

Mod-5A Wind Turbine Generator Program Design Report

Volume II—Conceptual and Preliminary Design Book 1

General Electric Company
(Advanced Energy Programs Department)

August 1984

Prepared for
National Aeronautics and Space Administration
Lewis Research Center
Cleveland, Ohio 44135
Under Contract DEN 3-153

for
U.S. DEPARTMENT OF ENERGY
Conservation and Renewable Energy
Division of Wind Energy Technology
Washington, D.C. 20545
Under Interagency Agreement DE-AI01-79ET20305

DOE/NASA/0153-2
NASA CR-174735
84AEPD004

Mod-5A Wind Turbine Generator Program Design Report

Volume II—Conceptual and Preliminary Design Book 1

(NASA-CR-174735-Vol-2-Ek-1) MOD-5A WIND
TURBINE GENERATOR PROGRAM DESIGN REPORT.
VOLUME 2: CONCEPTUAL AND PRELIMINARY
DESIGN, BOOK 1 Final Report, Jul. 1980 -
Jun. 1984 (General Electric Co.) 374 p

N86-15722

Unclas
03436

G3/44

General Electric Company
(Advanced Energy Programs Department)



August 1984

Prepared for
NATIONAL AERONAUTICS AND SPACE ADMINISTRATION
Lewis Research Center
Under Contract DEN 3-153

for
U.S. DEPARTMENT OF ENERGY
Conservation and Renewable Energy
Division of Wind Energy Technology

DISCLAIMER

This report was prepared as an account of work sponsored by an agency of the United States Government. Neither the United States Government nor any agency thereof, nor any of their employees, nor any of their contractors, subcontractors or their employees makes any warranty, express or implied, or assumes any legal liability or responsibility for the accuracy, completeness, or usefulness of any information, apparatus, product, or process disclosed, or represents that its use would not infringe privately owned rights. Reference herein to any specific commercial product, process, or service by trade name, trademark, manufacturer, or otherwise, does not necessarily constitute or imply its endorsement, recommendation, or favoring by the United States Government or any agency thereof. The views and opinions of authors expressed herein do not necessarily state or reflect those of the United States Government or any agency thereof.

Printed in the United States of America

Available from:

National Technical Information Service
U.S. Department of Commerce
5285 Port Royal Road
Springfield, VA 22161

Volume I, Executive Summary

Volume I contains an overview of the MOD-5A Program. These topics are covered:

- Objectives of the MOD-5A Program
- Description of the Final Design (Model 304.2)
- Cost of Energy
- Power Output
- Trade-Off Studies
- Development Tests
- Analyses of Loads and Dynamics
- Manufacturing and Quality Assurance and Safety Plans

Volume II, Conceptual and Preliminary Design

These sections comprise Volume II, which is divided into two books, as follows:

- Book 1
- 1.0 Summary
 - 2.0 Introduction
 - 3.0 Design Requirements
 - 4.0 Conceptual Design Studies
 - 5.0 Design, Development, and Optimization
 - 6.0 System Dynamics Analysis
 - 7.0 System Loads Analysis

- Book 2
- 8.0 Development Tests
 - 9.0 Design Criteria
 - Appendix A System Specification
 - Appendix B Design Load Tables

Volume III, Final Design and System Description

These sections comprise Volume III, which is divided into two books, as follows:

- Book 1
- 1.0 Summary
 - 2.0 Introduction
 - 3.0 System Description - Model 304.2
 - 4.0 Rotor Subsystem
 - 5.0 Drivetrain Subsystem
 - 6.0 Nacelle Subsystem
 - 7.0 Tower and Foundation Subsystems

<u>Book 2</u>	8.0	Power Generation Subsystem
	9.0	Control and Instrumentation Subsystems
	10.0	Manufacturing
	11.0	Site and Erection
	12.0	Quality Assurance and Safety
	13.0	FMEA, RAM and Maintenance
Appendix A		C.F. Braun & Company - Foundation Design Criteria
Appendix B		GE - Product Assurance Program Plan for the MOD-5A WTG Program
Appendix C		GE - System Safety Plan for the MOD-5A Program
Appendix D		GE - MOD-5A Configuration Management Plan
Appendix E		GE - MOD-5A Defect Reports for Development Hardware
Appendix F		GE - MOD-5A Program Quality Assurance Requirements for the Control of Raw Materials and the Blade Fabrication Process
Appendix G		GE - Statement of Work for the Erection of the MOD-5A WTG Yaw, Nacelle and Blade Subsystems

Volume IV, Drawings and Specifications

This volume contains the numbered drawings and specifications for the final design of the MOD-5A wind turbine. The volume is divided into five books, as follows:

<u>Book 1</u>	47A380002 through 47A380030
<u>Book 2</u>	47A380031 through 47A380068
<u>Book 3</u>	47A380074 through 47A380126
<u>Book 4</u>	47A380128 through 47A387125
<u>Book 5</u>	47D381002 through 47D387130

MOD-5A WIND TURBINE GENERATOR
DESIGN REPORT
VOLUME II, BOOK 1

<u>Section</u>	<u>Page</u>
1.0 <u>SUMMARY</u>	1-1
2.0 <u>INTRODUCTION</u>	2-1
3.0 <u>DESIGN REQUIREMENTS</u>	3-1
3.1 Introduction	3-1
3.2 Specifications	3-1
3.3 Cost of Energy	3-9
3.4 Advanced Technology	3-11
4.0 <u>CONCEPTUAL DESIGN STUDIES</u>	4-1
4.1 Introduction	4-1
4.2 Weight and Cost Estimating Relationships (WCERs)	4-3
4.2.1 Weight and Cost Estimating Relationship	
Sizing Parameters	4-4
4.2.2 Site Items	4-5
4.2.3 Site Erection Items	4-9
4.2.4 Rotor Items	4-9
4.2.5 Drive Train	4-10
4.2.6 Nacelle Items	4-11
4.2.7 Tower Items	4-12
4.2.8 Control Items	4-12
4.2.9 Spares	4-13
4.2.10 Special Items	4-13
4.2.11 Land Costs	4-13
4.2.12 Cluster Costs	4-13
4.2.13 Operation and Maintenance	4-14
4.2.14 Transportation	4-14
4.2.15 Performance	4-14

4.3	Subsystem Tradeoff Studies	4-17
4.3.1	Introduction	4-17
4.3.2	Blade Material Study	4-22
4.3.3	Blade Articulation Study	4-29
4.3.4	Upwind or Downwind Rotor Study	4-37
4.3.5	Torque Control Study	4-41
4.3.6	Tower Height Study	4-45
4.3.7	System Rotational Velocity Study	4-48
4.3.8	Gearbox and Nacelle Configuration Study	4-56
4.3.9	Rotor Stopping Technique Study	4-63
4.4	System Size Studies	4-71
4.4.1	Optimization Procedure	4-71
4.4.2	Cost of Energy Minimization	4-77
4.5	Conceptual Design Development, (Model 204.0)	4-79
4.5.1	Configuration	4-79
4.5.2	Performance	4-97
4.5.3	Weight Summary	4-97
4.5.4	Cost Summary	4-101
4.5.5	Cost of Energy	4-101
5.0	<u>DESIGN, DEVELOPMENT, AND OPTIMIZATION</u>	5-1
5.1	Introduction	5-1
5.2	Model 204.0 Design	5-1
5.3	Model 204.1 Design	5-4
5.4	Model 204.2 Design	5-6
5.5	Model 204.3 Design	5-9
5.6	Model 204.4 Design	5-11
5.7	Model 204.5 Design	5-12
5.8	Model 204.6 Design	5-17
5.9	Model 304.0 Design	5-25
5.10	Model 304.1 Design	5-27
5.11	Model 304.2 Design	5-29
5.11.1	Configuration	5-29
5.11.1.1	Rotor Subsystem	5-29
5.11.1.2	Drive Train Subsystem	5-34
5.11.1.3	Nacelle Subsystem	5-37

5.11.1.4	Tower and Foundation	5-39
5.11.1.5	Power Generation Subsystem	5-41
5.11.1.6	Control and Instrumentation Subsystem	5-45
5.11.2	Performance	5-49
5.11.3	Weight Summary	5-53
5.11.4	Cost Summary	5-53
5.11.5	Cost of Energy	5-53
6.0	<u>SYSTEM DYNAMICS ANALYSIS</u>	6-1
6.1	Introduction	6-1
6.2	Methods of Analysis	6-3
6.2.1	Natural Frequency Analysis	6-3
6.2.2	Aeroelastic Stability	6-5
6.3	System Modes and Natural Frequencies	6-9
6.3.1	Baseline Design - Model 304.2	6-9
6.3.1.1	Model Description	6-9
6.3.1.2	Natural Modes and Frequencies	6-18
6.3.2	Sensitivity Studies	6-23
6.3.2.1	Tower Frequency Sensitivity to Foundation Stiffness	6-23
6.3.2.2	Sensitivity of Tower Loads to Tower Fundamental Frequency	6-29
6.3.2.3	System Frequency Sensitivity to Bearing and Yaw Drive Stiffness	6-35
6.4	Aeroelastic Stability	6-44
6.4.1	Classical Flutter Divergence	6-44
6.4.2	Blade Flap-Lag-Pitch Instability	6-44
6.4.3	Coupled Rotor and Tower Instabilities	6-45
6.4.4	Blade Stall Flutter	6-45
6.4.5	Blade/Aileron Flutter	6-46
6.5	Control System	6-58
6.5.1	Overview	6-58
6.5.2	Control System Frequency and Time Response	6-61
6.5.2.1	Frequency Response	6-61
6.5.2.2	Time Response	6-68

6.6	Structure/Control System Interaction	6-79
6.6.1	Background	6-79
6.6.2	Sensitivity Studies with Tip Controlled Wind Turbine	6-79
6.6.3	Applicability to Current MOD-5A Control System Design	6-82
7.0	<u>SYSTEM LOADS ANALYSIS</u>	7-1
7.1	Introduction	7-1
7.2	Methods of Analysis	7-1
7.2.1	Aeroelastic Codes	7-1
7.2.2	Load Statistics	7-5
7.2.3	Wind Models	7-10
7.2.4	Verification of Codes and Models	7-17
7.2.5	Design Operating Conditions	7-21
7.3	Interfaces and Coordinate Axes	7-26
7.4	Interface Design Loads - Model 304.2	7-34
7.5	Component Design Loads	7-44
7.5.1	Ailerons	7-44
7.5.2	Blades	7-57
7.5.2.1	Primary Bending Loads	7-57
7.5.2.2	Blade Pressure Loading	7-57
7.5.2.3	Balance Requirements	7-60
7.5.3	Rotor Hub	7-60
7.5.3.1	Teeter Brakes	7-61
7.5.3.2	Teeter Bearings	7-61
7.5.3.3	Rotor Bearing	7-67
7.5.4	Gearbox/Drive Train	7-67
7.5.5	Yaw System	7-68

List of Abbreviations

LIST OF FIGURES		
Figure No.	Title	Page
4-1	Cost of Energy History	4-2
4-2	WCER Development Example - Gearbox	4-11
4-3	Output Power and Wind Speed Cumulative Distribution	4-16
4-4	System Configuration Selection Logic Flow	4-18
4-5	Blade Material Trade-Off Study - Flow Diagram	4-24
4-6	Blade Cost and Weight - Parametric Summary	4-25
4-7	Typical Blade Cross-Sections	4-26
4-8	Rotor Types	4-30
4-9	Comparison of the Aerodynamic Performance of Teetering and Independently Coned Rotors	4-32
4-10	Comparison of Loads for Independently Coned vs. Teetered Rotors	4-33
4-11	Blade Fatigue Load Summary	4-34
4-12	Control Flap Equivalent of 25% Partial Span Control	4-43
4-13	Ground Clearance vs. Cost Comparison	4-47
4-14	Benefits of Two-Speed Operation	4-53
4-15	Speed Ratio Sensitivity	4-55
4-16	Sensitivity of Cost of Energy to Rotor Speed Ratio	4-55
4-17	Non-Integrated Gearbox Quill Shaft Drive	4-58
4-18	Fully-Integral Gearbox	4-60
4-19	Rotor-Integrated Gearbox	4-61
4-20	Gearbox and Bedplate Trade-Off Flow Chart	4-62
4-21	Relative Sizes of Drivetrain Configurations	4-64
4-22	Simplified Diagram of the Overspeed Protection Study, Baseline Phase A Results	4-65

LIST OF FIGURES (Cont'd)
Title

Figure No.	Title	Page
4-23	Major Parameters Optimization Flow Chart	4-73
4-24	Blade Cost and Weight Estimating Procedure	4-76
4-25	Results of Tip Speed Variation and Power Density Variation	4-78
4-26	Design Evolution	4-82
4-27	MOD-5A Conceptual Design, Model 204.0	4-83
4-28	MOD-5A Production Plant Layout	4-84
4-29	Description of the Blade	4-85
4-30	Partial Span Control Mechanism	4-86
4-31	Pitch Hydraulics Block Diagram	4-88
4-32	Hub, Shaft, and Teeter Arrangement	4-89
4-33	Nacelle Cross-Section	4-91
4-34	Rotor Integrated Hybrid Gearbox	4-92
4-35	Yaw Drive	4-94
4-36	Tower and Foundation	4-95
4-37	Protected Aisle Compartment	4-96
4-38	Operating Mode Description	4-102
4-39	Cost of Energy Contributions	4-103
4-40	Cost of Energy and Capital Costs	4-104
5-1	Centered Bearing Blade Support	5-21
5-2	Selected Rotor Support Configuration	5-22
5-3	Variable Speed Subsystem Schematic	5-23
5-4	MOD-5A Model 304.2	5-30
5-5	Rotor Subsystem	5-32
5-6	Rotor Support Assembly	5-35

LIST OF FIGURES (Cont'd)
Title

Figure No.	Title	Page
5-7	Nacelle Profile	5-38
5-8	Tower and Foundation	5-40
5-9	Electrical Equipment Location	5-43
5-10	Power Generation Diagram	5-44
5-11	MOD-5A Control Subsystem Block Diagram	5-46
5-12	Cycloconverter	5-48
5-13	Power and Wind Speed Probability for Design Wind Regime	5-50
5-14	Power and Wind Speed Probability for Wind Regime in Kahuku, HI	5-52
6-1	Wind Turbine Model Substructures	6-4
6-2	Features of Aeroelastic Program, GETSTAB	6-7
6-3	Features of Aeroelastic Program, AILSTAB	6-8
6-4	Rotor/Yoke Finite Element Model	6-10
6-5	Coupled Mode Shapes	6-19
6-6	MOD-5A Frequency Placement Model 304.2	6-21
6-7	Tower Frequency Model	6-24
6-8	Tower Y Bending and Torsion Frequencies vs Rotational Foundation Stiffness	6-27
6-9	Tower Z Bending and Axial Frequencies vs Rotational Foundation Stiffness	6-28
6-10	Probability Distribution for Tower Base Bending Moment M_y -Alternating	6-32
6-11	Probability Distribution for Tower Base Bending Moment M_z -Alternating	6-33
6-12	Variation of Tower Fatigue Moments with Natural Frequency	6-34
6-13	Sign Conventions	6-36

LIST OF FIGURES (Cont'd)

Figure No.	Title	Page
6-14	Effect of Rotor Teetering Stiffness on Teeter Frequency	6-37
6-15	Effect of Radial Teeter Bearing Stiffness on Drive Train Frequency	6-38
6-16	Effect of Radial Teeter Bearing Stiffness on Blade Torsional Frequency	6-39
6-17	Effect of Yoke Bearing Stiffness on Tower Torsion and Second Lateral Bending Frequencies	6-41
6-18	Effect of Yaw Bearing Stiffness on Tower Fundamental Frequency	6-42
6-19	Effect of Yaw Stiffness on Chord Cyclic and Tower Torsion Frequencies	6-43
6-20	Stability with Free, Unbalanced Aileron	6-48
6-21	Stability with Free, Mass-Balanced Aileron	6-49
6-22	Free Aileron Stability at 6 rpm vs. Mass Balance	6-50
6-23	Stability with Unbalanced Aileron and 8 rad/sec Hinge Stiffness	6-51
6-24	Unbalanced Aileron Stability Boundary with Control System Stiffness	6-54
6-25	Unbalanced Aileron Stability Boundary with Hinge Dampers and Free Aileron	6-55
6-26	Comparative Effects of Stiffness and Damping Impedance on Aileron Stability	6-56
6-27	MOD-5A Flutter Boundary Shown in Terms of Aileron Root Impedance	6-57
6-28	General Control System Block Diagram	6-59
6-29	System Control Plan	6-59
6-30	Power Generation Operation Regions	6-60
6-31	Control System Rotational Dynamics	6-62
6-32	Linear Model of Speed Control Loops	6-64

LIST OF FIGURES (Cont'd)

Figure No.	Title	Page
6-33	Open Loop Gain/Phase Characteristics of Rotor Speed Loop	6-65
6-34	Rotor Speed Loop Hardware Implementation Representation	6-67
6-35	Generator Speed Loop LaPlace Representation	6-69
6-36	Time Response For Step Wind Change at $V_W = 45$ mph	6-69
6-37	Time Response For Step Wind Change at $V_W = 45$ mph	6-70
6-38	Time Response For Wind Gust at $V_W = 32$ mph	6-71
6-39	Time Response For Wind Gust at $V_W = 45$ mph	6-76
6-40	Time Response For Wind Gust Plus Turbulence	6-77
6-41	Time Response For Loss-of-Load Shutdown	6-78
6-42	MOD-5A Control System Schematic	6-84
6-43a	Tip Angle Response - GE Baseline	6-85
6-43b	Tip Angle Response - Boeing Baseline	6-86
6-44a	Hub Torque Response - GE Baseline	6-87
6-44b	Hub Torque Response - Boeing Baseline	6-88
6-45	Effect of Rotor Speed Gain and Pitch Servo Time Constant on Response	6-89
7-1	GETTS Analysis Flow	7-2
7-2	Features of the TRAC Code	7-4
7-3	Fatigue Load Types	7-6
7-4	Procedure for Determining Life Cycle Fatigue Loads	7-7 & 7-8
7-5	Development of Mean Wind Variation Model	7-12
7-6	Development of Large Rotor-Enveloping Gust Mode	7-13
7-7	Development of Local Turbulence Wind Model	7-15

LIST OF FIGURES (Cont'd)

Figure No.	Title	Page
7-8	Simulation of MOD-1 Shutdown, Using the Trac Code	7-18
7-9	Comparison of MOD-1 Shutdown Test Blade Loads with Theoretical Predictions	7-19
7-10	Test and Correlation with Theory of MOD-1 Type I Fatigue Loads	7-20
7-11	Frequency of Occurrence of MOD-2 Type II Load Measurements	7-22
7-12	Comparison of MOD-5A Type II Load Predictions with Scaled MOD-2 Measurements	7-23
7-13	Sign Conventions	7-31
7-14	Aileron Coordinate System	7-32
7-15	System Dimensions and Interfaces	7-33
7-16	Blade Flapwise Bending Moment Probability Distributions	7-36
7-17	Blade Chordwise Bending Moment Probability Distributions	7-37
7-18	Tower Root Bending Moment Probability Distributions	7-39
7-19	Rotor Torque Probability Distribution	7-40
7-20	Yaw Bearing Bending Moment and Drive Torque Probability Distributions	7-41
7-21	Blade Limit Loads	7-42
7-22	Aileron Aerodynamic Loads for Hurricane Conditions with the Blades Horizontal, and the Ailerons Undelected	7-47
7-23	Aileron Aerodynamic Loads for Hurricane Conditions with the Blades Vertical and the Ailerons Deflected 90°	7-48
7-24	Aileron Aerodynamic Limit Loads for a 25% Overspeed Condition, with the Ailerons Deflected 45°	7-49

LIST OF FIGURES (Cont'd)
Title

Figure No.	Title	Page
7-25	Aileron Inertial Limit Loads for a 25% Overspeed Condition with the Ailerons Deflected 45°	7-50
7-26	Mean Aerodynamic Aileron Loads at Rated Wind Speed, 50th Percentile Cyclic Loads are 15% of Shown Mean Loads	7-51
7-27	Mean Aileron Inertial Factors (G_x , G_y , G_z)	7-52
7-28	Aileron Normalized Fatigue Load Probability Distribution. Used for all Aerodynamic Loads, and Inertial Normal Force (G_z)	7-54
7-29	Aileron Normalized Fatigue Load Probability Distribution. Used for Radial and Lateral Inertial Loads (G_x & G_y)	7-55
7-30	Aileron Normal Force Inertial Factor (G_z) 50th Percentile Cyclic Values	7-56
7-31	Airfoil Pressure Coefficients, Shown for Sections at $\chi = .25$, $.55$ and $.95$	7-59
7-32	MOD-5A Teeter Brake Schedule	7-62
7-33	Teeter Angle Probability Distributions for Normal Operation	7-64
7-34	MOD-5A Gearbox Torque Duty Cycle	7-69

LIST OF TABLES
Title

Table No.	Title	Page
3-1	System Design Requirements	3-4 to 3-7
3-2	Major GE MOD-5A Specifications	3-8
3-3	Cost of Energy Computation	3-10
4-1	MOD-5A Weight and Cost Estimating Relationship (WCERS)	4-6
4-2	Major Trade Studies and Selection at the Conceptual Design Review	4-19
4-3	Trade-Off Summary Score Sheet (Format)	4-20
4-4	Conceptual Design - Cost and Weight of the 100th Unit	4-27
4-5	Blade Material Trade-Off at the System Level	4-28
4-6	Trade-Off Score Sheet, Independent Coning vs. Teetering	4-36
4-7	Rotor Weight and Cost Summary for 350-Ft Diameter	4-37
4-8	Summary of the Upwind vs. Downwind Trade-Off	4-40
4-9	Summary of Torque Control Study	4-44
4-10	Wind Speed Distribution in Amarillo, TX.	4-51
4-11	Persistence Analysis	4-52
4-12	Trade-Off Study Summary	4-57
4-13	Sizing Optimization Accounts	4-72
4-14	Cost of Energy Computation	4-77
4-15	Model 204.0 Configuration	4-80
4-16	MOD-5A Design Innovations	4-81
4-17	Availability Analysis Summary	4-98
4-18	Cost of Energy Report for Model 204.0	4-99/4-100
4-19	Cost of Energy Summary for the Baseline System	4-105

LIST OF TABLES (Cont'd)
Title

Table No.	Title	Page
5-1	Model 204.0 Configuration	5-3
5-2	Model 204.1 Configuration	5-5
5-3	Model 204.2 Configuration	5-8
5-4	Model 204.3 Configuration	5-10
5-5	Model 204.5 Configuration	5-13
5-6	Cost of Energy Report Model 204.5 - First Unit	5-14
5-7	Cost of Energy Report Model 204.5 - 100th Unit	5-15
5-8	Model 204.6 Configuration	5-18
5-9	Model 304.0 Configuration	5-26
5-10	Model 304.1 Configuration	5-28
5-11	Model 304.2 Configuration	5-31
5-12	Design Energy Output	5-51
5-13	Model 304.2 Weight Summary	5-54
5-14	Cost Summary for the First Unit	5-55
5-15	Cost Summary for the Second Unit	5-56
5-16	Cost Summary for the Third Unit	5-57
5-17	Cost Summary for the 100th Unit, Single Installation	5-58
5-18	Cost Summary for the 100th Unit, Clustered Installation	5-59
6-1	Tower Model Data, Element Properties	6-11
6-2	Rigid Body Bedplate Model	6-12
6-3a	Rotor Support/Yoke Model	6-13
6-3b	Bearings and Electrical Grid, Point to Point Stiffness Elements	6-14

LIST OF TABLES (Cont'd)

Table No.	Title	Page
6-4	Blade Properties	6-15
6-5	Yaw Bearing and Upper Yaw Adapter	6-16
6-6	Teeter Bearing	6-16
6-7	Yoke/Rotor Support to Nacelle Coupling Stiffness	6-17
6-8	MOD-5A Model 304.2 System Natural Frequencies	6-20
6-9	Weibull Distribution from Statement of Work	6-30
6-10	Root Mean Cubed Tower Load Comparison	6-31
6-11	Model 304.2 Control System Parameter Definition	6-63
6-12	Time Response Simulation Run Listing	6-72
6-13	Time Response Plot Identification	6-73
6-14	Significant Model Parameters	6-80
7-1	Classification of Wind Models	7-11
7-2	Formulas for the MOD-5A Wind Turbulence Model	7-16
7-3	MOD-5A Wind Bin and Fatigue Cycle Summary	7-24
7-4	Gust Amplitudes Used for the MOD-5A Fatigue Loads Analysis	7-25
7-5	Critical Limit Load Conditions	7-27
7-6	Additional Transient Events Analyzed	7-28
7-7	System Interfaces	7-29
7-8	One-G Interface Loads (Model 304.2)	7-30
7-9	Typical Load Histogram Presentation	7-35
7-10	Normalized Fixed System Limit Load Summary	7-43
7-11	Formulas Needed to Combine Aileron Aerodynamics and Inertial Loads	7-45

LIST OF TABLES (Cont'd)
Title

Table No.	Title	Page
7-12	Teeter Bearing Normal Operating and Limit Load Specification	7-65
7-13	Ratio of Specification to Model 304.2 Loads-Teeter Bearing	7-65
7-14	Normal Start-up and Shutdown Loads (kips)	7-66
7-15	Teeter Bearing Stiffness Requirements	7-67
7-16	Rotor Bearing Design Loads	7-70
7-17	Yaw Bearing Design Loads	7-70

1.0 SUMMARY

1.0 SUMMARY

This report documents the work accomplished during the conceptual and preliminary design phases of NASA Contract DEN3-153. The program described in this report was designated the MOD-5A Wind Turbine Generator by the U.S. Department of Energy, and is a key element of the national Wind Energy Program (see Section 2).

Section 3 summarizes the system design requirements that were used to develop the MOD-5A baseline configuration.

Section 4 defines the program's design objectives, and describes the results of system sizing optimization and cost of energy studies, composite rotor and two-speed gearbox innovations, and detailed trade-off studies that led to the selection of the baseline conceptual design configuration.

Section 5 contains the detailed configurational design update leading to the current system configuration, with detailed subsystem design descriptions, supporting system performance analysis, and verification of previously performed trade-off studies.

Section 6 details all of the results of all of the system dynamic analyses in support of the trade-off studies and the design activities.

Section 7 presents the evolution of the system loads that were used to evaluate and design the MOD-5A wind turbine's major structural elements.

Section 8 summarizes all of the development tests that were conducted in support of the design activities.

Section 9 summarizes the structural and dynamics design criteria by which the structural and load analyses were conducted.

2.0 INTRODUCTION

2.0 INTRODUCTION

In 1973, a national Wind Energy Program was established to develop the technology to make wind energy systems cost competitive with conventional power generation systems, and to accelerate the commercial use of wind energy.

The United States Department of Energy (DOE) has overall management responsibility for this program. The NASA-Lewis Research Center has the responsibility for managing the development of large horizontal-axis wind turbines for the DOE.

Under contract to NASA, the Advanced Energy Programs Department of the General Electric Company (GE-AEPD) was engaged in the development of an advanced multi-megawatt wind turbine generator designated the MOD-5A WTG. Participating in this program, as subcontractors to GE-AEPD are Gougeon Brothers, Inc. (GBI) for the wood laminae blades, Philadelphia Gear Corporation (PGC) for the gearbox, and the Chicago Bridge and Iron Company (CBI) for the steel shell tower, site work, foundation and WTG erection.

The goal of the MOD-5A program was to develop a reliable, commercially feasible wind energy system, able to produce electricity at a cost of energy of 3.75 cents per kilowatt hour, or less, in mid-1980 dollars, at a site with an annual average wind speed of 14 mph.

The general approach to the implementation of the MOD-5A WTG Program was the initiation of a multi-phased, 71 month effort, consisting of 47 months for conceptual design, preliminary design, final design, fabrication, assembly, installation and checkout, followed by 24 months of operational support and design improvements. In addition, development and qualification testing of materials, parts, and components were included as part of the preliminary design phase to ensure that the MOD-5A would perform and endure, as designed.

The program began in July 1980. It was organized into three design phases: conceptual design, which was completed in March 1981, preliminary design, which was completed in May 1982, and final design, which started in June 1982. Each design phase culminated in a comprehensive design review,

which had two main objectives: an in-depth review of the design's technical adequacy, and verification that the program's requirement for cost of energy was being met.

During the conceptual design phase, comprehensive trade-off and system sizing studies were conducted around a baseline configuration. The goal of these studies was to arrive at a concept with the greatest potential to meet the project's objectives: a cost of energy of 3.75 cents per kilowatt hour in mid-1980 dollars, a 30-year life, and safe operation, with acceptable risk to the program and equipment. As part of this activity, a cost, cost of energy, and weight accounting procedure was developed. This procedure tracked the effects of the sizing and trade-off studies. In addition, a manufacturing plan was developed to support the projected program costs for the fabrication of the 100th MOD-5A production unit.

After NASA and the Department of Energy approved the conceptual design, the program progressed into the preliminary design phase. During this period the recommended baseline configuration, an upwind wind turbine, with a 400-foot laminated wood and epoxy rotor and a power rating of 5.0 MW, was evaluated further. The outcome of the preliminary design would be used in the final development phases. In conjunction with the preliminary design activity, qualification of the wood-epoxy laminate blade materials, and key components and subsystems were conducted. These tests continued during the final design phase.

The development produced a wind turbine design rated at 7300 kW, with a 400-foot rotor with lightweight, wood-epoxy laminated blades, aileron control and a tower and nacelle system designed for reliability and ease of maintenance. As a result of the optimum size and the numerous technical advances, this third-generation machine would be expected to achieve a cost of energy competitive with the cost of conventional forms of power generation.

3.0 DESIGN REQUIREMENTS

3.0 DESIGN REQUIREMENTS

3.1 INTRODUCTION

The goal of the MOD-5A project was to develop a cost effective wind turbine that could be used in many applications in the electric utility market. The intent was to stimulate innovation and introduce advanced technology that would achieve a low cost of energy at an acceptable risk to the equipment and the program. Technical and economic feasibility were emphasized. Trade-off decisions favored the lowest cost of energy and a mature product.

The technical requirements and specifications were identified in Contract DEN 3-153, Statement of Work (SOW), Exhibit B. The System Specification for the MOD-5A Wind Turbine Generator, includes the statement of work requirements, and more detailed requirements for the design of the model 304.2 MOD-5A Wind Turbine Generator. (304.2 was the last model number assigned during the MOD-5A program.) This document is included in the appendix of this report.

The design process comprised the conceptual, preliminary, and final phases. During the conceptual design phase, trade-off and size optimization studies were conducted, to identify an optimum system. More detailed design was done in the preliminary and final design phases. Major changes were made as the result of a study that reassessed the risks during the final design phase.

3.2 SPECIFICATIONS

The statement of work required the MOD-5A to be:

- o designed for use by electric utility companies,
- o capable of generating at least one megawatt,
- o able to produce energy at less than 3.75 cents/kwh (1980\$) in a mean wind of 14 mph,
- o designed to deliver three phase, 60 Hz power,
- o designed for a useful operational life of 30 years,
- o configured with a horizontal-axis and a propellor.

These requirements were intended to permit the maximum design flexibility within the constraints imposed by the user, size, cost of energy, life, and configuration.

The system design requirements developed for the conceptual design phase are shown in Table 3-1. The comment column indicates areas in which a requirement acted as a design driver. The statement of work requirements were evaluated during the conceptual design phase. The recommendations that resulted from this evaluation are summarized below:

1. Use the cost of installed equipment or the capital cost, as well as the cost of energy. An electric utility will be able to evaluate these costs more readily than cost of energy, because of the uncertainty in wind resources.
2. Retain the extreme wind specification with 0.1 shear exponent.
3. Permit signals from a common sensor to be used by the control system, operational instrumentation system, and engineering instrumentation system. The signals must be buffered before they are sent to the engineering information system.
4. Obtain additional wind data for use in determining wind shear effects up to 500 ft.
5. Use the wind gust definition in NASA PIR #151 and use a Rayleigh gust amplitude distribution as a better match to the PNL-Battelle data than the Statement of Work definition. Also, use empirical dispersion factors to define turbulence induced response loads.
6. Specify a Response Spectra seismic method rather than the Uniform Building Code method.
7. Increase the minimum operating temperature to -22°F , if site data permits.
8. Specify 24-hour rain accumulation, and rate.
9. Specify shipping and storage requirements.
10. Use a 150 MW cluster for determining the number of units. This size is appropriate for a single 230 kV grid connection or 3kV connections.
11. Use more reasonable cluster distribution line costing, at 34.5 kV, of \$45,000 to \$55,000 per mile, depending on conductor size, instead of nearly \$90,000 per mile.

During later phases of the program, the extreme wind shear exponent, noted in item 2, was lowered from 0.1 to 0.04. The wind gust definition, noted in item 5, was adopted. The cluster size, noted in item 10, was raised to 175 MW during the preliminary design phase.

The ambient temperature range for wind turbine operation was specified during the final design to be 0°F to 104°F. This range was ample for the proposed installation in Hawaii. The minimum temperature reduces the risk of fatigue crack propagation in some steel components.

GE specifications were prepared for the major components, listed in Table 3-2. Industry and government documents and standards that were used during the design are referenced in a GE specification.

Table 3-1 System Design Requirements

Requirement	Criteria/Value		Comments
Cost of Energy	o	Less than 3.75 ¢/KWH (1980) (SOW)	o Major driver in all areas
	o	Goal - minimize cost of energy with acceptable risk	o Reduce labor and material costs
			o Increase performance and availability
Operational Wind Regime	o	14 MPH mean (SOW) at 32.8 ft. above grade with variable wind shear.	o Driver for combined tip speed, speed ratio, solidity to minimize COE
	o	Cut-in at below 10% of rating (GE)	o Determines tip length and startup time values
	o	Cut-out wind to minimize COE (GE)	o Goal of less than 12 minutes with 25% tip, 14 MPH (hub) established
			o Determines speed where COE stops decreasing or loads start increasing
			o 44 MPH (hub) established for SOW wind

Table 3-1 System Design Requirements
(Continued)

Requirement	Criteria/Value		Comments
Extreme Wind	o	120 MPH (SOW) at 32.8 ft. above grade with 0.1 wind shear exponent.	o Driver for tower and foundation o Minimize load by $< 45^\circ$ orientation to wind (weather- vaning) to decrease COE
Limit Thrust	o	115% speed, 1.2 C_L design point with 4 σ gust (GE)	o Driving load on parts of blades
Emergency Feather	o	Max negative C_L on tip (-1.5) Low C_L inboard	o Not as critical as limit thrust condition
Seismic	o	Zone 3-UBC (SOW)	o Not a design driver
	o	Analyze as 0.5G with response spectra	o 0.3G, 25 in. maximum response less than extreme wind limit loads on system

Table 3-1 System Design Requirements
(Continued)

Requirement	Criteria/Value		Comments
Cyclic Loads	o	30 year life (SOW)	o 35,000 start, stop and gear-shift cycles established from hourly data analysis
	o	Fatigue load factors determined from MOD-0 and MOD-2 and gust model (SOW turbulence)	o Driving load on parts of blades and hub for 2×10^8 cycles over life time
Frequency Placement	o	Avoid resonances	o Drives bell section to tower, high RPM and RPM ratio to increase energy capture
	o	Tower bending between 1.1 and 1.8P	o Driver for gearbox stiffness and active (control system) or passive damping
	o	Drivetrain torsion below 0.9P and $\geq 25\%$ critical damping	o Preliminary design phase requirements for system
	o	Blade cyclic modes away from odd $(N \pm .2)P$ (except teeter)	
	o	Blade collective and fixed system modes away from even $(N \pm .2)P$	

Table 3-1 System Design Requirements
(Continued)

Requirement		Criteria/Value		Comments
Availability	o	0.92 minimum design for 100th unit between cut-in and cut-out (SOW)	o	Design goals established based on RAM analysis
			o	0.960 for cluster
			o	0.932 for single site
			o	Design features for maintenance
Critical Failure Modes	o	Sense and control for failures which might cause human injury or require major (over 20% of capital cost) repair (SOW)	o	Redundancy checks established for critical sensors
			o	Single tip shutdown requirement established
	o	Single degradation shall not cause hazard (SOW)	o	Failsafe unit established to protect from controller malfunction
	o	Automatic shutdown on loss of grid power (SOW)	o	Stored energy shutdown power established

Table 3-2. Major GE MOD-5A Specifications

<u>NUMBER</u>	<u>TITLE</u>
47A380011	System Specification
47A380002	Structural Design Criteria
47A380013	Control System Specification
47A380022	Support Tower and Foundation Specification
47A380052	Electrical Fabrication and Workmanship
47A380053	Electrical Equipment Design and Test
47A380054	General Welding Specification
47A380047	Bolt Pretensioning Specification
47A380048	Material Finish Specification
47A380083	Three Stage Speed Increaser
47A380094	7500 KVA Variable Speed Generator Subsystem
47A380124	Aileron Structure
47A380104	Aileron Actuator
47A380110	Rotor Hydraulic Power Supply
47A380111	Yaw Hydraulic Power Supply
47A380108	Gearbox Lubrication Cooler
47A380116	Material Control Specification
47A380012	Slipring Assembly Specification
47A380062	Material Control Specification

3.3 COST OF ENERGY

The objective of the MOD-5A program was to develop a cost effective wind turbine generator that could be used in many applications in the utility market. The intent was to stimulate innovation and introduce advanced technology that would achieve a low cost of energy at an acceptable risk to the equipment and the program. The design should provide a low cost of energy and a machine that could be produced in volume. Within the boundary of acceptable risk, a minimum cost of energy was the design driver.

A method for computing the cost of energy was defined in contract DEN 3-153, exhibit E, and is summarized in Table 3-3. The costs were calculated and reported in mid-1980 dollars. The cost of energy formula uses an annual cost in the numerator and an expected annual energy capture in the denominator.

The annualized cost is based on the costs of installed equipment, interconnection costs, land costs, periodic replacement costs, and operation and maintenance costs. Values for fixed charge rates and levelizing factors were specified and were used to compute annual costs for each category. The annual energy capture was computed by multiplying the estimated output energy by an availability factor that was obtained from a reliability, availability and maintainability analysis. No cluster performance loss was included, since the wind turbine generators were spaced at intervals of 10 times the rotor diameter.

The cost of energy calculation assumes a 30-year operational and amortization life for the equipment, and a privately-owned utility. The calculation provides a uniform basis of comparison for the projected cost of electricity of various energy conversion technologies. The algorithm used to optimize size, power rating and other variables was designed to search for arrangements with a minimum cost of energy.

Table 3-3 Cost of Energy Computation

o $COE = \frac{\text{LEVELIZED ANNUAL COST}}{\text{AVAILABLE ANNUAL ENERGY}}$ (IN MID-1980 \$)
(REFERENCE SOW EXHIBIT "E")

o LEVELIZED ANNUAL COST INCLUDES

CAPITAL COST AT 0.18 FIXED CHARGE RATE

LAND COST AT 0.15 FIXED CHARGE RATE

O&M COST AT 2.0 LEVELIZING FACTOR

PERIODIC REPLACEMENT LEVELIZED COST

o AVAILABLE ANNUAL ENERGY INCLUDES

SYSTEM POWER CHARACTERISTICS

SYSTEM LOSSES

SOW 14 MPH MEAN WIND REGIME

SCHEDULED AND UNSCHEDULED MAINTENANCE

3.4 ADVANCED TECHNOLOGY

Many innovative designs were used or were considered for use on the MOD-5A wind turbine generator. The 400-ft. rotor was one innovation that reduced the cost of energy significantly. The blade material, blade attachment, variable speed generator, aerodynamic control using ailerons, and push-pull yaw drive are other innovations used in the final design. Advanced technology was also used in intermediate designs. Although this technology was not included in the final model, it may be of use in other wind turbine generators. These designs include free tip overspeed protection, weathervane capability, rotor integrated gearbox, passive control of drivetrain spring-damper characteristics, two speed operation, and underrunning and slip clutch control of drivetrain torque.

The initial size optimizations, with a minimum cost of energy as the goal, indicated that the rotor diameter should be roughly 300 ft. Later a comprehensive analysis of the weight and cost estimating relationships for large wind turbines indicated that a 400-ft. rotor diameter would reduce the cost of energy significantly.

Laminated wood and epoxy was selected as the material for the rotor because of its light weight, the ability to control the surface finish and the ability to tailor its properties using the lay-up of alternating materials. These properties yielded high performance and the low cost of energy. During the preliminary design, when the center blade was optimized with continuous wood construction, the external yoke was developed to attach the blade to the drivetrain using a blade teeter shaft. This innovative design was developed further when bolsters were added to the center blade to localize the area in which large openings and reinforcements were needed.

A variable speed generator was included during the final design phase, to reduce risk and gearbox cost, and to increase operational flexibility. The arrangement was based on the Scherbiustat type of variable speed drive. It comprises a wound rotor induction generator and a static cycloconverter. The variable speed generator drives the turbine at low speeds for starting and generates power at rotor speeds of 11 rpm to 17 rpm. The generation mode

provides generator airgap torque control both for drivetrain damping and for limiting the maximum torque. Reactive power control was provided for operation in either a constant var or a constant voltage mode. The subsystem arrangement and control modes were innovative applications.

The aileron control development and testing advanced wind turbine technology. Ailerons regulated the rotor torque. The MOD-5A ailerons extend from 60% of the blade radius to the tip. They comprise three driven sections on the trailing 40% of the airfoil. Wind tunnel tests and subscale MOD-0 tests were used to develop and demonstrate the characteristics of the aileron arrangement. Each driven section had two segments, to allow the main blade to flex. The control arrangement provided mechanically independent sections to increase reliability. A tip-to-tip structural wood spar was provided by locating the ailerons on the outside of the main structure. This spar was designed with structurally efficient finger joints.

The push-pull yaw drive is another advanced feature. The drive was developed during the MOD-1 program, and it was tested on one NASA MOD-0A wind turbine. Caliper brakes and hydraulic actuators held and retracted, then gripped and pushed or pulled mating flanges across the yaw bearing. By avoiding gear teeth on the bearing flanges, a more cost effective drive was achieved and backlash was avoided.

In the first design for rotor torque control, which was called partial span control, the outer 25% of each blade was moveable. A free-tip overspeed protection arrangement was designed for the partial span control. The MOD-5A airfoil uses NACA series 64XXX sections to optimize performance and fabrication. The control sections at the blade tips were designed with an unrestrained pitch equilibrium position that produced retarding rotor torque. This feature, proven by test on NASA's MOD-0 wind turbine, was used in the free-tip overspeed protection, in which releasing the pitch control restraint resulted in a passive shutdown. This innovative feature was expected to minimize the chances of rotor overspeed.

The MOD-5 rotor with partial span control could be weathervaned while parked. In this innovative design, proven by test on the NASA MOD-0 wind turbine, one tip control was rotated to maximize drag on one blade while the blades are

horizontal and the yaw is free. The blades are pushed into alignment with high wind. In this position the blades minimize drag area and reaction forces seen by the tower and foundation.

The initial gearbox design used an advanced technology that may be useful in smaller wind turbines. This design was called the rotor integrated gearbox. The rotor support bearing was integrated into the external gearbox structure to minimize interfaces and couplings and to permit a compact configuration. The first planetary stage of gearing was cantilevered on the rotor support shaft, which let it move with respect to the case with no load reaction. Torsional stiffness and damping control of the first stage ring gear were provided by passive torsion bar springs and viscous flow hydraulic dampers. This passive control of drivetrain dynamics avoided the potential excitation of structural modes that a more active control could produce.

The first plan for the generator subsystem used a synchronous generator. A two-speed gearbox permitted more efficient rotor operation. The low speed was automatically selected for low wind operation and performance predictions indicated that two-speed operation provided most of the energy capture benefits of a variable speed generator.

With the synchronous generator, drivetrain torque was constrained between zero and 1.4 times the rated torque in a generating direction. This was done by an overrunning clutch and a slip clutch in the high speed shaft of the drivetrain. The overrunning clutch prevented the generator from motoring the rotor and permitted the rotor to underrun the generator during brief periods of low wind, thereby avoiding a shutdown and start-up cycle. This clutch was also used for two-speed shift control. The slip clutch limited the torque that could be reacted between the gearbox and generator, prevented the generator from imposing fault torques on the gearbox, and avoided loss of synchronism by permitting brief slips in response to gusts. This response to gusts permitted the rotor torque control to react more slowly, and minimized fluctuations in the blade loads caused by the torque control.

ORIGINAL PAGE IS
OF POOR QUALITY

4.0 CONCEPTUAL DESIGN STUDIES

4.0 CONCEPTUAL DESIGN STUDIES

4.1 INTRODUCTION

During the conceptual design phase an optimized MOD-5A configuration was developed. The resulting baseline configuration evolved as a result of detailed subsystem trade-off studies using developed weight and cost estimating relationships, and an optimization of rotor size.

Detailed descriptions of the major tasks performed in the conceptual design phase are in the following sections, including:

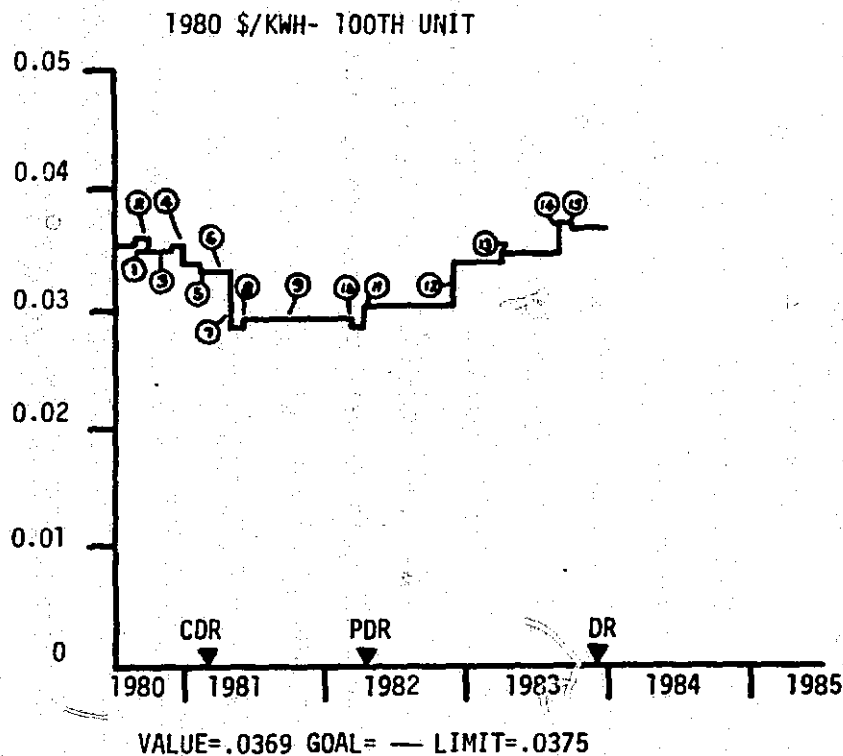
1. Weight and cost estimating relationships developed for the sizing optimization
2. Performance calculations
3. Major trade studies
4. Sizing optimization to minimize cost of energy
5. Conceptual design model 204.0

In addition to the detailed subsystem trade-off studies a series of analytical tasks were also performed in the conceptual design phase. These are discussed in other sections of the report, and include:

- 1) A study of automatic controls and safety
- 2) A volume production manufacturing plan
- 3) Evaluation of requirements
- 4) Analysis of the structural dynamics and aerodynamics
- 5) Verification of the loads prediction methods
- 6) Analysis of the utility interface stability
- 8) Determination of TV interference

The conceptual design phase began in July, 1980 and concluded with a design review in March, 1981. At this time, preliminary design activities were initiated.

The wind turbine proposed at the beginning of the conceptual design phase was rated at 4000 kW and had a glass fiber rotor 350 ft. in diameter. Model numbers were used to track significant changes in the configuration. The model number of the baseline system was changed from 101 to 102 when the rotor was changed from downwind to upwind of the shell tower. When the diameter was increased to 400 ft. the model number was changed to 104. A chart of cost of energy versus time by model number is shown in Figure 4-1.



KEY		
NO.	MODEL	COMMENT
1	101	Downwind 350 Ft. Dia, 4 MW, FRP Rotor, No Spec Relief, 69 KV Grid Connection
2	101	Detail Load, Cost and Weight Analysis
3	102	Upwind, 350 Ft. Dia, 4 MW
4	104	Initial Size Optimization, 400 Ft. Dia, 5 MW, 50 Ft. Ground Clearance
5	104.5	Revised Cluster Size to 150 MW with 30 Units, 50 Ft. Control Span
6	204.0	CDR Configuration, Wood Rotor with Steel Hub, 16.7 Ft. Blade Root Chord, Weathervane Loads
7	204.1	Aggressive Allowables, Detailed Torque Analysis 12.8/17.9 RPM, 6.2 MW, Rotating Shift
8	204.2	Raised Lower RPM for Better Tower Separation 13.2/17.9 RPM
9	204.3	Continuous Wood Center Blade with Steel Yoke, Non-Rotating Shift
10	204.4	Upated Gearbox Torque with Slip Coupling, 7.3 MW, 175 MW Cluster with 24 Units
11	204.5	Full Area Extreme Wind Loads with Spec Exponent Change, 40 Ft. Ground Clearance, 10% Blade Thickness Increase with Revised Allowables
12	204.6	Size Effect on Wood Allowables, NASA Turbulence Effect on Loads, 19.5 Ft Blade Root Chord, 13.7/16.9 RPM
13	204.0	Risk Reduction Analysis, Variable Speed Generator, Stand Alone Gearbox, Radial Bearing Rotor Support, 25 Ft. Blade Root Chord
14	304.1	50 Ft. Ground Clearance for Frequency Control
15	304.2	Alleron Control .4R, .4C and Low Speed Stopping Brake

Figure 4-1 Cost of Energy History

When the blade material study and size optimization were completed, the baseline design was designated model 204.0. This model had a teetered, 400-ft., laminated wood rotor, partial span control, a rotor-integrated gearbox and two-speed operation.

4.2 WEIGHT AND COST ESTIMATING RELATIONSHIPS (WCERS)

In order to optimize the size of the system and minimize the cost of energy, the weight and cost of subsystems were defined as functions of major parameters, such as rotor diameter and power rating.

This section discusses the development of the weight and cost estimating relationships that were used to optimize the system configuration and minimize the cost of energy. The techniques used to validate these relationships and a description of the performance calculations used to calculate energy capture are included. Thirteen cost categories were used:

1. Site items
2. Transportation
3. Installation
4. Rotor
5. Drivetrain
6. Nacelle
7. Tower
8. Remote control
9. Spares
10. Special items
11. Land
12. Cluster
13. Operation and Maintenance

To calculate the system cost, the 13 major components of cost were subdivided into 33 cost categories. Each of the costs is expressed as a function of one or more of six design parameters: rotor diameter, power density, tip speed, speed ratio, ground clearance, and rotor solidity. (Solidity is defined as the area of the blades divided by the area swept by the rotor, or, the percentage of the swept area that is filled by the blades). Some of these categories are also used to define components of the weight of the wind turbine generator system.

The relationships were originally developed for rotor diameters between 150 and 550 ft. Equipment designed for this range of sizes was analyzed for

continuous trends that expressed the cost and weight as a function of the design parameters. The trend relationships provided information necessary for sizing optimization. After the initial size optimization, updated costs and weights were calculated for point designs with 300, 350, 400, and 500-ft. rotor diameters. These values were used to validate the previous relationships. The cost and weight relationships were then adjusted to reflect the more accurate values from the point design calculations. This section uses the values as of June, 1981, in 1980 dollars.

4.2.1 WEIGHT AND COST ESTIMATING RELATIONSHIP SIZING PARAMETERS

The rotor diameter is the most significant sizing parameter. Other variables, such as area, are expressed in terms of the rotor diameter to minimize the number of parameters.

The power density is defined as the maximum power generated per square foot of the area swept by the rotor. The power density varied between 25 and 60 W/sq. ft. The rated power is calculated from this variable.

The tip speed varied between 250 and 450 ft. per second. This parameter, with the diameter, was used to define the high rotor speed. A variable defining the ratio of the two rotor speeds identified the lower rotor speed. This ratio varied from 1.0 (for a single speed rotor) to 2.0 (for a high speed equal to twice the low speed).

The ground clearance is the distance from the local ground grade line to the bottom of the rotor with the blades oriented vertically. A range of 25 to 150 ft. was considered for ground clearance. The tower height is calculated from the ground clearance and the rotor diameter.

The rotor solidity had a range of 2.5 to 4.0%. Solidity, tip speed and rotor diameter affect the rotor performance. High solidity creates high drag and consequently favors low speeds, but the blades are structurally efficient. Higher speeds permit low torque ratings, but require slender, less structurally efficient blades.

The rotor torque and cluster size are also important in optimizing the size of the system. The rotor torque is calculated from power and rotor speed. The

cluster size was set at a rated power of 150 MW, which permits a dual grid connection at 69 kV with intra-cluster connections at the same level. The number of units varies with unit power rating and size.

4.2.2 SITE ITEMS

The site-related items fell into three categories: foundation, ground equipment, and special items.

The foundation design was influenced by the overturning moment caused by extreme winds and by limit thrust. For rotor diameters between 150 and 550 ft., with a spread concrete foundation and approximately triple reinforcing bar content, the cost varied as shown in Table 4-1, line 110. Weight was not related to the foundation cost, since concrete would be supplied locally. The data required two equations, with a shift at a rotor diameter of 405 ft.

The ground equipment consists of the step-up transformer and its protection, circuit breakers, relays, auxiliary transformers, and an enclosure. The cost and weight equations are shown in Table 4-1, line 120. The cost of special items, such as soils survey, finish grading, and fencing, was defined as a fixed cost that is not related to weight. The equation is shown on line 130 of Table 4-1.

Table 4-1 MOD-5A Weight and Cost Estimating Relationship (WCERS)

LINE NUMBER	VOLUME PRODUCTION ITEM	(LB.) WEIGHT RELATIONSHIP (As Of June 1981)	(1980\$) COST RELATIONSHIP (As Of June 1981)
110	Foundation	None	If $D < 405$ Ft: $C_{110} = (118.2)D^{1.244}$ If $D \geq 405$ Ft: $C_{110} = (25.26)D^{1.501}$
120	Ground Equipment	$W_{120} = (10)P_R$	$C_{120} = 121,000 + (7.3)P_R$
130	Special	None	$C_{130} = 53,440$
310	Installation	None	$C_{310} = 36,000 + (54.8)D^{1.4} - 400D$
350	Integration and C/O	None	$C_{350} = 15,500 + (0.018)D^{2.5}$
410	Blades (Wood)	$W_{410} = (6.4726 \times 10^{-10})D^{3.1}(V_T)^{2.45}$	If $D < 400$ Ft: $C_{410} = (4.2576 \times 10^{-7})D^{2.7}(V_T)^{1.8}$ If $D \geq 400$ Ft: $C_{410} = (3.614 \times 10^{-10})D^{3.6}(V_T)^{2.1}$
420	PSC Hydraulics	$W_{420} = (0.0384)D^2 + 3,000$	$C_{420} = 13,100 + (22)D$
421	PSC Structure	$W_{421} = (5.844 \times 10^{-7})D^{4.138}$	$C_{421} = (5.468 \times 10^{-6})D^{3.839}$
430	Yoke, Shaft	$W_{430} = (57,606)(D/400)^{2.17} e^{[(2.3 \times 10^{-6})(W_{410} - 135,000)]}$	$C_{430} = 1.66 W_{430}$
520	Gearbox	$W_{520} = (38,775)Q_R(0.043) + (RWT)(0.124)$ Where Q_R = Rotor Torque (Ft-lb), Derived from P_R , V_T and 90% Efficiency $RWT = W_{410} + W_{420} + W_{421} + W_{430}$	$C_{520} = A Q_R^{0.627} + (33.7)(RWT)^{0.647}$ If $Q_R < (2.75 \times 10^6)$, $A = 36.03$ If $(2.75 \times 10^6) \leq Q_R < (3.85 \times 10^6)$, $A = 41.63$ If $Q_R \geq (3.85 \times 10^6)$, $A = 48.09$
530	Highspeed Shaft	$W_{530} = 500 + 0.65P_R$	$C_{530} = 5,000 + (3.033)P_R$

D = DIAMETER (FT); P_R = RATING (KW); V_T = TIP SPEED (FPS); GCL = GROUND CLEARANCE (FT)

C_{110} = COST ATTRIBUTED TO ITEM IN LINE 110

Table 4-1 MOD-5A Weight and Cost Estimating Relationship (WCERS)
(Continued)

LINE NUMBER	VOLUME PRODUCTION ITEM	(LB.) WEIGHT RELATIONSHIP (As Of June 1981)	(1980\$) COST RELATIONSHIP (As Of June 1981)
540	Generator	$W_{540} = 5.6P_R$	$C_{540} = (417.4)P_R^{0.64}$ If $P_R > 4500$: $C_{540} = (521.76)P_R^{0.64}$
610	Bedplate	If $D < 411$ Ft: $W_{610} = (4.417)D^{1.563}$ If $D \geq 411$ Ft: $W_{610} = (7.035 \times 10^{-4})D^{3.016}$	$C_{610} = 0.70W_{610}$
620	Hydraulic System	$W_{620} = 7,100 + 0.946D^{1.4}$	$C_{620} = 14,000 + 12.75D$
646	Fairing and Miscellaneous	If $D < 407$ Ft: $W_{646} = (0.1014)D^{2.021}$ If $D \geq 407$ Ft: $W_{646} = (170.2)D^{0.7852}$	If $D < 403.5$ Ft: $C_{646} = (0.01094)D^{2.618}$ If $D \geq 403.5$ Ft: $C_{646} = (82.96)D^{1.129}$
660	Sliprings, Electrical	$W_{660} = 1,500$	$C_{660} = 20,600$
670	Controls and Instrumentation	$W_{670} = 2,000$	$C_{670} = 45,300$
680	Yaw Subsystem	$W_{680} = (0.6886)D^{1.795}$	If $D < 395$ Ft: $C_{680} = (0.02312)D^{2.467}$ If $D \geq 395$ Ft: $C_{680} = (2.345 \times 10^{-8})D^{4.775}$
710	Tower	If $D < 398$ Ft: $W_{710} = (0.2309)D^{2.433}$ + $e[(9.166 \times 10^{-3})(GCL-50)]$ If $D \geq 398$ Ft: $W_{710} = (6.872 \times 10^3)D^{3.020}$ + $e[(9.166 \times 10^{-3})(GCL-50)]$	$C_{710} = 0.99 W_{710}$ (Includes Erection)
720	Lift	$W_{720} = 1,000$	$C_{720} = 20,000$
740	Cabling	$W_{740} = 20(D+GCL)$	$C_{740} = 45(D+GCL)$

D = DIAMETER (FT); P_R = RATING (KW); V_T = TIP SPEED (FPS); GCL = GROUND CLEARANCE (FT)

Table 4-1 MOD-5A Weight and Cost Estimating Relationships (WCERS)
(Continued)

LINE NUMBER	VOLUME PRODUCTION ITEM	(LB.) WEIGHT RELATIONSHIP (As Of June 1981)	(1980\$) COST RELATIONSHIP (As Of June 1981)
810	Modem	None	$C_{810} = 500$
820	Remote Display	None	$C_{820} = 2,000$
930	Spares	None	$C_{930} = 24,000 + 100$
1000	Profit	None	$C_{1010} = (0.010)(\text{Total of other Costs})$
1020	Assembly and Test	None	$C_{1020} = 4939D^{0.5}$
1030	Contingency	None	$C_{1030} = 0$
1110	WTG Land	None	$C_{1110} = (0.01722)(1.8)D^2$
1140	Road Land	None	$C_{1140} = (0.01722)(140)D$
1240	Substation	None	$C_{1240} = 6.68P_R$
1250	Transportation and Road	None	$C_{1250} = (492.6)(P_R/D^{0.4873})$
240	Transportation	None	$C_{240} = (0.09)(\text{Total Weight})$
1340	Yearly Operation and Maintenance	None	$C_{1340} = 4,500 + 1.78P_R + 100$

D = DIAMETER (FT); P_R = RATING (KW); V_T = TIP SPEED (FPS); GCL = GROUND CLEARANCE (FT)

4.2.3 SITE ERECTION ITEMS

The installation, integration and checkout cost items are in this category.

Installation is defined as any on-site erection, excluding the construction of the foundation and tower. It includes lifting the nacelle and rotor assemblies, attaching them to the tower, and renting lifting equipment. The cost is shown on line 310 of Table 4-1.

The integration and checkout costs are shown on line 350 of Table 4-1. They include system and subsystem checks from the initial stages of installation, until the system is approved with customer acceptance.

4.2.4 ROTOR ITEMS

The rotor cost and weight items include the blade, the partial span control (PSC) hydraulic subsystem, PSC structural elements, and the structure between the center blade and the rotor integrated gearbox.

The blade cost and weight varied with rotor diameter, and to a lesser extent, with tip speed and solidity. The relationships were derived from almost eighty wood blade designs encompassing the ranges of size, tip speed and solidity. The cost of the larger systems was more sensitive to size and tip speed, so the cost relationship is expressed in two equations. The cost and weight relationships are shown on line 410 of Table 4-1. Relationships for wood, steel and glass fiber were developed, but only the equations for the wood construction are shown.

Structural considerations such as frequency placement, buckling, limit load and fatigue stresses were included in the mini-design algorithms that were used to develop weight equations for the rotor, nacelle and tower systems.

The PSC hydraulics rotate with the blade, thereby avoiding the need for rotating fluid couplings. The weight and cost of a reservoir, a pump, accumulators, valves, and related piping are included on line 420 of Table 4-1.

The cost and weight of the structural joint between the PSC and the blade, the rotating shaft and bearings, actuator, and control valving are shown on line 421 of Table 4-1.

The yoke and shaft section includes the attachment to the main blades, the teeter bearings and restraint, and the low speed shaft up to the joint where the rotor is attached to the drivetrain. The weight for these items depends on the blade weight, as shown on line 430 of Table 4-1. The cost of this yoke and shaft varies directly with the weight.

4.2.5 DRIVETRAIN

The drivetrain items are the gearbox, high speed shaft, and the generator and accessories.

The transmission, or gearbox, consists of step-up gearing, stiffness and damping control equipment, a speed changer, the rotor support bearing, and a structural case. The rotor weight and torque were important variables in the cost and weight equations, as shown in line 520 of Table 4-1. There were discrete changes in the cost equation at torque levels which required partial disassembly for shipping or field gearing assembly. Figure 4-2 is a plot of cost vs. torque, indicating both the original data and the data validated by the point designs.

The high speed shaft includes one-way and torque limiting couplings and a floating shaft. The cost and weight equations are shown on line 530 of Table 4-1.

The generator category includes the synchronous generator, exciter, instrument transformers and surge protection equipment. The cost and weight equations are shown on line 540 of Table 4-1. The cost depended on the power rating and required two equations, with a split at a power rating of 4500 kW.

4.2.6 NACELLE ITEMS

The nacelle category includes the bedplate structure, the yaw hydraulic and gearbox lubrication systems, the fairing structure and miscellaneous items, sliprings at the rotor and yaw interfaces, electrical wiring, the control system and instrumentation, and the yaw structural and drive items.

The bedplate cost and weight, shown on line 610 of Table 4-1, are sensitive to the rotor weight moment. The relationship required two equations, with a break at a rotor diameter of 411 ft. This break results from having to break down the bedplate structure for shipping and handling.

The weight and cost of the lubrication system are shown on line 620 of Table 4-1.

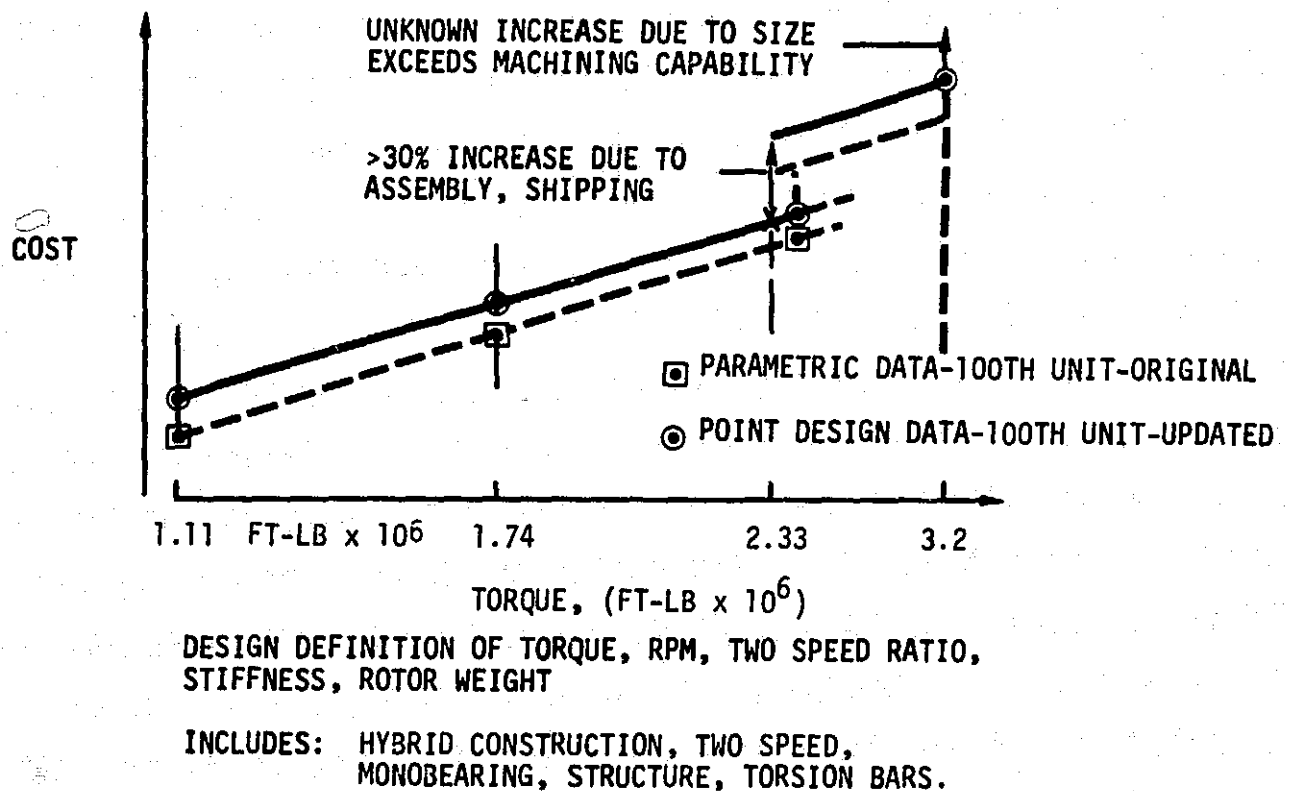


Figure 4-2 WCER Development Example - Gearbox

The cost and weight equations for the fairing and miscellaneous items are shown on line 646 of Table 4-1. The slipring cost and weight do not vary with any of the design parameters, as shown on line 660. The controller and instrumentation cost and weight are also constants as shown on line 670.

The yaw subsystem consists of the bearing, the structure on both sides, and the hydraulic push-pull yaw drive. The design of the structure was influenced most by the rotor weight moment. The yaw drive design was a function of rotor tilt angle, which produces a yaw torque, and rotor size. As shown on line 680 of Table 4-1, the relationships for cost and weight were related to the rotor diameter. The weight data fit a single equation, but the cost data required two equations, with the break at a rotor diameter of 395 ft.

4.2.7 TOWER ITEMS

The shell structure from the yaw bearing area to the foundation, the elevator, and the cabling from the yaw slipring to the electrical equipment on the ground are the cost and weight items included in the tower category.

The design factors for the tower were stiffness, fatigue, and extreme wind loads. Wind loads vary with blade area and the moment varies with the tower height. The weight varied with the ground clearance and rotor diameter, in two equations that split at a rotor diameter of 398 ft. The cost equation depended on weight, and included the cost of tower erection. The tower weight and cost equations are shown on line 710 of Table 4-1. The elevator weight and cost are constants, as shown on line 720, because the design does not depend on the tower height.

The cost of cabling depends on the height of the tower, as shown on line 740 of Table 4-1.

4.2.8 CONTROL ITEMS

The cost for the main controller and instrumentation are covered in line 670 of Table 4-1. The remote display and control lines for the remote site communications modulator-demodulator and terminal are addressed individually in lines 810 and 820. The costs are fixed and this equipment does not affect the weight of the system.

4.2.9 SPARES

Spares are defined as the allocation of spare parts per wind turbine generator in a cluster. Spare parts will be stocked at the cluster level. The spare parts will not affect the weight of the system. The cost of the parts varies with the rotor diameter plus a constant term. Line 930 in Table 4-1 defines the equation.

4.2.10 SPECIAL ITEMS

Profit is defined as 10% of all cost items, as shown on line 1010 of Table 4-1. Factory assembly and test costs that were not included in the cost of the hardware appear on line 1020. This cost varies with system size. A contingency cost is also included in the special items category. It is a measure of uncertainty in the weight and cost estimating relationships. This cost, shown on line 1030, was reduced as data was validated by the point design definitions.

4.2.11 LAND COSTS

The land costs were defined for a site with an area of 1.2 times the rotor diameter by 1.5 times the rotor diameter. A land buffer between machines was not used. At the rate of \$750 per acre, the cost is shown on line 1110 of Table 4-1.

Within a cluster, costs for the roadway and transmission line right-of-way were calculated for a fixed cluster power rating. The allocation to each unit depends on diameter, as shown on line 1140.

4.2.12 CLUSTER COSTS

Cluster-related costs reflect the cost of transmission line construction, at the rate of roughly \$90,000 per mile for 69 kV and the cost per unit of the grid connection substations. Roadbed improvement is included in the transmission line cost. The per unit cost data was developed from a 150 MW farm with each unit placed at intervals of 10 times the rotor diameter to permit wind recovery between units.

The substation cost depends on the power rating, as shown in line 1240 of Table 4-1. The cost per unit of the transmission line and road improvement

varied with the rotor diameter and the product of the rotor diameter and power, as shown on line 1250 of Table 4-1.

4.2.13 OPERATION AND MAINTENANCE (O&M)

Operating and maintenance costs are based on a two-shift maintenance crew for the 150 MW cluster and expendable supplies. Maintainability data confirmed that the costs for unscheduled failures, repair times, and scheduled maintenance were within the crew costs. As shown on line 1340 of Table 4-1, the costs per unit depend on the rotor diameter and the power rating.

4.2.14 TRANSPORTATION

Transportation costs, shown on line 240 of Table 4-1, are related to the sum of the weights of the system components. Increased costs for large loads that are difficult to ship were included originally, but were eliminated since they were found to be unnecessary. The shipping cost is based on a 2000 mile trip from the factory to the site.

4.2.15 PERFORMANCE

The system performance was computed from an envelope power coefficient curve that varies with solidity. Wind duration characteristics were converted from the reference height of the anemometer to hub height. The wind speed at the hub height was used over the full rotor diameter, with appropriate corrections for tilt, teeter, elastic deflection and yaw error.

Drivetrain and electrical system losses were included in the calculation of grid power. Gearbox and rotor bearing losses were based on fixed and variable losses:

$$\text{(Gearbox)} \quad P_{\text{out}} = P_{\text{in}} - (0.015) (P_R + [P_{\text{in}}/P_R])$$

Electrical losses were treated similarly:

$$\text{(Electrical)} \quad P_{\text{out}} = P_{\text{in}} - (A) (P_R + [P_{\text{in}}/P_R]^{1.8}) - (0.015)(P_{\text{in}}/P_R)^{1.8}$$

where P_R = Rated output power

P_{out} = Power out of item

P_{in} = Power input to item

and A varies with P_R ; it is approximately equal to 0.014

The exponent of 1.8 in the equation for electrical losses matches vendor data. This term is well known for losses that include resistive losses (proportional to I^2R), hysteresis, and eddy current losses. The last term reflects transmission losses between the generator and the grid tie.

Energy was calculated from the area under the output power versus wind speed curve, for wind speeds between the cut-in speed (14 mph) and the cut-out speed (45-60 mph) The design wind duration Weibull curve is defined by:

$$P(V \geq V_1) = e^{[-(V_1/C)^K]}$$

where V, V_1 are in meters/sec at 32.8 ft.
 $C = 7.17$ meters/sec
 $K = 2.29$

The design variable wind shear characteristic used to extrapolate the design wind to hub elevation Z is:

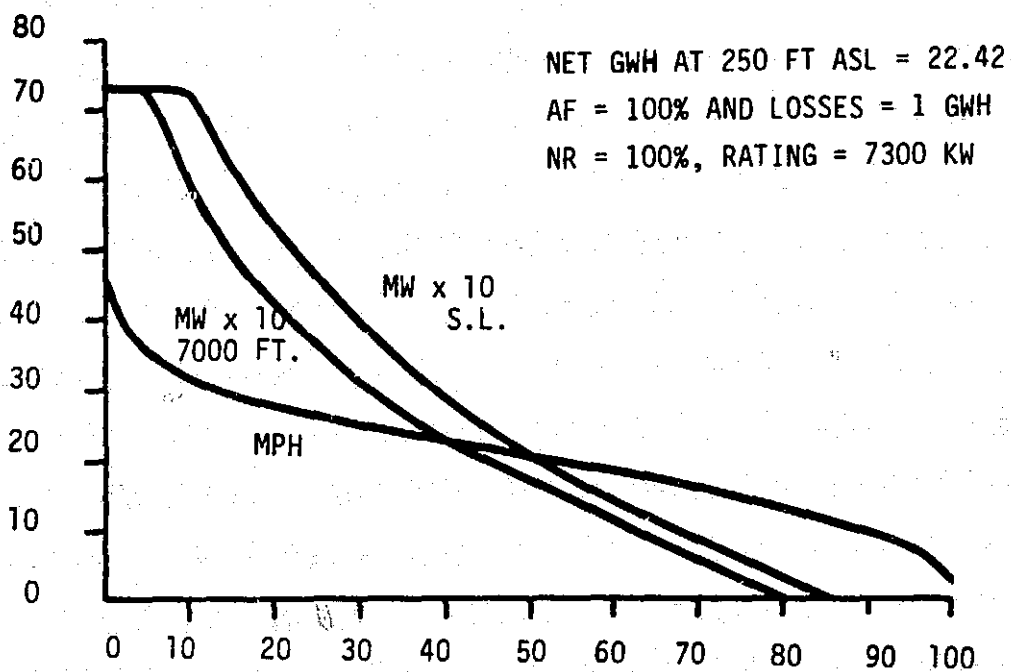
$$\begin{aligned} V_Z/V_R &= (Z/Z_R)^\alpha \\ \alpha &= \alpha_0 [1 - \log(V_R)/\log(V_H)] \end{aligned}$$

where V_Z = Wind speed at elevation Z (m/s)
 V_R = Wind speed at elevation Z_R (m/s)
 Z, Z_R = Elevations in consistent units
 α_0 = 0.35, zero speed shear exponent
 V_h = 67 m/s, homogeneous wind speed

Cumulative annual distributions of the hub height design wind speed and typical net output power are shown in Figure 4-3.

The calculated energy was reduced by start-up, shutdown, speed shift, and auxiliary power energy values, then multiplied by an availability factor to obtain average annual net energy.

CUMULATIVE MOD - 5A (304.2) WIND-POWER & ENERGY
HUB
V(MPH) & MW*10 AT ZH FT



CUMULATIVE PROBABILITY, PERCENTILE

Figure 4-3 Output Power and Wind Speed Cumulative Distribution

4.3 SUBSYSTEM TRADE-OFF STUDIES

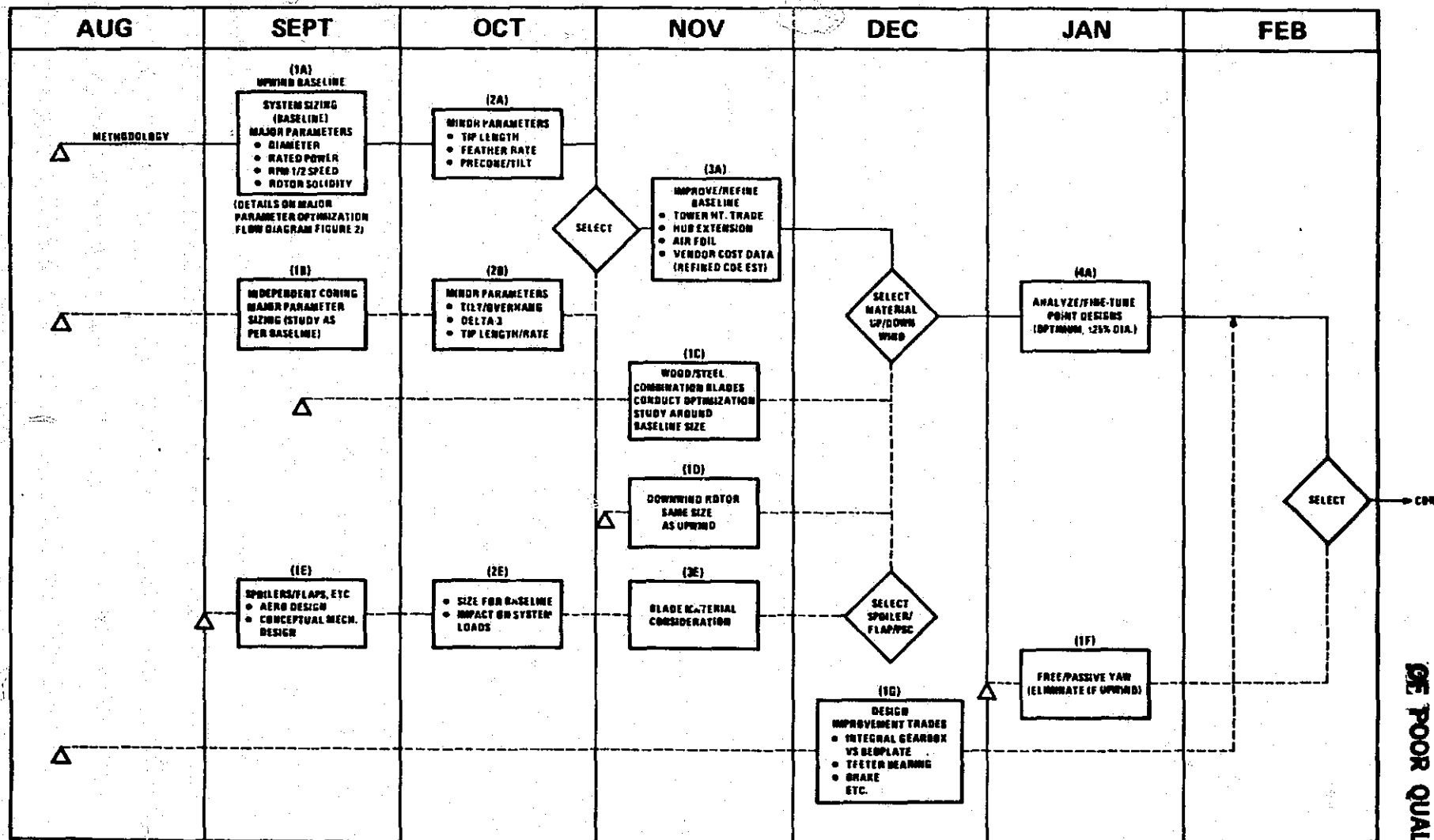
4.3.1 INTRODUCTION

Eight major trade-off studies were conducted during the conceptual design phase. These studies are summarized in Table 4-2. The results of four of these studies, torque control, system speed, gearbox configuration, and rotor stopping technique, were changed in the preliminary and final design phases after studies that reassessed the technical risks. The reasons for change are noted in this section, and are discussed in detail in section 5. The trade-off studies were performed both in parallel and in series with the size optimization study, so that the best results were included in the design.

The criteria for evaluating each trade-off are shown in Table 4-3, the summary score sheet. Each criterion received a qualitative or quantitative score. The cost of energy was the major deciding factor, but the other measures, including qualitative (best, 2nd best, etc.) factors, were necessary for an adequate evaluation. Technical criteria and measures of performance were tabulated for each trade-off study. For example, cost, reliability, complexity, and the risks that factory or field assembly would involve, were carefully examined in the blade material study. In a trade-off study, a possible design was evaluated against either the baseline configuration or a model that developed from the baseline configuration.

The costs for the trade-off items were calculated for the 100th unit in a 1000 unit production run, produced commercially according to a manufacturing plan. Special facilities, spares, or maintenance costs were also included, if they were appropriate. This plan was designed to meet wind power goals in a competitive market, with volume production. The flow chart and schedule by which the trade-off studies and size optimization were performed is shown in Figure 4-4.

The baseline system optimization and the evolution of the design is described by the solid-line path. The dashed lines indicate several alternatives. The following are brief descriptions of the various steps labeled on Figure 4-4.



ORIGINAL PAGE IS
OF POOR QUALITY

Figure 4-4 System Configuration Selection Logic Flow

**Table 4-2. Major Trade Studies and Selection at
the Conceptual Design Review**

Study	Alternate Considered	Selection	Attributes
1. Blade Material	<ul style="list-style-type: none"> • Fiberglass (Epoxy & Polyester) • Steel • Wood Epoxy 	<ul style="list-style-type: none"> • Wood Epoxy 	<ul style="list-style-type: none"> • Lightest Weight • Lowest Cost
2. Blade Articulation	<ul style="list-style-type: none"> • Independent Coned Blades • Teetered Rotor 	<ul style="list-style-type: none"> • Teetered Rotor 	<ul style="list-style-type: none"> • Allows Upwind • Least Tech Risk • Lowest Cost
3. Wind Orientation	<ul style="list-style-type: none"> • Upwind • Downwind 	<ul style="list-style-type: none"> • Upwind 	<ul style="list-style-type: none"> • Lowest Cost • Lowest Sound
4. Torque Control	<ul style="list-style-type: none"> • Flaps • Partial Span Control 	<ul style="list-style-type: none"> • Partial Span Control 	<ul style="list-style-type: none"> • Lowest Cost • Most Reliable Startup
5. Tower Height	<ul style="list-style-type: none"> • Ground Clearance 25' to 125' 	<ul style="list-style-type: none"> • 50' Ground Clearance 	<ul style="list-style-type: none"> • Cost Insensitive 25' to 75' • Can move in either direction to accommodate other drivers
6. System RPM	<ul style="list-style-type: none"> • One Speed • Two Speed Mechanism (Up to 2:1) • Two Speed Electric (Up to 2:1) 	<ul style="list-style-type: none"> • Two Speed Mechanism 1.3:1 Speed Ratio 	<ul style="list-style-type: none"> • Greater Energy Capture • Lower Coe • System Flexibility
7. Gearbox/Nacelle Configuration	<ul style="list-style-type: none"> • Separate Gearbox • Integral Gearbox • Rotor Integrated Gearbox 	<ul style="list-style-type: none"> • Rotor Integrated Gearbox 	<ul style="list-style-type: none"> • Most Efficient System • Lowest Weight • Lowest Coe
8. Rotor Stopping Technique	<ul style="list-style-type: none"> • Partial Span Control Stopping • Stopping Brake 	<ul style="list-style-type: none"> • Partial Span Control 	<ul style="list-style-type: none"> • Significant Stopping Torque Margin • No New Hardware for This Feature • Lowest Coe

Table 4-3. Trade-Off Summary Score Sheet (Format)

Item	Units	Baseline	Trade A	Trade B	Remarks
Design Complexity	(Qual)				
Manufacturing Complexity	(Qual)				
Transportation	(\$)				
Erection	(\$)				
Reliability	(Qual, #)				
Maintainability, O&M	(Qual, \$)				
Availability	(%)				
Environmental Impact Sound, TVI	(DB-SPL)				
Safety	(Qual)				
Technical Risk	(Qual)				
<u>Trade Specific Items</u>					
Weight	(K lb)				
Installed Cost	(K\$)				
Annual Energy Capture	(GWH)				
Maximum Efficiency	(%)				
Plant Factor	(%)				
Cost of Energy	(\$/Kwh)				

Recommendation _____

- (1A) This step represents the size optimization of the upwind baseline system. The objective of this task was to determine the combination of diameter, rated power, rotor speed, rotor speed ratio and solidity that resulted in the lowest cost of energy. The baseline was updated accordingly. This study contained an evaluation of both one- and two-speed rotor operation.
- (2A) Variations in blade tip length, feather rate, and rotor precone and tilt were analyzed to further refine and lower the cost of the baseline system.
- (1B) & (2B) These steps comprise the independent coning trade-off study, which was conducted in parallel with the baseline optimization (1A and 2A). Parameter variation studies were performed similarly to the baseline study, but over a smaller range. The appropriate weight and cost estimating relationships for the blade and hub, and the energy capture algorithms, were used to reflect the differences in design. A choice between the best independently-coned rotor and the current baseline was made. That choice became the new baseline.
- (3A) This step included trade-off studies and refined the baseline. During this time, improved cost estimates became available from the vendors and system sizing parameters were re-evaluated. Studies on tower height, hub extension and airfoil type were performed. The tower height study assessed the increase in cost versus the increased energy capture for a higher tower. The hub extension study assessed the costs of making an extra foot or more of hub instead of a foot of blade. Shipping considerations were a factor in the hub extension study, so it was deferred until an optimum rotor diameter had been established. The output of this step was the best upwind, composite blade configuration.
- (1C) The wood, steel and TFT glass fiber composite blade designs were deferred until this step in order to allow the blade subcontractors to develop better cost estimating procedures. The wood and steel materials were analyzed for a smaller range of sizes than the glass fiber composite, since initial cost data for the materials allowed the selection of the appropriate material arrangement at a size near the optimum rotor diameter, which was found in step 1A.
- (1D) This step analyzed a downwind system of the same size as the optimum upwind system. Previous studies by GE and by Boeing indicated that there was not much difference in the cost of upwind and downwind configurations. However, if independent coning had been selected for the baseline configuration, the downwind rotor would have had a lower cost of energy, because the blade would deflect away from the tower. However, rotor noise might have been a problem.
- (1E, 2E & 3E) Blade torque control studies began early. Costs for the final torque control designs were compared to the design for partial span control. Only the optimum system was designed. The final decision was deferred, to coincide with the blade material selection, since the choice of blade material might affect the choice of a torque control system.

- (4A) The selections made in this step were used to define the point designs for the final costing. The point designs of the optimum system and systems +25% in rotor diameter were analyzed. The resulting costs were compared with earlier estimates used in the parametric sizing studies and configuration trade-offs. The relationships used in these studies were updated to incorporate the new data.
- (1F) A free, or passive, yaw system was to be considered only if the final design was a downwind system.
- (1G) Design improvement trade-off studies were conducted throughout the conceptual design phase. Periodically, the results of these studies were incorporated into the baseline design..

Model 104.5 was the outcome of the conceptual design studies. This configuration and the trade-off and size studies were reviewed extensively by GE and NASA before proceeding to the preliminary design phase. Descriptions of the eight major trade-off studies in Table 4-2 follow.

4.3.2 BLADE MATERIAL STUDY

An extensive trade-off study evaluated blades made of TFT reinforced glass fiber, steel and laminated wood and epoxy, based on the cost of the 100th unit. The results of this study indicated that laminated wood and epoxy was the most effective material for a rotor with a large diameter. TFT glass fiber was a close second, and steel was a distant third. Other composite materials, such as filament-wound glass fiber, were not evaluated because the resources were insufficient.

Figure 4-5 is a flow-plan outlining the salient features of the study. The studies established material allowables, developed a parametric data base, performed many size and configuration evaluations at the system level, and evaluated the cost of the material and configuration. All of these tasks were performed with three supporting subcontractors: Chicago Bridge & Iron (CBI) for the steel studies, Structural Composites, Inc. (SCI) for the TFT glass fiber studies, and Gougeon Brothers, Inc. (GBI) for the wood studies. All the subcontractors were maintained on contract throughout the conceptual design phase, to provide design and costing support.

The subcontractors developed parametric cost and weight data, based on early load data. These costs, in terms of dollars-per-pound for chordwise blade sections of different sizes, capable of carrying different loads, determined

the costs of various blade configurations, using a GE computer program, called SECTION. The program determined the weight and cost of a blade using parametric data, including configuration, loads, material and properties, and power rating. Many configurations were evaluated by SECTION, to determine the optimum cost and weight characteristics for each material.

The blade configuration contained joints associated with partial span control, and a root joint and a field joint required by shipping considerations. The subcontractors provided cost and weight data for these joints. Parametric cost and weight data for the joints were integrated into the program.

The results of the parametric study is summarized in Figures 4-6. The curve of cost and weight versus size is clearly exponential. The figure shows that the wood blade weighs the least and is the least costly. The preliminary evaluation of aerodynamics indicated that the NACA series 64XXX airfoil operating in a flow regime between laminar and turbulent, allows the thickness-to-chord ratio to increase 30% to 50% without any noticeable deterioration in performance. This airfoil series, as shown in Figure 4-7, is concave near the trailing edge, so it would not be suitable for welded steel or glass fiber winding without a costly development program. The use of female molds in building the wood blade allows the 64XXX airfoil to be used without increased manufacturing costs.

When the trade-off study was completed, laminated wood and epoxy was selected as the baseline material. However, wood and glass fiber ranked so closely, that conceptual designs were completed for both glass fiber and wood blades. The two subcontractors, SCI and GBI, prepared cost analyses for blades 300, 400, and 500 ft. in diameter, using the geometry and skin thickness defined by GE.

The normalized costs for a unit of each material, produced in volume, is summarized in Table 4-4.

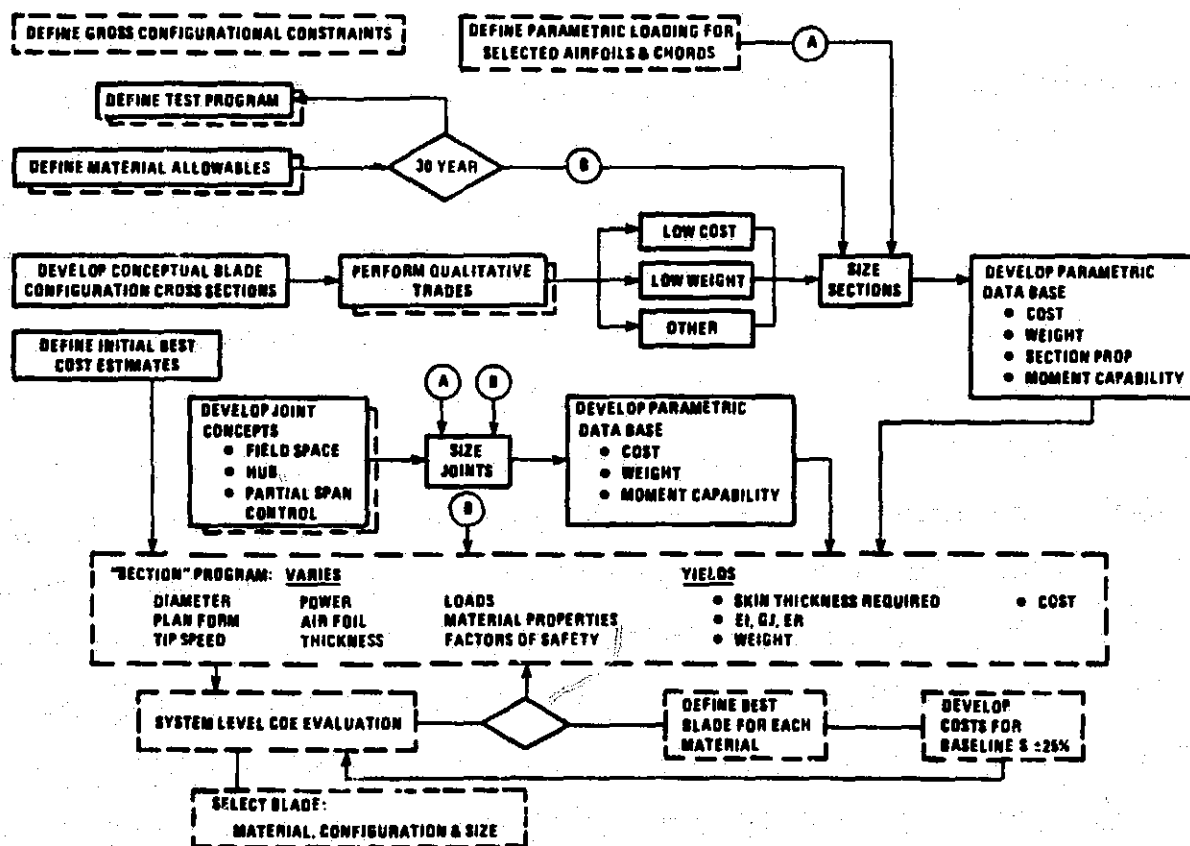


Figure 4-5 Blade Material Trade-Off Study - Flow Diagram

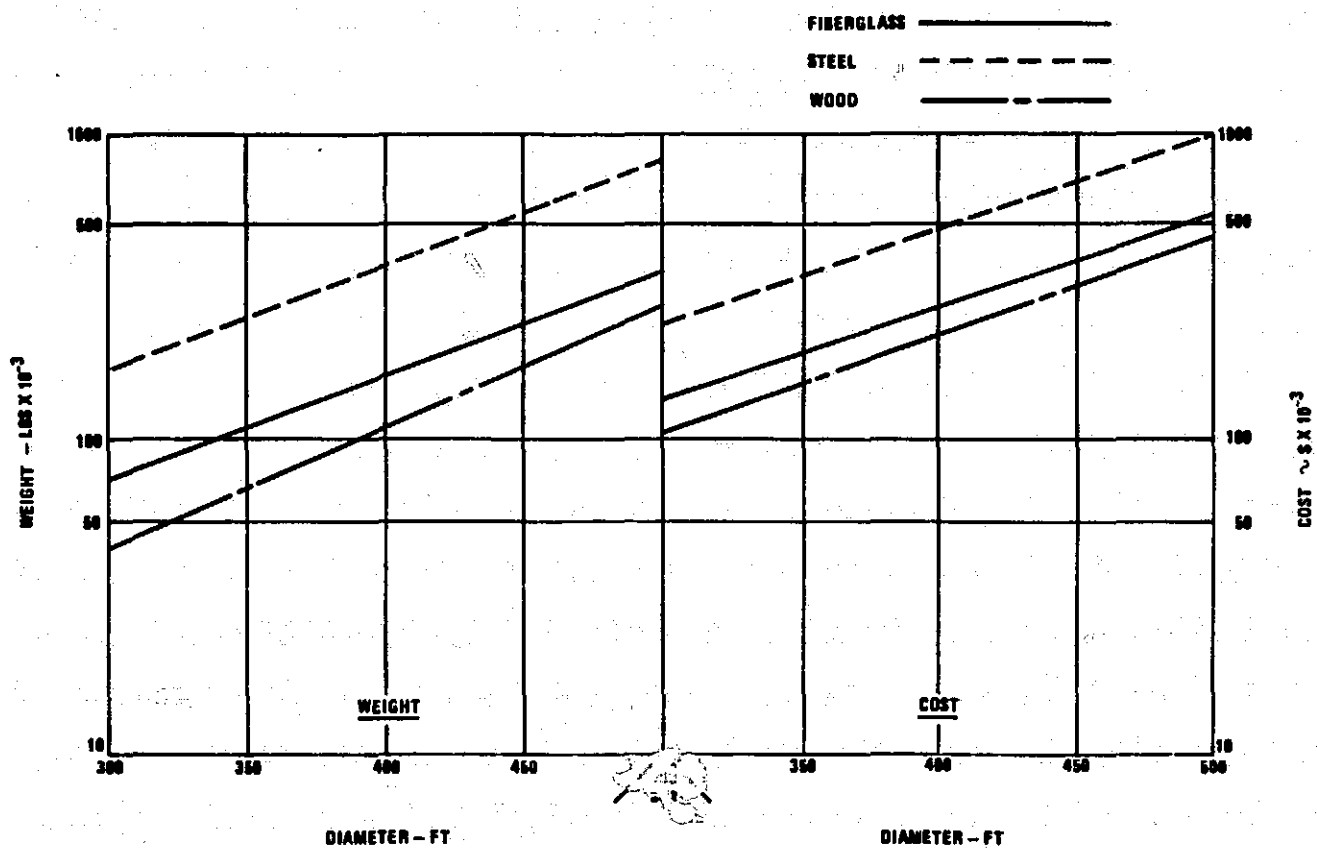


Figure 4-6 Blade Cost and Weight - Parametric Summary

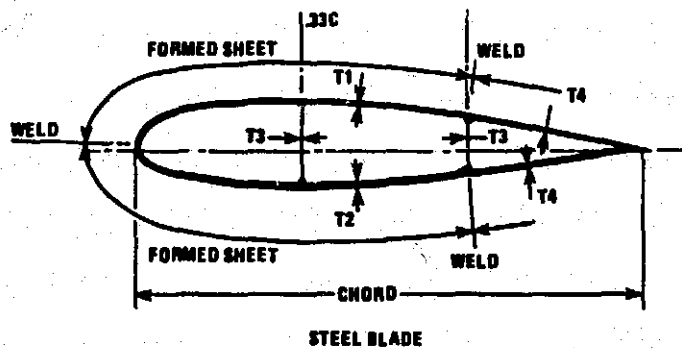
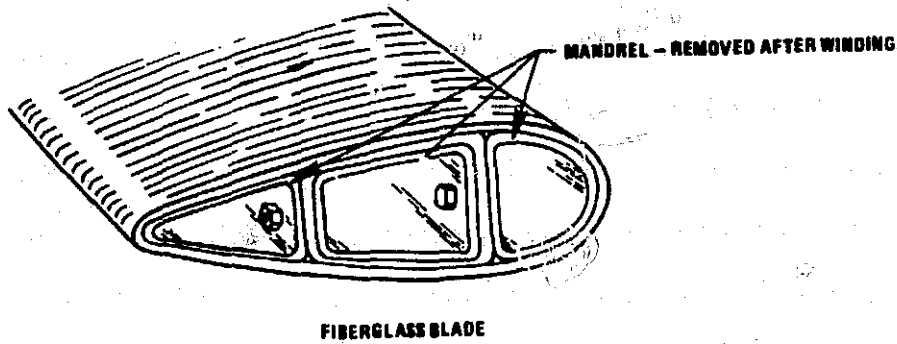
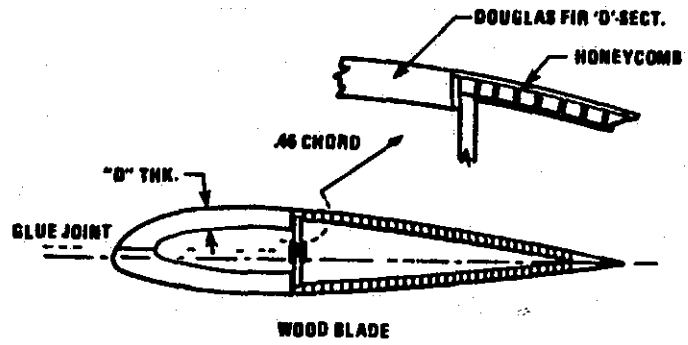


Figure 4-7 Typical Blade Cross-Sections

Table 4-4. Conceptual Design - Cost and Weight of the 100th Unit

Diameter - Ft.	300	350	400	500
Field Joint Req'd.	No	No	Yes	Yes
Cost - K\$				
Fiberglass	135.2	159.4	299.1	636.1
Wood	89.7	138.8	183.7	360.2
Steel	170.6	247.1	363.0	689.6
Weight - K-Lbs.				
Fiberglass	98.9	125.0	244.3	716.9
Wood	51.3	75.6	139.5	318.8
Steel	165.0	261.0	395.0	800.0

- Std. labor rates
- S. E. U. S.
- Construct OH
- Direct lab. support
- Mat'l. burden
- Dir. lab. OH
- Construct G&A
- Depreciation
Plant - S. I. @ 30 yrs.
Equip. - S. L. @ 20 yrs.
- Cost of money
Assume 25% front
Fin 75% @ 12%
- Plant - 30
- Equip - 20
- Profit 6% aft. tax
- Assume 45% state & fed. tax

Notes: 1. Normalized 100th unit costs based on subcontractor quotes.
2. One set i. e. two blades plus joints.

The costs evaluated for the conceptual design supported the selection of wood. The materials were also evaluated at the system level, as shown in Table 4-5. The lower costs of energy and the reduction in risk to the program, based on the performance of the wood blades in MOD-OA, also endorsed the selection of wood. A more detailed description of this study is given in Volume III, section 4.1.

Table 4-5. Blade Material Trade-Off at the System Level

Item	Units	Baseline	A	B	Remarks
Blade Material		Fiberglass	Wood	Steel	
Complexity	Qual	Baseline	Less	Less	Process control
Transportation	K \$	Baseline	23 less	26 more	Weight dependent
Reliability	Qual	Baseline	Same	Same	
Maintainability, O&M	Qual	Baseline	Same	More	Painting
Availability	%	Baseline	Same	Same	.96 goal
Environmental	Qual	Baseline	Same TVI Less sound	Worse TVI Less Sound	Material dependent Speed dependent
Safety	Qual	Baseline	Same	Less	Single steel load path
Risk	Qual	Baseline	Less	Same	MOD-OA history
Diameter	Ft	402	400	400	
Tip speed	Ft/Sec	400	350	325	Wood, Fiberglass Optimized
Weight	K LB	1349	1209	1627 (A)	3/81 WCER 100th unit
Installed cost	K \$ (1980)	3602	3366	4100 (B)	3/81 WCER 100th unit
Annual energy capture	GWH	20.56	19.21	19.80 (C)	Lower wood CP - A
Cost of energy	c/KWH(1980)	3.33	3.32	3.90	Wood has least cost, risk

- A Based on parametric data
 B Based on 3/81 cost data
 C Extrapolated

4.3.3 BLADE ARTICULATION STUDY

The NASA MOD-0 and MOD-1 wind turbines used a rigid rotor. Each blade was firmly attached to a stiff hub. The rigid rotor is not mechanically complex, but each blade must react airloads independently. Large vibratory moments are transferred through the hub to the drivetrain, bedplate and tower. The teetering rotor was recommended by the MOD-1A study to reduce loads. It was adopted in later designs, including Boeing's MOD-2 and Hamilton Standard's WTS-4. The teetered rotor was selected as the baseline configuration for the MOD-5A. During the conceptual design, the rigid hub was not considered. However, a trade-off study was performed for an independently coned configuration, in which each blade has its own flap hinge. Figure 4-8 shows this hub configuration, and the rigid hub and teeter hub configuration.

The potential load relief provided by independent coning was the motivation for investigating this configuration. In the teetered rotor configuration, no flapwise moments are transmitted to the fixed system, and vibratory blade root moments are approximately half those of a rigid rotor. Independent coning provides even more load relief. In the independent cone configuration the blade flap hinges are near the center of rotation. No flapwise moments are transmitted to the fixed system, and both steady and vibratory flapwise moments at the blade root are zero. As shown in Figure 4-8, the blade always seeks an equilibrium flap angle so that the root moment caused by airloading is balanced by the centrifugal restoring moment. The reduction in bending moment on the inboard portions of the blade and hub reduce the structure needed in these areas.

For this study, rotor design loads were calculated for the teetered and independently coned configurations. Comparative weights and costs were derived from these design loads. Simultaneously, the performance and energy capture of both configurations were computed. The energy capture and cost data were combined to furnish the cost of energy of the two configurations. The final decision between the two configurations was based on this information and qualitative factors. The cost of other components of the system were not significantly different, so the costs of energy were based only on the rotor.

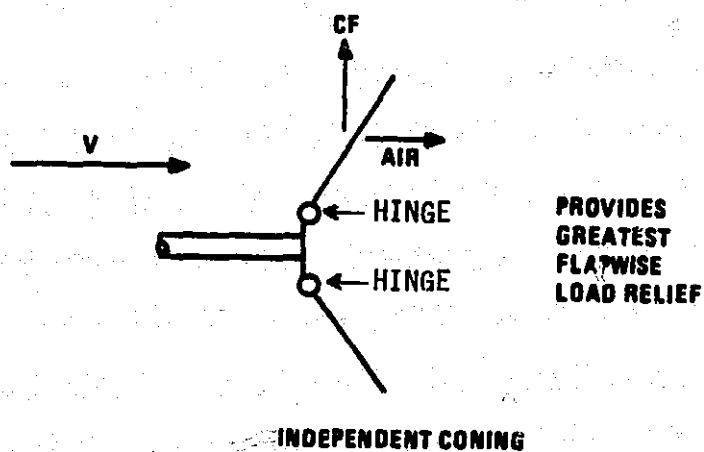
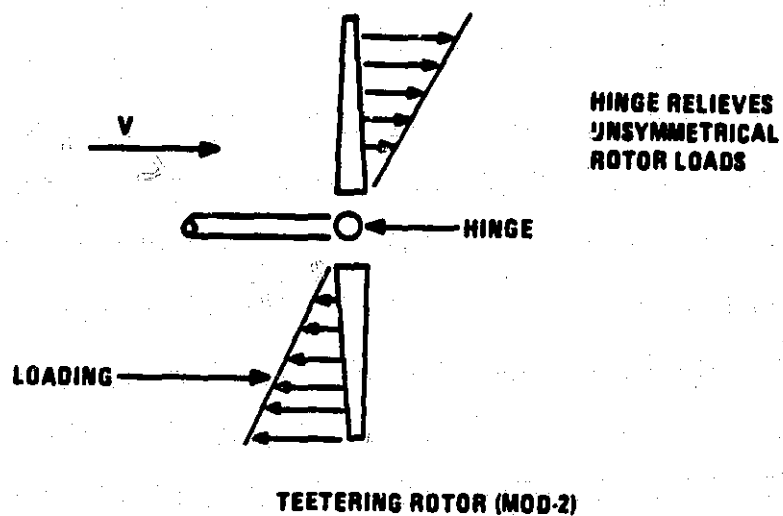
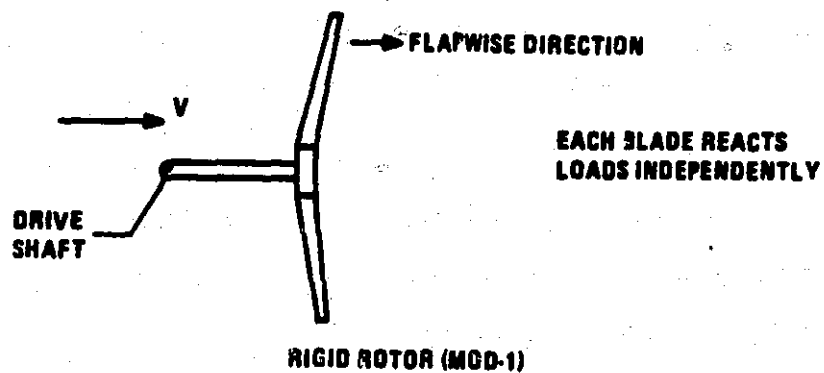


Figure 4-8 Rotor Types

At this time the MOD-5A baseline configuration was an upwind teetered rotor, with 9° of shaft tilt. Independent coning was best implemented by a downwind rotor, because of tower clearance considerations, so the study focused on this configuration. Detailed comparisons were made at a diameter of 350 ft. However, enough conceptual design data was generated to extend the results to other sizes. The results of the study are highlighted below.

The efficiencies of the teetered and independently coned rotors are shown in Figure 4-9. The maximum efficiency was 3.5% less for an independently coned rotor. The percentage of loss becomes less at higher tip speed ratios in lower wind speeds, because the blades do not cone as much in that range of speeds.

The power coefficient versus the velocity ratio, shown in Figure 4-9, determined the energy capture of the teetered and independently coned rotors. The performance of the teetered rotor was adjusted for the 9° tilt, and the performance of the downwind independently coned rotor was adjusted for tower shadow blockage. Each of these deductions amounted to approximately 1%. Although the difference in the maximum power coefficient was 3.5%, the loss in energy capture with the independently coned configuration was only 2%. This was because at low wind speeds, the difference in efficiency is less than 3.5%, and at wind speeds above the rating the efficiency does not matter.

Rotor cost and weight estimates were developed for each configuration on the basis of the design loads. Blade limit loads are shown in Figure 4-10. The difference in chord bending loads was due to lower gravity moments on the lighter, independently coned blades. These chord loads were not design drivers for either configuration. The limit flap bending loads, however, were design factors and independent coning had a significant advantage in this area. Flapwise fatigue loads were also design factors at some blade spanwise locations. Independent coning had a decided advantage, particularly at the inboard blade stations, as shown in Figure 4-11.

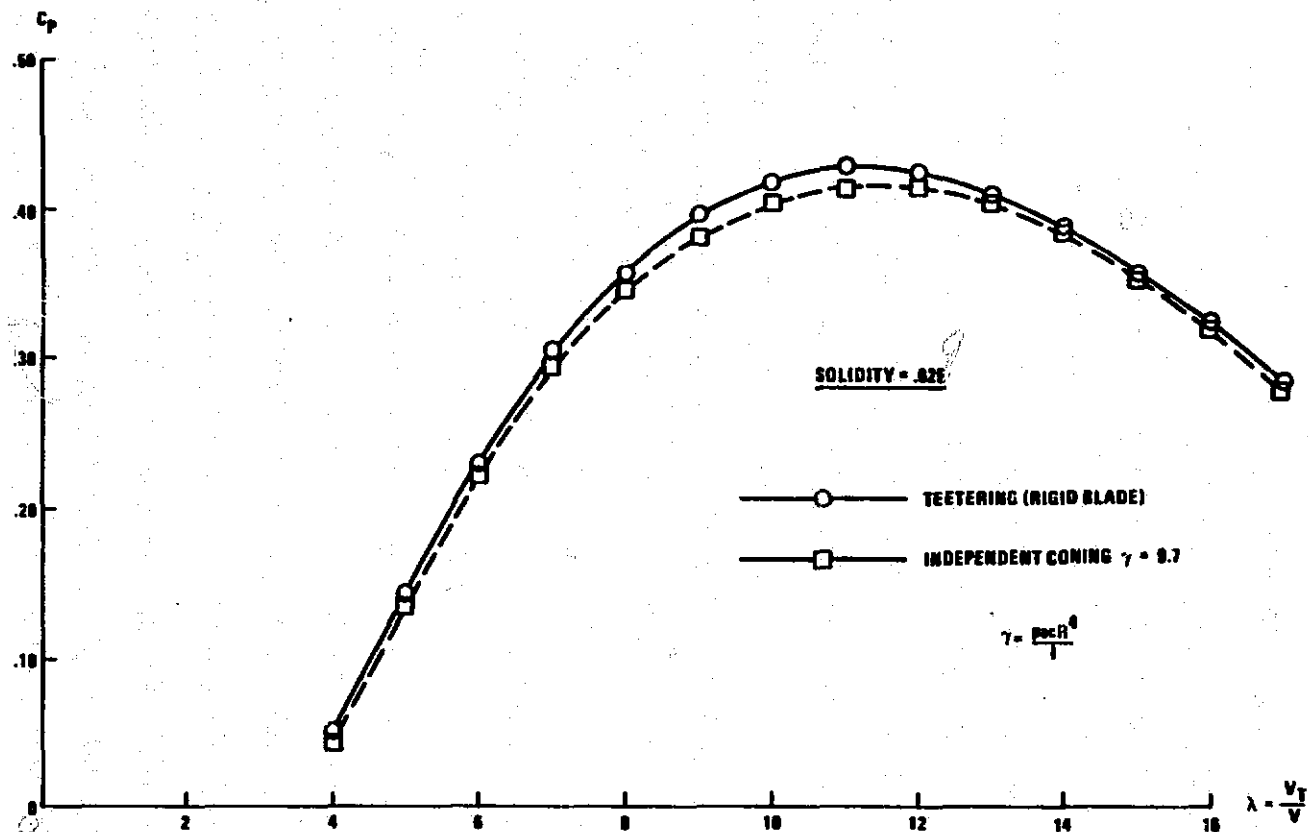


Figure 4-9 Comparison of the Aerodynamic Performance of Teetering and Independently Coned Rotors

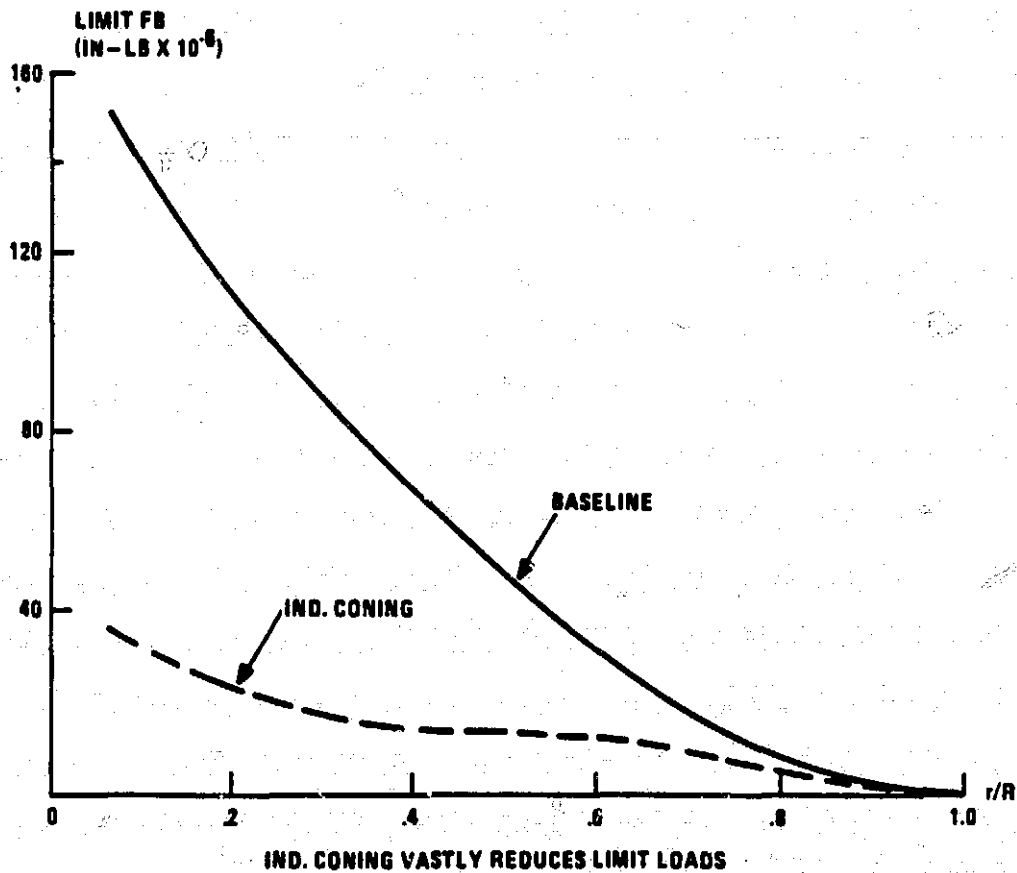
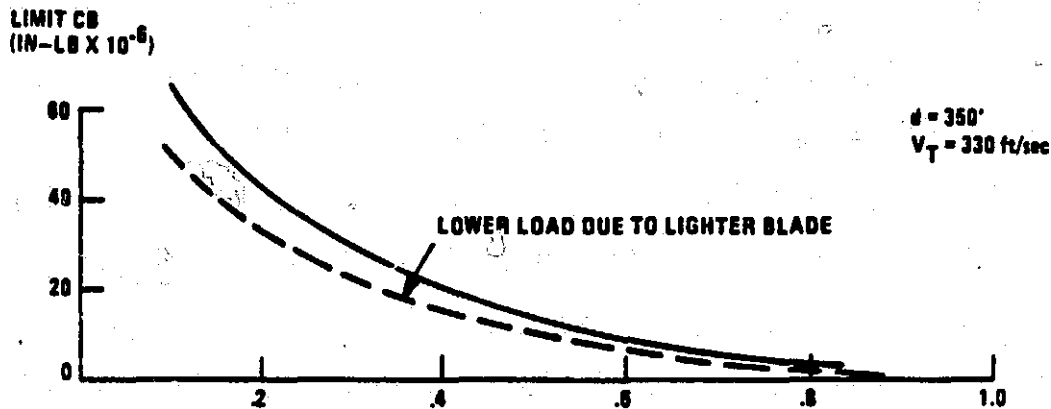


Figure 4-10 Comparison of Loads for Independantly Coned vs Teetered Rotors

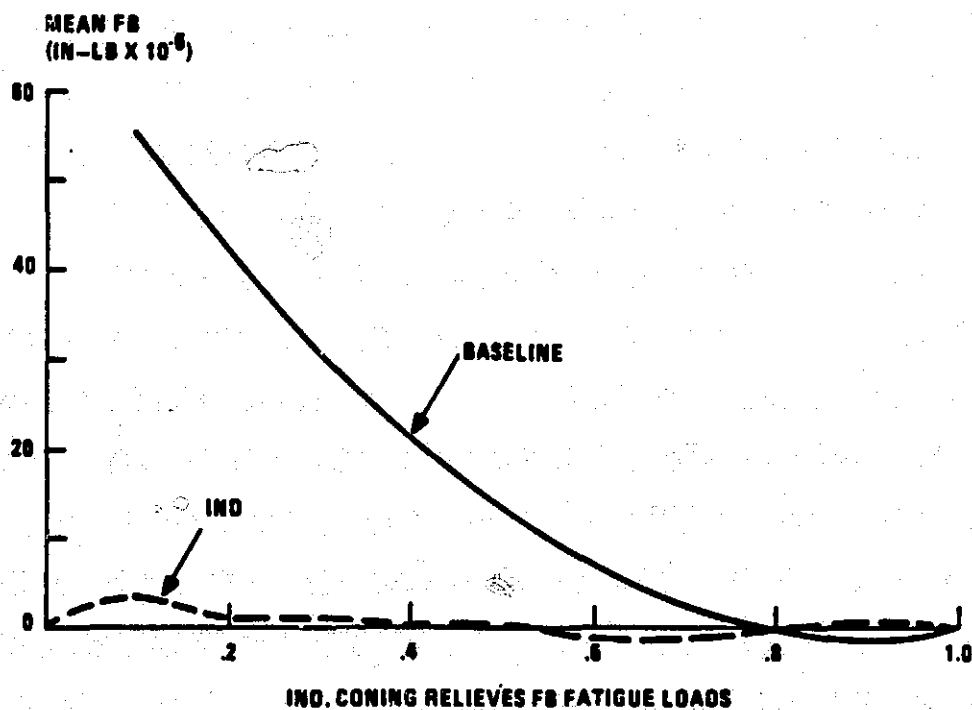
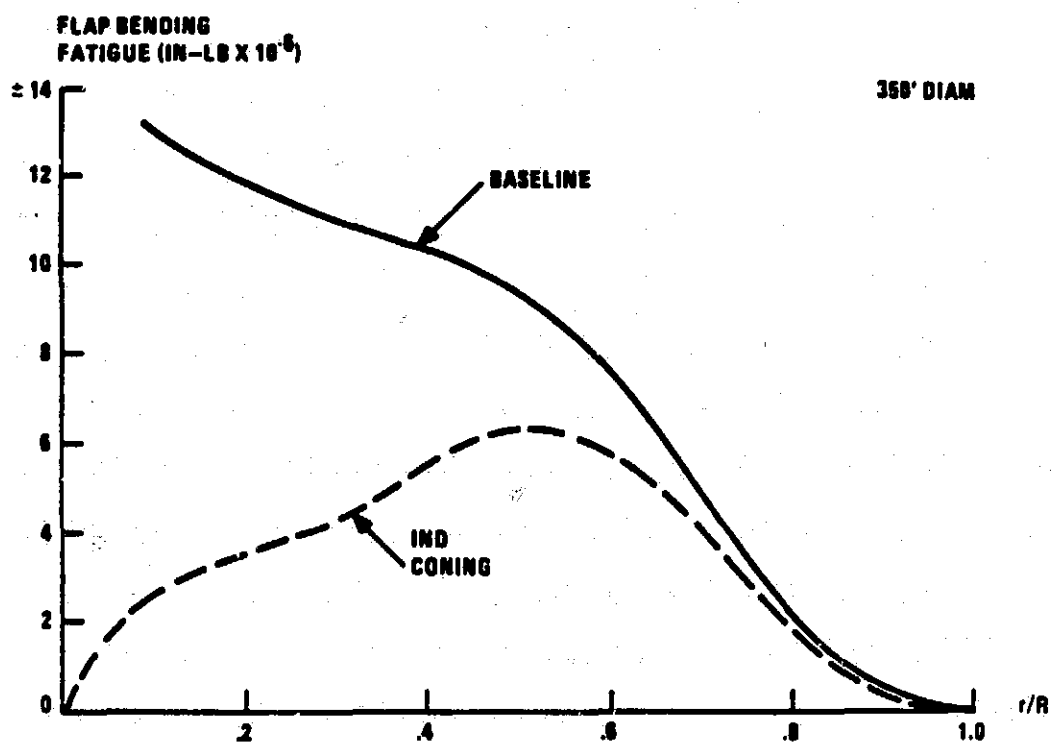


Figure 4-11 Blade Fatigue Load Summary

The lower loads associated with the independently coned rotor allowed a 30% savings in blade and hub weight, as indicated in Table 4-6. The total rotor cost was reduced by a smaller percentage, because, although the hub was lighter, it was more complex.

The trade-off summary sheet is in Table 4-7. Substantially reduced rotor loads on the independently coned rotor resulted in a significant savings in rotor weight. On the other hand, the energy capture of the independently coned rotor was 2% less than that of the teetered rotor. The savings were not quite enough to overcome this difference in energy capture, although the cost of energy of the coned rotor was within .5% of the cost of energy of the teetered rotor. There were two other reasons for using the teetered rotor. The downwind coned rotor generated much more noise than the upwind teetered rotor and the teetered rotor was less of a risk because it had been extensively analyzed and tested on recent wind turbine generators. Consequently, the independently coned rotor was dropped from consideration in the MOD-5A program.

Table 4-6. Trade-Off Score Sheet, Independent Coning vs. Teetering

Item	Units	Baseline	Ind/Cone	Remarks
Design Complexity	(Qual)	Baseline	(-)	Hub
Manufacturing Complexity	(Qual)		(-)	Hub Structure Assessed 1.37 Complexity Factor
Transportation	(\$)		Saves \$9K	Lighter Weight
Erection	(\$)		Even	More Parts but Less Sensitive to Gusts
Reliability	(Qual, #)		Even	
Maintainability, O&M	(Qual, \$)		(-)	2 More Bearings
Availability	(%)		Even	
Environmental Impact Sound, TVI	(DP-SPL)		(-)	Higher Sound - Downwind (Greater than 10 dB)
Safety	(Qual)		(+)	Less Sensitive to Gusts
Technical Risk	(Qual)		See Remarks	<ul style="list-style-type: none"> • In Field, less risk because of reduced gust sensitivity • Programmatic - Engineering Design more straightforward with baseline
Trade Specific Items				
Blades				
Hub				
Energy Capture				
Weight	(K Lb.)	Baseline	Saves 63.5	Result of Major Reduction in Loads
Installed Cost	(K \$)		Saves 47.5	
Annual Energy Capture	(GWH)		Loses 2%	
Maximum Efficiency	(%)	.43	.415	
Plant Factor	(%)	Baseline	Same	
Cost of Energy	(\$/KWH)	"	Approx. 1/2% Higher	

Recommendation - Baseline Upwind Teetering

Table 4-7. Weight and Cost Summary for 350-ft. Rotor

	Baseline	Ind. Coning
Blades (Lb.)	124,200	79,600
<u>Hub (Lb.)</u>	<u>92,500</u>	<u>73,600</u>
Total	216,700	153,200
Delta		-63,500
Blades (\$)	188,000	116,500
<u>Hub (\$)</u>	<u>152,000</u>	<u>185,000</u>
Total	340,000	301,500
Delta		-38,500

NOTE: Costs are based on 100th Unit

4.3.4 UPWIND OR DOWNWIND ROTOR STUDY

The MOD-5A proposal was for a coned rotor, downwind of the tower. As a result of analysis and technical direction from NASA, the configuration was changed to an unconed rotor, upwind of the tower.

An upwind rotor involves the least aerodynamic interaction between the tower and rotor. The upwind location was favored from an energy capture standpoint, because it prevented the tower from blocking a small region in the rotor swept area. This blockage created large cyclic load variations in the blade and tower structures of a downwind rotor. Even though a small reduction in the wind upwind of the cylindrical tower was predicted by potential flow theory, the impact of this reduction on cyclic loads and noise was minor compared to that of the downwind rotor, because the angle of attack change was small.

The disadvantages of the upwind configuration were a need for blade to tower clearance, and the impracticality of a free yaw or a coned rotor. The elastic deflection of the blade, caused by thrust loading, was towards the tower. Adequate clearance for this deflection and teeter motion had to be provided. Straight rotor and tilted rotor configurations were examined to provide blade to tower clearance; a 9° tilt was chosen. The tilt reduced the rotor swept area, thereby reducing the energy capture and raising the cost of energy. However, this tilted rotor cost of energy was less than that with a vertical rotor. The vertical rotor required a longer bedplate with higher moment loading caused by the greater offset distance of the rotor's center of gravity from the tower. Sound was minimized because of the increased tower clearance from the tilt.

The tilted rotor produced a yaw torque when operating. The torque had to be considered when the size of the yaw restraint and drive system was established. A downwind rotor, with no rotor tilt, would have avoided this requirement, but since the yaw restraint and drive system was not costly and was needed for maintenance, the upwind orientation was favored.

A coned rotor, which would balance the thrust loads, with the centrifugal loads, was not practical in the upwind orientation, because of tower clearance factors. Coning is not advantageous for shutdown loads on the portions of the blade that experience reverse thrust caused by the action of the control surface.

The main advantage of a downwind rotor was the reduced concern over blade deflection. The ability to accommodate a coned rotor, and the potential for free yaw operation were also advantageous.

One drawback of the downwind rotor was that the rotor thrust load moment adds to, rather than subtracts from, the rotor weight moment at the yaw bearing. This problem, and an increasing weight moment caused by coning and elastic deflection, resulted in higher structural loads and cost in the yaw area. Also, the fabrication cost of the hub section for a coned rotor was significantly higher than the cost of a more uniform hub section for an unconed rotor. The benefits of coning were not balanced by the added cost of the more complex center blade.

As shown in Table 4-8, the upwind orientation with an unconed, tilted rotor produces a system with a lower cost of energy than the best downwind configuration. Consequently, the upwind rotor was selected as the baseline system for the final design.

Table 4-8 Summary of the Upwind vs Downwind Trade-Off

ITEM	UNITS	UPWIND	DOWNWIND	REMARKS
ROTOR DETAIL	-	9° TILT	9° REONE	TILT FOR CLEARANCE, CONE FOR LOADS RELIEF, FOR MODEL 102 (350 FT)
BLADE WT	KLB	BASLINE	-20	WEIGHT SAVINGS DUE TO LOADS RELIEF
HUB WT	KLB		+19	MORE COMPLEX HUB FROM PRECONE
ROTOR COST	K\$(1980)		+45	BLADE COST DECREASES LESS THAN HUB COST INCREASE
YAW COST	K\$(1980)		+	YAW DRIVE IS -6K FOR PASSIVE, BUT BEARING COST WILL INCREASE DUE TO LARGER OVERHANG AND ADDITIVE MOMENT
COMPLEXITY	QUAL		WORSE	DUE TO HUB FABRICATION
ENVIRONMENTAL	QUAL		WORSE	10 DB HIGHER SOUND LEVELS DOWNWIND
RISK	QUAL		SAME	
ENERGY CAPTURE	GWII/YR		-.36	PRECONE AND TOWER SHADOW EFFECT
MAXIMUM Cp	-		-3.6%	PRECONE
O & M COST	\$/YR(1980)		SAME	
TOTAL COST	K\$(1980)		+45+	YAW BEARING COST INCREASE NOT ESTI-MATED
COST OF ENERGY	¢/KWH(1980)		+.054	

4.3.5 TORQUE CONTROL STUDY

During a trade-off study of torque control methods, the baseline partial span control was compared with a flap control. (Later in the program the flaps became known as ailerons.) The comparison was made when the blade was made of glass fiber. The partial span control involved the outer 25% of each blade, and the flap control involved the outer 50% of each blade and 30% of the trailing edge, as shown in Figure 4-12.

1. Flaps were operationally inferior to partial span control because a motor-assisted boost was required to start the rotor. They were also less effective at lower rotor speeds. In addition, blade deflection limited the flap length to approximately 10 ft.
2. The reliability, availability and maintainability assessment ranked flaps lower, because the number of components was greater.
3. Ten independent flap sections per blade were required versus one partial span control. Five times as many hydraulic joints, actuators, hinges, and attachment points were required for two flap sections driven by one actuator. The failure rate of the flap system would be higher since there are five times as many items to fail. Consequently, availability would be lower.
4. The flap system extends to 50% of the span. The area beyond 25% of the span back from the tip of the 400-ft. diameter rotor cannot be reached by a utility truck with a 100-ft. lift. More elaborate procedures would be required to get access to part of the flap control.

The flap system was an inferior choice from the point of view of performance, operating and maintenance. The concept could be rejected if its cost advantages were not enough to offset the disadvantages. Since the absolute cost differences were not defined, a relative difference between the two concepts was estimated. The basic blade materials were assumed to cost and weigh the same, ignoring for the moment, hardware for flap hinges, actuators, the mechanism, and field joints. This assumption was logical assuming the blades had the same geometry, loads, and construction. The flap configuration required more complex production and handling. For the lengths of interest and for 300 to 400 ft. diameters, the TFT blade with a partial span control was wound in two major pieces and the flap blade was wound in three major pieces, the inboard, outboard and flap sections. The flap section is cut into the individual flaps. The attachment of ten flap sections with hinges and actuators was a more complex operation than the attachment of one partial span control section actuator.

The flap configuration was estimated to require 50% more labor. The difference in cost was about 11%, since the labor content of the blade was 22%.

The hardware costs were assumed to be the same for flaps and partial span control mechanisms, although it was possible that five small sets of flap hardware cost more than one large partial span control.

Thus, the only other cost savings would arise if the partial span control required an extra field joint. An extra joint would be required only if the blade diameter was 350 to 400 ft., which would mean that the inboard section of the blade could not be shipped in one piece. An estimate from SCI indicated a field joint would be 9% of the blade cost. Thus, below 350 ft. the partial span control had a clear cost advantage. Above 350 ft., the cost of the two concepts were equal, especially when the extra starting motor for the flaps was considered.

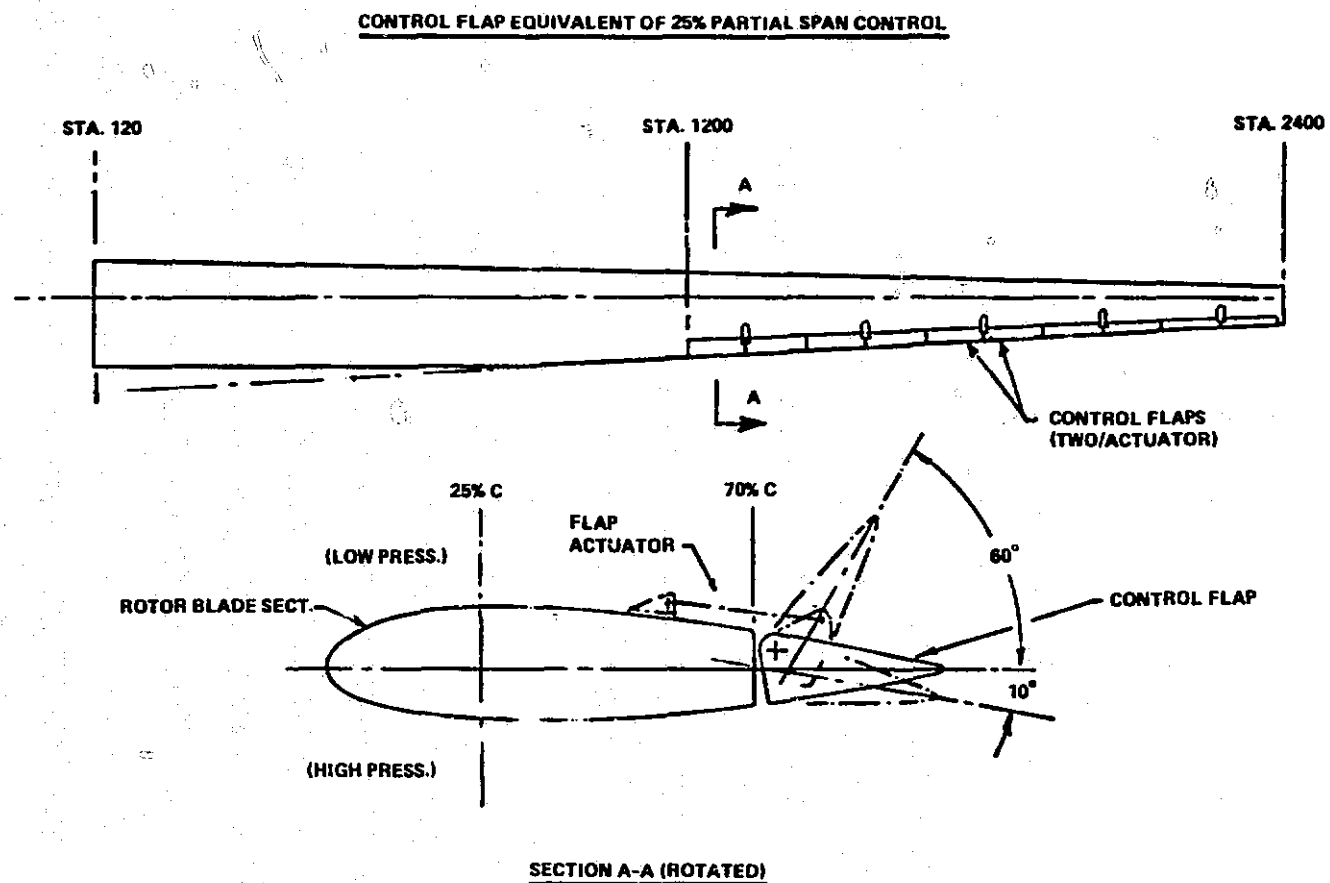


Figure 4-12 Control Flap Equivalent of 25% Partial Span Control

During conceptual design, flap control was shown to be technically inferior, and was shown to have operating and maintenance disadvantages. The study is summarized in Table 4-9. Flap control was rejected and the baseline partial span control concept was retained.

Table 4-9. Summary of Torque Control Study

Item	Units	PSC Baseline	Flap Configuration	
			350' Dia	350' Dia
Design Complexity	Qual.	+	-	-
Manf. Complexity	Qual.	+	-	-
RAM	Qual.	+	-	-
Tech. Risk	Qual.	+	-	-
Safety	Qual.	0	0	0
Rel. Wt.	-	0	0	0
Rel. Cost	-	0	-	0
Rel. COE	-	0	-	0

+ is favorable, - is unfavorable, 0 is neutral.

This study was reevaluated during the final design. The blade was made of laminated wood and epoxy and the partial span control was a substantial steel fabrication that was attached to the blade through tapered, bonded studs. As the design developed, the weight of the partial span control grew from about 20,000 lb. per blade to nearly 40,000 lb. per blade. This weight influenced gravity loads and decreased the blade elastic bending frequency. The frequency was near a strong 2 per revolution excitation and would have meant a further increase in loads and size.

NASA also obtained test data from the flap control on the MOD-0 test machine. (At this point, the flaps became known as ailerons.) A 30% chord and a 38% chord aileron control were designed for the MOD-5A. Wind tunnel testing, described in section 8.4.2, provided much better performance data than the data available during conceptual design. A three-actuator aileron arrangement

on the outer 40% of each blade appeared to be feasible and cost effective. The final baseline also included a variable speed generator subsystem that would be able to motor the rotor during start-up, and could overcome the lack of starting torque associated with ailerons.

Because of the cost and weight reductions, avoiding joints between wood and steel, better blade frequency placement, and the availability of test data, ailerons became the torque control method during the final design. This change is described in detail in section 4.2 of Volume III.

4.3.6 TOWER HEIGHT STUDY

The original plan for optimizing the tower height was modified somewhat because of the design relationships between the tower, foundation, and the erection. Chicago Bridge and Iron (CBI) was the subcontractor responsible for these activities. Data from CBI, based on the cost of the 100th unit, included the effects of factory and field tower fabrication. Ground clearance became the significant variable for the evaluation, rather than tower height, since the height is half the rotor diameter plus ground clearance. This automatically adjusts tower height for various rotor diameters.

Fatigue loading was not a critical design factor for the tower design, because the ratio of weld fatigue allowables to ultimate allowables was usually greater than the ratio of dispersed fatigue to limit load. Analyses of dynamics indicated that fatigue excitation was reduced by about 10% with increasingly high ground clearances, as a result of more uniform wind across the rotor disk.

The results of the study indicated that tower cost increases linearly with increasing ground clearance. Energy capture varies slightly less than linearly, as a function of ground clearance. The initial study showed that the cost of energy is essentially constant from a minimum 25-ft. ground clearance to about 60 ft. for a rotor 400 ft. in diameter. Above 60 ft., the tower cost increases faster than the value of the additional energy captured, so cost of energy increases correspondingly.

The tower frequency was tuned by adjusting the tower height and by designing the conical bell section of the tower so that it could be raised or lowered for the same ground clearance. A larger ground clearance provided more latitude for tuning and the opportunity to obtain a lower bending frequency.

Access to the tip control mechanism from a 95 - 100 ft. lift utility truck was a very useful feature. From a maintenance standpoint, the ground clearance should be about 50 ft. or less, since the tip length was approximately 50 ft. This maintenance consideration was not crucial, since an access door in the tower and blade support and access structure can be provided for approximately \$5,000 of recurring cost.

These results indicated that:

1. Cost of energy is insensitive to ground clearance from 25 ft. to 60 ft., and increases with increasing clearance.
2. Access does not have a significant influence.
3. The upper end of the clearance range provides the maximum design flexibility.

Therefore, 50 ft. was selected as the tower ground clearance at the end of the conceptual design phase. During the preliminary and final design phases, this selection was evaluated further, considering cost, maintenance, and frequency placement requirements.

During preliminary design, the ground clearance was changed from 50 ft. to 40 ft. on model 204.5 and the sensitivity of the cost of energy to tower height was reevaluated. Relative costs and relative energy capture are shown in Figure 4-13. Note that the slope of the energy curve decreases, while the slope of the cost curve increases. This behavior resulted in a flat, then increasing curve of cost of energy vs. ground clearance.

The ground clearance was raised to 50 ft. for model 304.1 during the final design. This increase was necessary to lower the tower stiffness so that the

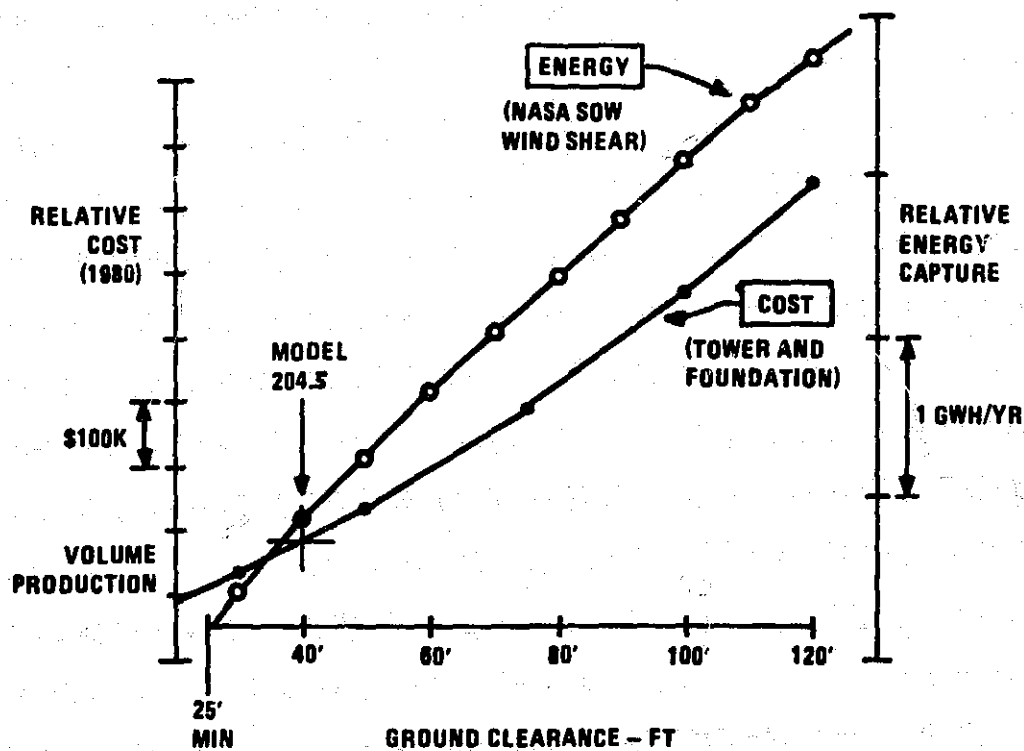


Figure 4-13 Ground Clearance vs Cost Comparison

system bending frequency requirements were satisfied. The NASA design wind shear characteristic is representative of an open plain, so wind speed increases significantly with height. Some good wind sites, however, have very little wind shear and, therefore, very little increase in energy with increases in tower height. The lowest practical ground clearance was the most universally applicable.

4.3.7 SYSTEM ROTATIONAL VELOCITY STUDY

One of the key trade-off studies conducted during the conceptual design phase evaluated the impact of rotor speed on the cost of energy. Studies evaluated single-speed and two-speed operation. During the preliminary design, variable speed generation was investigated, and rejected then because of its high cost of energy. In the final design phase, however, reduction of risk to the system led to the selection of a variable speed generator. The operating plan for the variable speed generator was based on the conceptual design work, for a generator that delivers power in two speed ranges.

Operation at a constant tip speed ratio, and maximum power coefficient is not practical over the broad wind speed range from the cut-in to the cut-out speeds. The wind variation is 3:1 or more. This range of rotor speed is prohibited by system dynamics and equipment costs. Conceptual design studies showed that two-speed operation could capture 99% of the energy available with a constant tip speed ratio for wind velocities from the cut-in speed to the rating. A two-speed system also captures 2% more energy than an optimized single-speed system.

Two-speed systems with ratios of up to 2:1 were studied. A ratio of 1.45:1 had the lowest cost of energy for the 350 ft. rotor diameter, 4 MW system.

Mechanical and electrical systems of two-speed operation were examined. The mechanical system shifted gears in the gearbox, which increased rotor speed to generator speed. The last stage of the gearbox had the shift mechanism and the more costly high torque planetary gear stages were not changed.

The gear changer that was studied could operate while the drivetrain was rotating, but not loaded. Two shift strategies, cold and warm, were

developed. In a cold shift, the rotor was stopped before the gears were shifted. In a warm shift, the shift was made while the rotor was turning. Warm shifts took less time than cold shifts. The warm shift occurred with the drivetrain unloaded. Drivetrain power was removed through the action of the rotor's aerodynamic controls.

GE's ENCAPT and WINDOPT computer codes were used during the conceptual design to compute the energy capture and the cost of the system for variations in the maximum tip speed and the ratio of the two rotor speeds. The system costs were computed for warm and cold shifts. Shift losses were included indirectly.

Comparisons were made on the basis of a torque limited system. The selected torque value during conceptual design was 2.333 million ft.-lbs. The gear size with this value was consistent with the manufacturing capability of Philadelphia Gear Corporation to make an epicyclic unit with sleeve-type planet bearings.

The site conditions assumed for these studies were from Amarillo, Texas, based on PNL-Battelle's hourly wind data from October, 1978 through December, 1979. This information included data taken at height's of 9.1 m and 45.7 m. This data was very similar to the Weather Bureau's data for Amarillo, Texas, taken over 10 years.

PNL's wind data was evaluated for the changes in wind speed that would prompt shifting between high gear and low gear. Static shifts for start-up were not included, since the logic counted only changes between the cut-in and rated speeds in a wind speed band.

For the evaluation, the data was sorted by 6-hour periods, and a cumulative probability and wind power analysis was performed. Wind data was sorted into 1 m/s (2.237 mph) bins and the transition of the 9 m/s bin (from 8.0 to 8.99 m/s) at a hub height of 250 ft. (76.2 m) was counted as a shift. This bin represents a hysteresis band for the shift of 17.9 to 20.1 mph at hub height. The raw data at 45.7 m was shifted to 76 m, using the design definition for variable wind shear.

As shown in Table 4-10, a total of 7258 hours of operation was expected in the design wind, 4222 hours at high speed and 3036 at low speed. 752 shifts were predicted. The shift logic based a shift decision on a one-hour average wind speed without considering the number of shifts that occurred in a period. Actual shift logic would limit shifting to once per six-hour period. A persistence analysis was also performed. As presented in Table 4-11, there were 1229 hours of operation at or above the rated speed, and 5931 hours of operation between the cut-in and rated speeds. There were 375 start-ups, with 205 start-ups for operation lasting 12 hours or less.

If the 752 shifts are cold, each shift counts as a start-up and the total number of start-ups would be 1127. As each start-up presents a significant change in mean loading, the total number of start-ups was important for determining fatigue life on some rotor and hub elements. A small contingency was added to the 1127 cycles and for a 30-year design life, 35,000 start-ups were used in fatigue calculations.

Shift losses are related to the quantity and type of shifts. For Model 104.5, a warm shift would take 4 minutes, losing 108.5 kW-hrs. and a cold shift would take 10.4 minutes, losing 321.7 kW-hrs per shift. At 3.5 cents/kW-hrs., a warm shift strategy would cost \$2,601 per year in lost energy and a cold shift strategy would cost \$7,713. An equivalent break-even hardware cost for the warm shift was \$28,400. A warm shift design was used during the preliminary design until model 204.3, when a cold shift strategy was adopted to reduce the risk of overspeed, in spite of the increased cost of energy.

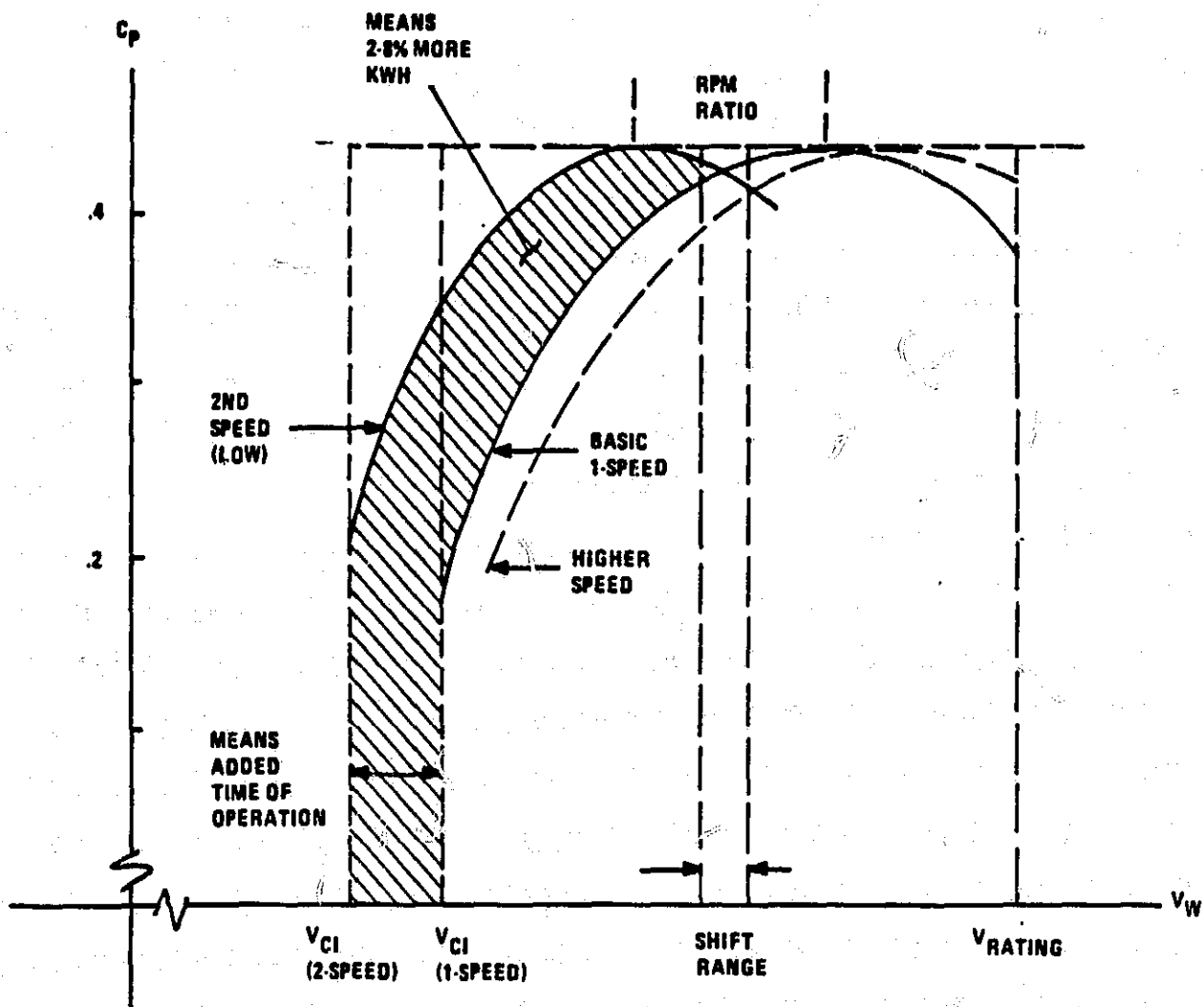
The benefits of multi-speed operation are most dramatic where the single-speed power coefficient characteristic of the rotor is high, but narrow. Two-speed operation provides a much better overall power coefficient characteristic, as shown in Figure 4-14. The basic MOD-5A rotor characteristic was fairly broad, so the benefits of two-speed operation were less dramatic, but were still significant.

Table 4-10 Wind Speed Distribution in Amarillo, TX.

<p>DATA SCALED TO 76 M. BINS ARE 6 HOUR GROUPS</p> <p>AVERAGE WIND SPEED = 8.31 METERS PER SECOND</p> <p>POWER IN THE WIND = 3329.44 KW-HR PER SQUARE METER PER YEAR</p> <p>DATA ANALYSIS BINS 27 AND 28 PLUS 1 BIN, OR MORE</p> <p>OUT OF RANGE FROM 9 BIN TO 9 BIN</p>						
MPS (Meters per Second)	BIN 1-600	7-1200	13-1800	19-2400	SUM	CUM
1	3	3	3	11	20	20
2	33	58	38	31	160	180
3	54	106	99	38	297	477
4	121	136	144	74	475	952
5	136	197	197	96	626	1578
6	224	253	218	149	844	2422
7	255	267	229	140	891	3313
8	236	218	199	142	795	4108
9	295	202	264	241	1002	5110
10	277	179	226	234	916	6026
11	295	161	152	250	858	6884
12	220	114	137	155	626	7510
13	143	84	92	118	437	7947
14	129	71	72	58	330	8277
15	61	56	52	48	217	8494
16	39	30	22	18	109	8603
17	14	25	15	6	60	8663
18	7	15	17	6	45	8708
19	2	13	10	6	31	8739
20	4	1	4	3	12	8751
21	3	1	0	1	5	8756
22	1	0	0	0	1	8757
23	2	0	0	0	2	8759
24	1	0	0	0	1	8760
25	0	0	0	0	0	8760
26	0	0	0	0	0	8760
UPSHIFTS 27	-	-	-	-	376	0
DOWNSHIFTS 28	130	112	65	69	376	0
TOTAL HOURS OF HIGH SPEED OPERATION = 4222						
TOTAL HOURS OF LOW SPEED OPERATION = 3036						

Table 4-11 Persistence Analysis

CONTINUOUS HOURS	BELOW CUT-IN	CUT-IN TO-RATED	RATED TO CUT-OUT	ABOVE CUT-OUT	CUT-IN TO CUT-OUT
1	105	109	114	5	49
2	71	66	43	2	31
3	35	63	31	0	23
4	30	46	23	1	12
5	24	36	24	0	13
6	21	36	10	0	16
7	21	27	20	0	9
8	16	37	11	1	8
9	12	25	10	0	3
10	4	34	5	0	22
11	7	22	5	0	9
12	4	15	3	0	10
13	1	12	4	0	6
14	7	13	2	0	10
15	2	18	1	0	12
16	3	13	0	0	6
17	2	10	1	0	8
18	1	10	0	0	6
19	0	5	0	0	3
20	0	6	1	0	9
21	0	5	1	0	6
22	1	13	0	0	10
23	1	3	0	0	7
24	0	7	1	0	6
25	0	4	0	0	4
26	0	1	0	0	3
27	1	5	0	0	4
28	0	3	1	0	2
29	0	3	0	0	2
30	0	3	0	0	5
31	0	2	0	0	2
32	0	1	0	0	2
33	0	0	0	0	0
34	0	0	0	0	2
35	0	0	0	0	1
36	0	2	0	0	3
37	0	0	0	0	1
38	0	0	0	0	3
39	0	1	0	0	2
40	0	0	0	0	4
41	0	0	0	0	1
42	0	1	0	0	0
43	0	0	0	0	0
44	0	0	0	0	2
45	0	0	0	0	1
46	0	0	0	0	0
47	0	1	0	0	1
48	0	0	0	0	2
49 to 177	0	9	0	0	36
SUMMATION OF COUNTS IN PERSISTENCE COLUMNS					
8760	1579	5931	1229	21	7160



- LOWER CUT-IN
- LONGER OPERATION
- HIGHER POWER AT CONSTANT TORQUE
OR LOWER TORQUE AT CONSTANT POWER

Figure 4-14 Benefits of Two-Speed Operation

The model 102.0 system was examined for the sensitivity of energy capture to the rotor speed ratio. These results are illustrated in Figure 4-15, which shows that a broad range of rotor speed ratios yielded a fairly constant cost of energy. The best ratio for energy capture was 1.45. Further analysis on the model 104.2, illustrated in Figure 4-16, shows that the cost of energy was constant for ratios between 1.3 and 1.5. A smaller ratio was advantageous for tower bending and drivetrain torsional frequency placement, so a ratio of 1.3 was selected.

With this ratio, the gearbox flexibility could be controlled to provide a natural frequency below 0.9 per revolution (0.9P) at both speeds. The best tower bending frequency is above 1.1P, at the higher rotor speed, and below 1.8P at the lower rotor speed. Straddling the 2P line is also practical if the necessary softness is difficult or expensive. An increase in rotor speed is also practical to raise the critical frequency window. These frequency characteristics were identified in the point design definitions during the conceptual design phase.

When the model 102.0 system was operated at a 14% higher torque and 14% lower rotor speed, for the best single speed system, 96% of the ideal "maximum C_p " rotor energy capture was obtained from operation below the rating. This statistic confirmed the fact that the rotor was already efficient, and that it had a broad high power coefficient characteristic.

For two-speed operation, 99% of the ideal maximum power coefficient energy was captured. When compared with the best single-speed machine, total energy capture increased by 3%, and the cost of energy decreased by 4.4%. Operating time increased by 7%.

An electrical system for providing two-speed operation was evaluated during conceptual design. A pole amplitude modulated generator provided two-speed capability, but the cost of this arrangement was almost \$31,000 above the cost of the shifting gearbox.

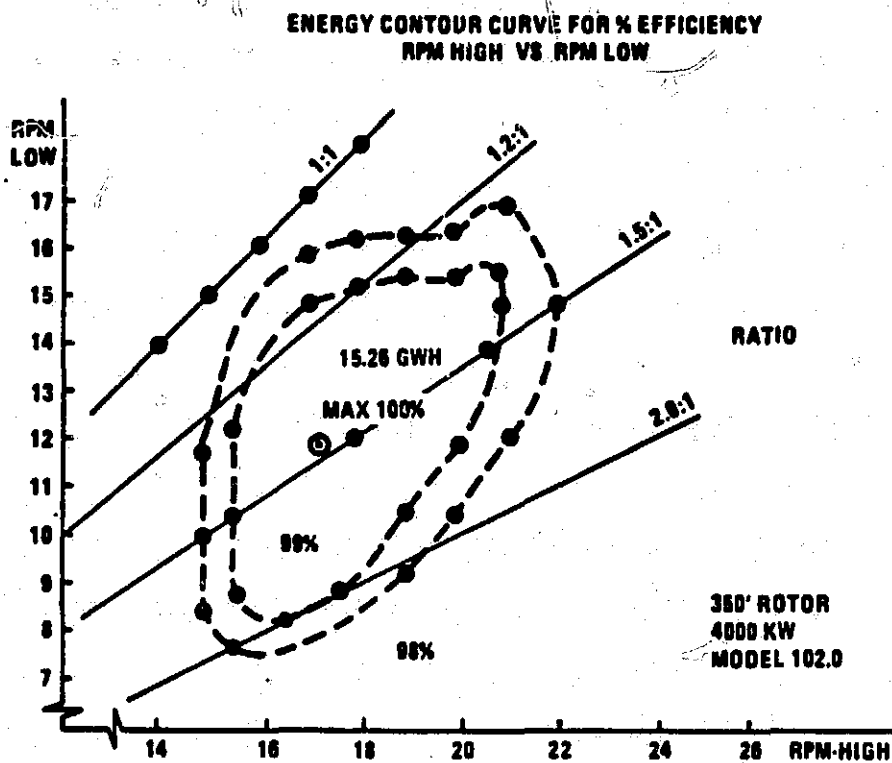


Figure 4-15 Speed Ratio Sensitivity

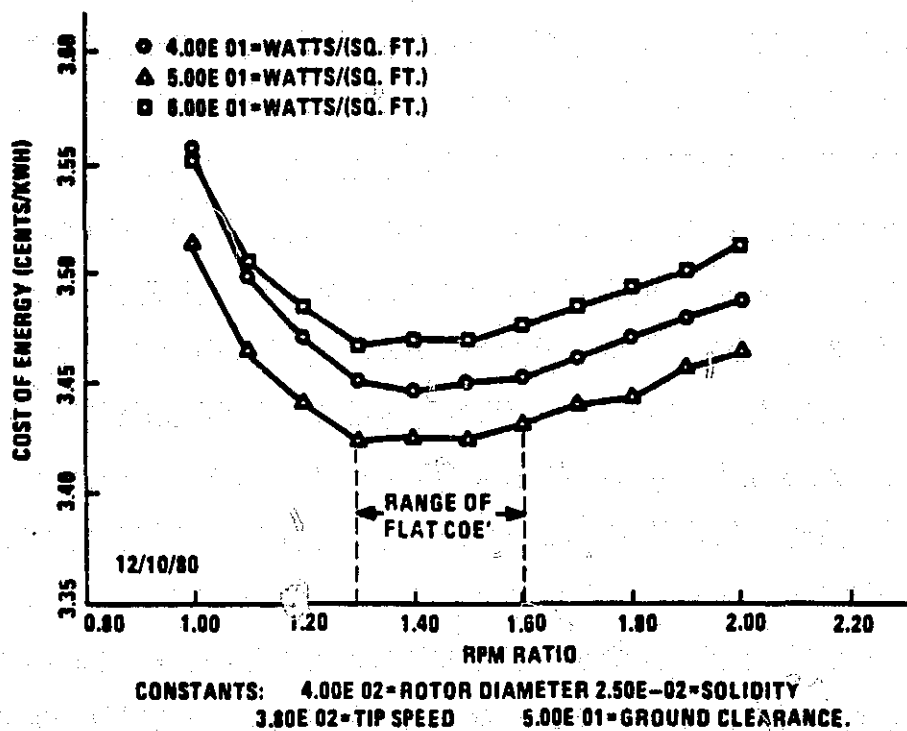


Figure 4-16 Sensitivity of Cost of Energy to Rotor Speed Ratio

The results of the conceptual design phase evaluation are shown in Table 4-12. A mechanical, two-speed, warm-shift configuration was selected as the baseline for the preliminary design, with the following conclusions:

1. Two-speed operation can capture a substantial amount of the 4 to 5% of the energy lost by a single-speed wind turbine from cut-in to rating because of the off-peak C_p operation.
2. Warm shifting is more cost effective than cold shifting.
3. For a cold-shift design, 35,000 start cycles are appropriate for fatigue. This number was used for design purposes. It is not what the machine would see.
4. Two-speed operation is cost effective, including deductions for shift loss, in warm or cold shifting systems.
5. Electrical two-speed systems are less cost effective than mechanical two-speed systems.
6. Constant velocity ratio implementation was not cost effective.

4.3.8 GEARBOX AND NACELLE CONFIGURATION STUDY

The gearbox was the component of the drivetrain that connects the rotor to the generator. It was the most substantial element of the nacelle. The gearbox converts the high rotor torque input from the low speed shaft to a low torque, high speed output for the generator. To extend the operational capability of the turbine into the lower wind speeds, the gearbox provides the capability to change speeds. An integrated gearbox provides bearing supports for the rotor, and some torsional compliance and damping to alleviate torque overloads caused by wind gusts and includes structural elements that replace some of the usual nacelle functions. This strategy offered many possible nacelle configurations besides the conventional simple speed increaser on a bedplate. The strategy could extend to a completely integrated concept. All of these design concepts were evaluated and are summarized in the following paragraphs.

The separate gearbox is shown in Figure 4-17. This conventional approach used an "off-the-shelf" gearbox for only the speed increaser function. Rotor support was provided by separate bearing and shaft assemblies. Torsional compliance in the drivetrain was obtained either by means of a torsionally

Table 4-12 Trade-Off Study Summary

Item	Units	Baseline Mechanical 2-Speed (Warm) 104.5	Baseline Mechanical 2-Speed (Cold) 104.5	Electrical 2-Speed (Warm)	Mechanical 2-Speed (Warm) Optimum	1-Speed Optimum	Remarks
Design complexity	(Qual)	Medium	Moderate	Moderate	Medium	Moderate to low	Baseline has synchro-mesh shifter
Manufacturing complexity	(Qual)	Moderate to medium	Moderate	Moderate	Moderate to medium	Moderate to low	
Transportation	\$ 1980	Base	Same	+70	+3950	-350	Electrical shift equip. weighs 500 = more -2500 = for shifter +3000 = for cabling & generator windings higher RPM sys. weighs more.
Erection	(\$)	Base	Same	Same	Same	Same	
Reliability	(Qual)	Base	Slight +	Slight +	Same	Slight +	Cold shift & electrical shift have fewer parts
Maintainability	(Qual)	Base	Same	Slightly better	Same	Slightly better	Gearing is reliable
Availability	(%)	Base	Same	Same	Same	Slight +	Fewer parts have less inspection
Environmental impact	(Qual)	Base	Same	Same	Worse	Same	All upwind higher tip-speed sound increase
Safety	(Qual)	Base	Same	Same	Same	Same	
Technical risk	(Qual)	Base	Slightly less	Slightly less	Slightly more	Less	Higher RPM risk increase Fewer parts decrease risk.
Speed	(RPM)	17/13.2	Same	Same	19/14.7	17	All for 1.3 speed ratio
Tip speed (max)	(FPS)	356	Same	Same	400	Same	Constant 3.06% solidity basis
Torque	(MFP)	2.333	Same	Same	Same	Same	Constant torque comparison basis
Power	(KW)	5125	5125	5125	5700	5125	
Operating Time	(Hours)	7092	7092	7092	6824	6537	
Energy capture below rating & shift loss	(%)	99.2-.63	99.2-1.67	99.2-.38	98.7-.65	95.5	
Weight	(KLB)	Base	Same	(+.5)	(+28.1)	(-2.5)	810205 WCERS
Installed cost	K\$ 1980	Base	(-16)	(+30.9)	(+80)	(-45)	810205 WCERS
Annual energy capture	(GWH)	19.63	19.48	19.63	20.24	19.02	Includes shift losses and .96 availability
Specific energy	(KWH/FT ²)	158.1	156.9	158.1	163.1	153.3	
Plant factor	(%)	.437	.434	.437	.405	.424	
Cost of energy	c/KWH (1980)	Base	(-.011)	(+.020)	(-.030)	(+.068)	810205 WCERS
<p>Recommendation: The baseline warm shift model 104.5 is recommended as offering the best combination of low COE and low risk, while the higher speed system has lower COE, plant factor, weight, cost and qualitative factors are negative.</p>							

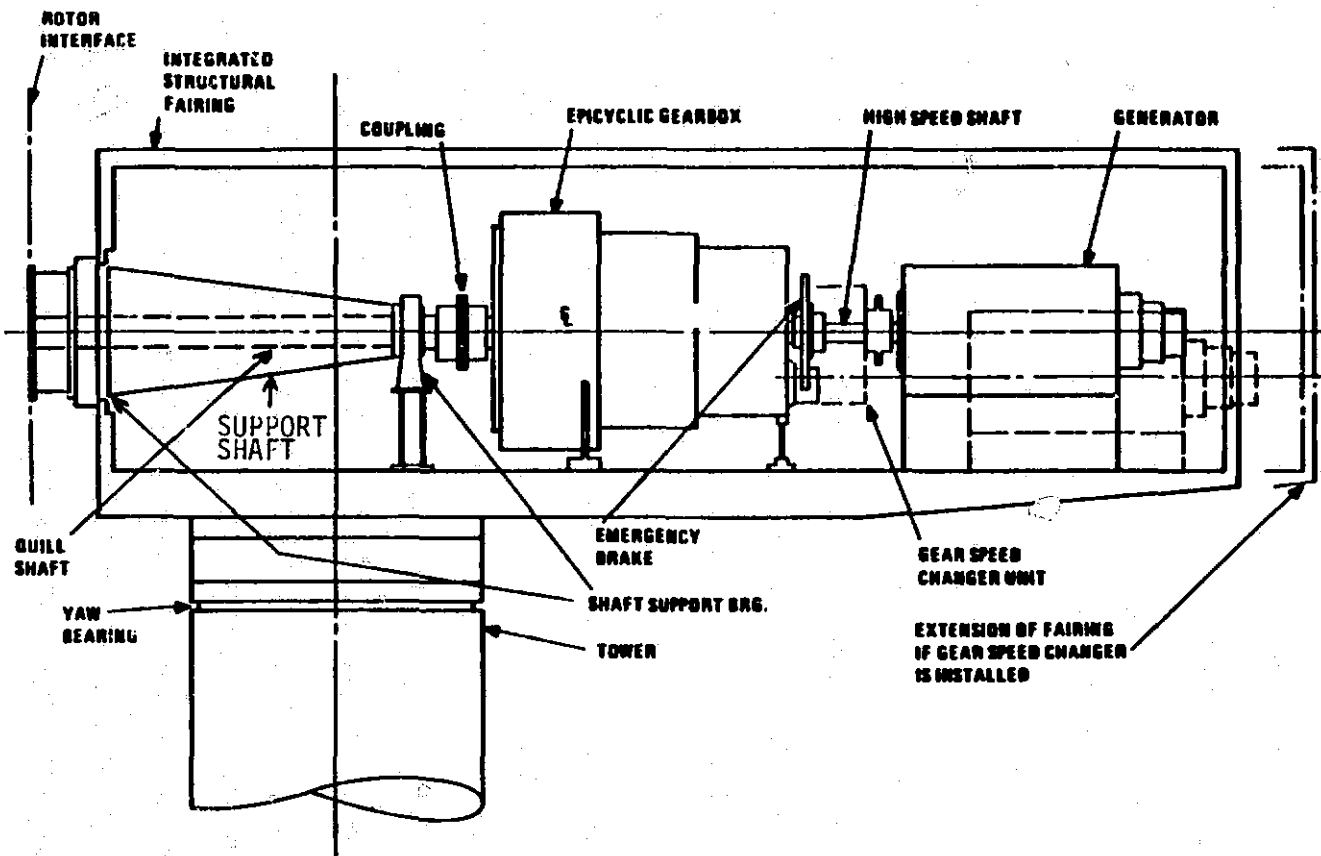


Figure 4-17 Non-Integrated Gearbox Quill Shaft Drive

soft shaft, which makes it difficult to provide damping, or by a spring support for the whole gearbox. The entire assembly was mounted on a bedplate structure. The simplicity of this assembly was very attractive. However, it required too much assembly work, and resulted in a larger nacelle configuration than necessary. Since this configuration was based on existing hardware and technology, production in large quantities would not reduce costs.

The fully integrated gearbox configuration, shown in Figure 4-18, integrated all structural functions normally provided by the nacelle and bedplate into the gearbox casing. The rotor support was provided internally with bearings, compliance control was internally provided by torsion bars, and the casing of the gearbox was extended to form the tower interface at the yaw bearing. A small, bolted-on cantilevered structure supported the generator. The housing structure would be monolithic, to provide a reliable load path. However, the fabrication of this structure had some disadvantages, and the size and weight of the structure was a drawback to handling and shipping. It would be very costly to ship this configuration to most sites. For these reasons, the fully integrated gearbox was ruled out.

A rotor-integrated gearbox, shown in Figure 4-19, was finally selected during the conceptual design. It was an optimum between the two designs described above. While most functions were integrated into the gearbox housing, the size and weight of the housing were within the railroad shipping envelope. Furthermore, the arrangement could be disassembled into two halves, neither exceeding 60 tons, for transportation to less accessible sites.

The gearbox was a hybrid, consisting of an epicyclic first stage and parallel shaft second and third stages. The logic for the selection of this arrangement is based on minimizing the cost of energy, as shown in Figure 4-20. If all the stages were parallel shaft, the high input torque would require a very large bull gear and pinion in the first stage. For a machine the size of the MOD-5A, the cost of a large parallel shaft configuration exceeds the cost of an equivalent epicyclic stage, so an epicyclic first stage was selected. The second and third stages transmit progressively lower torques at increasingly higher speeds, so parallel shaft arrangements are

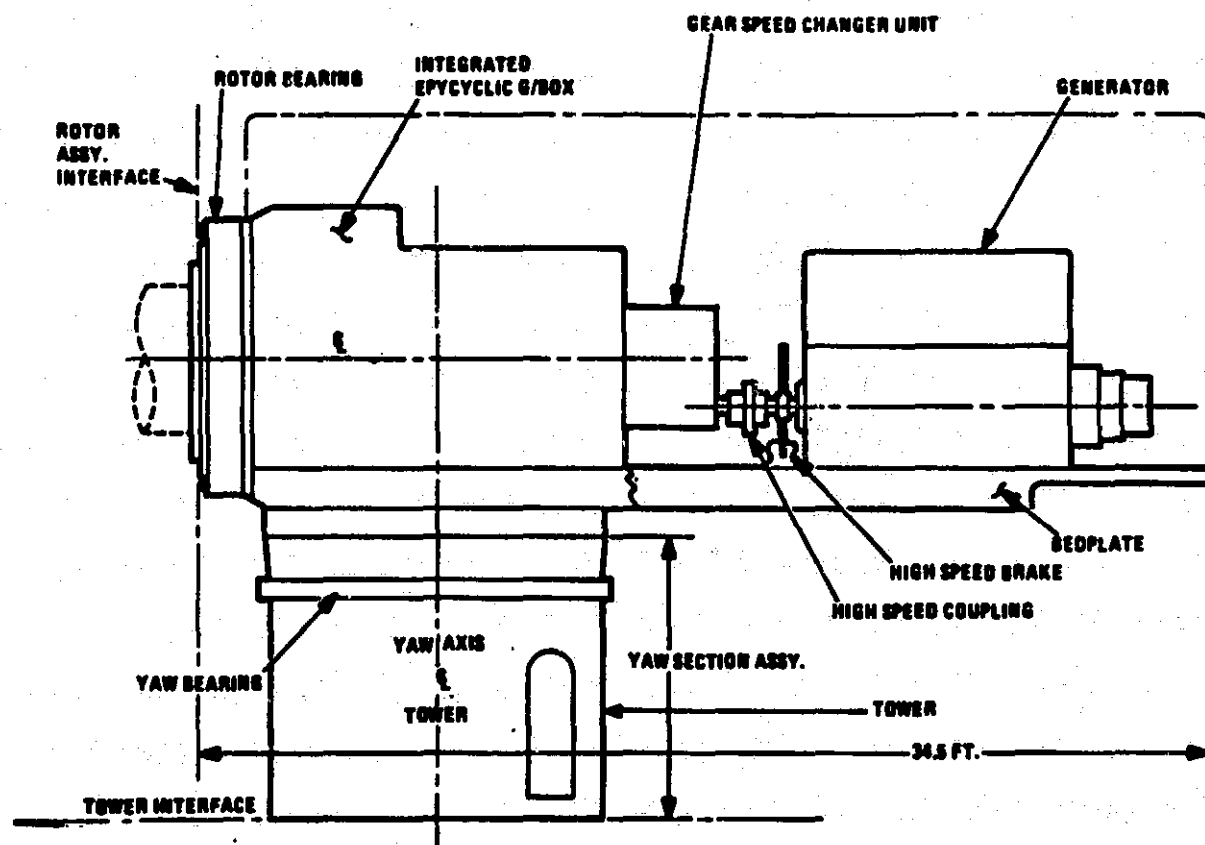


Figure 4-18. Fully-Integral Gearbox

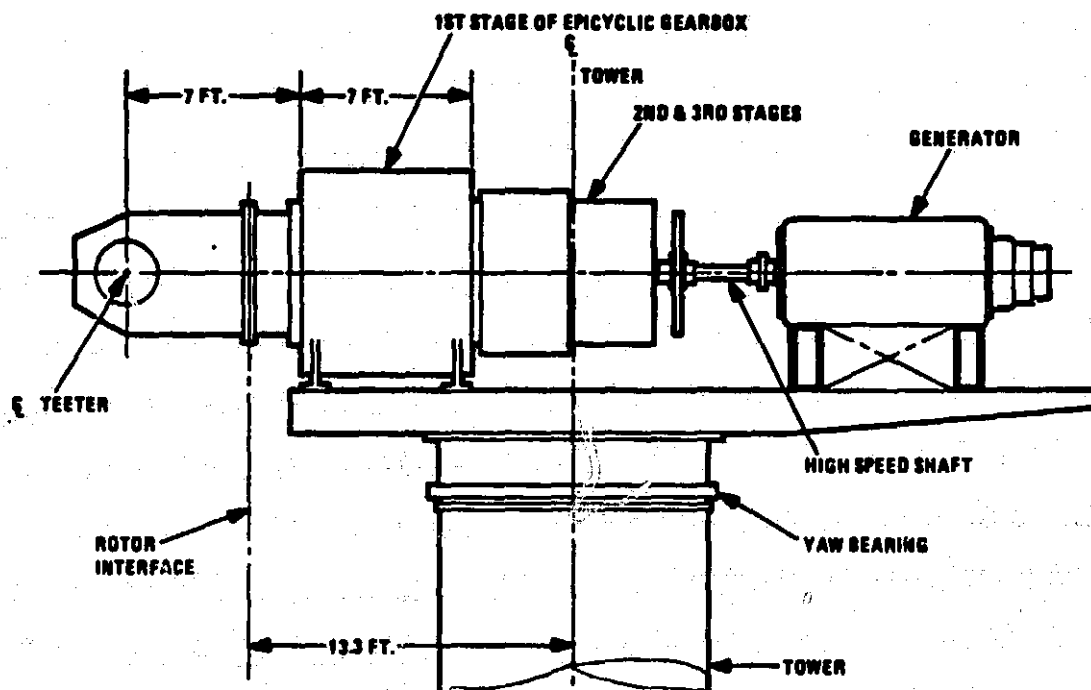


Figure 4-19. Rotor-Integrated Gearbox

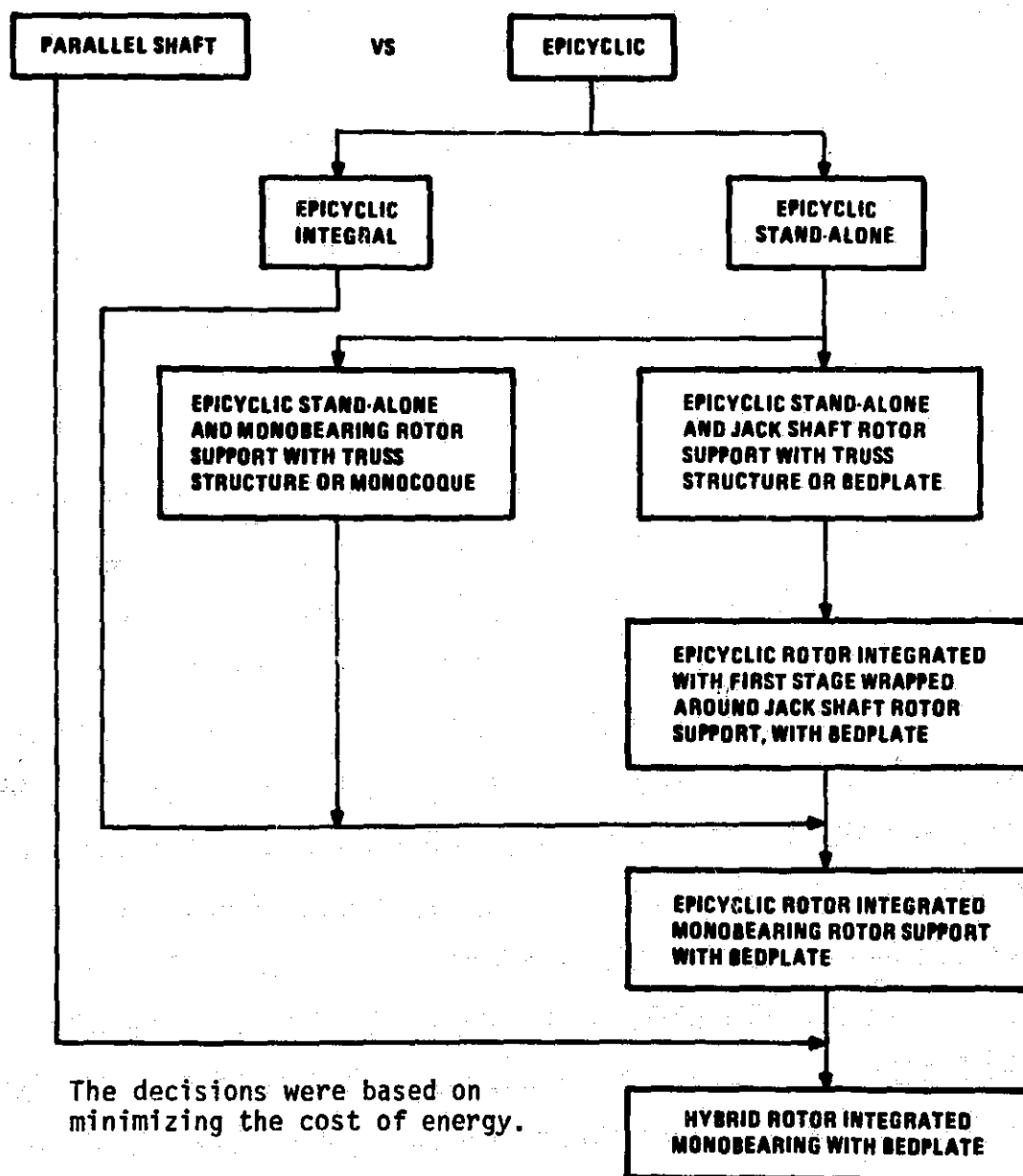


Figure 4-20 Gearbox and Bedplate Trade-Off Flow Chart

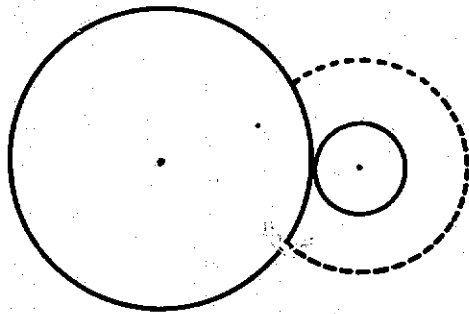
feasible for these stages. The combination of epicyclic and parallel shaft stages offered the most economical configuration for the shipping envelope and handling constraints. The relative sizes of the gearing configurations that were examined are shown in Figure 4-21.

During the final design phase, this issue was reopened. The rotor integrated gearbox was more expensive and more complex than the estimates had predicted. Some potential suppliers were unable to produce quotes. Furthermore, rearranging the rotor support function would reduce the risk of a combined bending fatigue and torque failure on the rotor support shaft. The lowest system and gearing cost was obtained by reverting to a stand-alone speed increaser with a single ratio. A nacelle box frame structure provided the rotor support function, and a variable speed generator subsystem provided the speed change and compliance control functions. These changes are described in section 5.8.

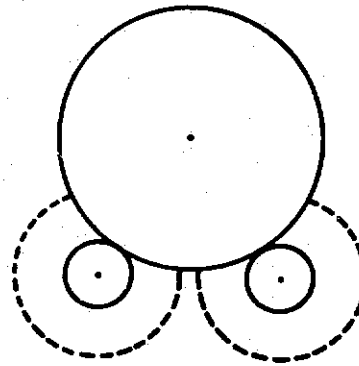
4.3.9 ROTOR STOPPING TECHNIQUE STUDY

The rotor stopping technique trade-off study involved an evaluation of the reliability of the partial span control mechanism. These two independent tip systems each had three levels of redundancy. This design was compared to a partial span control system with less redundancy, and with the addition of a mechanical rotor brake, referred to as a last resort brake. The criteria were a reliable, safe shutdown system and a minimized impact on the cost of energy.

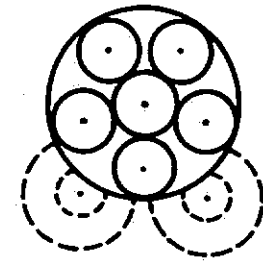
The partial span control subsystem, shown schematically in Figure 4-22, consisted of a hydraulic pressure supply mounted on the hub, and movable blade tips controlled by actuators. The blade tips are the outer 25% of the blade span. The system was designed with several levels of redundancy. First, during normal operation, the servo-controlled primary system positions and holds the tips anywhere between the power and feathered positions. The pressure and actuator piston areas were designed to overcome the highest possible reaction torques, and the tip rotational inertia. Hydraulic fluid was supplied by a hydraulic pump and hydraulic accumulators at the proper pressure and flow rate and was ported by servo valves on each tip to the actuator. The emergency feather valve was the second system. When the system loses electrical power, the emergency feather valve actuates, blocking the



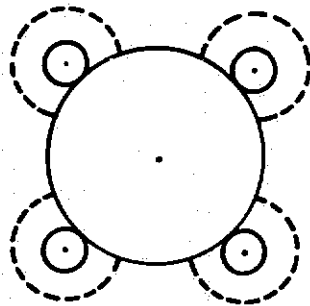
PARALLEL SHAFT- 1 LOAD PATH



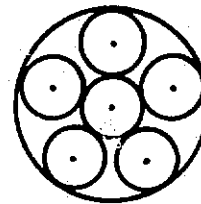
PARALLEL SHAFT- 2 LOAD PATHS



HYBRID

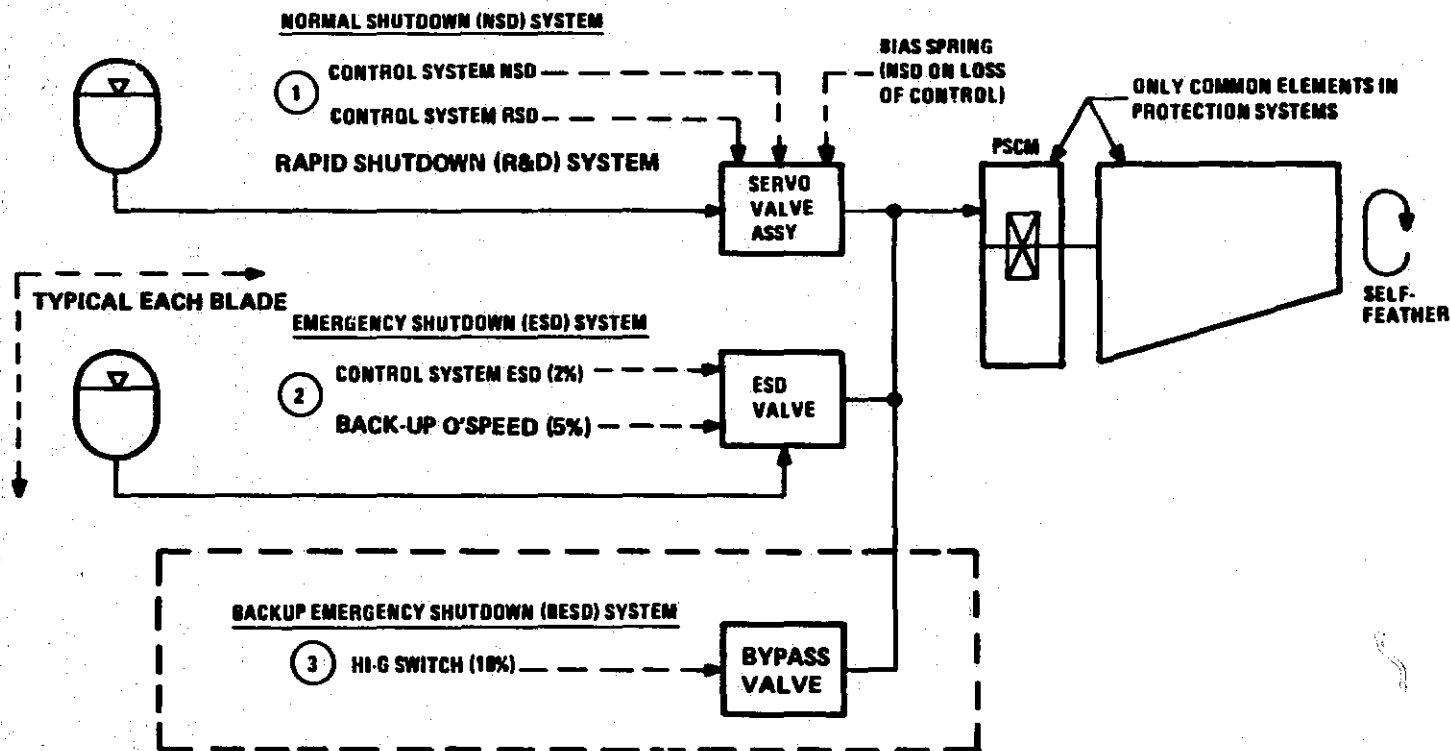


PARALLEL SHAFT- 4 LOAD PATHS



EPICYCLIC

Figure 4-21 Relative Sizes of Drivetrain Configurations



- NOTES:**
- ① CONTROL SYSTEM WORKS OFF D.C. PWR. FROM STATION BATTERY
 - ② BACK-UP OVERSPEED IS INDEPENDENT A.C. POWERED SYSTEM, FEATHERS ON LOSS OF A.C., AND UTILIZES HUB MOUNTED SENSOR, SEPARATE FROM CONTROL SYSTEM SENSOR
 - ③ BESD USES D.C. PWR, ACTUATED FROM BLADE MOUNTED HI-G SWITCH
 - ④ SERVO VALVE & ESD ARE EXERCISED BEFORE EACH START
 - ⑤ ESD VALVES TO BE SHEAR SEAL TYPE TO MINIMIZE VULNERABILITY TO CONTAMINATION

Figure 4-22 Simplified Diagram of the Overspeed Protection Study, Baseline Phase A Results

servo valve and providing pressure to the actuator from the accumulators in the direction that will feather the blade. The third level of redundancy took advantage of the fact that the tip was hinged at a point where the aerodynamic moments act to drive the blade tips towards a shutdown position. A by-pass valve was connected to both sides of the actuator and the accumulator. It was electrically controlled and could be operated to hydraulically connect both sides of the actuator. In this condition, the aerodynamic torque drives the tip towards the feathered position, aided by hydraulic pressure on the actuator piston. The tip was feathered by the pressure on the blind end of the actuator.

The aerodynamic braking systems for each blade were completely segregated, separate pumps. The accumulator bank on each blade was separated by check valves from the other blade, so that a complete loss of pressure in one blade would not impair the operation of the other blade. Only one operational tip was needed to stop the rotor.

Each blade was fully instrumented with sensors indicating pump operation, accumulator charge pressure, fluid reservoir level and blade tip angle. The emergency feather system tripped upon loss of power. The basic failure modes were:

1. Pump Malfunction
2. Valve Malfunction
3. Catastrophic Leakage
4. Blade Jam

Pump malfunction will be detected by the pump discharge pressure switch, which initiates a shutdown. Any valve malfunction will cause the blade tips to be in different positions. The discrepancy would be detected by the control system and the system would initiate a shutdown, either through servo valve control or emergency feathering of the functional blade. Electrical power loss triggers the emergency feather system and initiates shutdown. Catastrophic leakage in any circuit would be detected by the individual pressure sensors, but would not affect other hydraulic circuits because of the presence of isolating check valves. The pressure loss would cause an emergency shutdown command and the unaffected blade would effect the shutdown.

This brief description of the partial span control shows that a single-point failure of the partial span control was manageable. The system would be reliable and safe.

A last-resort brake system, in lieu of some of the redundancy in the partial span control, was an alternative technique for stopping the rotor. The logical location for a braking system capable of protecting against overspeed was at the low speed rotor shaft. This location avoided loading the gear train.

A rotor brake on the low speed shaft has to absorb the total kinetic energy stored in the rotating mass, and the energy added to the rotating system by the wind during the deceleration. It was assumed that the rotor speed at the time of brake application was 15% above the rated speed and the corresponding rotor input torque was about two times the rated torque. The total kinetic energy of the rotor was computed as follows:

$$KE = \frac{1}{2} I \omega^2$$

where:

I = rotor moment of inertia, slug ft. sq.

ω = rotor speed, radians/second

At a 15% overspeed, $\omega = 17.9 \times 1.15 \times 2\pi/60 = 2.16$ radians/second. With a rotor moment of inertia of 50×10^6 slug-ft. sq., the total kinetic energy is:

$$\begin{aligned} KE &= (0.5) \times 50 \times 10^6 \times (2.16)^2 \\ &= 116.64 \times 10^6 \text{ ft-lb (149,923 btu)} \end{aligned}$$

Assuming that the rotor is stopped in 26 seconds, the total energy absorbed from the wind in that time, based on a MOD-1 analysis, was approximated by:

$$W.E. = 2\pi N_i T_i \times 2/3 \times 26 \text{ seconds} \times 2454/3600$$

where:

W.E. = wind energy

N_i = rotor speed at time of brake application, 17.9 x 1.15 rpm

T_i = rotor torque at time of brake application, 2 x rated torque of 2.7×10^6 ft-lb

$$W.E. = \frac{(2\pi)(17.9)(1.15)(5.4 \times 10^6)}{33,000} \times \frac{2}{3} \times \frac{2454}{3600} \times 26 = 250,072 \text{ btu}$$

The total energy to be absorbed by the brake is 399,995 btu. If a mean temperature rise of 750°F is permitted in the steel disk, each pound of steel absorbs 75 btu. The total weight of disk material required to absorb the 399,995 btu is:

$$M_{\text{steel}} = 399,995/75 = 5333.3 \text{ lbs}$$

One disk, with an outer diameter of 144 in., an inner diameter of 60 in. and 1.5 in. thick, weighing 5,446 lbs., meets the heat sink requirements. The number of Goodyear type SLC 19 brake calipers was derived by taking the ratio of the total heat to be absorbed in the MOD-5A to the total heat absorbed in the MOD-1 brake design.

$$\frac{Q_{5A}}{Q_1} = \frac{399,995}{32,133} = 12.44$$

This calculation indicates that the MOD-5A needed a minimum of 12.5 brakes of the type used on MOD-1. For proper spacing this was increased to 16, or 4

brakes per quadrant. The circumference of a disk with a diameter of 12 ft. will easily accommodate the 16 brakes. The available brake torque is given below.

Holding power of each brake:

$$F = 2 \times P \times A \times \mu \text{ (lbs)}$$

P = applied hydraulic pressure, 3000 psi

A = brake piston area

μ = coefficient of friction, .3

The SLC 19 brake has 3 pistons with 3.5 in. diameters, thus

$$A = \frac{(3.5)^2 \pi}{4} \times 3 = 28.9 \text{ sq. in.}$$

$$F = 2 \times 3000 \times 28.9 \times .3 = 51,954 \text{ lbs.}$$

$$\text{Total brake torque} = F \times R \times N_b \text{ (ft-lb)}$$

where: R = action radius, 5.8 ft.

N_b = number of calipers, 16

$$T = 51,954 \times 5.8 \times 16 = 4.8213 \times 10^6 \text{ ft-lb}$$

The total brake torque is below the required value of two times the rated rotor torque, which equals 5.4×10^6 ft-lb. Accordingly, the number of calipers had to be increased. Twenty calipers was the next number of brake calipers that could be accommodated efficiently. This required the minimum circumference to equal 40 ft., resulting in a outer diameter of 12.75 ft. for each disk. Since the calipers would be attached to the gearbox, which was only 144 in. wide, an outrigger structure would be added to the gearbox and bedplate to support the calipers. One alternative, using two smaller disks was even less attractive, because of the lack of space between the bedplate and blade hub.

It was decided during conceptual and preliminary design that partial span

control with the redundant features noted in this section, was satisfactory for rotor stopping duty. This decision was re-examined during the final design, when ailerons were selected for the rotor torque control.

Ailerons are not able to stop the rotor completely, so a rotor stopping brake was added to the final design, to provide complete stopping. The aileron subsystem was designed with three mechanically independent sections on each blade and the stopping brake was designed to stop the rotor with one aileron section jammed. This stopping brake only dissipates the kinetic energy of the rotor at a reduced speed, and it does not have to dissipate wind energy. Since wind energy contributed significantly to the energy requirements for a last resort brake, the aileron stopping brake described in Volume III, section 4.5.7 was designed with less disk mass and fewer calipers.

4.4 SYSTEM SIZE STUDIES

The system sizing studies were the essence of the conceptual design effort. They became an integral part of the baseline optimization and were instrumental in the evaluation of independent coning and alternate blade materials. Although many design parameters, such as the tilt, could be changed during the preliminary design phase without affecting the entire design, the sizing parameters, particularly the rotor diameter, were fixed at the end of the conceptual design phase.

Sizing studies were conducted for these parameters:

1. Rotor diameter
2. Rated electrical power (P_{re}), defined as power density
3. Rotor solidity (σ)
4. Rotor speed (N_H), defined as tip speed
5. Ratio of rotor speeds (N_H/N_L) for two-speed operation
6. Tower height, defined as ground clearance (GCL)

The cost and weight accounts that were used for the optimization are shown in Table 4-13.

The original baseline diameter was 350 ft. The sizing studies stipulated that the range of rotor diameters and rotor areas to be evaluated encompass values between 50% smaller and 50% larger than the original baseline design. Blade diameters between 150 ft and 550 ft. were evaluated.

4.4.1 OPTIMIZATION PROCEDURE

The baseline sizing optimization study used the weight and cost estimating relationships described in Section 4.2. The study resulted in the optimum combination of system parameters for the minimum cost of energy. The procedure that determined these parameters is described in detail below:

Figure 4-23 is a flow chart of the major parameter optimization and is shown as if one parameter at a time were varied. The actual algorithm used in the WINDOPT computer code has multi-variable optimization using the steepest descent method. To read the chart, follow the logic flow from top to bottom.

Table 4-13. Sizing Optimization Accounts

COST	WEIGHT
Rotor (including blades)	Rotor
Drivetrain (including gearbox and shafting items)	Drivetrain gearbox Shaft items (shaft, brake, etc.)
Nacelle (including access, installation, rotor support, control system, etc.)	Nacelle
Generator	Generator
Yaw subsystem	Yaw subsystem
Tower (structural)	Tower
Site interface (electrical and remote control)	Site interface (electrical)
Foundation and site preparation	
Farm interconnection	--
Erection	--
Transportation	--
Spares	--
Operation and maintenance	--

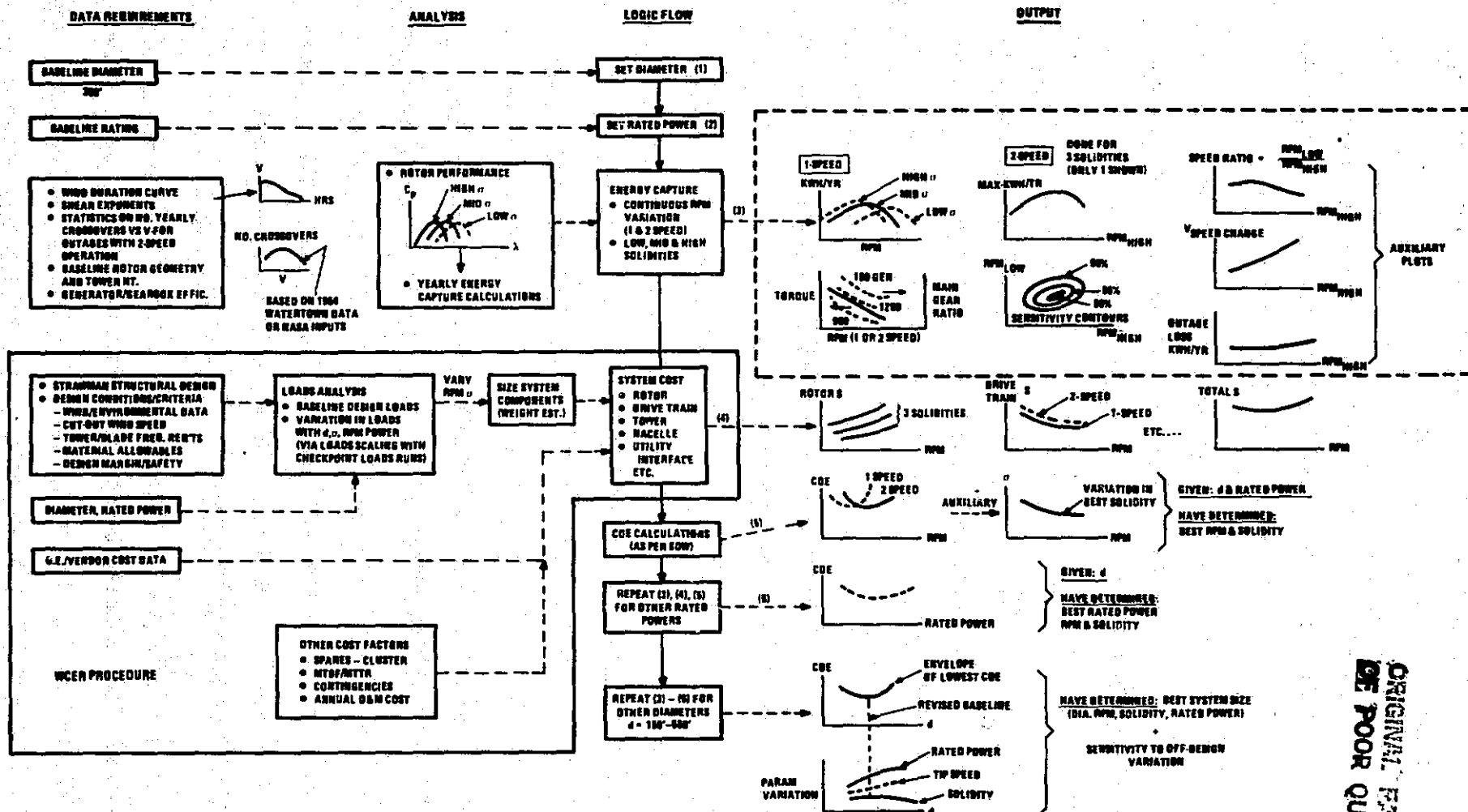


Figure 4-23 Major Parameter Optimization Flow Chart

The data requirements, analysis, and output columns clarified each step. Steps one and two initialized the diameter and power rating to 350 ft and 4 MW, the proposed baseline values. In step three the yearly energy capture was computed as a continuous function of rotor speed for rotors with low, medium (baseline), and high solidities. These calculations followed the procedure outlined in section 4.2.15. For the case of a two-speed rotor, actual wind data was used to compute the energy losses incurred during rotor speed changes. This data was the number of speed changes that occurred every year as a function of wind speed. For the two-speed studies, the most important variables were the upper rotor speed and the ratio of the two rotor speeds. The studies searched for the change-over wind speed that maximized energy for a given set of variables. The rotor speeds were subject to the restriction that the maximum torque at the lower rotor speed was less than or equal to the maximum torque at the higher rotor speed. Typical energy capture plots are sketched in Figure 4-23. For single speed operation, energy per year versus rotor speed was plotted for various solidities. The plots of rated torque and gear ratio versus rotor speed applied to both single and two-speed operation. The torque and gear ratio data were used to determine the size, weight and cost of the gearbox. Energy capture versus the higher rotor speed was plotted, and auxiliary plots supplied the corresponding optimum speed ratio and change-over wind speeds. Related data was shown in the form of sensitivity contours, in which curves of constant energy were shown on a graph of low versus high rotor speed. The contours were used to determine how exact the selected rotor speed had to be, to be consistent with the natural frequency separation requirements of the tower.

The fourth step of the procedure was to determine the costs associated with operation at various rotor speeds and solidities. The costs were determined from the weight and cost estimating relationships. Design driving loads were first computed for the sizing parameters: diameter, solidity, tip speed and rated power. The variation in loads as a function of sizing parameters was determined using loads scaling formulae, supplemented by "check case" load runs, which ensured that the trends were accurate for given values of the sizing parameters. A table was entered into the program, to find the critical design loads. The loads were used to determine the size of the structural elements of the system. For example, the procedure that was used to determine

the size of the blades is illustrated in Figure 4-24. For a given set of sizing parameters, a table was entered and a set of design loads was determined, using wind data. For fatigue loads, only the cut-out speed was used to establish conservative trends. The design loads and blade geometry were entered into a "blade section" subroutine, which computed the mass distribution and stresses. The stresses were compared to the material limits and skin thickness and revised, if necessary, to yield a predetermined margin of safety. Blade costs were generated, based on their planform geometry and cross-sectional dimensions. In particular, the subcontractors provided data on cost per foot and per pound, given the weight per foot and the chord length. This data was integrated over the blade length and the joint costs were added, to estimate the total blade cost and weight, excluding the hub. This procedure is more involved than the simple power formula previously used to scale cost and weight from a known baseline. However the extra work was justified by the increased accuracy in the resulting trends and because of the very large range being investigated. For other system components, such as the gearbox and generator, the weight and cost estimating procedures were simply based on the rate of change around the baseline. For example, generator costs depend on the power rating, and gearbox costs can be determined from the rated torque and gear ratio.

In step five, costs for the individual components, the entire system, spares, site preparation and operation and maintenance were determined. The cost of energy was calculated according to the formula in the statement of work. Cost of energy was plotted as a function of rotor speed; the "bucket" in the curve defined the optimum for the current diameter and power rating. A cross plot was produced to show cost of energy versus rotor diameter for constant power ratings.

Steps three through five were repeated for other power ratings until an optimum system was established at the current diameter. The optimum configuration is not necessarily the point of maximum energy capture; it is the combination of energy capture and cost that yields the lowest cost of energy. Finally, other diameters were analyzed to complete the system sizing study.

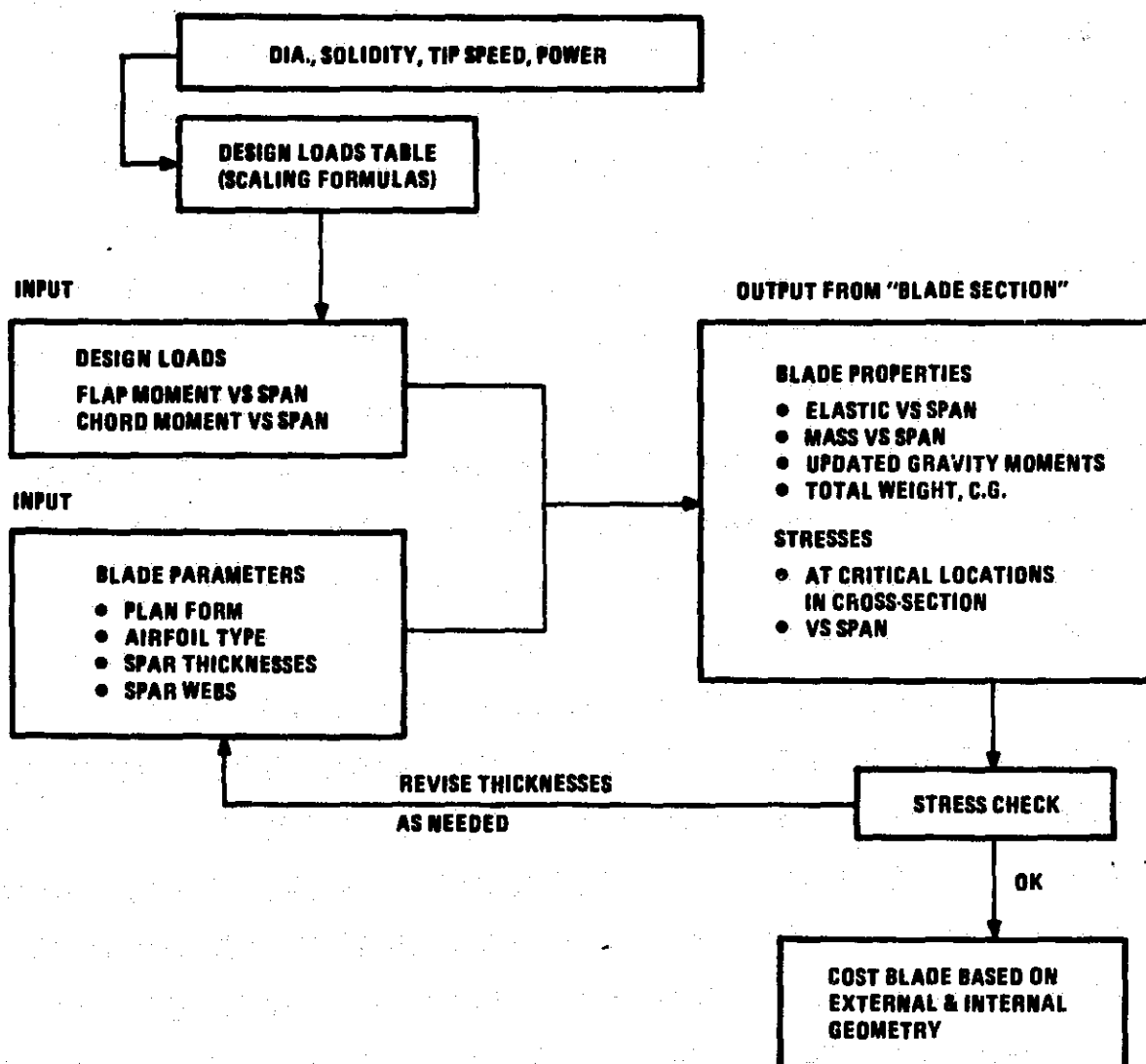


Figure 4-24 Blade Cost and Weight Estimating Procedure

4.4.2 COST OF ENERGY MINIMIZATION

The cost of energy was computed in accordance with the design specification procedure shown in Table 4-14. The objective was to reduce the cost of energy by optimizing the system sizing parameters.

A computer code called WINDOPT optimized the cost of energy using multi-variable scan and maximum slope techniques. A representative output is shown in Figure 4-25. The output illustrates the system's sensitivity to rotor diameter and power density. The other sizing variables were held constant at the values noted.

The results of the sizing optimization indicated that the system with the lowest cost of energy had an upwind, 400-ft wood rotor on a 250 ft. tower and a 5000 kW rating. This configuration was identified as Model 204.0 at the conclusion of the program conceptual design phase.

- o Cost of Energy = $\frac{\text{LEVELIZED ANNUAL COST}}{\text{AVAILABLE ANNUAL ENERGY}}$ (IN MID 1980 \$)(SEE WORK STATEMENT, EXHIBIT E)
- o LEVELIZED ANNUAL COST INCLUDES:
 - CAPITAL COST AT 0.18 FIXED CHARGE RATE
 - LAND COST AT 0.15 FIXED CHARGE RATE
 - OPERATING & MAINTENANCE COST AT 2.0 LEVELIZING FACTOR
 - PERIODIC REPLACEMENT LEVELIZED COST
- o AVAILABLE ANNUAL ENERGY INCLUDES:
 - SYSTEM POWER CHARACTERISTIC
 - SYSTEM LOSSES
 - STATEMENT OF WORK 14 MPH MEAN WIND REGIME
 - SCHEDULED AND UNSCHEDULED MAINTENANCE
 - AVAILABILITY DETERMINED FROM RAM ANALYSIS

Table 4-14. Cost of Energy Computation

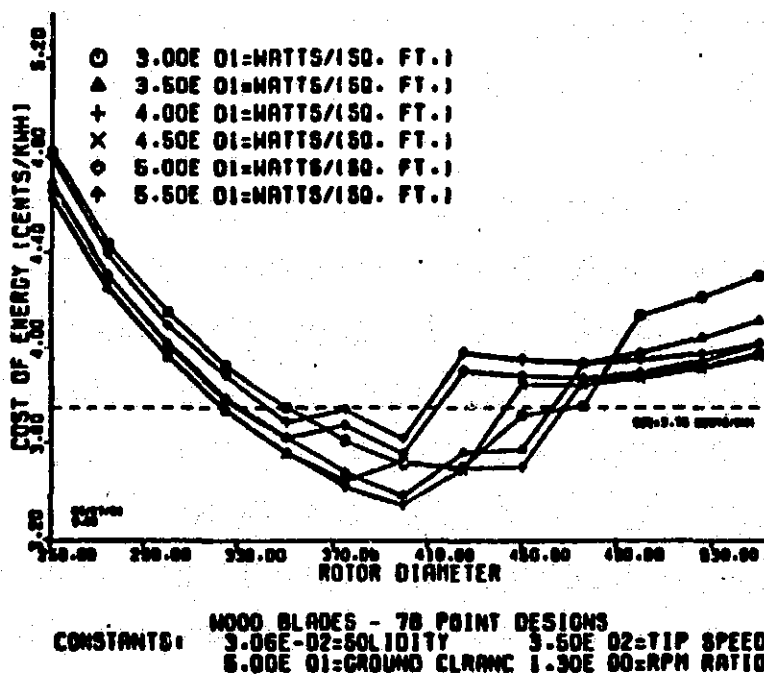


Figure 4-25 Results of Tip Speed Variation and Power Density Variation

4.5 CONCEPTUAL DESIGN DEVELOPMENT (MODEL 204.0)

The evolution of the conceptual design of the MOD-5A is shown in Figure 4-26. The development of weight and cost estimating relationships, trade-off studies, and size optimization, which were described in the preceding sections, resulted in the Model 204.0 configuration as the conceptual design baseline. The major characteristics of this design are shown in Figure 4-27 and in Tables 4-15 and 4-16.

4.5.1 CONFIGURATION

The model 204.0 configuration was optimized for a minimum cost of energy in a mean wind speed of 14 mph, measured at 32.8 ft. above the grade. The cost of the installed equipment assumed that this unit is the 100th of a production run of 1,000 units. A special production plant, illustrated in Figure 4-28, was used to develop manufacturing data.

Rotor - The rotor was 400 ft. in diameter, located upwind of the tower at an angle of 9° for clearance between the blade and the tower. The blade construction is shown in Figure 4-29. Each blade was divided into three sections. The tip section was moveable, for rotor torque control. The inner blade section was attached to the steel hub with threaded stud inserts, which were bonded with epoxy into the wood. The inner blade and outer blade sections were attached in the field with a finger joint. Stud joints attached the steel partial span control, shown in Figure 4-30, to the wood outer blade and tip sections.

The load carrying parts of the blade were made of 0.10-in. thick, rotary cut Douglas fir veneer, bonded with epoxy at room temperature in female molds. The upper and lower surfaces were made separately. The mold surface provided excellent control of the contour and surface finish. After bonding the upper and lower surfaces together with a shear web, the trailing edge was added and the blade was wrapped with glass fiber. The reverse curvature of the NASA 64XXX airfoil was made possible by using the molding process. This shape provided good performance of the structurally efficient thick blade.

Partial Span Control - The partial span control structure, illustrated in Figure 4-30, comprised two steel weldments, a shaft 16 in. in diameter,

Table 4-15 Model 204.0 Configuration

System Weight (lb)	1,209,124
Installed Cost (Volume, 1980 \$)	3,366,377
Annual Energy (GWH, SOW wind, 0.96 AF)	19.21
Cost of Energy (Volume, 1980 \$)	3.32

Rotor 301,604 lb.

- o Upwind of tower
- o 400-ft. diameter
- o 350 ft/sec tip speed
- o 12.8/16.7 rpm, two-speed operation
- o Laminated wood blades and tip
- o 64-XXX Airfoil, 234 in. root chord, 3.06% solidity
- o 25% (50 ft.) hydraulically powered partial span control -90° motion
- o Steel hub, stud joints with blade
- o Steel partial span control, stud joints with blade and tip
- o Hub mounted hydraulic power unit 9° tilt, ±9° teeter allowance
- o Shaft-hub interface with low friction teeter bearings and brake type restrictor. Shaft bolts to 1st stage of gearbox

Drivetrain 235,119 lb.

- o Hybrid rotor integrated gearbox, 2.34 million ft-lb input torque
- o Planetary 1st stage gearing, split parallel shaft 2nd stage
- o 3rd stage underrunning shifter, warm shift procedure, inching drive
- o Stiffness and damping control at 1st stage
- o Rotor and gear supported by two-row monobearing integrated into gear case with load path to bedplate
- o In-line slipring access, shaft drive lube pump, rotor lock, parking brake
- o Floating high speed shaft
- o 5,000 kW, 1,200 rpm synchronous generator

Nacelle 116, 956 lb.

- o Bedplate type with wiring, piping runs under flooring
- o Mountings for gearbox, generator, control electronics, high voltage cabinet
- o Insulated weather fairing
- o Lubrication system for gearbox and bearings on lower platform
- o Yaw structural adapters and bearing
- o Hydraulic power supply and push-pull yaw drive
- o Yaw slipring

Tower 505,798 lb.

- o 14.5 ft. diameter steel shell
- o 250 ft. to rotor hub
- o 50 ft. tapered bell for tuning
- o Internal cable lift and ladder

Foundation

- o Spread footing, reinforced concrete
- o About 960 cubic yards
- o Anchor bolts for tower attachment

Electrical 49,627 lb.

- o Walk-in aisle switchgear and control enclosure
- o 5,000 kVA oil-filled transformer with fused switch
- o 69 kV nominal interface
- o 150 MVA radial feeder cluster, with 30 units

Maintenance

- o Permanent cluster crew

Table 4-16 MOD-5A Design Innovations

FEATURE	MAJOR BENEFIT
<p><u>ROTOR</u></p> <ul style="list-style-type: none"> • WEATHERVANING ROTOR ASSY • WOOD LAMINATE BLADES (MULTI-MEGAWATT APPLICATION) • TILTED ROTOR (INCLINED AXIS) • HIGH EFFICIENCY ROTOR 	<ul style="list-style-type: none"> • REDUCE HURRICANE LOADS BY FACTOR OF <u>TWO</u> • REDUCES SYSTEM COST AND WEIGHT, WITH PROVEN TECHNOLOGY • SMALLER, LIGHTER NACELLE AND SUPPORT STRUCTURE • HIGH PERFORMANCE AIRFOIL SECTION (64XXX) AND GOOD SURFACE FINISH (1/4 ROUGH) IMPROVES ENERGY CAPTURE
<p><u>GEARBOX</u></p> <ul style="list-style-type: none"> • HYBRID EPICYCLIC/PARALLEL SHAFT DESIGN • INTEGRAL ROTOR BEARING ARRANGEMENT • ADJUSTABLE GEARBOX COMPLIANCE • TWO SPEED GEARBOX 	<ul style="list-style-type: none"> • HIGH TORQUE CAPABILITY AT INPUT, LOW COST AT HIGH SPEED END • SIGNIFICANT REDUCTION IN MOMENTS ON NACELLE SUPPORTS. REDUCE BEDPLATE WEIGHT AND COST. • PROVIDES LOAD ALLEVIATION AND DRIVE TRAIN TUNING. • OPTIMIZES ENERGY CAPTURE.
<p><u>YAW DRIVE</u></p> <ul style="list-style-type: none"> • PUSH-PULL, HYDRAULIC SYSTEM 	<ul style="list-style-type: none"> • PROVIDES ACTIVE YAW CONTROL AT LOW COST, WITH HIGH RELIABILITY • ELIMINATES BACKLASH

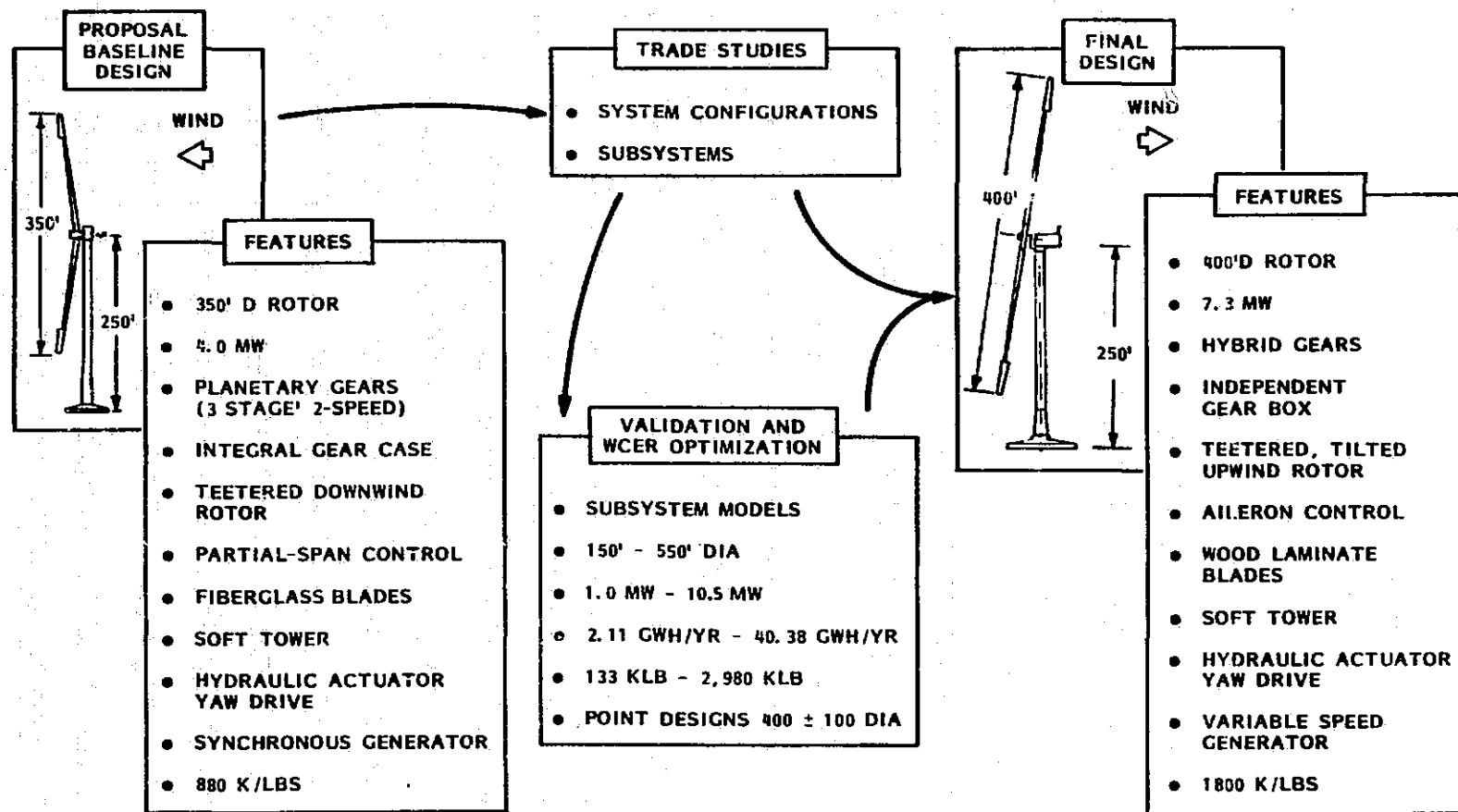


Figure 4-26 Design Evolution

MOD-5A CONCEPTUAL DESIGN

MODEL 204

TOOTH UNIT COST: \$3,366K
COST: 3.32¢/KWH
\$/KW: \$873

OPERATIONAL CHARACTERISTICS

RATED POWER	5000 KW @ .98PF
RATED WIND SPEED	29.5 MPH @ 250 FT.
CUT-IN/CUT-OUT WIND SPEED	14/44 MPH @ 250 FT.
MAXIMUM WIND SPEED (SURVIVAL)	150 MPH @ 250 FT.
ROTOR DIAMETER	400 FT.
BLADES	2
ROTOR LOCATION & CONFIGURATION	UPWIND/TEETERED
PITCH CHANGE	25% PARTIAL SPAN CONTROL
ROTOR RPM	12.8/16.7 RPM
TOWER	250' (TO HUB CENTERLINE)
ENERGY CAPTURE/YR.	19.21×10^6 KWH (14 MPH ANNUAL AVERAGE WIND SPEED @ 32 FT.)
TOTAL WT. ON FOUNDATION	1209 KLB

FEATURES

- MOD0 LAMINATE BLADES WITH HIGH PERFORMANCE AIRFOIL
- TILTED ROTOR (9°)
- INTEGRATED ROTOR SUPPORT GEARBOX
- TUNABLE STIFFNESS IN GEARBOX MOUNTING
- SIMPLIFIED MICROPROCESSOR CONTROL SYSTEM
- SOFT SHELL TOWER, INTERNAL LIFT, TUNABLE BELL SECTION AT BASE
- OVERRUNNING COUPLING IN H.S. SHAFT TO REDUCE LOW WIND ENERGY LOSS

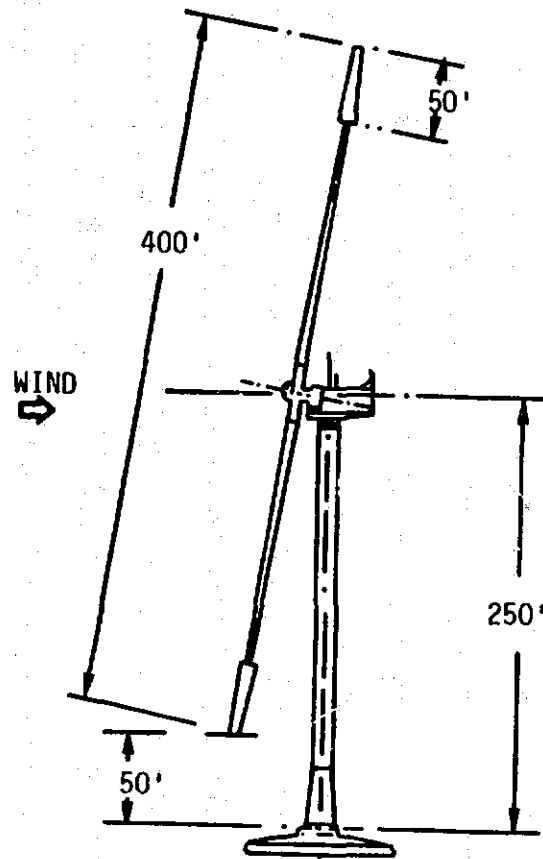
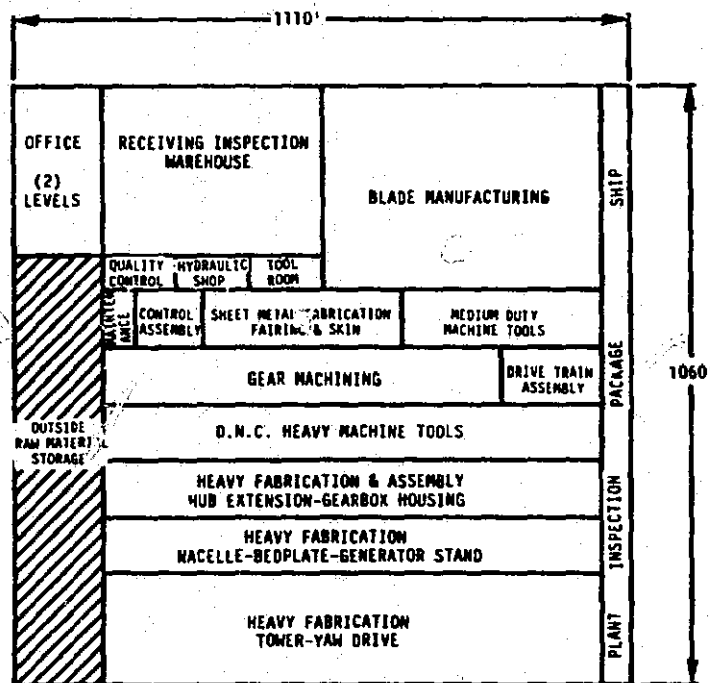


Figure 4-27 MOD-5A Conceptual Design, Model 204.0



MOD-5A PRODUCTION PLANT LAYOUT

- NEW, DEDICATED, VERTICALLY INTEGRATED PLANT
 - SOUTHEAST USA
 - HIGH EFFICIENCY
 - HIGH MAKE-TO-BUY RATIO
 - SIZE: 1 MILLION/FT²
 - PLANT COST: \$100 MILLION
 - EQUIPMENT COST: \$82 MILLION
- PRODUCTION RATE - 30/MONTH
- ESTIMATED DIRECT HOURS PER WTG: 40,780
- TOTAL EMPLOYEES: 11,029
 - DIRECT: 7,058
 - SUPPORT: 1,765
 - SALARIED: 2,206
- BURDENED PRODUCTION WAGE RATE AVERAGE: \$30.00/HOUR
- OVERHEAD RATIO: 2.7 (TYPICAL HEAVY INDUSTRY)
- SELL PRICE (INSTALLED): \$3,243K

ORIGINAL PAGE IS
OF POOR QUALITY

DETAILED MANUFACTURING ANALYSIS
VALIDATES OUTPUT OF MCER'S
FOR COST AND COE COMPUTATION

Figure 4-28 MOD-5A Production Plant Layout

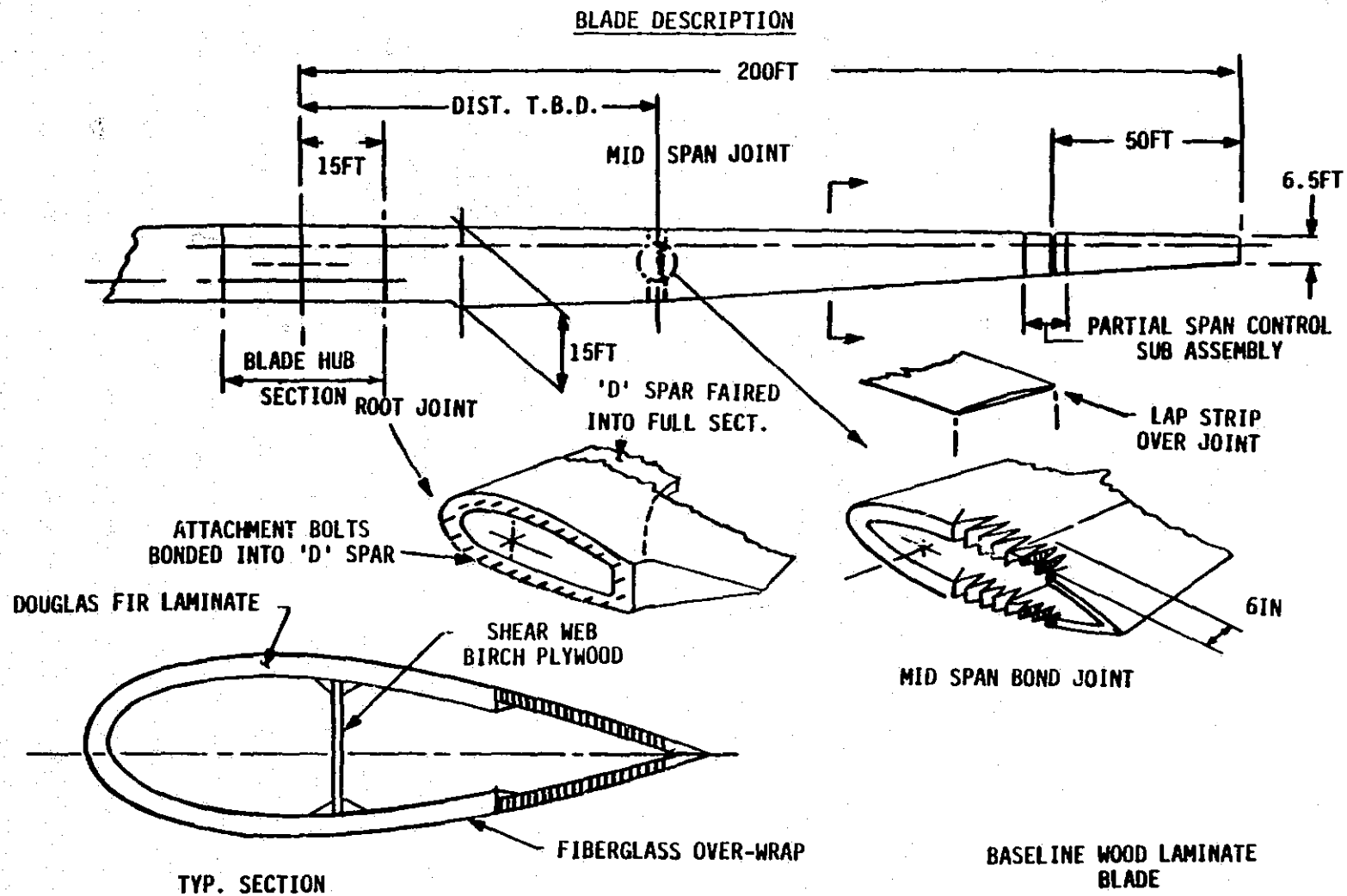


Figure 4-29 Description of the Blade

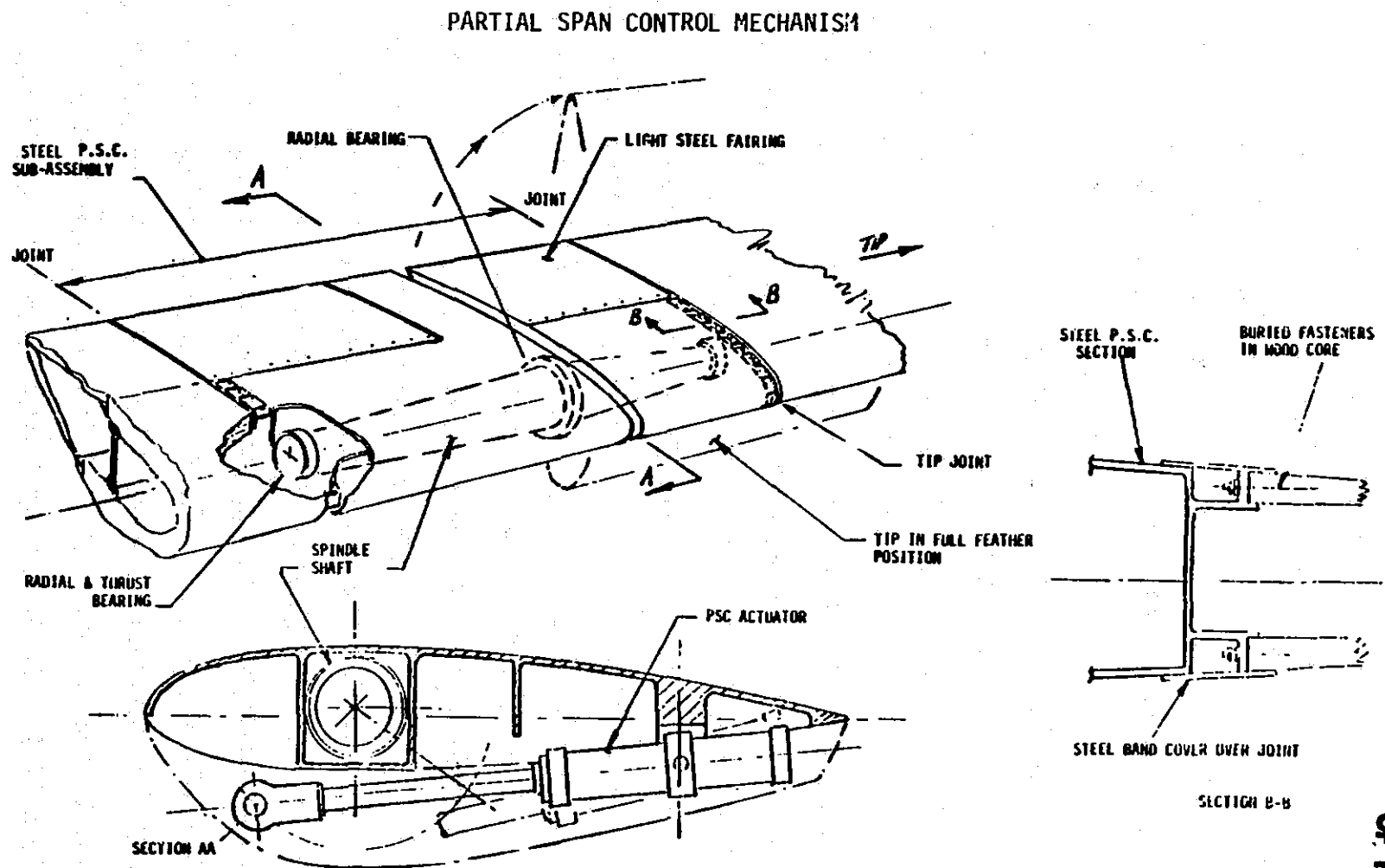


Figure 4-30 Partial Span Control Mechanism

bearings and an actuator. A servo valve, located near the actuator, controlled the position of the actuator, which rotated the 50 ft. tip through a direct crank arm. The hydraulic supply system for the actuators was located on the hub and a separate emergency feather accumulator was provided for each blade, as shown in Figure 4-31. The steel weldments were attached to the outer blade and tip sections with studs, and were covered with light, airfoil-shaped skins. The tapered shaft was secured to the outermost weldment and was retained by bearings in the innermost weldment.

The weldments provided load paths, which transferred the tip shear and bending loads from the stud plane into the shaft. The radial bearings were separated by 80 in., to carry bending loads into the shaft. The innermost bearing also reacted centrifugal loads. The shaft and bearings were assembled into a flanged compression tube that "plugged into" the innermost weldment and was secured at the actuator location.

The actuators were conventional, but had been modified for use in centrifugal accelerations of 20 g. The modifications included stop tubes and heavy duty seals and guide rings. A separate emergency valve system and control circuit controlled emergency tip feathering as a backup for the normal tip control through the servo valves and system controller. Only one tip was required to feather to stop the rotor. The separated control and hydraulics provided for the motion of at least one tip.

Hub and Shaft - An oval steel hub transmitted loads between the blades, and provided structure for the redistribution of rotor weight, torque, and thrust loads from the shell to the teeter bearing housings. The shaft was a flanged, steel tube weldment. The design of the shaft was driven by the cyclic bending moment that occurred because of the rotor weight. The teeter bearing trunnion shafts were bolted to the flattened sides of the tube and the flange was bolted to the gearbox.

The hub, shaft, and teeter elements are illustrated in Figure 4-32. A large oval cutout on one side of the hub allowed the shaft to enter and was also large enough to permit inspectors to enter. The flanges on either side of the cutout provided a gripping surface for the teeter motion restrictors attached to the shaft.

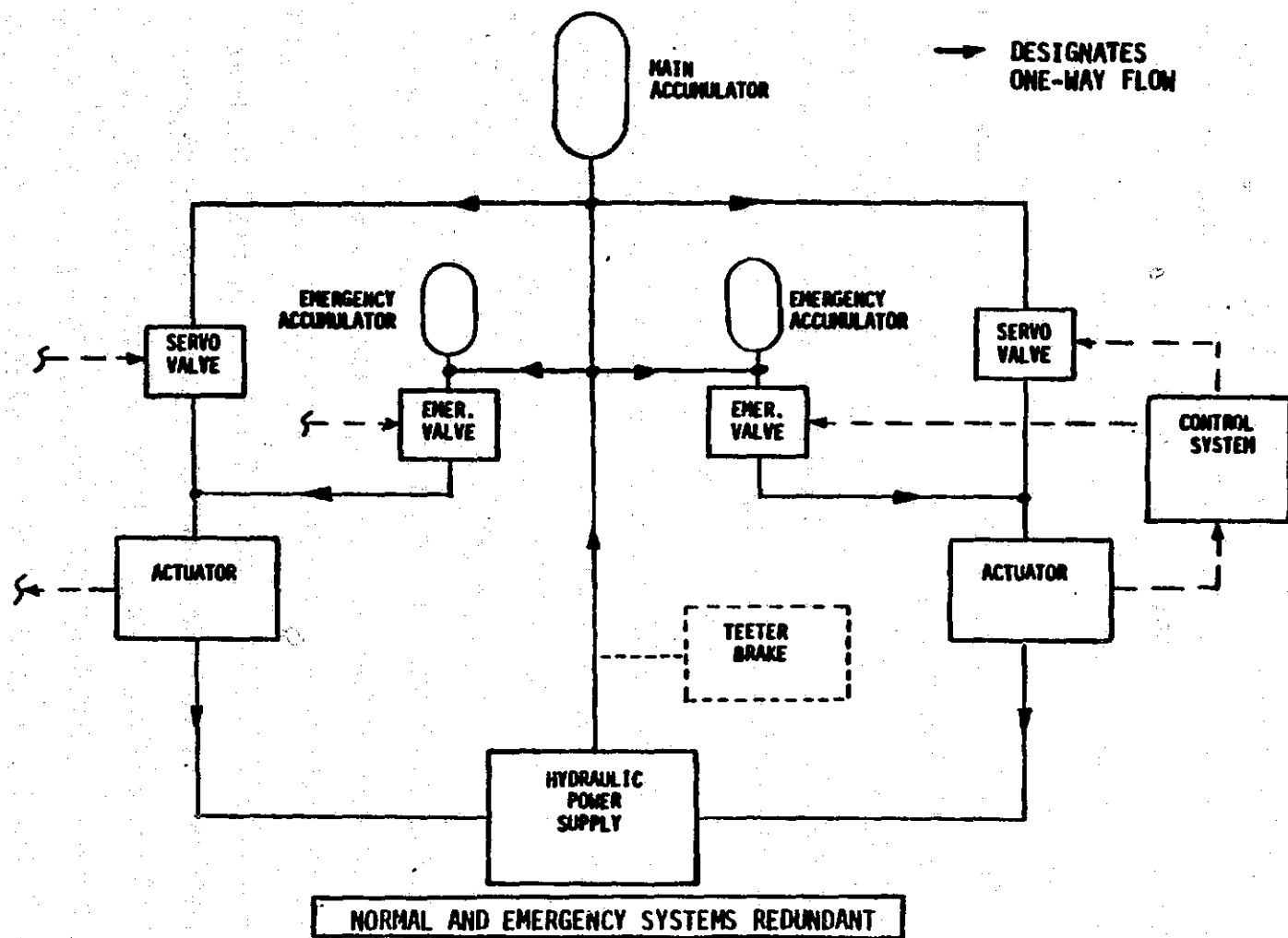
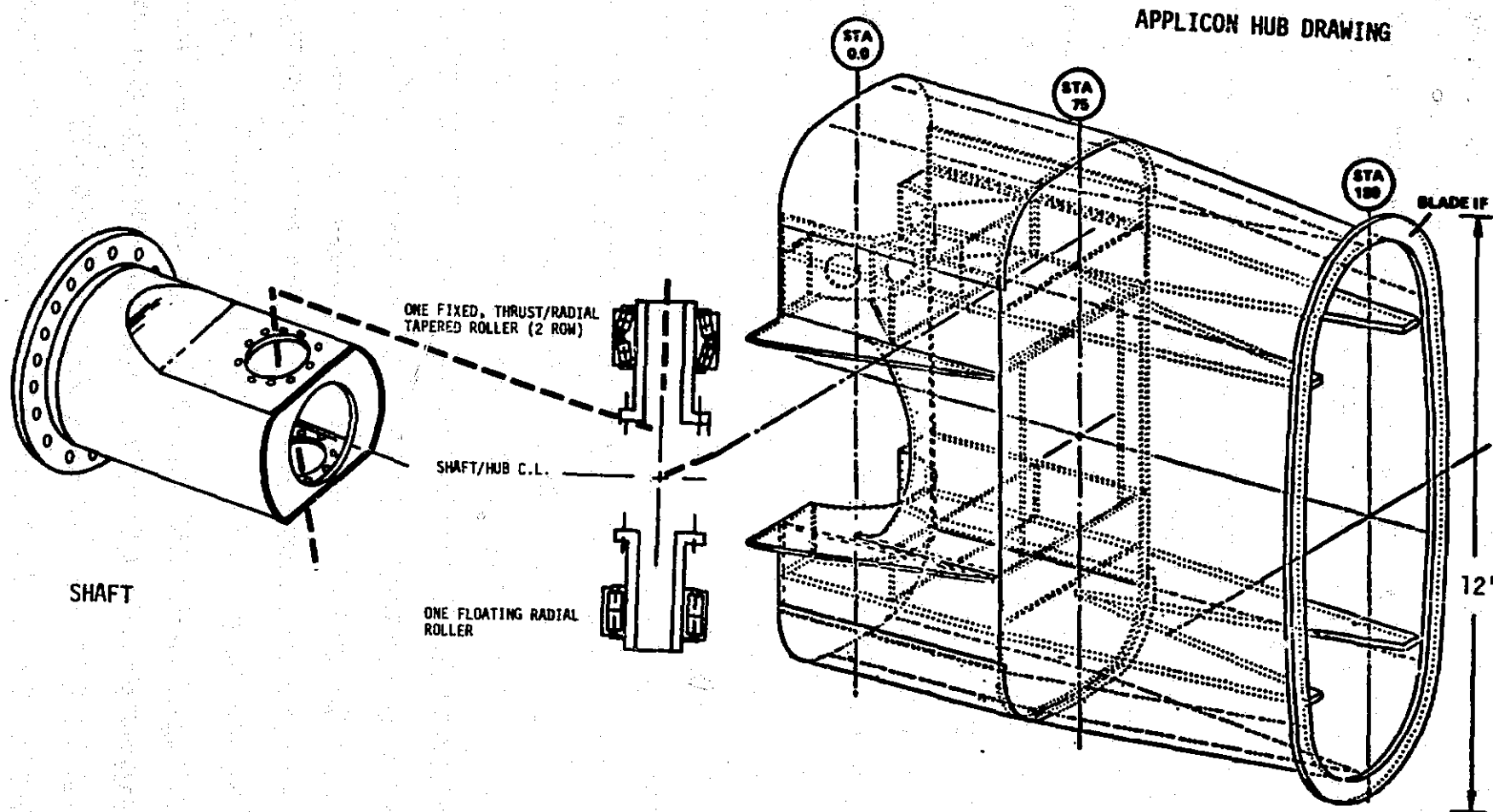


Figure 4-31. Pitch Hydraulics Block Diagram



ORIGINAL PAGE IS
OF POOR QUALITY

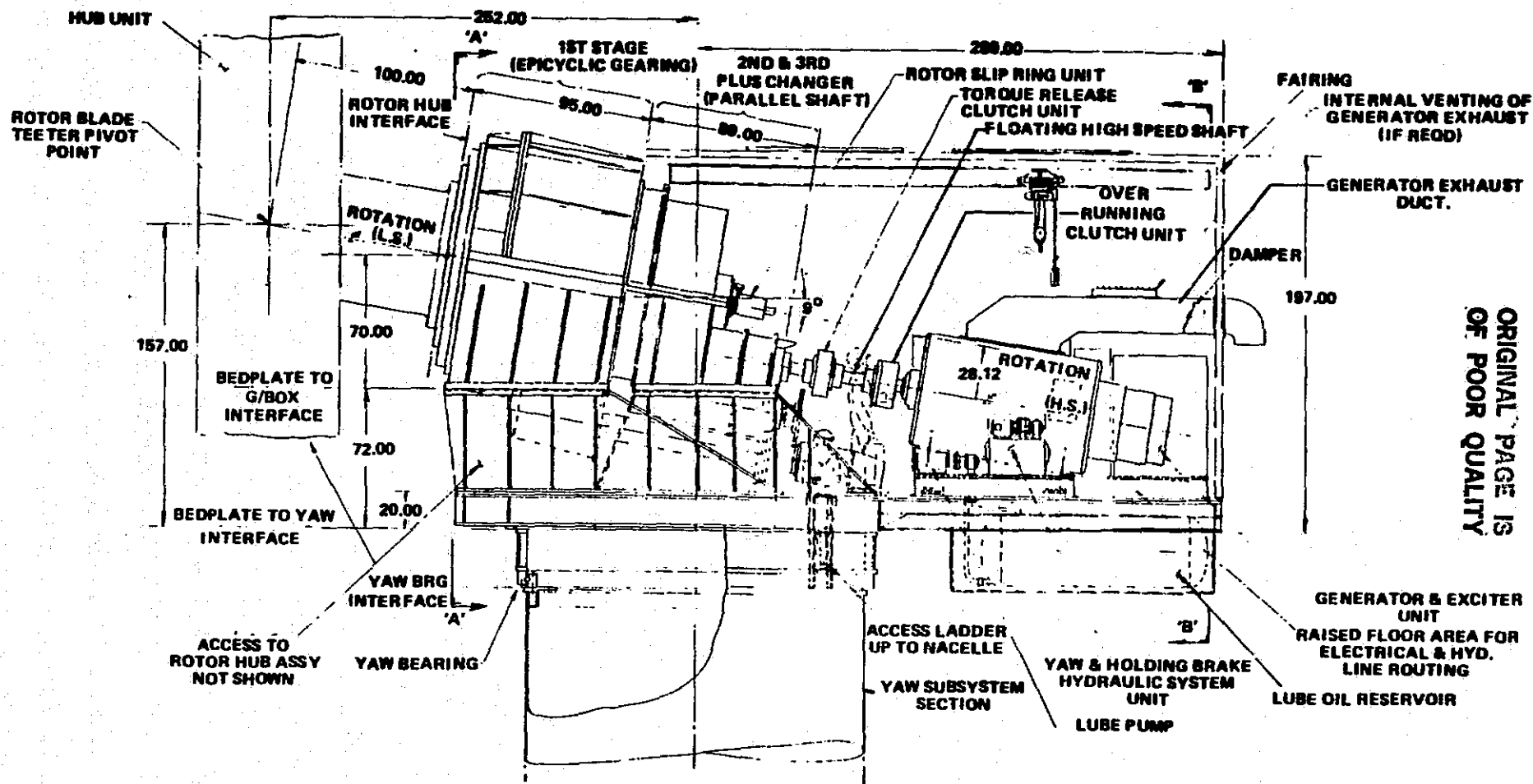
Figure 4-32 Hub, Shaft and Teeter Arrangement

Teeter motion through angles up to 9° was permitted by oil bath lubricated bearings. Torque, thrust and weight loads were carried by radial bearings when the rotor was vertical. Weight loads were carried by the thrust capability of the tapered bearing set when the rotor was horizontal. The bearing assemblies were designed so that they could be replaced without disassembling the entire rotor.

Nacelle - The nacelle assembly is shown in Figure 4-33. Rotor thrust and weight loads were transmitted from the shaft, through the main bearing in the gearbox, into the gearbox case structure, the bedplate, and the yaw to the tower structure. Torque was reacted through the gearbox case. Power flowed through the gearbox to the highspeed shaft and generator. The bedplate provided mounting structure for the gearbox, generator, yaw hydraulic subsystem, gearbox lubrication subsystem, an environmental fairing, and electrical equipment. A maintenance hoist, aircraft warning lights and wind sensors were mounted on the fairing, which provided protection from the environment for the generator and other nacelle subsystems.

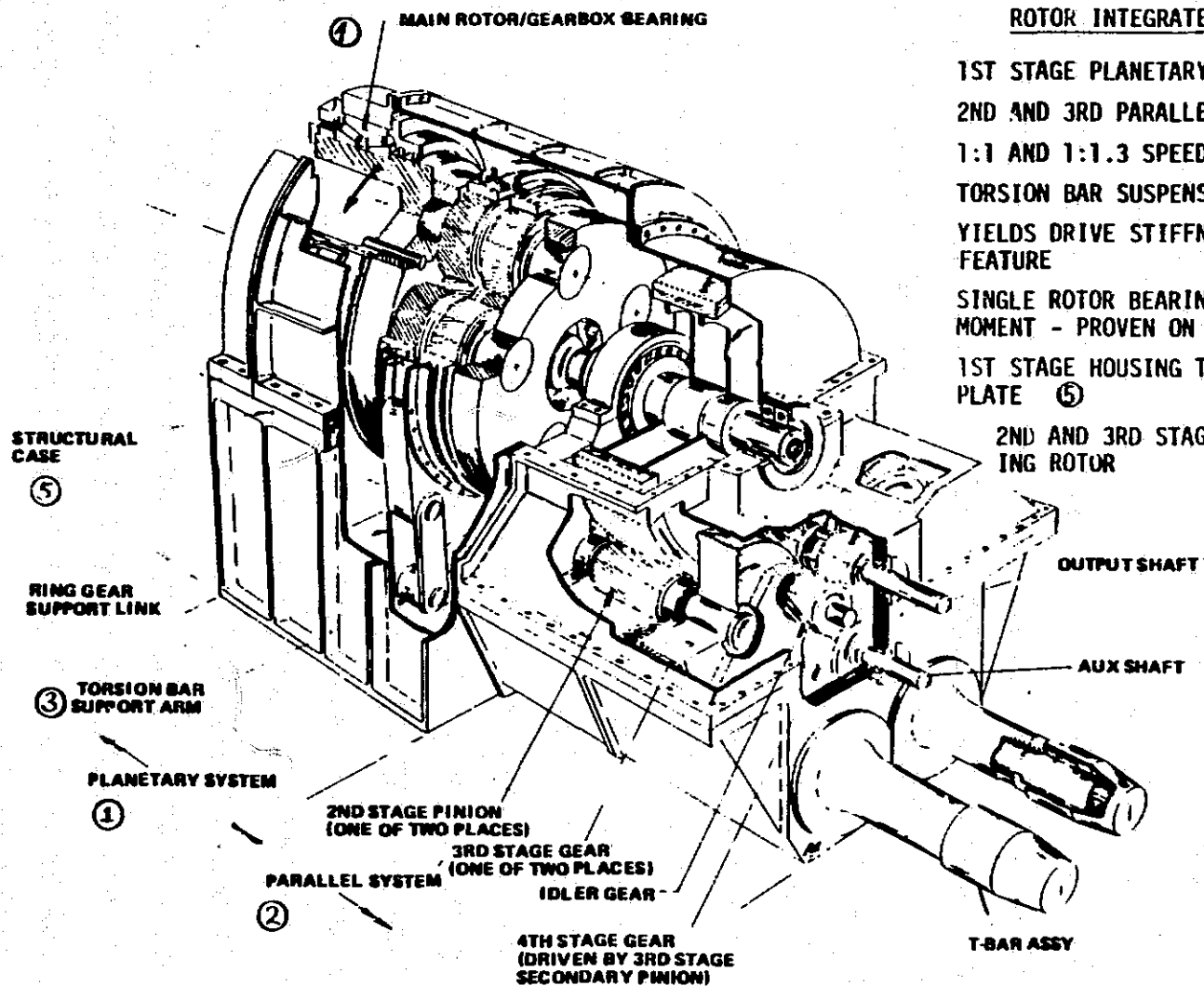
Drivetrain - The 5000 kW synchronous generator operated at 1200 rpm and delivered 4160 V. A highspeed shaft connected the generator and gearbox through gear couplings, an overload release clutch and a one-way underrunning clutch. The overload clutch did not allow torques greater than 175% of the rated torque to reach the gearbox from the generator. The underrunning clutch aided speed changing and allowed the rotor to underrun the synchronous generator speed during transient low winds.

Several features were provided by the gearbox, shown in Figure 4-34. The main bearing supported the rotor and the large, first-stage planetary gear. A floating sun shaft connected the first stage to the bull gear of the split path, parallel shaft second stage. The two third stage gears drove two shafts. The auxiliary shaft was always connected to the gearing. It provided an external parking brake and inching drive interface. The output shaft was connected through a gear changer to either the upper pinion or the lower gear and idler for two-speed operation. The first stage ring gear was rotationally restrained by a dashpot and torsion bar linkage, to provide good drivetrain



ORIGINAL PAGE IS
OF POOR QUALITY

Figure 4-33 Nacelle Cross-Section



ROTOR INTEGRATED HYBRID GEARBOX

1ST STAGE PLANETARY ①

2ND AND 3RD PARALLEL SHAFT ②

1:1 AND 1:1.3 SPEED CHANGE RATIOS

TORSION BAR SUSPENSION ③

YIELDS DRIVE STIFFNESS AS REQUIRED AND DAMPING FEATURE

SINGLE ROTOR BEARING SIZED TO CARRY ROTOR OVERTURNING MOMENT - PROVEN ON MOD-1 ④

1ST STAGE HOUSING TRANSMITS LOAD DIRECTLY INTO BED-PLATE ⑤

2ND AND 3RD STAGES CAN BE REMOVED WITHOUT DISTURBING ROTOR

ORIGINAL PAGE IS
OF POOR QUALITY

Figure 4-34 Rotor Integrated Hybrid Gearbox

damping and stiffness characteristics. A small slipring was mounted on the back of the gearbox in line with the main bearing axis. The slipring provided a route for power and control signals to the rotor. A shaft-driven pump provided operating lubrication oil during normal operation, and an electric motor driven pump provided oil during starting and emergency operations.

Yaw - The yaw assembly, shown in Figure 4-35, consisted of the upper and lower interface structures, the yaw bearing, the yaw slipring, the yaw drive, and the tower lift support and landing deck. A bolted interface was provided with the bedplate and a weld interface was provided with the tower. The push-pull yaw drive was installed on the nacelle side of the yaw bearing. Fixed and moveable brakes gripped a flange to hold the nacelle or to rotate the nacelle in a ratchet-action motion. A centrally located slipring was the route for main power, control and instrumentation circuits. The cable climbing lift was protected by the tower. The yaw bearing was a grease-lubricated crossed roller bearing.

Tower and Foundation - The tower is shown in Figure 4-36. The upper 200 ft. was a steel shell, 14.5 ft. on the outer diameter. Wall thicknesses varied from 0.5625 in. at the top to 1.4375 in. at the transition between the tower and the flared base. The lower 30 ft. of the tower was a tapered bell-shaped shell with a base flange secured to the foundation with anchor bolts. A spread foundation, with extra reinforcing bar, was designed for soils at a general site.

Electrical Equipment - Ground-mounted electrical equipment was designed into a protected aisle arrangement shown in Figure 4-37 and connected to the main transformer for voltage step-up to the 69 kV grid. Main power switching and protective devices were installed in metal-clad compartments. The site control interface was located at one end of the structure. The control interface communicated with the wind turbine control, which was a programmable controller located in the nacelle.

A cluster of 30 units was used in the baseline 150 MW configuration, with multiple 69 kV grid ties. The cluster would have a permanent maintenance crew of four workers, and a central spare parts storage location.

FEATURES

- ① **CROSSED ROLLER BEARING**
(BEST COMPROMISE, COST AND PERFORMANCE)
- ② **MOUNTED IN TOP TOWER SECTION**
 - CLEAN INTERFACE WITH NACELLE
 - FACTORY ASSEMBLY AND C/O
 - MECHANISM ACCESSIBLE
- ③ **SPRING CENTERED GRIPPERS**
RIDE ON BRAKE DISK
- ④ **ALL BEARING BOLTS ACCESSIBLE**
- ⑤ **YAW SLIP RING ACCESSIBLE**

DESIGN EMPHASIZES LOW COST AND EASE OF MAINTENANCE

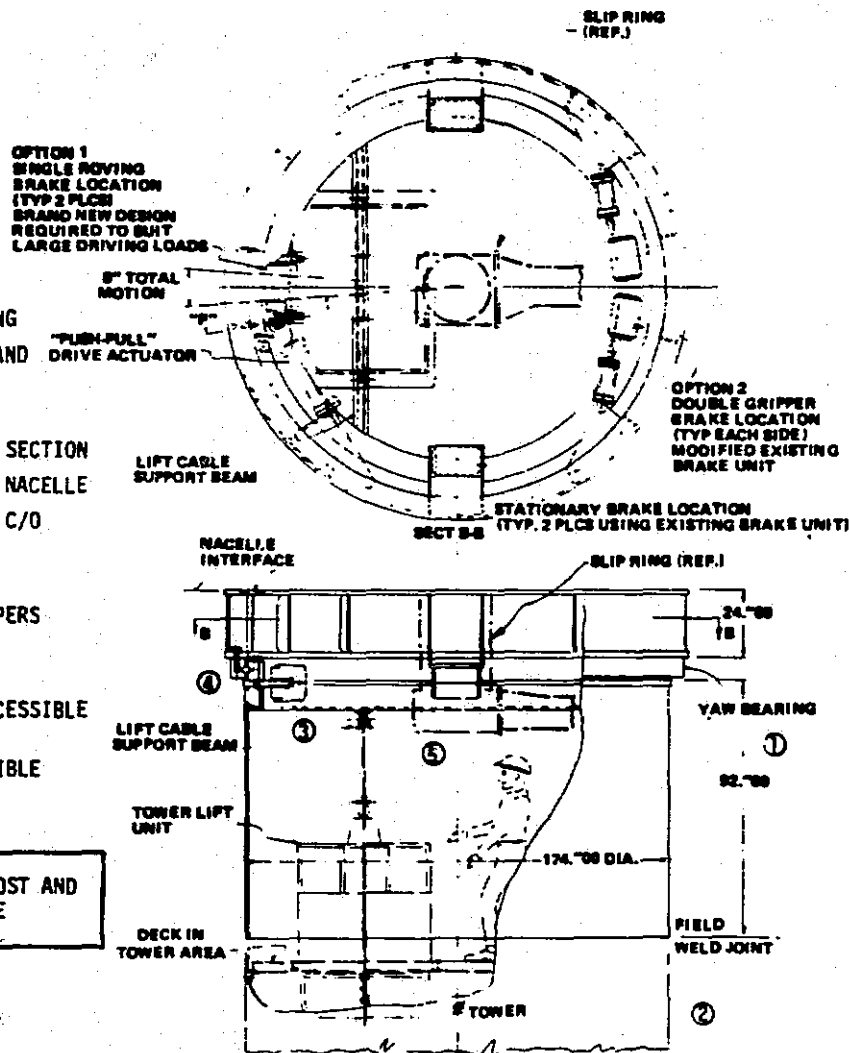


Figure 4-35. Yaw Drive

**ORIGINAL PAGE IS
OF POOR QUALITY**

14'-6"

TOP ACCESS DOOR

PLATFORM

FIELD SEAM BY CD

6 x 4 x 1 CIRCUMFERENTIAL STIFFENER ANGLE (TYP) 10 REQ'D

10 REQ'D

SHELL

20 RINGS @ 10'-0" = 200'-0"

233'-6"

PLATFORM

LADDER

TRANSITION KNUCKLE

BELL DOOR

68'-4"

ELEVATION

t = 0.5625

t = 0.625

t = 0.6875

t = 0.750

t = 0.8125

t = 0.8125

t = 0.875

t = 0.9375

t = 1.00

t = 1.0625

t = 1.0625

t = 1.125

t = 1.1875

t = 1.250

t = 1.250

t = 1.3125

t = 1.375

t = 1.4375

t = 1.4375

t = 1.4375

t = 1.500

t = 1.500

t = 1.250

t = 1.125

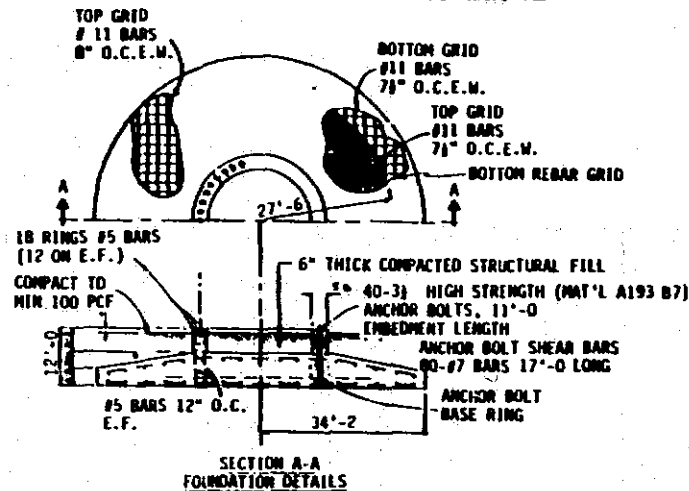
2'-8 13 32

2'-1 25 32

8'-7 13 16

10'-0

10'-0



- SPREAD FOUNDATION - HEAVY REBAR
- STANDARD TOWER/FOUNDATION INTERFACE BOLTING
- TOWER SECTORS FIELD WELDED INTO CYLINDERS
- "SPYDER" LIFT & FULL LENGTH LADDER
- TWO PLATFORMS FOR A/C WARNING LIGHT MAINTENANCE
- 10 CIRCUMFERENTIAL STIFFENERS
- TOWER WEIGHT: 510,050 LBS
- FOUNDATION: 738 CUBIC YARDS

DESIGN DETAILED TO CONFIRM COSTS

Figure 4-36 Tower and Foundation

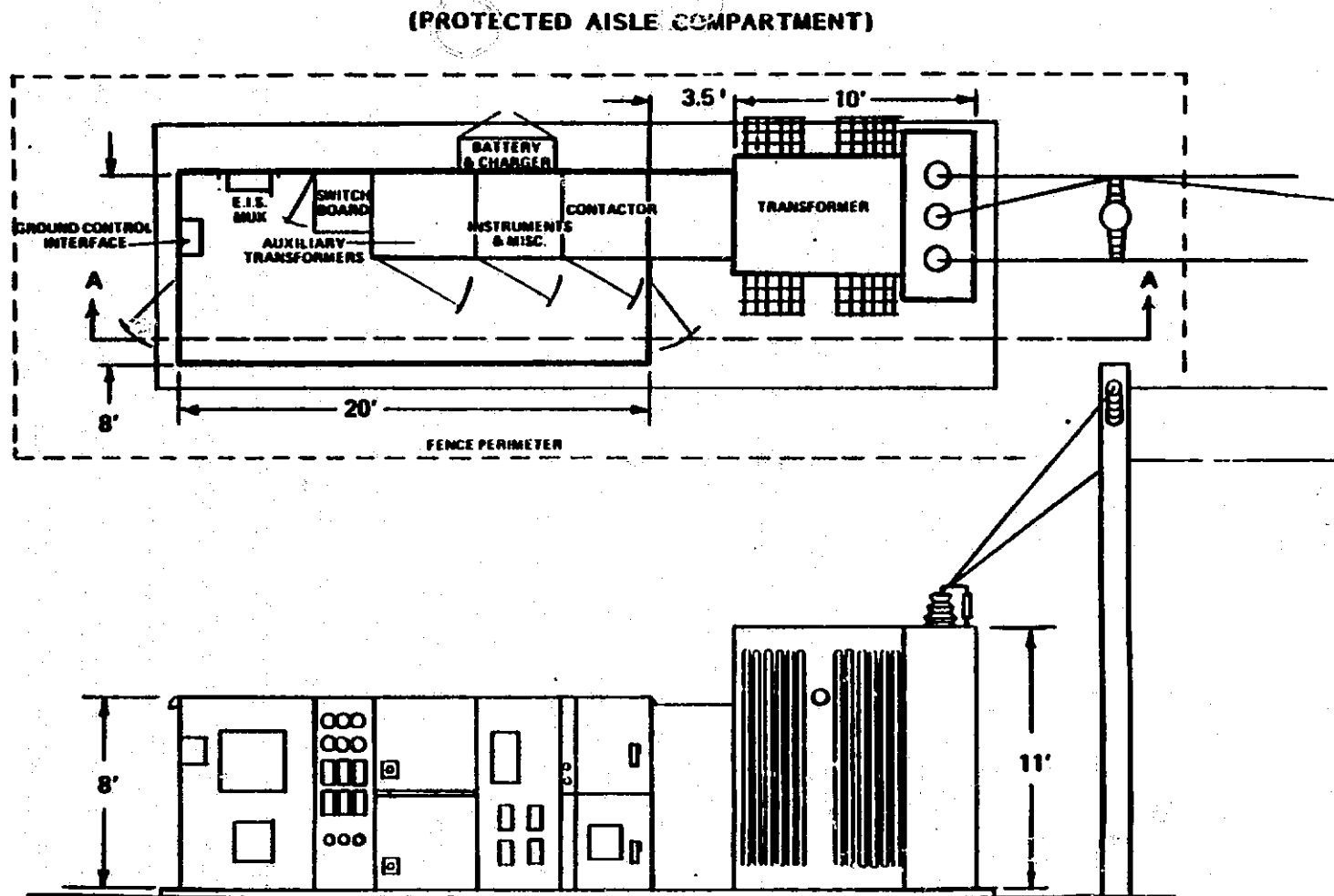


Figure 4-37 Protected Aisle Compartment

4.5.2 PERFORMANCE

The MOD-5A model 204.0 operated in the wind speeds shown in Figure 4-38. The rated power, 5000 kW, was reached at a wind speed of 27.5 mph, at the high rotor speed of 16.7 rpm. The mechanical and electrical losses were about 10% in these conditions, so the rotor output was about 5550 kW. When the wind speed exceeded 44 mph, a high wind shutdown began. Very little energy is available from winds above 44 mph for the design wind duration characteristics. Operation in higher winds requires a design for higher shutdown loads.

At 14 mph, the wind supplies enough torque to start rotation and to accelerate the rotor to operating speed in less than 10 minutes. Once the system is on-line, it delivers power in wind speeds as low as 11.5 mph. For temporary wind speeds below 11.5 mph the rotor would not be able to overcome parasitic losses and would underrun the generator synchronous speed briefly. Prolonged low wind would cause a shutdown initiated by the low rotor speed.

Around 21-23 mph, automatic gear changing achieved the maximum rotor efficiency. Average power was sensed and the control system would use the partial span control to reduce the output power to zero, and cause the rotor to underrun the lower operating speed. Then the gear change would be made while the drive train was rotating, but not loaded. Finally, the partial span control would be moved to speed up the rotor to synchronous speed and resume power generation.

For a mean wind speed of 14 mph, measured at 32.8 ft. above the grade, the net energy output was predicted to be 19.21 million kW-hrs per year. An availability factor of 0.96 was used for the volume production cluster installation, as shown in Table 4-17.

4.5.3 WEIGHT SUMMARY

The MOD-5A model 204.0 weight above the foundation was estimated to be 1,209,124 lb. A weight breakdown is shown in Table 4-18 in the fourth column. Weight percentages are shown in the seventh column.

Table 4-17 Availability Analysis Summary

**AVAILABILITY ANALYSIS
SUMMARY**

ITEM	SINGLE SITE	CLUSTER
AVAILABILITY	.934	.962
UNSCHEDULED EVENTS/YR/WTG	28	28
<u>TOTAL DOWNTIME/YR</u>	578 HRS	336 HRS
● SCHEDULED	94 HRS	94 HRS
● UNSCHEDULED	484 HRS	242 HRS

**SINGLE SITE AVAILABILITY EXCEEDS MINIMUM REQUIREMENT OF .92
CLUSTER AVAILABILITY EXCEEDS DESIGN GOAL OF .96**

Table 4-18 Cost of Energy Report for Model 204.0

CGE REPORT MODEL 204.0								
SUBASS. ABBREV.	ITEM NAME ABBREV.	REF. NUM.	WEIGHT TWOOTH UNIT	COST (1980) TWOOTH UNIT	DOLLARS PER LB.	% OF TOTAL WT.	% OF COE	COE CONTRIB. (1980 CENTS)
SITE	FOUNDATION	110		203,976			5.76	.19
	GRD EQUIP	120	49,647	161,710	3.26	4.11	4.56	.15
	SPECIAL	130		53,440			1.51	.05
			49,647	419,126		4.11	11.83	.39
TRANSPORT.	TRANSPORT.	240		108,821			3.07	.10
ERECTION	INSTALL.	310		116,604			3.30	.11
	INTEG&C.O.	350		73,100			2.06	.07
			0	189,904		.00	5.36	.18
ROTOR	BLADES	410	167,273	219,025	1.31	13.83	6.18	.21
	PCS HYDR	420	9,144	21,900	2.40	.76	.62	.02
	PCS STRUC	421	13,179	20,528	1.56	1.09	.58	.02
	HUB	430	112,008	185,932	1.66	9.26	5.25	.17
			301,604	447,385		24.94	12.63	.42
DRIVE-TRA.	TRANSMIS.	520	199,122	518,156	2.60	16.47	14.62	.49
	HI SPEED	530	3,727	20,056	5.38	.31	.57	.02
	GEN & EXCI	540	32,270	133,074	4.12	2.67	3.76	.12
			235,119	671,288		19.45	18.95	.63
NACELLE	BEDPLATE	610	51,540	36,078	.70	4.26	1.02	.03
	HYD SYST.	620	11,257	19,100	1.70	.93	.54	.02
	FAIR., MISC	646	18,399	70,992	3.86	1.52	2.00	.07
	SLP, ELEC.	6600	1,500	20,600	13.73	.12	.58	.02
	INST & COM	670	2,000	45,300	22.65	.17	1.28	.04
	YAW SUB.	680	32,260	62,371	1.93	2.67	1.76	.06
			116,956	254,441		9.67	7.18	.24
TOWER	TOWER	710	495,798	490,840	.99	41.00	13.85	.46
	PERS. LIFT	720	1,000	20,000	20.00	.08	.56	.02
	CABLING	740	9,000	20,250	2.25	.74	.57	.02
			505,798	531,090		41.83	14.99	.50
REM-CTRL	LINE-MODEM	810		500			.01	
	REM-DISP.	820		2,000			.06	
			0	2,500		.00	.07	.00

Table 4-18. Cost of Energy Report for Model 204.0

Table 4-18 Cost of Energy Report for Model 204.0 (con't)

COE REPORT MODEL 204.0								
SUBASS. ABBREV.	ITEM NAME ABBREV.	REF. NUM.	WEIGHT 100TH UNIT	COST (1980) 100TH UNIT	DOLLARS PER LB.	% OF TOTAL WT.	% OF COE	COE CONTRIB. (1980 CENTS)
SPARES	SPARES	930		28,100			.75	.03
SPECIAL	PROFIT	1010		256,481			7.24	.24
	ASM/TEST	1020		97,882			2.76	.09
	GR'TH BUGT	1030		170,987			4.83	.16
			0	525,350		.00	14.83	.49
LAND	WTG LAND	1110		4,959			.12	
	ROAD LAND	1140		964			.02	
			0	5,923		.00	.14	.00
CLUSTER	SUBSTATION	1240		33,164			.94	.03
	TRANSM ETC	1250		131,948			3.72	.12
			0	165,112		.00	4.66	.15
O&M REFS. 400-699	YEARLY O&M	1340		17,337			5.44	.18
TOTALS:								
WEIGHT 100TH UNIT.....			653,679					
COST 100TH UNIT.....			1,373,114	ROTOR, NACELLE AND DRIVE TRAIN				
COE CONTRIB. (1980 CENTS)...			1.29					
REFS 400-799								
TOTALS:								
WEIGHT 100TH UNIT.....			1,159,477					
COST 100TH UNIT.....			1,904,204	ROTOR, NACELLE, DRIVE TRAIN AND TOWER				
COE CONTRIB. (1980 CENTS)...			1.78					
REFS 100-1399								
TOTALS:								
WEIGHT 100TH UNIT.....			1,209,124					
COST 100TH UNIT.....			3,366,377	GRAND TOTALS				
COE CONTRIB. (1980 CENTS)...			3.32					

4.5.4 COST SUMMARY

Volume production cost estimates in 1980 dollars are shown in Table 4-18 in the fifth column. A levelized profit of 10%, noted in line 1010 of Table 4.5.4, was added to the sum of all other costs. Because of an uncertainty in the cost, a 5% cost growth budget (reference line 1030) was maintained.

4.5.5 COST OF ENERGY

The cost of energy for model 204.0 was 3.32 ¢/kWh (1980\$). Each contribution toward the cost of energy is shown in the ninth column of Table 4-18. Percentages are shown in the eighth column. The relative cost of energy percentages are shown diagrammatically in Figure 4-39. A summary of the size optimization results that led to the selection of model 204.0 is shown in Figure 4-40. A summary of first unit, single site volume production unit, and cluster volume production unit installations is shown in Table 4-19.

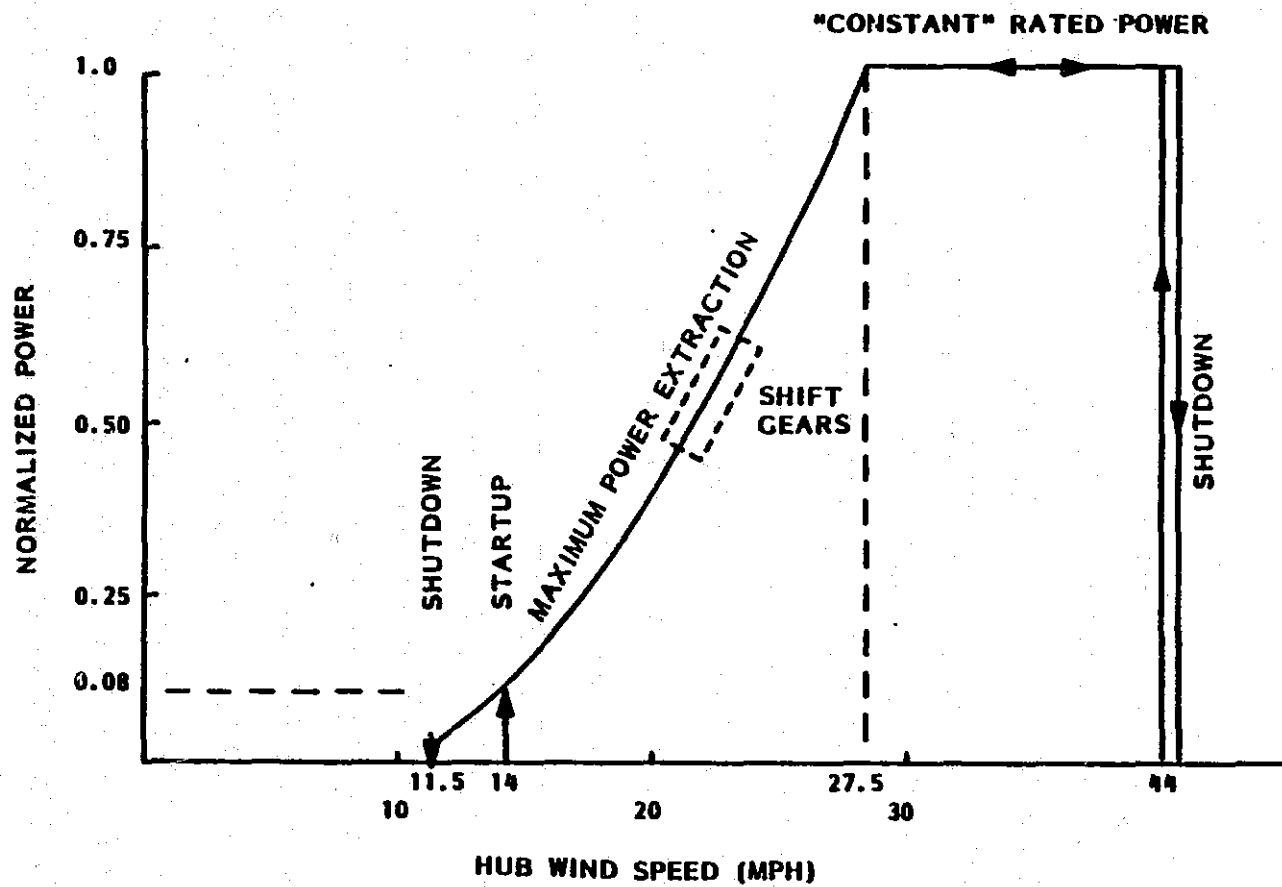
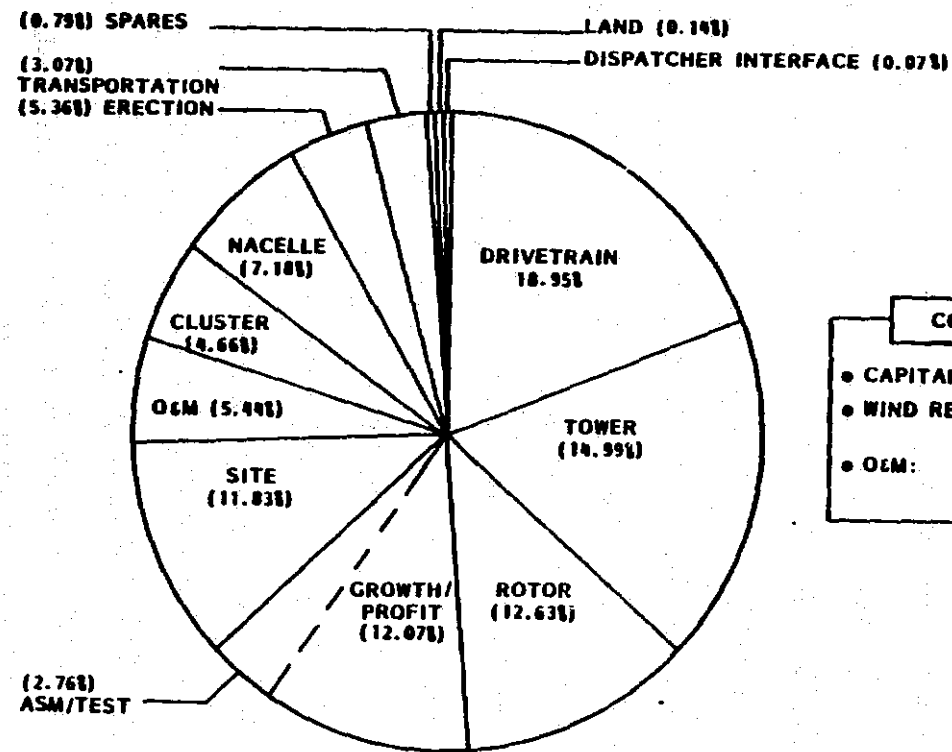
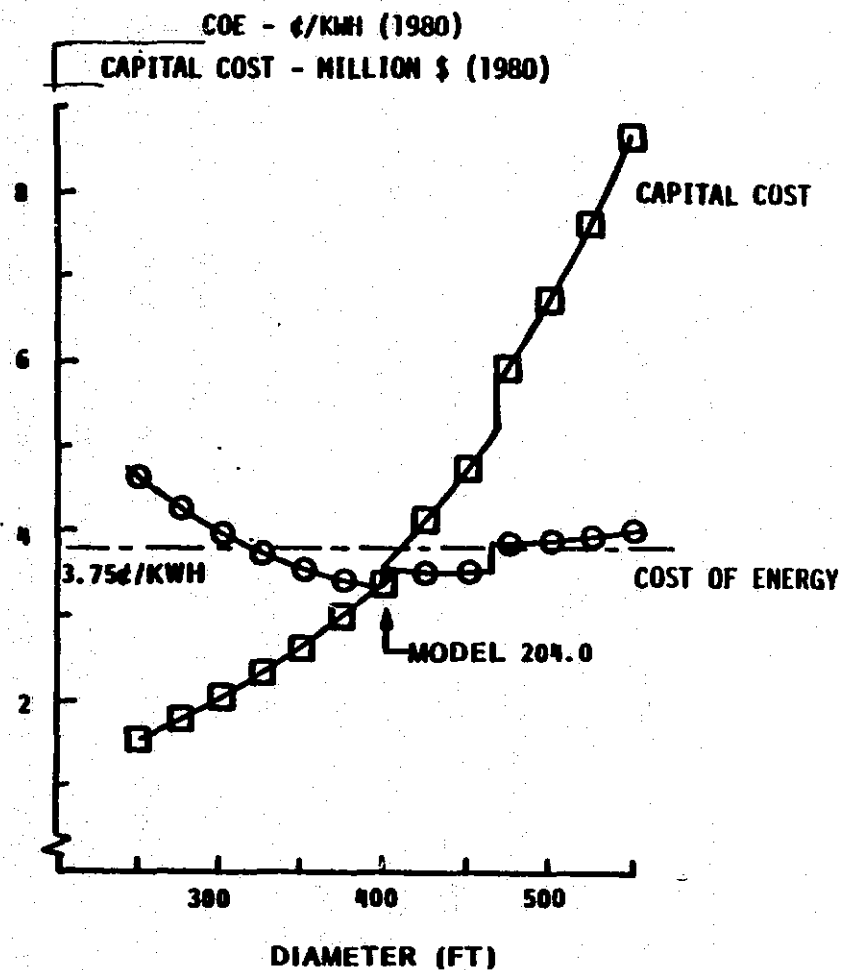


Figure 4-38 Operating Mode Description



COE SENSITIVITIES	
• CAPITAL COST:	\$100,000 ≈ 0.1¢/KWH
• WIND REGIME:	1 MPH (AVG) ≈ 0.24¢/KWH
• O&M:	\$10,000/YR ≈ 0.1¢/KWH

Figure 4-39 Cost of Energy Contributions



- 100TH UNIT
- DISCONTINUITIES DUE TO GEARBOX MANUFACTURING AND SHIPPING
- MODEL 204.0 CONFIGURATION WITH WOOD LAMINATE ROTOR SYSTEM
- 40 WATTS/FT-SQ POWER DENSITY
- 14 MPH (10M) 50M WIND REGIME

Figure 4-40 Cost of Energy and Capital Costs

Table 4-19 Cost of Energy Summary for the Baseline System

Model 204.0

ITEM	1ST UNIT	100TH UNIT SINGLE SITE	100TH UNIT CLUSTER (150 MW)
COST (1980 K\$)	10070	3230 ⁽¹⁾	3366 ⁽²⁾
AVAILABILITY	.880	.932	.960
O&M (1980 K\$)	34.6	21.9	17.3
ANNUAL ENERGY (GWH, SOW)	17.61	18.65	19.21
COE (\$/KWH 1980)	10.69	3.36	3.32

(1) Cost for the single site include higher installation costs.

(2) Cluster site cost includes interconnections.

ORIGINAL PAGE IS
OF POOR QUALITY

5.0 DESIGN, DEVELOPMENT AND OPTIMIZATION

5.0 DESIGN DEVELOPMENT AND OPTIMIZATION

5.1 INTRODUCTION

This section describes the preliminary and final design phases of the MOD-5A development and optimization. There were eight intermediate system model numbers between 204.0 at the end of conceptual design, and the final model 304.2. A summary of each model's features, and of the work leading to the model is given in this section. The discussion of each version starts with the newly defined baseline and describes the progression of design refinement. A new model number was designated when the design was changed significantly.

5.2 MODEL 204.0 DESIGN

The MOD-5A Model 204.0 was the baseline configuration at the end of the conceptual design phase. A summary of this configuration is shown in Table 5-1.

Features of the model 204.X series that were not changed during design development are identified with an "X". The 204.0 model was rated at 5000 kW. A two-speed rotor integrated gearbox supported the 400 ft., laminated wood rotor from the nacelle. A steel shell tower, 14.5 ft. in diameter, supported the nacelle, at a rotor hub height of 250 ft. The gearbox drove a synchronous generator. The outer 50 ft. of each blade was movable to control rotor torque.

The turbine cut in at wind speeds above 14 mph and cut out at wind speeds above 44 mph, both measured at hub height. The lower operating speed was used in light winds for the most efficient use of the rotor. An automatic shift to the higher speed was made when higher winds occurred while the rotor was turning, but unloaded. Shifting speed while rotating was called warm-shifting.

The preliminary design phase started in March, 1981. This phase extended the range of operating wind speeds and improved the wind turbine generator's performance. Also, the cost contingency plan in effect during the conceptual design phase was reduced as a more detailed design evolved.

8
The high wind cut-out point was extended from 44 mph to 60 mph to avoid nuisance shutdowns caused by gusty winds. An increase in the teeter motion restricting force became necessary, to accommodate the higher cut-out speed during shutdowns, and this increase added slightly to the center blade loads. Energy capture was not significantly increased by a higher cut-out speed, since the wind distribution has only 29.5 hours per year at speeds greater than 44 mph, measured at the hub.

The gearbox sizing and costs were driven by rated torque and an overload service factor of 2.0 during the conceptual design phase studies. The preliminary gearbox design used a torque duty cycle that was derived from the wind speed distribution and the two-speed operating plan. The duty cycle was more advantageous than the service factor approach, so a 16% increase in the torque rating was possible without modifying the geartrain design. Because of the torque increase, and a 7% increase in rated rotor speed, the system rating increased by 24% from 5,000 kW to 6,200 kW, with no change in the gearing.

Table 5-1 Model 204.0 Configuration

System Weight (lb)	1,209,124
Installed Cost (Volume, 1980 \$)	3,366,377
Annual Energy (GWH, SOW wind, 0.96 AF)	19.21
Cost of Energy (Volume, 1980 cents/Kwh)	3.32

Rotor 301,604 lb.

- X Upwind of the tower
- X 400 ft. diameter
- o 350 ft/sec tip speed
- o 12.8/16.7 rpm, two-speed operation
- X Laminated wood blades and tip
- o 64-XXX Airfoil, 200 in. root chord, 3.06% solidity
- X 25% (50 ft.) hydraulically powered partial span control -90° motion
- o Steel hub, stud joints with blade
- X Steel partial span control, stud joints with blade and tip
- X Hub-mounted hydraulic power unit 9° tilt, ±9° teeter allowance
- X Shaft-hub interface with low friction teeter bearings and brake type restrictor. Shaft bolts to 1st stage of gearbox

Drivetrain 235,119 lb.

- o Hybrid rotor integrated gearbox, 2.34 million ft.-lb. input torque
- o Planetary 1st stage gearing, split parallel shaft 2nd stage
- o 3rd stage underrunning shifter, warm shift procedure, inching drive
- X Stiffness and damping control at 1st stage
- X Rotor and gear supported by two-row monobearing integrated into gear case with load path to bedplate
- X In-line slipring access, shaft drive lube pump, rotor lock, parking brake
- X Floating high speed shaft
- o 5,000 kW, 1,200 rpm synchronous generator

Nacelle 116, 956 lb.

- X Bedplate type with wiring, piping runs under flooring
- X Mountings for gearbox, generator, control electronics, high voltage cabinet
- X Insulated weather fairing
- X Lubrication system for gearbox and bearings on lower platform
- X Yaw structural adapters and bearing
- X Hydraulic power supply and push-pull yaw drive
- X Yaw slipring

Tower 505,798 lb.

- X 14.5 ft. diameter steel shell
- o 250 ft. to rotor hub
- X 50 ft. tapered bell for tuning
- X Internal cable lift and ladder

Foundation

- X Spread footing, reinforced concrete
- X About 960 cubic yards
- X Anchor bolts for tower attachment

Electrical 49,627 lb.

- o Walk-in aisle switchgear and control enclosure
- o 5,000 kVA oil-filled transformer with fused switch
- X 69 kV nominal interface
- o 150 MVA radial feeder cluster, with 30 units

Maintenance

- X Permanent cluster crew

A higher rotor speed and the material properties of the laminated wood blade were investigated simultaneously. Test data in the wood literature supported an increase in allowable properties for wood. Consequently, the rotor speed was increased from 16.7 rpm to 17.9 rpm, while an efficient solidity and profile geometry were maintained.

In May, 1981, the MOD-5A model number was changed to 204.1 to incorporate these changes.

5.3 MODEL 204.1 DESIGN

A summary of the Model 204.1 configuration is shown in Table 5-2. This model had a cost of energy of 2.83 cents/Kwh, a 15% reduction from model 204.0. Continued refinement of the design required a change in operating speed and a change in energy capture.

Dynamics analysis on model 204.1 showed that at the lower operating speed, excitation at twice per revolution ($2 \times 12.8 = 25.6$ rpm) was too close to the tower bending frequency, which occurs around 23 rpm. Consequently, it was necessary to increase the lower speed to 13.25 rpm. This change had a small affect on energy capture, but increased the frequency separation to an acceptable level.

A more detailed analysis of energy capture then determined that teetered rotor performance was less than previously estimated. Teetering tends to smooth the rotor blade variational forces, because the blade attack angles produced by teeter motion are more constant. While teetering reduces the loads it also smooths the power production at a slightly lower level than a rigid hub rotor would provide. The more detailed analysis indicated a 4.2% reduction in energy capture when wind speeds are below the rated value.

In July, 1981, the MOD-5A model number was changed to 204.2 to incorporate the change from a rigid hub rotor to a teetered rotor configuration.

Table 5-2 Model 204.1 Configuration

System Weight (lb)	1,202,201
Installed Cost (Volume, 1980 \$)	3,311,378
Annual Energy (GWH, SOW wind, 0.96 AF)	23.3
Cost of Energy (Volume, 1980 cents/Kwh)	2.83

Rotor 277,822 lb.

- o Upwind of tower
- o 400 ft. diameter
- o 375 ft/sec tip speed
- o 12.8/17.9 rpm, two-speed operation
- o Laminated wood blades and tip
- o 64-XXX Airfoil, 200 in. root chord, 3.06% solidity
- o 25% (50 ft.) hydraulically powered partial span control -90° motion
- o Steel hub, stud joints with blade
- o Steel partial span control, stud joints with blade and tip
- o Hub-mounted hydraulic power unit
- o 9° tilt, ±9° teeter allowance
- o Shaft-hub interface with low friction teeter bearings and brake type restrictor. Shaft bolts to 1st stage of gearbox

Drivetrain 239,567 lb.

- o Hybrid rotor integrated gearbox, 2.71 million ft.-lb. input torque
- o Planetary 1st stage gearing, split parallel shaft 2nd stage
- o 3rd stage underrunning shifter, warm shift procedure, inching drive
- o Stiffness and damping control at 1st stage
- o Rotor and gear supported by two-row monobearing integrated into gear case with load path to bedplate
- o In-line slipring access, shaft drive lube pump, rotor lock, parking brake
- o Floating high speed shaft, slip coupling
- o 6,200 kW, 1,200 rpm synchronous generator

Nacelle 116,956 lb.

- o Bedplate type with wiring, piping runs under flooring
- o Mountings for gearbox, generator, control electronics, high voltage cabinet
- o Insulated weather fairing
- o Lubrication system for gearbox and bearings on lower platform
- o Yaw structural adapters and bearing
- o Hydraulic power supply and push-pull yaw drive
- o Yaw slipring

Tower 505,798 lb.

- o 14.5 ft. diameter steel shell
- o 250 ft. to rotor hub
- o 50 ft. tapered bell for tuning
- o Internal cable lift and ladder

Foundation

- o Spread footing, reinforced concrete
- o About 960 cubic yards
- o Anchor bolts for tower attachment

Electrical 62,058 lb.

- o Walk-in aisle switchgear and control enclosure
- o 6,200 kVA oil-filled transformer with fused switch
- o 69 kV nominal interface
- o 150 MVA radial feeder cluster, with 24 units

Maintenance

- o Permanent cluster crew

5.4 MODEL 204.2 DESIGN

A summary of the Model 204.2 configuration is shown in Table 5-3. Further studies showed that a significant improvement in the blade structure could be made by eliminating the steel hub section and the stud joints that attached the hub to the wooden blade sections. In addition, a safety and risk reduction study prompted a modification in the procedure for changing the rotor speed.

The steel hub of the rotor blade originated in the conceptual design phase trade-off studies, in order to join the different materials of the main blade. As the design progressed, the steel and wood interface became less desirable. There was some risk of encountering problems that would require lengthy development programs, for example, the development of a wood stud with double the fatigue capability of the state of the art MOD-OA stud. A preferable design, described in more detail in section 4.1 of Volume III, was found by eliminating the joint made of different materials. This design used a wooden center blade section with finger joints that would be bonded in the field. With the wooden center blade, the rotor would have a continuous load path between the blades. A related analysis of methods for attaching the rotor to the hub resulted in the selection of an external steel yoke that supported the blade through the teeter axis bearing.

A concern about overspeed led to a revision in the procedure for changing rotor speed. The MOD-5A model 204.X series used two-speed operation to maintain the rotor efficiency near the optimum during subrated wind speeds. The lower rotor speed was preferred for lower wind speeds. The warm change procedure, specified for models 204.0 through 204.2, which is used while the rotor is turning, required the generator to be electrically disconnected from the grid, using aerodynamic control to change speeds, shifting gears, and resynchronizing the generator with the grid. Further consideration of this procedure raised concerns about safety and a cold change procedure, which was used while the rotor was not turning, was developed. The rotor would be stopped before shifting gears, to minimize the possibility that a malfunction in the aerodynamic control could cause an overspeed while the generator was not connected to the grid. The cold change reduces the net energy capture

slightly, because during the 10 minutes required for each speed change, there is no power delivery.

In September, 1981, the continuous center blade configuration and the revised procedure for changing speed were adopted in MOD-5A Model 204.3.

Table 5-3 Model 204.2 Configuration

System Weight (lb)	1,202,201
Installed Cost (Volume, 1980 \$)	3,311,339
Annual Energy (GWH, SOW wind, 0.96 AF)	21.6
Cost of Energy (Volume, 1980 cents/Kwh)	2.92

Rotor 277,804 lb.

- o Upwind of tower
- o 400 ft. diameter
- o 375 ft/sec tip speed
- o 13.25/17.9 rpm, two-speed operation
- o Laminated wood blades and tip
- o 64-XXX Airfoil, 200 in. root chord, 3.06% solidity
- o 25% (50 ft.) hydraulically powered partial span control -90° motion
- o Steel hub, stud joints with blade
- o Steel partial span control, stud joints with blade and tip
- o Hub-mounted hydraulic power unit
- o 9° tilt, ±9° teeter allowance
- o Shaft-hub interface with low friction teeter bearings and brake type restrictor. Shaft bolts to 1st stage of gearbox

Drivetrain 239,565 lb.

- o Hybrid rotor integrated gearbox, 2.71 million ft.-lb. input torque
- o Planetary 1st stage gearing, split parallel shaft 2nd stage
- o 3rd stage underrunning shifter, warm shift procedure, inching drive
- o Stiffness and damping control at 1st stage
- o Rotor and gear supported by two-row monobearing integrated into gear case with load path to bedplate
- o In-line slipring access, shaft drive lube pump, rotor lock, parking brake
- o Floating high speed shaft, slip coupling
- o 6,200 kW, 1,200 rpm synchronous generator

Nacelle 116,956 lb.

- o Bedplate type with wiring, piping runs under flooring
- o Mountings for gearbox, generator, control electronics, high voltage cabinet
- o Insulated weather fairing
- o Lubrication system for gearbox and bearings on lower platform
- o Yaw structural adapters and bearing
- o Hydraulic power supply and push-pull yaw drive
- o Yaw slipring

Tower 505,798 lb.

- o 14.5 ft. diameter steel shell
- o 250 ft. to rotor hub
- o 50 ft. tapered bell for tuning
- o Internal cable lift and ladder

Foundation

- o Spread footing, reinforced concrete
- o About 960 cubic yards
- o Anchor bolts for tower attachment

Electrical 62,058 lb.

- o Walk-in aisle switchgear and control enclosure
- o 6,200 kVA oil-filled transformer with fused switch
- o 69 kV nominal interface
- o 150 MVA radial feeder cluster, with 24 units

Maintenance

- o Permanent cluster crew

5.5 MODEL 204.3 DESIGN

A summary of the Model 204.3 configuration is shown in Table 5-4. As the preliminary design phase continued, the possibility of raising the gearbox torque rating and the system energy capture was examined.

The preliminary design of the gearbox was created by Philadelphia Gear Corporation (PGC) under a teaming arrangement. The gear size, life and cost were significantly influenced by the few overload cycles specified in the load/life duty cycle. Optimization studies showed that the torque rating could be increased if the gearbox torque was limited by a friction-type slip coupling.

The Model 204.3 gearbox had a 2.71 million ft.-lb. input torque rating and an effective design factor of 1.7. By lowering the effective design factor and maximum operating overload to 1.4, the rated torque could be raised to 3.20 million ft.-lbs. This increase in torque allowed a potential rating of 7,300 kW, using the same gearbox cost and arrangement, an 18% gain over the 6,200 kW rating of Model 204.3. Only a small increase in the electrical system rating and a rerating of the slip coupling would be necessary to complete this change.

The design cluster configuration was also reconsidered. The 150 MW cluster design had been maintained since the conceptual design phase studies. With a 6,200 kW unit rating, there were 24 units in the baseline cluster. Operations and maintenance costs depended on the number of units over which the cluster labor pool was allocated. To avoid an increase in unit operating and maintenance costs per unit the cluster rating was increased to 175 MW when each unit was uprated to 7,300 kW to maintain 24 units in the cluster. The cluster transmission line costs were not effectively altered, as only brief times at the higher rating were expected. The higher winds, during which the cluster reached the rating, aided cooling, so that no increase in conductor size was necessary.

In March, 1982, the system uprating and cluster uprating were included in MOD-5A Model 204.4.

Table 5-4 Model 204.3 Configuration

System Weight (lb)	1,177,722
Installed Cost (Volume, 1980 \$)	3,241,255
Annual Energy (GWH, SOW wind, 0.96 AF)	21.2
Cost of Energy (Volume, 1980 cents/Kwh)	2.92

Rotor 256,044 lb.

- o Upwind of tower
- o 400 ft. diameter
- o 375 ft/sec tip speed
- o 13.25/17.9 rpm, two-speed operation
- o Laminated wood blades and tip
- o Continuous wood center blade
- o 64-XXX Airfoil, 200 in. root chord, 3.06% solidity
- o 25% (50 ft.) hydraulically powered partial span control -90° motion
- o Steel yoke attachment at teeter axis
- o Teeter and brake shafts through blade
- o Steel partial span control, stud joints with blade and tip
- o Yoke-mounted hydraulic power unit
- o 9° tilt, ±9° teeter allowance
- o Low friction teeter bearings and brake type teeter restrictor.
- o Yoke bolts to 1st stage of gearbox

Drivetrain 236,866 lb.

- o Hybrid rotor integrated gearbox, 2.71 million ft.-lb. input torque
- o Planetary 1st stage gearing, split parallel shaft 2nd stage
- o 3rd stage underrunning shifter, cold shift procedure, (warm capability) inching drive
- o Stiffness and damping control at 1st stage
- o Rotor and gear supported by two-row monobearing integrated into gear case with load path to bedplate
- o In-line slipring access, shaft drive lube pump, rotor lock, parking brake
- o Floating high speed shaft, slip coupling
- o 6,200 kW, 1,200 rpm synchronous generator

Nacelle 116,956 lb.

- o Bedplate type with wiring, piping runs under flooring
- o Mountings for gearbox, generator, control electronics, high voltage cabinet
- o Insulated weather fairing
- o Lubrication system for gearbox and bearings on lower platform
- o Yaw structural adapters and bearing
- o Hydraulic power supply and push-pull yaw drive
- o Yaw slipring

Tower 505,798 lb.

- o 14.5 ft. diameter steel shell
- o 250 ft. to rotor hub
- o 50 ft. tapered bell for tuning
- o Internal cable lift and ladder

Foundation

- o Spread footing, reinforced concrete
- o About 960 cubic yards
- o Anchor bolts for tower attachment

Electrical 62,058 lb.

- o Walk-in aisle switchgear and control enclosure
- o 6,200 kVA oil-filled transformer with fused switch
- o 69 kV nominal interface
- o 150 MVA radial feeder cluster, with 24 units

Maintenance

- o Permanent cluster crew

5.6 MODEL 204.4 DESIGN

The configuration defined by model 204.4 was found to have design problems which required almost immediate changes. Analyses of blade strength, high wind shutdown, and extreme wind loads prompted major changes in this design.

An environmental effects analysis of strong sunlight indicated that temperatures on the blade surface could be high enough to affect allowable stress. Therefore, the allowable stress for the wood was reduced, because of the analysis of temperature and the results from phase A of the wood strength versus temperature testing. The blade thickness then had to be increased by 10% for the same chord, to accommodate the lower stresses. The weight of the wind turbine increased by 1%, because of these changes.

The dynamic analysis of transient shutdown loads indicated that high limit loads were produced in 60 mph, 45° inflow conditions. The cut-out wind speed was then reduced from 60 mph to 50 mph, to meet load requirements.

The length of the movable tip was then studied. The loads resulting from a longer 90 ft. tip were reduced in the mid-blade region, but increased for the inner blade. The longer tip cost more and required an increase in capability of the wood to steel joint. A swept tip or a passive way of scheduling tip motion for shutdowns would be advantageous, but difficult to design. The 50 mph cut-out wind speed and the 50 ft. tip were selected as the best arrangement.

NASA reduced the extreme wind shear exponent from 0.1 to 0.04. This reduced the extreme wind at the hub height from nearly 150 mph to 130 mph. By reducing the hub height from 250 ft. to 240 ft., the tower could be redesigned for broadside blade exposure to extreme wind. The previous design had relied on weathervaning. Manually controlled weathervaning was kept in the design, but automatic, failsafe operation was deleted. The tower weight increased slightly, because of higher loads.

These changes were incorporated in model 204.5 late in March, 1982.

5.7 MODEL 204.5 DESIGN

The model 204.5 configuration is summarized in Table 5-5. This configuration was reviewed by NASA during a preliminary design review in April, 1982.

The major weights take advantage of projected reductions from the first unit to volume production units. The cost of energy for the first unit of model 204.5 and the clustered 100th unit is shown in Tables 5-6 and 5-7.

Design work on model 204.5 concentrated on the rotor. Measurements by PNL-Battelle and analysis by NASA defined higher fatigue loads caused by wind turbulence. The chord and thickness were increased to compensate for the new fatigue loads and weight of the partial span control. This change made changes in the upper and lower operating speeds necessary to avoid load amplification.

Investigations by the NASA-Lewis Research Center and PNL-Battelle, which examined wind turbulence, resulted in the definition of an interior turbulence specification. This definition was used to recalculate the system's loads. The 50th percentile fatigue load was doubled. Consequently, the average fatigue load was raised, but the infrequent large gust loads were not raised. The turbulent load analysis is discussed in section 7.0.

Table 5-5 Model 204.5 Configuration

System Weight (lb)	1,277,065
Installed Cost (Volume, 1980 \$)	3,349,655
Annual Energy (GWH, SOW wind, 0.96 AF)	21.1
Cost of Energy (Volume, 1980 cents/kwh)	3.03

Rotor 296,068 lb.

- o Upwind of tower
- o 400 ft. diameter
- o 375 ft/sec tip speed
- o 13.25/17.9 rpm, two-speed operation
- o Laminated wood blades and tip
- o Continuous wood center blade
- o 64-XXX Airfoil, 200 in. root chord, 3.06% solidity
- o 25% (50 ft.) hydraulically powered partial span control, -90° motion
- o Steel yoke attachment at teeter axis
- o Teeter and brake shafts through blade
- o Steel partial span control, stud joints with blade and tip
- o Yoke-mounted hydraulic power unit
- o 9° tilt, ±9° teeter allowance
- o Low friction teeter bearings and brake type teeter restrictor.
- o Yoke bolts to 1st stage of gearbox

Drivetrain 246,110 lb.

- o Hybrid rotor integrated gearbox, 3.2 million ft.-lb. input torque
- o Planetary 1st stage gearing, split parallel shaft 2nd stage
- o 3rd stage underrunning shifter, cold shift procedure, (warm capability) inching drive
- o Stiffness and damping control at 1st stage
- o Rotor and gear supported by two-row monobearing integrated into gear case with load path to bedplate
- o In-line slipring access, shaft drive lube pump, rotor lock, parking brake
- o Floating high speed shaft, slip coupling
- o 7,300 kW, 1,200 rpm synchronous generator

Nacelle 137,437 lb.

- o Bedplate type with wiring, piping runs under flooring
- o Mountings for gearbox, generator, control electronics, high voltage cabinet
- o Insulated weather fairing
- o Lubrication system for gearbox and bearings on lower platform
- o Yaw structural adapters and bearing
- o Hydraulic power supply and push-pull yaw drive
- o Yaw slipring

Tower 524,250 lb.

- o 14.5 ft. diameter steel shell
- o 240 ft. to rotor hub
- o 50 ft. tapered bell for tuning
- o Internal cable lift and ladder

Foundation

- o Spread footing, reinforced concrete
- o About 960 cubic yards
- o Anchor bolts for tower attachment

Electrical 73,200 lb.

- o Walk-in aisle switchgear and control enclosure
- o 7,300 kVA oil-filled transformer with fused switch
- o 69 kV nominal interface
- o 175 MVA radial feeder cluster, with 24 units

Maintenance

- o Permanent cluster crew

Table 5-6 Cost of Energy Report Model 204.5 - First Unit

SUBASS. ABBREV.	ITEM NAME ABBREV.	REF. NUM.	WEIGHT 100TH UNIT	COST FIRST UNIT	DOLLARS PER LB.	% OF TOTAL WT.	% OF COE	1ST UNIT COE CONTRIB.
SITE	FOUNDATION	110		309,800			2.88	0.28
	GRD EQUIP	120		232,925			2.19	0.21
	SPECIAL	130		160,600	2.99	5.84	1.91	0.19
			78,000	699,326		5.84	6.98	0.64
TRANSPORT.	TRANSPORT.	240		180,900			1.70	0.17
ERECTION	INSTALL	310		586,287			5.51	0.54
	INTEGRAL	330		913,200			8.59	0.83
			0	1,499,487		0.00	14.10	1.37
ROTOR	BLADES	410	229,653	1,510,002	6.58	17.20	14.20	1.28
	PCS HYDR	420	9,418	76,545	8.13	0.63	0.72	0.07
	PCS STRUC	431	46,950	264,200	5.63	3.32	2.49	0.24
	HUB	430	54,100	246,281	4.55	4.03	2.32	0.23
			339,721	2,097,328		25.40	19.72	1.92
DRIVE-TRA.	TRANSMTS.	520	196,050	1,280,975	6.53	14.48	12.05	1.17
	MT SPEED	530	3,920	32,912	8.40	0.23	0.31	0.03
	GEN & EXCI	540	46,140	224,176	7.03	3.46	3.03	0.30
			246,110	1,638,063		18.43	15.40	1.50
NACELLE	BEDPLATE	610	67,750	151,389	2.23	5.07	1.42	0.14
	HYD SYST	620	8,600	20,543	2.39	0.64	0.19	0.02
	FAIR. WISC	646	17,490	87,480	5.00	1.31	0.82	0.08
	SLP. ELEC	640	4,770	42,689	8.95	0.24	0.40	0.04
	INST & CON	670	3,060	137,859	45.38	0.23	1.29	0.13
	YAW SUB.	680	47,930	181,512	3.79	3.99	1.71	0.17
			147,600	621,272		11.06	9.84	0.97
TOWER	TOWER	710	510,700	947,023	1.85	26.25	8.90	0.87
	PERS. LIFT	720	1,250	19,209	12.39	0.12	0.18	0.02
	CABLING	740	12,000	91,079	4.26	0.90	0.48	0.05
			524,250	1,017,311		39.27	9.57	0.93
REM-CTRL	LINE-MODEM	810		728			0.01	0.00
	REM-DISP.	820		4,776			0.04	0.00
			0	5,504		0.00	0.05	0.01
SPARES	SPARES	930		115,547			1.09	0.11
SPECIAL	PROFIT	1010		640,977			6.22	0.60
	ASM/TEST	1020		1,635,774			15.38	1.50
	GR' TH BUGT	1030					0.00	0.00
			0	2,296,751		0.00	21.60	2.10
LAND	HTG LAND	1110					0.00	0.00
	ROAD LAND	1140					0.00	0.00
			0	0		0.00	0.00	0.00
CLUSTER	SUBSTATION	1240					0.00	0.00
	TRANSH ETC	1250					0.00	0.00
			0	0		0.00	0.00	0.00
OMW REFS. 400-699	YEARLY OMW	1340		41,703			4.36	0.42

TOTALS: ROTOR & NACELLE

WEIGHT 100TH UNIT..... 732,831
 COST FIRST UNIT..... 4,356,442
 1ST UNIT COE CONTRIB.... 3.98
 REFS 400-799

TOTALS: OVERALL TOTAL

TOTALS: ROTOR & NACELLE & TOWER

WEIGHT 100TH UNIT..... 1,257,081
 COST FIRST UNIT..... 5,373,974
 1ST UNIT COE CONTRIB.... 4.91

WEIGHT 100TH UNIT..... 1,339,081
 COST FIRST UNIT..... 10,213,142
 1ST UNIT COE CONTRIB.... 9.72

Table 5-7 Cost of Energy Report Model 204.5 - 100th Unit

SUBASS. ABBREV.	ITEM NAME ABBREV.	REF. NUM.	WEIGHT 100TH UNIT	COST 100TH UNIT	DOLLARS PER LB.	% OF TOTAL WT.	% OF COE	COE CONTRIB. (1980 CENTS)
SITE	FOUNDATION	110		241,400			6.81	0.21
	GND EQUIP	120	73,200	100,915	1.38	5.73	2.84	0.09
	SPECIAL	130		64,100			1.81	0.05
			73,200	406,415		5.73	11.46	0.35
TRANSPORT.	TRANSPORT.	240		115,851			3.27	0.10
ERECTION	INSTALL.	210		105,300			2.97	0.09
	INTEG&C.O.	350		68,300			1.93	0.06
			0	173,600		0.00	4.89	0.15
ROTOR	BLADES	410	194,600	271,141	1.39	15.24	7.64	0.23
	PCS HYDR	420	8,418	26,924	3.20	0.44	0.76	0.02
	PCS STRUC	431	38,920	69,854	1.79	3.05	1.97	0.06
	HUB	430	54,100	68,476	1.27	4.24	1.93	0.06
			296,048	436,395		23.18	12.30	0.37
DRIVE-TRA.	TRANSMIS.	520	196,050	639,074	3.26	15.35	18.02	0.55
	MT SPEED	530	3,920	14,259	3.64	0.31	0.40	0.01
	GEN & EXCI	540	44,140	140,448	3.04	3.61	3.96	0.12
			244,110	793,781		19.27	22.38	0.68
NACELLE	REDPLATE	610	57,587	57,028	0.99	4.51	1.61	0.05
	HYD SYST.	620	8,600	8,901	1.04	0.67	0.28	0.01
	FAIR. MISC	644	17,490	27,878	1.59	1.37	0.79	0.02
	SIP. ELEC	640	2,770	18,492	6.68	0.22	0.52	0.02
	TEST & COM	670	8,060	41,258	5.12	0.24	1.17	0.04
	YAM SUB.	680	47,930	64,504	1.39	3.75	1.87	0.06
			137,437	220,444		10.76	6.22	0.19
			210,700	532,010	1.06	37.99	15.20	0.46
TOWER	PERS. LIFT	730	1,420	9,539	6.75	0.12	0.27	0.01
	CABLING	740	12,000	22,130	1.84	0.94	0.62	0.02
			524,250	570,679		41.05	16.09	0.49
REM-CNTRL	LINE-MODEM	810		500			0.01	0.00
	REM-DISP.	820		2,000			0.04	0.00
			0	2,500		0.00	0.07	0.00
SPARES	SPARES	930		33,920			0.96	0.03
SPECIAL	PROFIT	1010		302,734			8.53	0.26
	ASN/TEST	1020		84,174			2.43	0.07
	GR'YH BUGT	1030						
			0	388,908		0.00	10.96	0.33
LAND	MTG LAND	1110		4,927			0.14	0.00
	ROAD LAND	1140		964			0.03	0.00
			0	5,923		0.00	0.14	0.00
CLUSTER	SUBSTATION	1240		48,708			1.37	0.04
	TRANS ETC	1250		132,885			3.75	0.11
			0	181,594		0.00	5.12	0.15
DEM REFS. 400-699	YEARLY DEM	1340		19,625			6.15	0.19
TOTALS: ROTOR & NACELLE								
WEIGHT 100TH UNIT.....			679,615					
COST 100TH UNIT.....			1,450,640					
COE CONTRIB. (1980 CENTS)...			1.24					
REFS 400-799								
TOTALS: ROTOR & NACELLE & TOWER								
WEIGHT 100TH UNIT.....			1,203,865					
COST 100TH UNIT.....			2,021,319					
COE CONTRIB. (1980 CENTS)...			1.72					
TOTALS: OVERALL TOTAL								
WEIGHT 100TH UNIT.....			1,277,065					
COST 100TH UNIT.....			3,349,625					
COE CONTRIB. (1980 CENTS)...			3.03					

Blade arrangements that would accommodate the higher loads and maintain acceptable frequency separation with a heavier partial span control were examined. Increased thickness separated the blade skins in the flap bending mode. To avoid a large decrease in performance, the blade chord profile was also increased, to retain the same thickness-to-chord ratio. At the blade root, the chord dimension was changed from 200 in. to 234 in. The increased thickness increased the section's modulus, which reduced stress levels to values consistent with allowable stresses. Energy capture was reduced 3% by these changes.

The larger blade was stiffer so it was necessary to increase the lower operating speed, to separate integer multiples of the operating speed and the elastic blade frequencies. The lower speed was increased from 13.25 rpm to 13.75 rpm. The upper speed was reduced from 17.9 rpm to 16.8 rpm, because the blade with the larger chord captured more energy at the lower speed.

The reduced upper speed might have decreased rated power by 7% because the drivetrain is torque limited. However, the evaluation of the gearbox duty cycle showed it to be favorable. The maximum overload torque was reduced. The slip coupling setting was lowered from 1.4 to 1.2 times the rated torque value, to permit a 3.38 million ft. lb. rating, which kept 7,300 kW at 16.8 rpm.

These changes influenced other areas of the design as well. A heavier partial span control was needed for the larger loads and larger blade mounting surface. The larger blade area resulted in higher extreme wind loads on the tower and a wider, heavier yoke. The mounting surface of the gearbox case was redesigned to be parallel to the drivetrain axis. The tilt was reduced from 9° to 7°, to avoid excessive bedplate depth.

This configuration was officially designated model 204.6 in August, 1982. Updated cost and weight details were available in December, 1982.

5.8 MODEL 204.6 DESIGN

Model 204.6 is summarized in Table 5-8. The growth of the weight of the partial span control, a simplified gearbox configuration, and reduced risk in the rotor support and other areas of the system were examined. The influence of size on the allowable fatigue strength for wood was also considered.

A fatigue crack was discovered in the rotor support shaft of the MOD-2 wind turbine generator in November, 1982. The rotor support shaft experiences reversed bending loads as the rotor revolves. To reduce the risk of a similar failure on the MOD-5A, several rotor attachments were examined. At the same time, it was found that competitive procurement for the rotor-integrated gearbox was limited because of its large bearing, structural case, stiffness and damping control and two-speed features. When the rotor support feature was eliminated from the gearbox the rotor attachment and rotor support structure could be designed with less risk. This change was also advantageous to the gearbox procurement and the alternative rotor attachment studies.

The gearbox was redesigned as a torque transfer, single-speed ratio, step-up unit. A significant reduction in the price resulted from these changes. Three vendors became interested. A variable-speed generator subsystem reduced shutdown loads on the partial span control structure. The speed range over which this subsystem operated and the control characteristics of the generator were able to replace the stiffness and damping elements and the two-speed stage that were integrated into the gearbox.

The volume of wood in the laminated wood and epoxy MOD-5A blades is over ten times the volume of wood in the MOD-0A wood blades. This volume was found to require that the allowable stresses be lowered because of the resulting higher probability of the blade containing a significant defect. This size factor was not addressed previously because of the many veneer butt, scarf, and surface joint discontinuities in the blades. These discontinuities were believed to have more impact on the allowable stresses than defects in the wood. However, lower allowable stress was established until tests could be made on large samples of wood. Allowable fatigue strength parallel to the wood grain was reduced by a third, and the size of the blade was recalculated.

Table 5-8 Model 204.6 Configuration

System Weight (lb)	1,486,242	
Installed Cost (Volume, 1980 \$)	3,663,532	
Annual Energy (GWH, SOW wind, 0.96 AF)	20.6	
Cost of Energy (Volume, 1980 cents/Kwh)		3.39

Rotor 365,920 lb.

- o Upwind of tower
- o 400 ft. diameter
- o 352 ft/sec tip speed
- o 13.75/16.8 rpm, two-speed operation
- o Laminated wood blades and tip
- o Continuous wood center blade
- o 64-XXX Airfoil, 234 in. root chord, 3.06% solidity
- o 25% (50 ft.) hydraulically powered partial span control, -90° motion
- o Steel yoke attachment at teeter axis
- o Teeter and brake shafts through blade
- o Steel partial span control, stud joints with blade and tip
- o Yoke-mounted hydraulic power unit
- o 7° tilt, ±9° teeter allowance
- o Low friction teeter bearings and brake type teeter restrictor. Yoke bolts to 1st stage of gearbox

Drivetrain 311,543 lb.

- o Hybrid rotor integrated gearbox, 3.38 million ft.-lb. input torque
- o Planetary 1st stage gearing, split parallel shaft 2nd stage
- o 3rd stage underrunning shifter, cold shift procedure, (warm capability) inching drive
- o Stiffness and damping control at 1st stage
- o Rotor and gear supported by two-row monobearing integrated into gear case with load path to bedplate
- o In-line slipring access, shaft drive lube pump, rotor lock, parking brake
- o Floating high speed shaft, slip coupling
7,300 kW, 1,200 rpm
synchronous generator

Nacelle 158,659 lb.

- o Bedplate type with wiring, piping runs under flooring
- o Mountings for gearbox, generator, control electronics, high voltage cabinet
- o Insulated weather fairing
- o Lubrication system for gearbox and bearings on lower platform
- o Yaw structural adapters and bearing
- o Hydraulic power supply and push-pull yaw drive
- o Yaw slipring

Tower 572,120 lb.

- o 14.5 ft. diameter steel shell
- o 240 ft. to rotor hub
- o 50 ft. tapered bell for tuning
- o Internal cable lift and ladder

Foundation

- o Spread footing, reinforced concrete
- o About 960 cubic yards
- o Anchor bolts for tower attachment

Electrical 78,000 lb.

- o Walk-in aisle switchgear and control enclosure
- o 7,300 kVA oil-filled transformer with fused switch
- o 69 kV nominal interface
- o 175 MVA radial feeder cluster, with 24 units

Maintenance

- o Permanent cluster crew

The size factor tests are described in section 8.1.6. The chord at the root was increased from 234 in. to 300 in. The thickness of the blade was also increased, to minimize the weight and cost growth for the large reduction in allowable fatigue strength.

The weight of the partial span control sections increased. This assembly is loaded in reversed chordwise bending every rotation, and is exposed to a large flapwise load reversal during the transition between operating and shutdown. A large portion of the structural weight is in the thick flanges. The flanges provide a rigid mounting interface for the wood stud joints. The larger blade cross section increased the flange area, but did not permit a reduction in thickness, so the weight increased.

The weight of the partial span control would have lowered the blade's flap bending frequency, but the larger blade was stiff enough to keep the frequency in an acceptable range at the selected operating speeds. Because the variable speed generator subsystem operated over a 0.6 rpm range in both low and high speeds, a minimum speed of 13.2 rpm was selected. The low range was 13.2 to 13.8 rpm and the high range was 16.2 to 16.8 rpm.

The partial span control spindle diameter had increased to 26 in. because of the thrust reversal that occurs from slowing the rotor aerodynamically. The bending loads produced by the thrust could be reduced if the rotor was slowed by shaft torque as well as aerodynamic control, until it reached lower speed. Shaft torque could be provided by either a brake or a generator capable of variable speed operation. The variable speed generator subsystem was selected because it provided flexibility in the selection of operating speeds, so it could control the dynamic behavior of the drivetrain, and provide back torque for most shutdowns.

An aileron torque control was studied at this time. Partial span control on model 204.6 was significantly heavier and more costly than the configuration used in the trade-off study. The aileron control was attractive, considering weight, cost, and integration with the blade, but there was not enough data to support a configuration change.

Consequently, aerodynamic testing on aileron controlled blade sections began, and the aileron control was established as an alternative to partial span control. Testing consisted of small wind tunnel models and a 125 ft. rotor on the MOD-0, a NASA research wind turbine in Sandusky, OH. Further description and discussion of aileron testing can be found in section 8.4.

Both internal and external rotor supports were examined. The goals were to minimize the volume of metal exposed to reversed bending and to avoid details that would concentrate stress in the blade. First, the rotor support function and the torque transmission function were separated. A low speed shaft with splined ends was placed between the gearbox and the rotor, to transmit torque. The shaft did not support the rotor, and had no torsional stiffness control requirements like the MOD-2's quill shaft.

The monobearing used to support the rotor was very large and costly. A double bearing located closer to the blade's center of gravity was examined. This bearing was smaller and could support the radial loading required to carry the rotor moment exerted by the rotor's weight. A bearing arrangement centered on the blade, as shown in Figure 5-1, was also examined. An arrangement that placed the double bearings in the yoke box structure and supported the yoke on a non-rotating spindle was the most practical arrangement. The low speed shaft passes through the spindle and is attached to the yoke on the side closest to the blade. This design is shown in Figure 5-2.

The variable speed generator was tentatively identified as similar to the Scherbiustat variable speed drive. A wound rotor or doubly fed machine was used. The stator circuit was directly connected to the 60 Hz grid, and the rotor circuit was connected to the grid through a thyristor ac to ac converter called a cycloconverter. The converter was mounted on the ground, to reduce weight in the nacelle. A simplified schematic of this arrangement is shown in Figure 5-3. A converter rating of 1500 kVA was selected. This permits the rotor to operate at just below 12 rpm to just above 17.5 rpm.

The generator control regulated airgap torque and reactive power. A control plan varied airgap torque with generator speed, so that zero to rated torque

ORIGINAL PAGE IS
OF POOR QUALITY

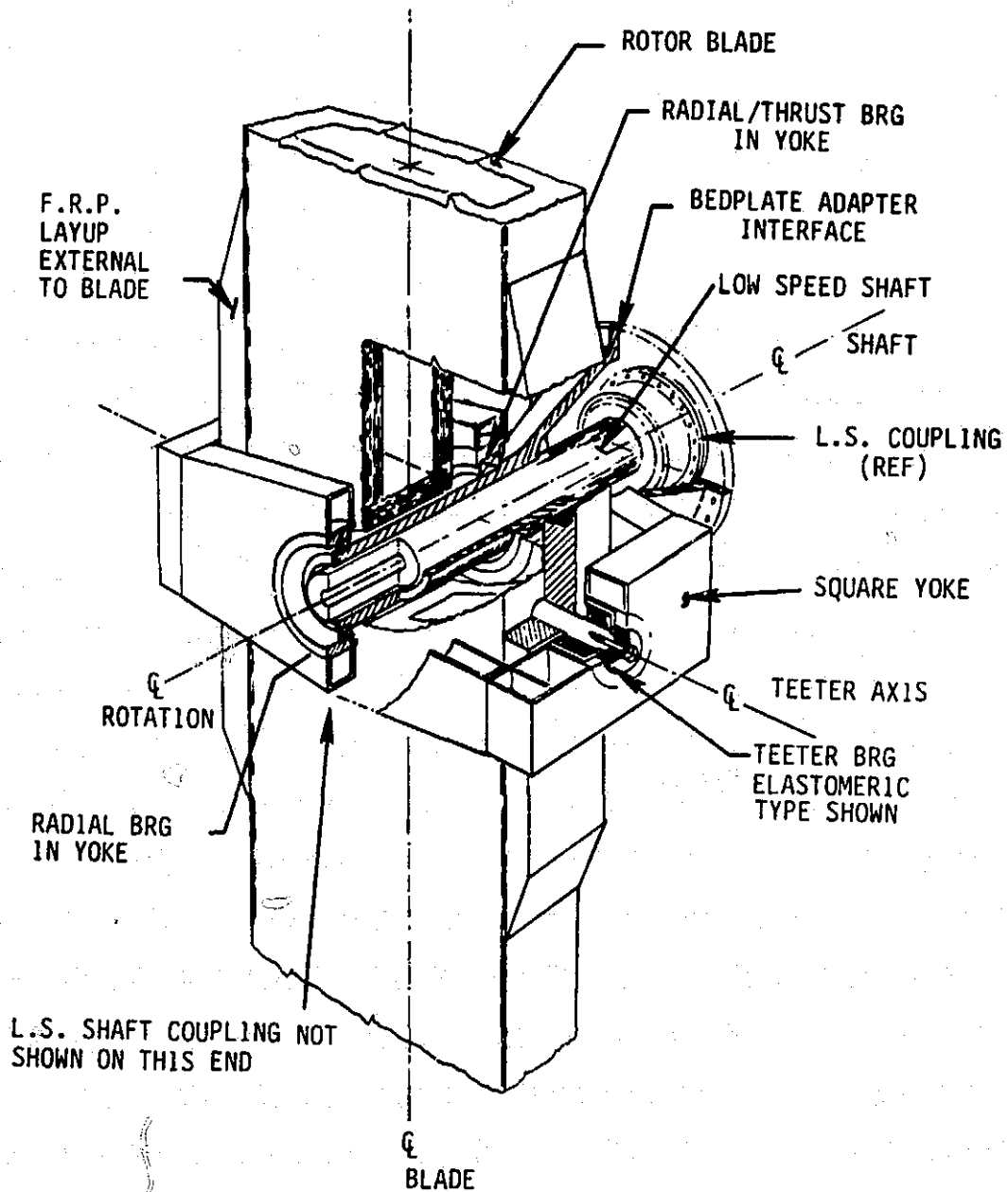


Figure 5-1 Centered Bearing Blade Support

SUPPORT CONFIGURATION INVESTIGATED (CONTINUED)

CONCEPT 3: NON-ROTATING SHAFT

2 RADIAL BEARINGS, 1 THRUST BEARING

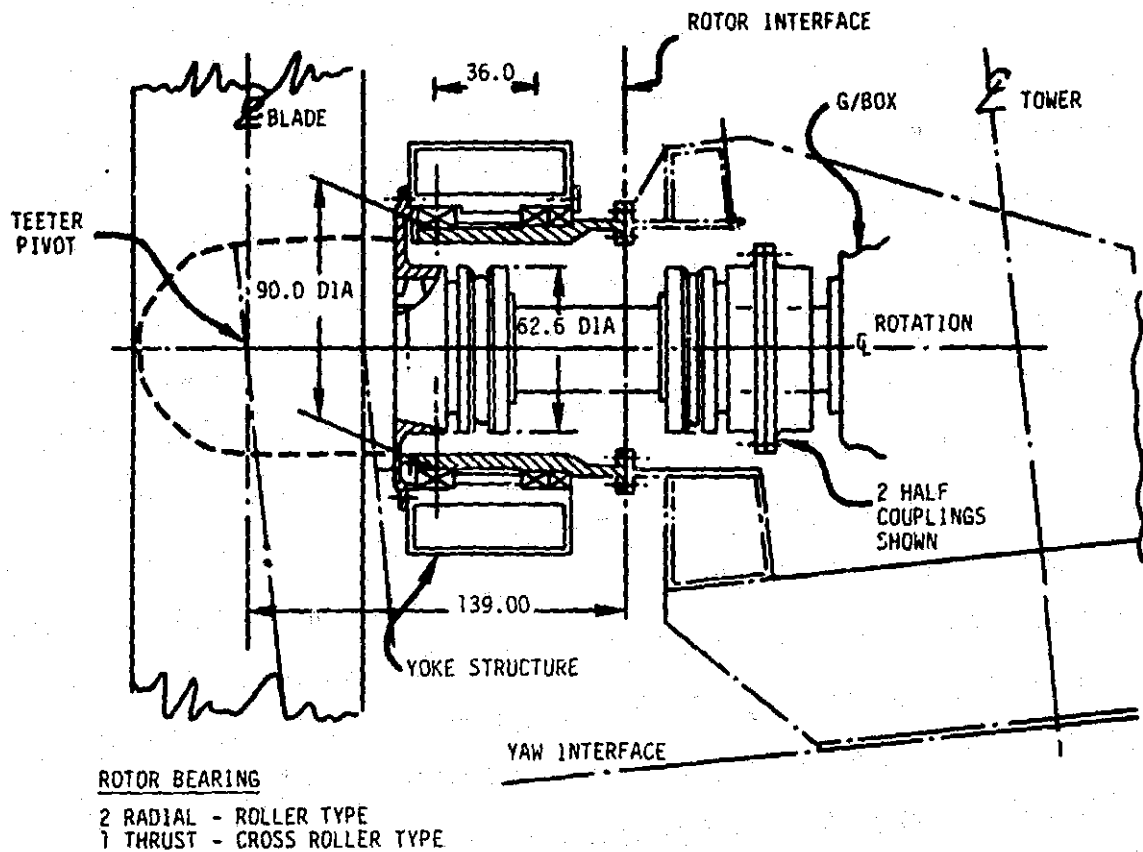


Figure 5-2 Selected Rotor Support Configuration

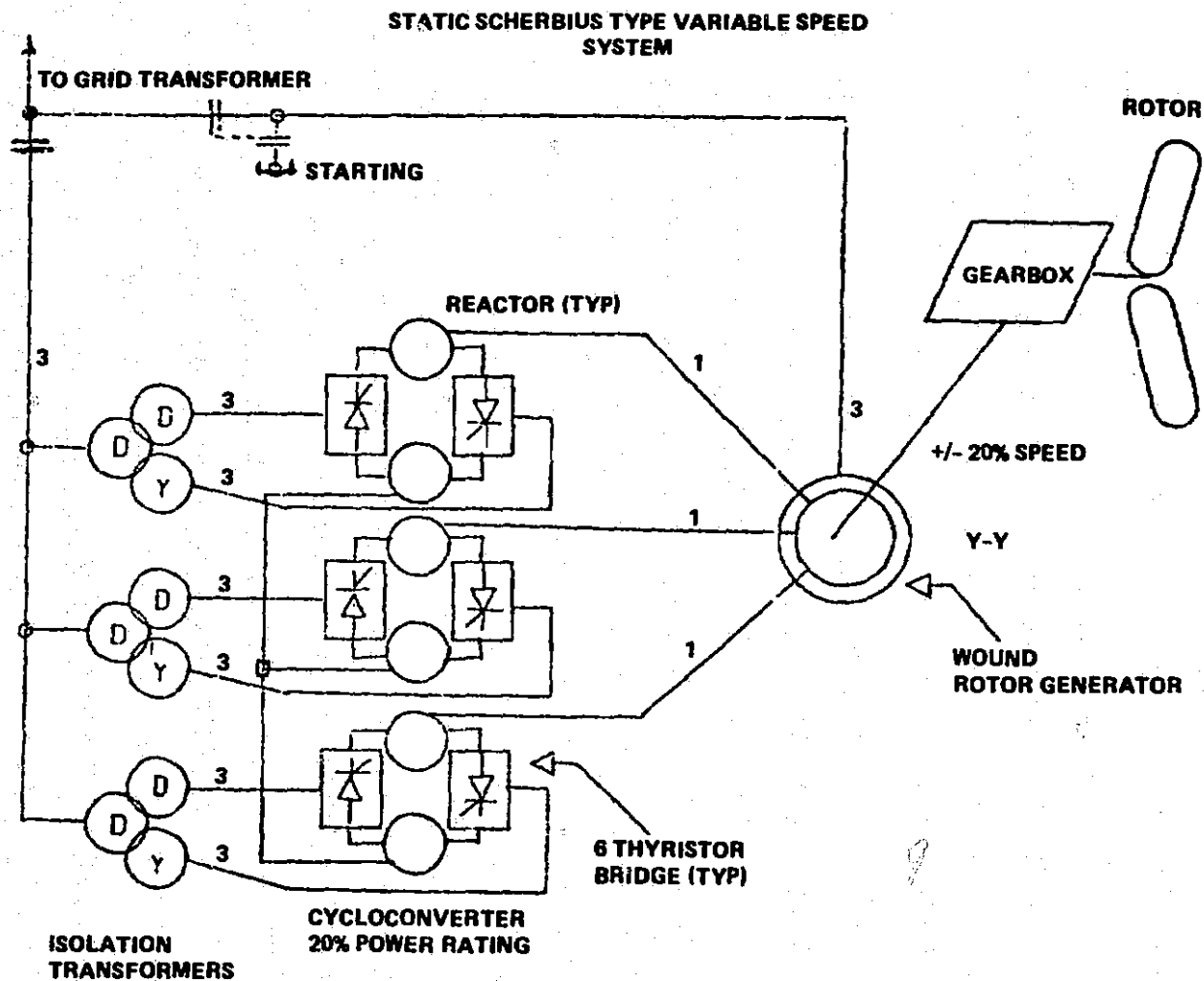


Figure 5-3 Variable Speed Subsystem Schematic

occurred with a 0.6 rpm speed change. The same dynamic behavior of the drivetrain would occur with a 3.5% slip coupling or induction generator. This behavior critically damps the first rotor oscillatory mode. Torque was limited to 10% above rating, independent of speed, so the generator control eliminated the friction slip coupling in the high speed shaft.

For start-up, partial span control tips were positioned at the proper angle and rotation began as a result of aerodynamic lift. If ailerons were used for aerodynamic control the rotor must be boosted to a starting speed to achieve the effective angle from which the aerodynamics would improve with increasing rotor speed. Thus, for purposes of starting an aileron controlled rotor, a starting circuit breaker was included in the switch gear, as shown in Figure 5-3. The stator is short-circuited when this circuit breaker is closed and the generator rotor can be energized by the cycloconverter to bring the main rotor up to 3 rpm.

A rotor support frame was added to the bedplate, to transfer loads from the spindle to the bedplate. This structure performed the function formerly performed by the gearbox case. An adaptor with radial ribs transferred loads from the circular spindle to a rectangle formed by the bedplate, two side plates, and a top plate. The side plates provide the section modulus to turn the corner into the bedplate with acceptable stress levels.

The blade teeter attachment was modified to reduce penetrations of the main box structure and to simplify the manufacture of the laminated wood and epoxy reinforced with glass fiber. Bolsters were added to the chordwise blade sides. The bolsters were simple slabs of wood and epoxy, augmented with glass fibers, with holes for the teeter bearing and teeter restrictor arm attachments. They were bonded to the main blade over a very large surface, which kept stress levels low. Only torque, weight and thrust loads were transferred into the bolsters, and the large blade bending loads were kept in the main blade. This change reduced the risk of a penetration-induced stress concentration on the main blade. The yoke became slightly heavier because a greater separation in the ears was needed to surround the bolsters.

The changes in this section were reviewed with NASA in January and March, 1983 and as a result, Model 304.0 was officially introduced in March, 1983.

5.9 MODEL 304.0 DESIGN

The configuration of model 304.0 is shown in Table 5-9. Higher energy capture was predicted for this configuration, since the cold shift used with the two-speed gearbox on model 204.6 had been eliminated. The blade had a higher loss because of profile drag, and the variable speed electrical subsystem had a higher loss than the synchronous electrical subsystem. Fortunately, the variable-speed electrical subsystem changed speed ranges while delivering energy to the grid, so the net energy output increased.

The major features of model 304.0 were an upwind laminated, 400 ft. in diameter, wood rotor with 50 ft. movable control tips, yoke, dual bearing support of yoke on nonrotating spindle, low speed shaft carrying only torque, single ratio gearbox, 7300 Kw variable speed generator, and a rotor support box structure on the bedplate. The shell tower, yaw structure drive, and foundation were the same as in the 204.X series.

Design loads were recalculated for model 304.0. The tower bending frequency was too high to significantly alleviate loads at the low end of the variable speed range. The sensitivity of loads to tower frequency is described in section 6.3.2. Analysis indicated that lengthening the tower by 10 ft. would sufficiently lower the tower frequency to avoid high loads.

The bedplate was widened by 20 in., to fit the gearbox and rotor support structure, with adequate access to the low speed shaft for assembly and maintenance. This change increased the weight of the bedplate and rotor adapter. A tilted gearbox adapter structure was also added to the nacelle. This structure interfaces the gearbox mounting surface, which was parallel to the shaft axis. The adapter was a better design than a 7° tilt incorporated in the gearbox case.

An improvement in the connection between low speed shaft and the gearbox was also made. A direct spline connection was more cost-effective than the original gear coupling and bolted flange. The gearbox planet carrier was modified to incorporate an internal spline and the gearbox oil lubrication path was extended to include the spline. The low speed shaft was extended to mate with the spline, which provides sufficient angular motion to accommodate assembly tolerances.

Table 5-9 Model 304.0 Configuration

System Weight (lb)	1,655,250
Installed Cost (Volume, 1980 \$)	3,855,200
Annual Energy (GWH, SOW wind, 0.96 AF)	21.2
Cost of Energy (Volume, 1980 cents/kwh)	3.46

Rotor 457,530 lb.

- o Upwind of tower
- o 400 ft. diameter
- o 352 ft/sec tip speed
- o 13.2-13.8/16.2-16.8 rpm
two range variable speed operation
- o Laminated wood blades and tip
- o Continuous wood center blade
- o 64-XXX Airfoil, 300 in. root chord,
3.06% solidity
- o 25% (50 ft.) hydraulically powered
partial span control, -90° motion
- o Steel yoke attachment at teeter axis
- o Teeter and brake shafts through blade
- o Steel partial span control, stud
joints with blade and tip
- o Yoke-mounted hydraulic power unit
- o 7° tilt, ±9° teeter allowance
- o Elastomeric teeter bearings
and brake type teeter restrictor.
- o Yoke supported on spindle with dual
bearings

Drivetrain 269,350 lb.

- o Floating torque shaft from yoke to
gearbox
- o Hybrid single ratio gearbox,
3.38 million ft.-lb. input
torque
- o Planetary 1st and 2nd stage gearing,
parallel shaft 3rd stage
- o In-line slipring access, shaft drive
lube pump, rotor lock, parking
brake, inching drive
- o Floating high speed shaft,
7,300 kW, 960-1440 rpm
wound rotor, induction generator

Nacelle 263,250 lb.

- o Bedplate type with wiring, piping
runs under flooring
- o Box type rotor support structure
with spindle, crane mount
- o Mountings for gearbox, generator,
control electronics, high voltage
cabinet
- o Insulated weather fairing
- o Lubrication system for gearbox
and bearings on lower platform
- o Yaw structural adapters and
bearing
- o Hydraulic power supply and
push-pull yaw drive
- o Yaw slipring

Tower 577,120 lb.

- o 14.5 ft. diameter steel shell
- o 240 ft. to rotor hub
- o 50 ft. tapered bell for tuning
- o Internal cable lift and ladder

Foundation

- o Spread footing, reinforced concrete
- o About 960 cubic yards
- o Anchor bolts for tower attachment

Electrical 88,000 lb.

- o Electrical equipment building with
cycloconverter and switchgear and
control
- o 7,300 kVA oil-filled transformer
with fused switch
- o 69 kV nominal interface
- o 175 MVA radial feeder cluster,
with 24 units

Maintenance

- o Permanent cluster crew

Other updates in the configuration were made in the rotor wood weight, partial span control, yoke, and lift subsystems. The partial span control spindle assembly increased from just under 4,000 lb. per blade to just over 7,000 lb. per blade, reinforcing the desire to use ailerons for torque control. The yoke weight significantly increased as a result of detailed stress analysis with new loads.

The elevator was changed to a traction drive, to comply with state and OSHA requirements.

In August, 1983, the system model was changed to 304.1 to reflect these changes.

5.10 MODEL 304.1 DESIGN

Details of the model 304.1 configuration are shown in Table 5-10. Model 304.1 was the heaviest configuration, and its cost of energy was too close to the maximum 3.75 cents/kWH in 1980\$. The results of wind tunnel testing on aileron models indicated an aerodynamic control using ailerons would be successful. The aileron conceptual design work was, therefore, expanded and incorporated into the rotor design.

The wind tunnel aileron tests, described in section 8.4.2, were performed on models with both plain and balanced or forward lip configuration and both 30% and 40% chord lengths. To avoid the expected noise problems which could be generated by a forward lip aileron, a 40% chord, plain aileron was selected. Three mechanically independent surfaces per blade were mounted on the outer 40%, or 80 ft., of the span. Each surface was driven by a hydraulic actuator and segmented to permit free motion with the main blade deflection.

Stopping calculations indicated that the ailerons might not be capable of stopping the rotor completely. A group of caliper brakes was added to the rotor support structure to engage a disk on the yoke. This low speed stopping brake also locks the rotor during maintenance. The holding brake on the high speed side of the gearbox was eliminated. The new brake location avoids loading the geartrain when the rotor is parked.

Table 5-10 Model 304.1 Configuration

System Weight (lb)	1,863,170
Installed Cost (Volume, 1980 \$)	4,184,885
Annual Energy (GWH, SOW wind, 0.96 AF)	21.2
Cost of Energy (Volume, 1980 cents/kwh)	3.74

Rotor 533,714 lb.

- o Upwind of tower
- o 400 ft. diameter
- o 352 ft/sec tip speed
- o 13.2-13.8/16.2-16.8 rpm
two range variable speed operation
- o Laminated wood blades and tip
- o Continuous wood center blade
- o 64-XXX Airfoil, 300 in. root chord,
3.06% solidity
- o 25% (50 ft.) hydraulically powered
partial span control, -90° motion
- o Steel yoke attachment at teeter axis
- o Teeter and brake shafts in bolster
- o Steel partial span control, stud
joints with blade and tip
- o Yoke-mounted hydraulic power unit
- o 7° tilt, ±9° teeter allowance
- o Elastomeric teeter bearings
and brake type teeter restrictor.
- o Yoke supported on spindle with dual
bearings

Drivetrain 259,636 lb.

- o Floating torque shaft from yoke to
gearbox
- o Hybrid single ratio gearbox,
3.38 million ft.-lb. input
torque
- o Planetary 1st and 2nd stage gearing,
parallel shaft 3rd stage
- o In-line slipring access, shaft drive
lube pump, rotor lock, parking
brake, inching drive
- o Floating high speed shaft,
7,300 kW, 960-1440 rpm
wound rotor, induction generator

Nacelle 328,700 lb.

- o Bedplate type with wiring, piping
runs under flooring
- o Box type rotor support structure
with spindle, crane mount
- o Mountings for gearbox, generator,
control electronics, high voltage
cabinet
- o Insulated weather fairing
- o Lubrication system for gearbox
and bearings on lower platform
- o Yaw structural adapters and
bearing
- o Hydraulic power supply and
push-pull yaw drive
- o Yaw slipring

Tower 653,120 lb.

- o 14.5 ft. diameter steel shell
- o 250 ft. to rotor hub
- o 50 ft. tapered bell for tuning
- o Internal traction elevator and
ladder

Foundation

- o Spread footing, reinforced concrete
- o About 960 cubic yards
- o Anchor bolts for tower attachment

Electrical 88,000 lb.

- o Electrical equipment building with
cycloconverter and switchgear and
control
- o 7,300 kVA oil-filled transformer
with fused switch
- o 69 kV nominal interface
- o 175 MVA radial feeder cluster,
with 24 units

Maintenance

- o Permanent cluster crew

A reduction in the weight of the center blade resulted from the decreased gravity loads without the partial span control. The weight and cost of the yoke and teeter assembly, however, increased, because the ear dimension was increased to provide acceptable fatigue stress levels.

The blade load carrying structure was laminated wood from tip to tip. Four field finger joints were used at 25% and 60% of the span to connect the blade modules. The inner blade trailing edge was bonded in the field to the structure, and the aileron subassemblies were secured by wood studs into load distribution ribs. The large number of studs in wood carrying main blade structural loads at the partial span control were eliminated from the design.

The model number was changed to 304.2 in September, 1983 to reflect the change to aileron control of the rotor. This configuration was reviewed with NASA in December, 1983.

5.11 MODEL 304.2 DESIGN

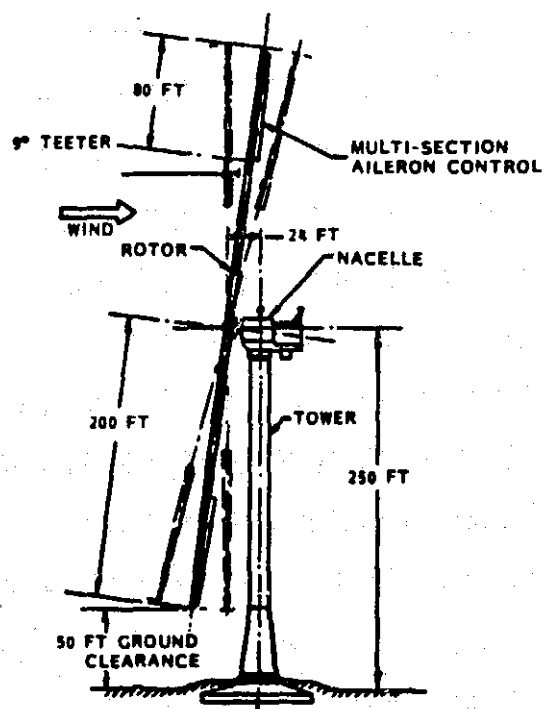
5.11.1 CONFIGURATION

The model 304.2 configuration is shown in Figure 5-4 and Table 5-11. Model 304.2 was the last design of the MOD-5A program.

5.11.1.1 Rotor Subsystem

The rotor subsystem of the MOD-5A wind turbine generator consists of all the rotating structures windward of the main rotor bearings. It is mounted by the main rotor bearings on the rotor support spindle, which is part of the nacelle assembly. The rotor subsystem is illustrated in Figure 5-5.

The major assemblies shown are the blade and ailerons. The rotor also includes the yoke, teeter bearings, brake subsystems, hydraulic subsystem and electrical subsystem. The yoke is a large steel fabrication that supports the blade from the teeter bearings to the main rotor bearings and the rotor support spindle. It transmits rotor torque through its forward shear web to the low speed shaft. The blade is attached to the yoke by the teeter bearing assemblies, which provide a degree of freedom to the blade perpendicular to the plane of rotation.



OPERATIONAL CHARACTERISTICS

RATED POWER	7300 KW AT 0.98PF
RATED WIND SPEED	32 MPH AT 250 FT
CUT-IN/CUT-OUT WIND SPEED	14/60 MPH AT 250 FT
MAXIMUM WIND SPEED (SURVIVAL)	130 MPH AT 250 FT
POWER CONTROL	MULTI-SECTION AILERONS
ROTOR RPM-SET SPEED	13.7/16.8 RPM ($\pm 10\%$)
ENERGY CAPTURE/YR	21.3 X 10 ⁶ KWH (NASA SPECIFIED WIND SPEED DURATION CURVE, 14 MPH AT 32 FT, 100 % AVAIL)
TOTAL WT ON FOUNDATION	1804 K-LB

FEATURES

- WOOD LAMINATE BLADES WITH HIGH PERFORMANCE AIRFOIL - UPWIND, TEETERED
- NON-ROTATING ROTOR SUPPORT
- HYBRID EPICYCLIC/PARALLEL SHAFT GEARBOX
- VARIABLE SPEED/CONSTANT FREQUENCY OPERATION, WITH 2 SET POINTS
- SOFT SHELL TOWER, TUNEABLE BELL SECTION

Figure 5-4 MOD-5A Model 304.2

Table 5-11 Model 304.2 Configuration

System Weight (lb)	1,803,926
Installed Cost (Volume, 1980 \$)	4,111,805
Annual Energy (GWH, SOW wind, 0.96 AF)	21.2
Cost of Energy (Volume, 1980 cents/kwh)	3.69

Rotor 474,470 lb.

- o Upwind of tower
- o 400 ft. diameter
- o 352 ft/sec tip speed
- o 13.2-13.8/16.2-16.8 rpm
 - two range variable speed operation
- o Laminated wood blades
- o Continuous wood blade, tip-tip
- o 64-XXX Airfoil, 300 in. root chord, 3.06% solidity
- o 40% (80 ft.) aileron control -90° motion 40% chord, 3 hydraulic actuators/blade
- o Steel yoke attachment at teeter axis
- o Teeter and brake shafts in bolster
- o Rotor stopping brake
- o Yoke-mounted hydraulic power unit
- o 7° tilt, ±9° teeter allowance
- o Elastomeric teeter bearings and brake type teeter restrictor.
- o Yoke supported on spindle with dual bearings

Drivetrain 259,636 lb.

- o Floating torque shaft from yoke to gearbox
- o Hybrid single ratio gearbox, 3.38 million ft.-lb. input torque
- o Planetary 1st and 2nd stage gearing, parallel shaft 3rd stage
- o In-line slipring access, shaft drive lube pump, inching drive
- o Floating high speed shaft, 7,300 kW, 960-1440 rpm wound rotor, induction generator

Nacelle 328,700 lb.

- o Bedplate type with wiring, piping runs under flooring
- o Box type rotor support structure with spindle, crane mount
- o Mountings for gearbox, generator, control electronics, high voltage cabinet
- o Insulated weather fairing
- o Lubrication system for gearbox and bearings on lower platform
- o Yaw structural adapters and bearing
- o Hydraulic power supply and push-pull yaw drive
- o Yaw slipring

Tower 653,120 lb.

- o 14.5 ft. diameter steel shell
- o 250 ft. to rotor hub
- o 50 ft. tapered bell for tuning
- o Internal traction elevator and ladder

Foundation

- o Spread footing, reinforced concrete
- o About 960 cubic yards
- o Anchor bolts for tower attachment

Electrical 88,000 lb.

- o Electrical equipment building with cycloconverter and switchgear and control
- o 7,300 kVA oil-filled transformer with fused switch
- o 69 kV nominal interface
- o 175 MVA radial feeder cluster, with 24 units

Maintenance

- o Permanent cluster crew

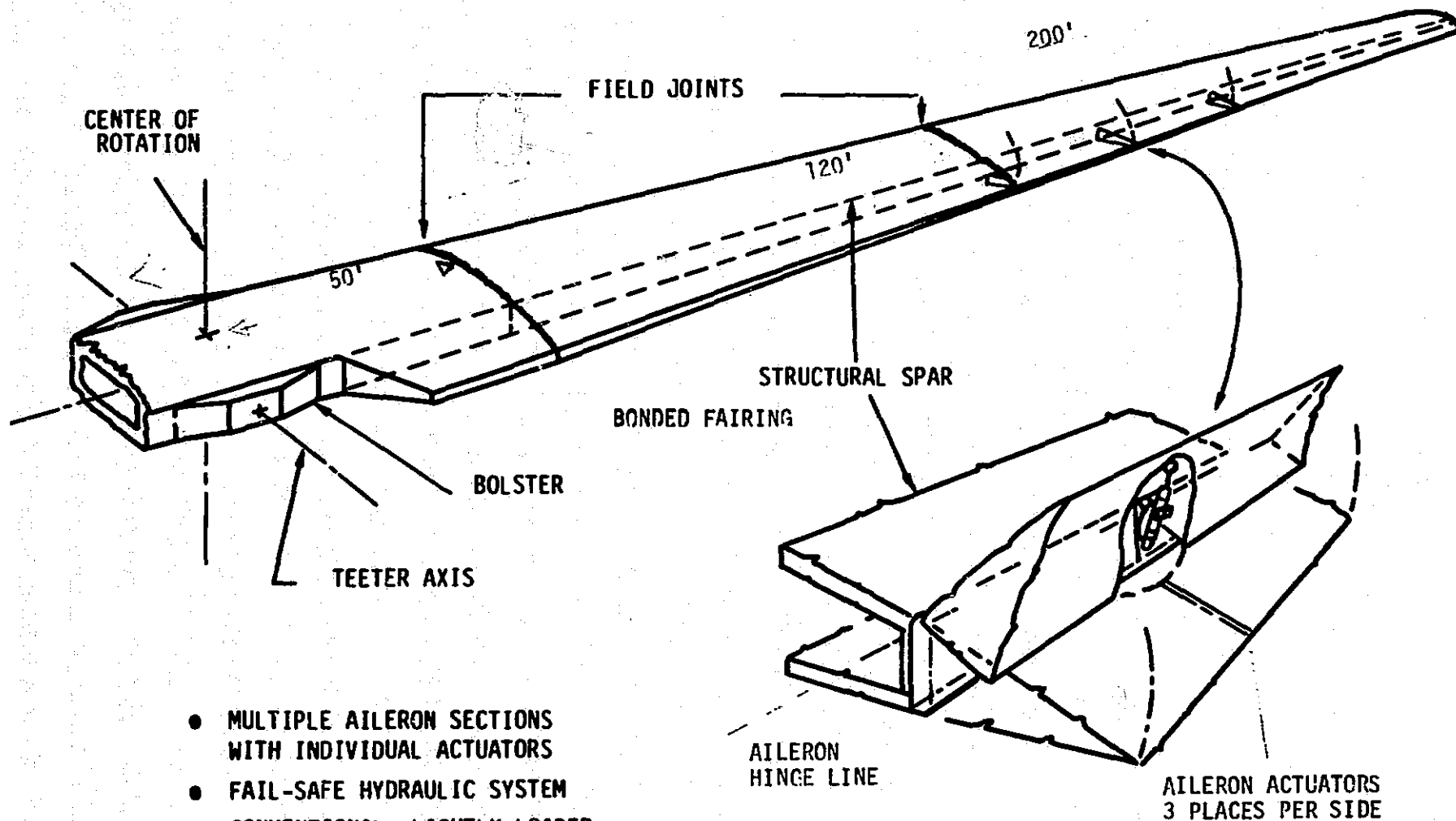


Figure 5-5 Rotor Subsystem

The laminated wood and epoxy blade is assembled from five segments: the center blade unit, two inner blade units and two outer units, which are bonded together in the field.

The ailerons form the trailing edge of the outer segments, from 60% to 100% of the span. They modify the rotor lift and drag characteristics to modulate system torque and control the rotor speed.

The rotor subsystem requires two braking subsystems, one for teeter motion and one to stop the rotor. The teeter brake stabilizes the teeter angle for low rotational speeds and high wind angle conditions. The teeter brake force is applied to four arms that are pinned to the blade bolster and slide through two sets of caliper brake assemblies for each arm. These calipers are mounted to the four corners of the yoke. They are actuated by the control subsystem. The rotor brake subsystem stops the rotor after the ailerons are deployed. The rotor brake torque is applied independently of the low speed shaft by means of a yoke-mounted brake disc and nacelle-mounted caliper brake sets.

The hydraulic subsystem provides the required pressure to the ailerons and teeter brakes. It is mounted on the outside of the yoke, to simplify its interfaces.

The electrical subsystem provides all power, command and signal functions to the rotor. Sliprings interface the rotating components with the non-rotating nacelle.

Lightning protection is built into the blades. A metal screen is used on the outer portion of the blade and conduit and conductors carry lightning currents to the yoke. The current is carried through the yoke to the nacelle and tower via a separate conduction path.

The five blade segments are assembled in the field. Ailerons, trailing edges, bolsters, hydraulic and electrical distribution systems and the teeter bearings and teeter shaft are also installed in the field. All subsystems are checked and the rotor is lifted as a unit into place on the yoke. The yoke assembly is also completed in the field, by installing the hydraulic power subsystem and associated hydraulic and electrical distribution lines. The yoke is installed on the nacelle support structure after the blade-to-yoke

interface is validated on the ground. The installation of the blade to the yoke completes the assembly of the rotor subsystem.

5.11.1.2 Drivetrain Subsystem

The drivetrain subsystem consists of all the elements that transmit power from the rotor to the generator. Power from the rotor passes through the torque plate, low speed shaft, speed increaser gearbox, and the high speed shaft to the generator. The gearbox increases the shaft speed with a set of gears with a ratio of 1 to 82.14. For example, if the low speed shaft turns at 16.8 rpm, the high speed shaft turns at 1380 rpm. The rotor support bearings supported the rotor and provided rotational freedom to the rotor.

The drivetrain is rated for 3.38×10^6 ft-lb of torque at the low speed shaft. Total system losses are approximately 10% at rated operating conditions and this torque rating provides 8,066 kW at 16.8 rpm (7,300 kW rating \times 1.105 = 8,066 kW). Friction causes some power loss in the drivetrain. The maximum power loss in the gears and bearings of the speed increaser is 3%. No loss is expected in the low and high speed shaft and coupling assemblies. The rest of the losses occur in the generator and electrical subsystem.

The rotor was supported on a pair of tapered roller bearings in a horizontal "king post" arrangement. The bearings were mounted on a stationary spindle that was part of the bedplate structure. The inner bearing races were stationary, and the outer races rotated with the yoke. In this arrangement the two bearings oppose the weight moment exerted by the rotor, the dead weight of the rotor, and the rotor thrust. The bearing arrangement is illustrated in Figure 5-6. The bearings were designed for grease lubrication. An automatic lubricator periodically injects a metered quantity of grease.

The torque plate transmits torque from the yoke to the low speed shaft. The outer diameter of the torque plate is bolted to the yoke, and the inner diameter of the torque plate interfaces with the low speed shaft, at a splined connection. The low speed shaft is a forging with a concentric inner passage, which protects an electrical conduit. Electric power, control and instrumen-

tation wiring run from a slip ring, mounted on the rear end of the gearbox, through the gearbox and low speed shaft to the rotor. They provide electric power and control to the hydraulic aileron actuation subsystem and other rotor controls.

ORIGINAL PAGE IS
OF POOR QUALITY

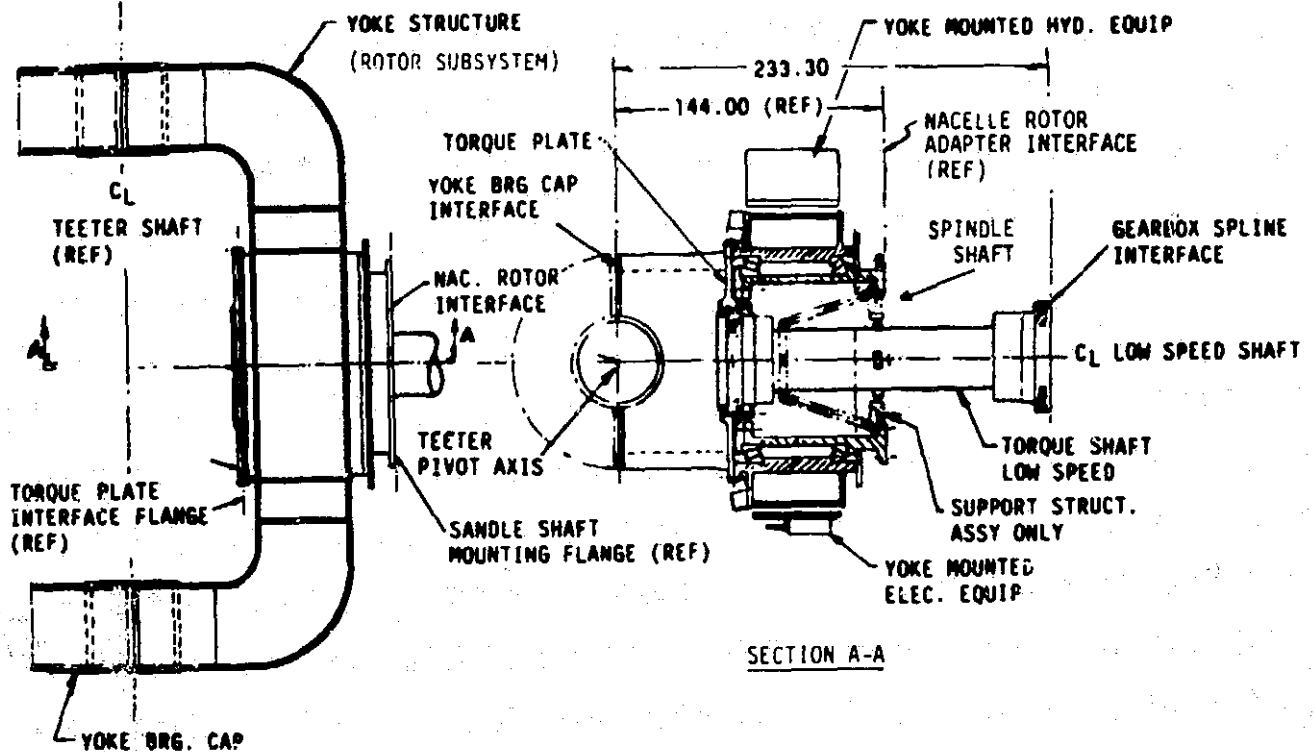


Figure 5-6 Rotor Support Assembly

The low speed shaft is connected directly to the first stage of the gearbox through a splined connection. The gearbox is a stand-alone, 3-stage unit. The first and second stages are epicyclic and the third stage has a parallel shaft design. The epicyclic stages are of conventional planetary arrangement, in which the input torque is transmitted to the planet cage and the output torque is transmitted by the sun wheel to the next stage. The output of the second stage is transmitted to the bull gear of the third stage. The bull gear turns a pinion, whose output drives the generator. The connection between the gearbox and generator is the high speed shaft assembly.

The gearbox and the splined interface between the gearbox and low speed shaft are lubricated by a central oil lubrication system. Two parallel pumps ensure that oil is available at all times. A motor-driven pump circulates oil during start-up and backs up the gear driven pump in the gearbox. The gear-driven pump circulates oil after the wind turbine reaches operating speed. Mobil SHC630 oil is circulated through the gearbox at 160 gpm and 25 psi. The oil temperature is kept between 60°F and 115°F by heaters or coolers, to maintain the proper viscosity for protecting the gears and bearings.

A 400 gallon oil reservoir was built into the gearbox. Other conditioning equipment, such as filters, heaters, and coolers were located either in the reservoir or on the lubricating subsystem platform.

The high speed shaft assembly used flex disc couplings to provide a low maintenance, floating shaft configuration.

The low speed brake was designed to assist the ailerons in stopping the rotor, when the rotor speed was 10 rpm or lower. The brake also prevented rotation during maintenance and servicing. The low speed brake consisted of a 10.5 ft. diameter steel disc mounted on the rear of the yoke and eight Goodyear SLC 19 brake calipers, mounted on the front rotor adapter. The brakes supply a holding torque of 3,000,000 ft-lb.

5.11.1.3 Nacelle Subsystem

The nacelle subsystem has key structural, dynamic and protective functions. The nacelle structure provides a load path from the rotor to the tower. The complex load consists of equipment dead weight, overturning moments, thrust, rotor dynamics and wind induced forces. In designing the structural elements, ultimate load levels and fatigue were design drivers. The nacelle provides the rotating interface between the rotor and gearbox in the form of a stationary spindle shaft, shown in Figure 5-6, and a pair of tapered roller bearings. The bearings support the 300,000 lb rotor and resist the associated dynamic forces, while providing rotational freedom to the rotor. Finally, the nacelle protects the drivetrain, generator, controls and power conditioning equipment from the environment. A profile of the nacelle subsystem is shown in Figure 5-7.

The largest, and perhaps most critical element of the nacelle is the bedplate. The bedplate, shown in Figure 5-7, is a large weldment made of structural shapes. The design includes details that meet the requirements of the fatigue load environment. All key welds are full penetration, all changes in section are smooth and gradual and there are no sharp corners. The bedplate material is A572 GR 50 steel and is specified to have controlled grain size and minimal inclusions and must meet a rigorous, low temperature Charpy V-notch test. Post-weld heat treatment was specified to assure that residual stresses are relieved. Similar design criteria were applied to the front adapter sections, side walls and roof sections.

The bedplate has a flat bottom made of 4 in. thick steel plate that is bolted to the flange of the upper yaw section. To reduce weight, lightly loaded sections of the bottom plate are made of 1 in. thick steel.

The spindle is a forging, made from ASTM A508, Class 4b steel, with controlled inclusion shapes and restrictions on phosphorus and sulphur. The forging must meet a rigorous, low temperature Charpy V-notch test. The spindle is bolted to the front face of the rotor adapter and supports the rotor on bearings.

The roof structure of the nacelle was designed to support a 5-ton utility crane. The crane is a service and maintenance tool and can reach and lift

ORIGINAL PAGE IS
OF POOR QUALITY

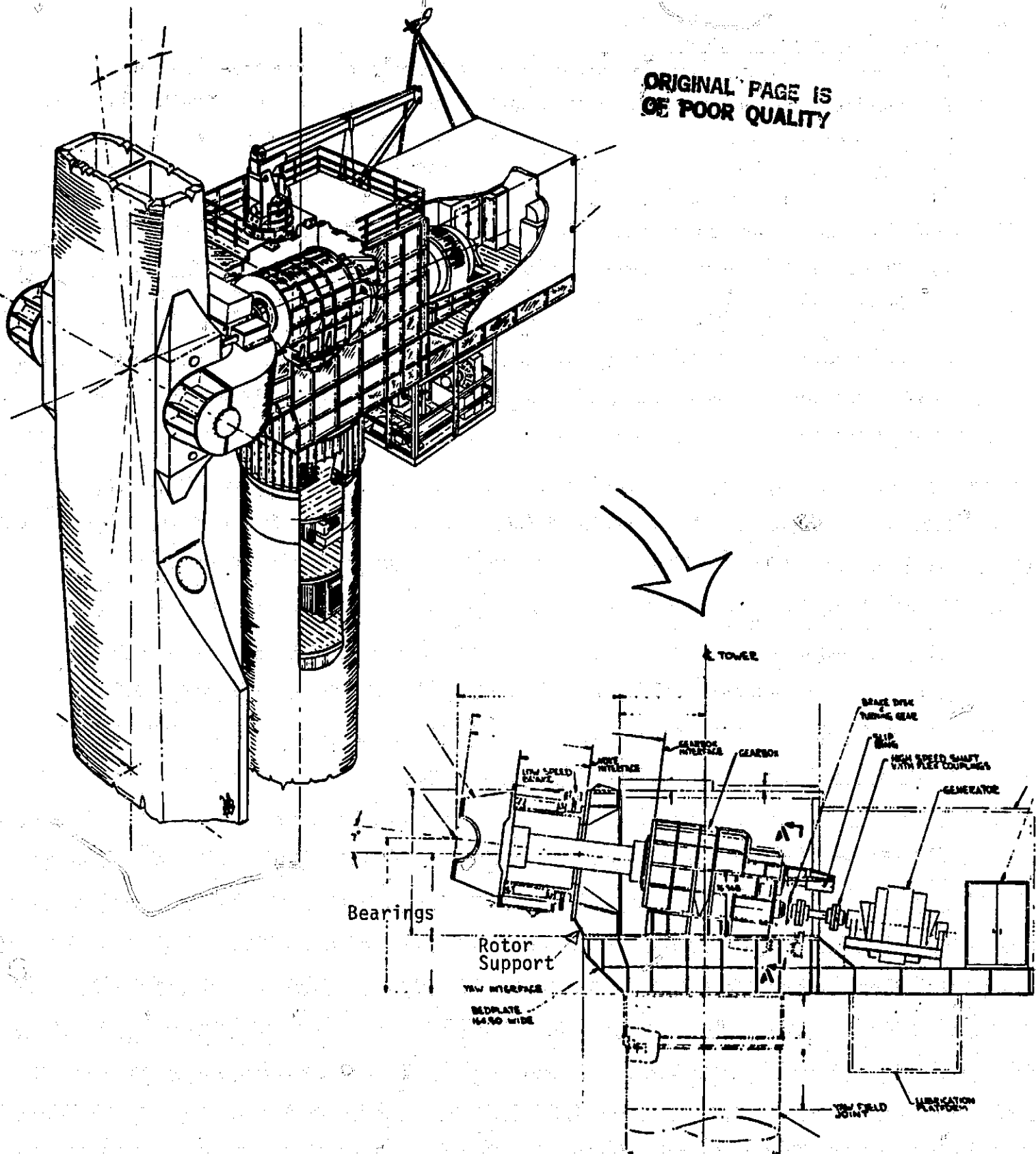


Figure 5-7 Nacelle Profile

most of the generator and drivetrain components, such as pinions, bearings and couplings. Also, the crane provides a hoist point for blade inspection and teeter bearing maintenance.

A fairing covers the aft section of the nacelle to protect the generator, control cabinet and power conditioning equipment. The fairing is made of light-weight galvanized steel with thermal insulation. The fairing was designed to resist wind pressure and live loads on the roof. A louvered vent, air filters and an exhaust fan are attached to the fairing. The fairing has access hatches and supports two wind sensor masts and aircraft warning lights. The gearbox lubrication subsystem was attached to the bottom of the bedplate.

All sections of the nacelle subsystem were designed to meet shipping size and weight requirements. The sections are bolted together in the field to form the overall structure. All exposed metal surfaces areas are painted in the factory with two coats of zinc-rich primer before the finish coat and touch-up paint are applied in the field.

5.11.1.4 Tower and Foundation Subsystem

The tower and foundation are shown in Figure 5-8. The tower is a cylindrical, welded steel structure made from formed plates. The cylinder has a 14.5-ft. diameter between the nacelle and an elevation of 50 ft.. Below 50 ft. the structure is conical, spreading out to a diameter of 22.5 ft. at the base. There are 25 sections, most of which are slightly less than 10 ft. high. The thickness of each section, which was determined by fatigue or buckling allowable stress and the frequency criteria, is different. The frequency criteria was that the tower stiffness would be such that the first bending frequency of the entire system would be approximately 0.34 Hz.

The tower base has reinforcements, called anchor chairs, that help distribute the tower loads into 96 anchor bolts. The anchor bolts are embedded about 4 ft. into the reinforced concrete ring wall of the foundation. The foundation is a spread foundation, 72 ft. in diameter and 9 ft. below the original grade level. The design requires approximately 1,000 cubic yards of concrete. This

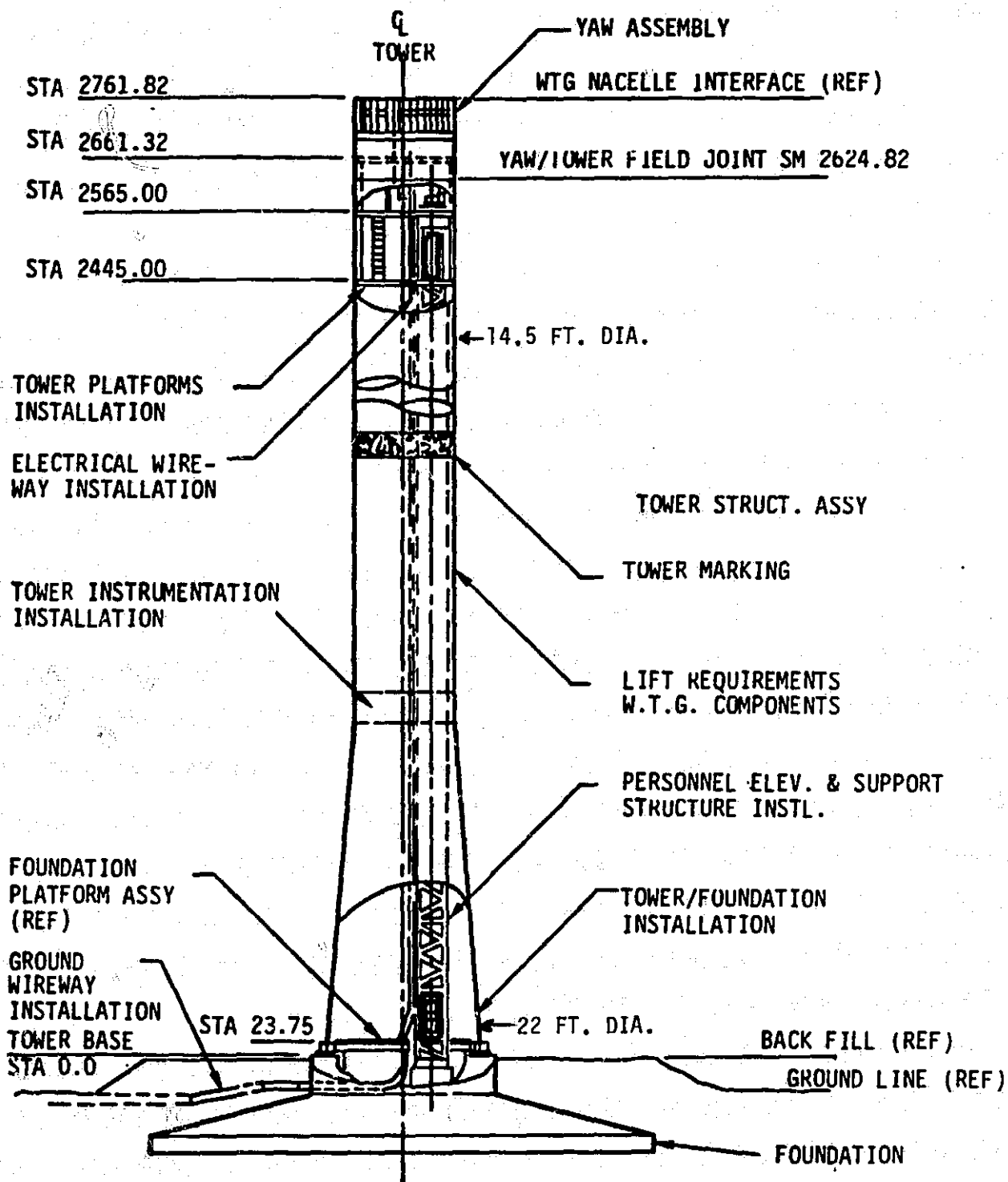


Figure 5-8 Tower and Foundation

design is a generic design; the foundation design should depend on the soil properties at the site. However, study has shown that except for some unusual sites, the design will be close to that described here.

The elevator and support structure are inside the tower. The elevator is a traction elevator, often used in grain elevator applications. The elevator meets ANSI/ASME 17.1a Part XV and, consequently, it will be acceptable in over 90% of the states without special permit requirements. The elevator support structure is only attached at the top of the tower, and it stands on a pivoted base to minimize stresses induced as the tower flexes. There are platforms at the top and bottom for entrance to the elevator. The tower has a door at the bottom to allow entrance to the interior of the tower and access to the elevator.

At the top of the tower there are two sections called the lower and upper yaw adapter sections. Between these sections, a large slewing ring bearing is mounted. The bearing allows the nacelle to rotate in the yaw azimuth, relative to the fixed tower. The yaw sections also include a yaw drive, yaw slipring, hydraulic power supply, and an automatic bearing lubrication system. All components are enclosed in the tower, to protect them from the weather. A ladder in the yaw section provides access to the nacelle through manholes in the bedplate floor.

5.11.1.5 Power Generation Subsystem

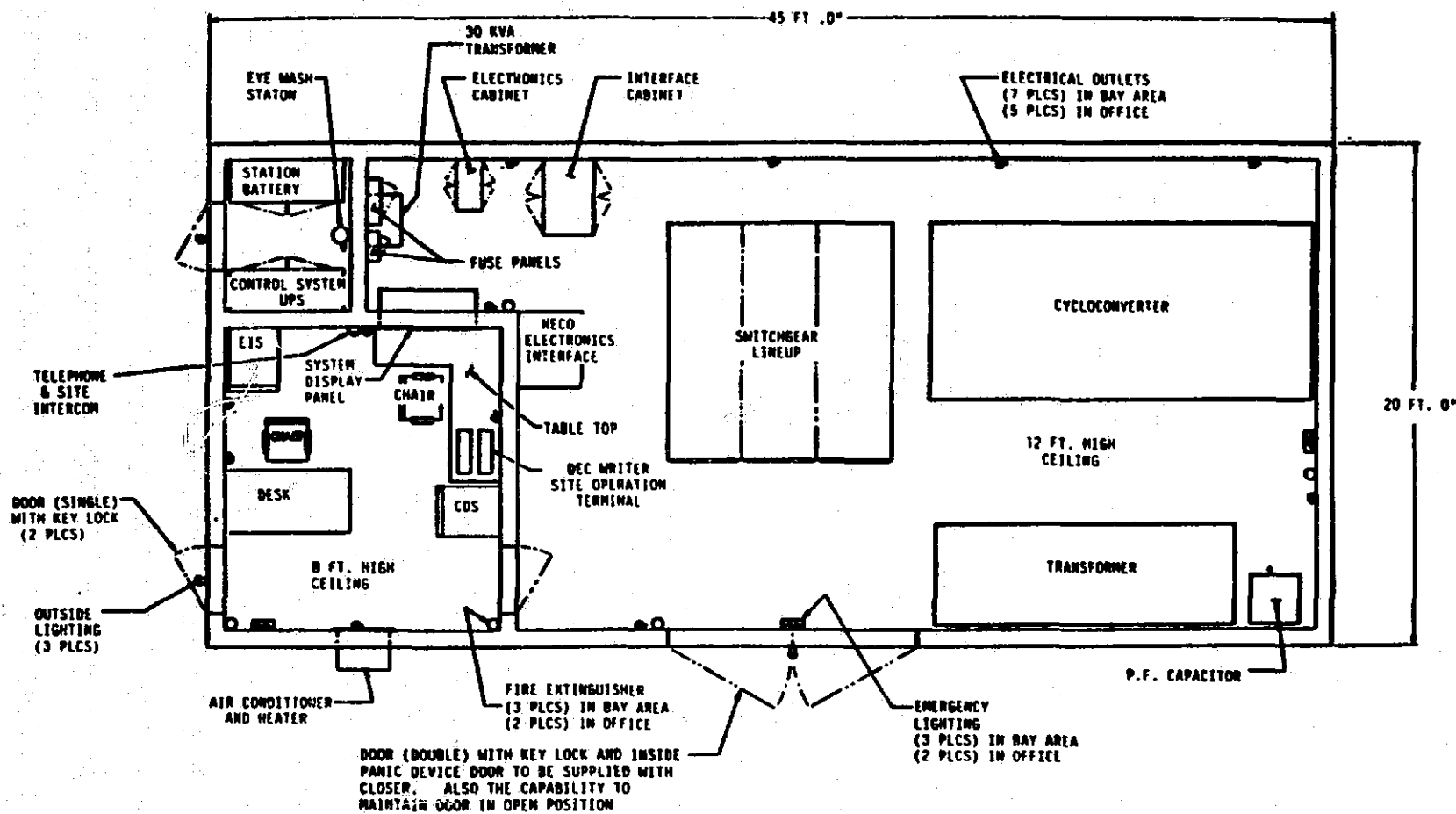
A variable speed generator and its associated power conversion equipment converts the mechanical energy of the wind turbine to useful electrical energy. Equipment locations at ground level are shown in Figure 5-9. A simplified, one-line diagram of the subsystem with protective relay numbers is shown in Figure 5-10.

The major components include the generator, sliprings, interconnections, power converter, harmonic filter, switchgear, step-up transformer, and station batteries. The components were chosen for a 30-year life and a maintenance interval of 6 months or more.

The generator is a 7500 kVA wound-rotor, 6 pole machine with a 6300 kVA stator, and a 1500 kVA rotor. A static power converter and its associated control maintain the output frequency at 60 Hz while the rotor speed varies. The stator and converter output is 4160 V. When singly excited, the generator also provided motoring duty to bring the rotor up to 3.5 rpm.

The converter and its controls are designed to regulate the generator's air gap torque, frequency and reactive power. This equipment is located in an enclosure near the base of the tower. The switchgear for stator short, stator tie, and converter tie functions, and associated relays are also located in the enclosure.

All electrical circuits between the rotating nacelle and the stationary support tower pass through the yaw slipring assembly.



ORIGINAL PAGE IS
OF POOR QUALITY

Figure 5-9 Electrical Equipment Location

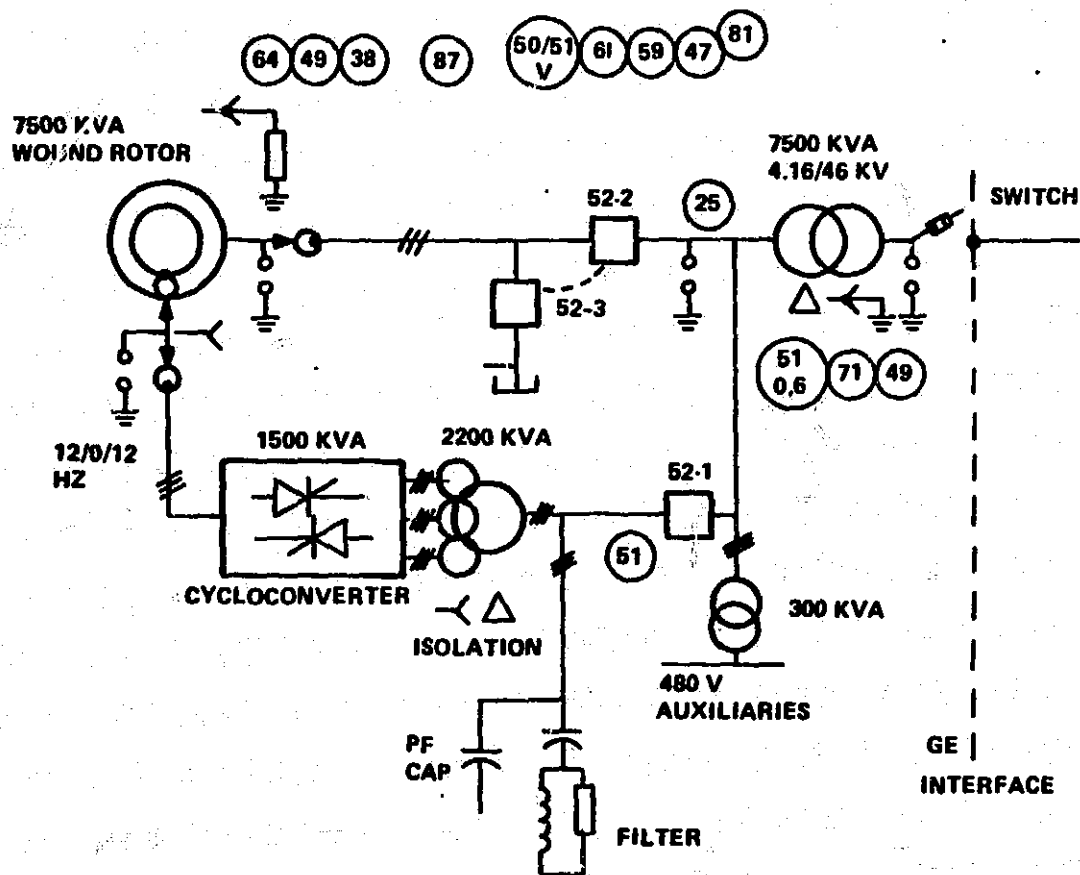


Figure 5-10. Power Generation Diagram

5.11.1.6 Control And Instrumentation Subsystems

A block diagram of the control subsystem is shown in Figure 5-11. The controller, signal conditioning, and the emergency shutdown panel are located in the nacelle in the controls equipment cabinet. The system display panel, operator's terminal, and the controls data subsystem are located in the office of the electrical equipment building at the base of the tower. There are also three data multiplexers; one is located on the yoke, one in the nacelle, and one in the electrical equipment building.

The controller is a microprocessor-based, programmable controller, the EPTAK 700, made by Eagle Signal. The basic functions of the controller are mode determination, automatic sequence operation, torque and speed control, and command and data interface.

The remote and site operator's terminals are "dumb" keyboard printers that print a summary of the operating data and transmit the operator's commands.

The control data subsystem is an engineering instrumentation subsystem that supports tests and initial operation. It receives operating data from the controller, and records and processes the data for a detailed report. The control data subsystem transmits the operator's commands to interrogate controller RAM locations and to alter operating parameters.

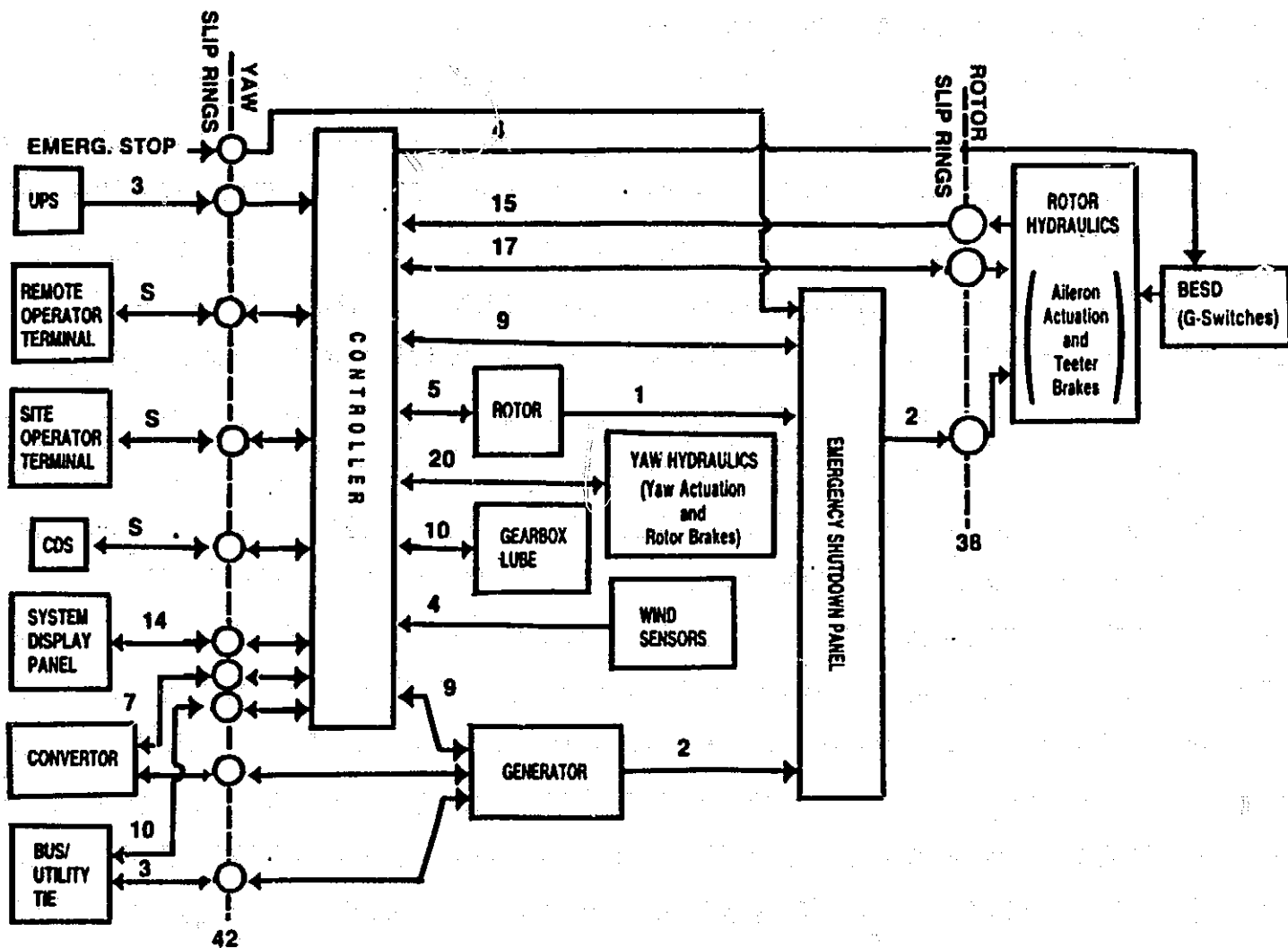


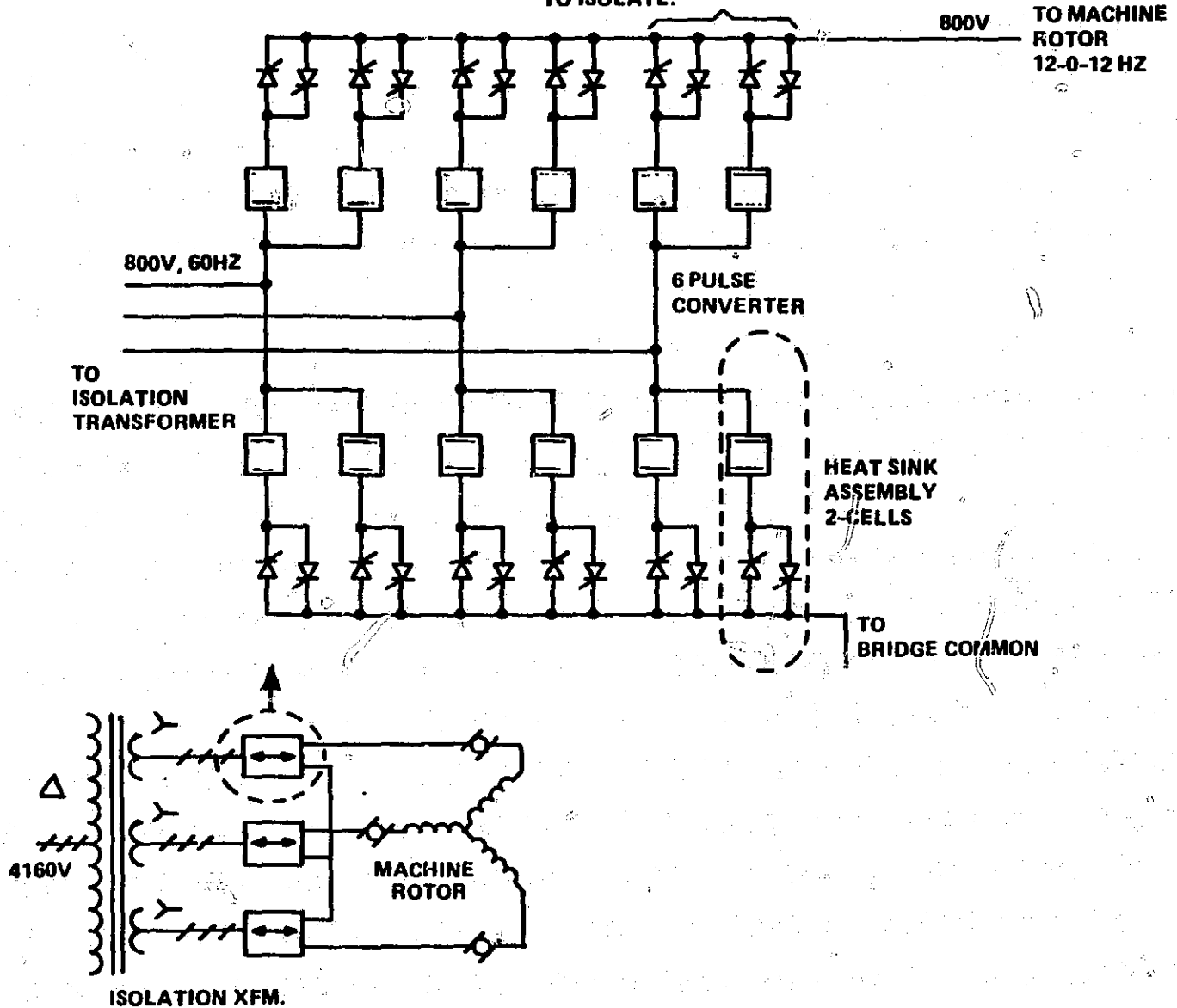
Figure 5-11 MOD-5A Control Subsystem Block Diagram

The system display panel contains hardware functions for shutdown, manual mode select, and controller reset. Basic operating performance parameters are displayed in engineering units. TV video display and the intercom are located in the system display panel.

The emergency shutdown panel functions independently of the controller. The emergency shutdown panel energizes feather valves that enable the controller to operate hydraulic servo valves. When deenergized, the feather valves cause the ailerons to feather. When the emergency shutdown panel loses the signal, it deenergizes the feather valves for a shutdown that is analogous to a "deadman stick" operation.

A cycloconverter for the variable speed generator subsystem is shown in Figure 5-12. The converter has a local controller that communicates with the wind turbine controller in the nacelle. This local controller operates switchgear, controls converter operation, and provides converter fault detection.

**100% REDUNDANT ARRANGEMENT
WILL OPERATE WITH ONE CELL
SHORTED/BLOWN FUSE
TO ISOLATE.**



**CONVERTER: 500 KVA (1/3 OF CYCLOCONVERTER)
CIRCUIT IS STANDARD REVERSING D.C. DRIVE ARRANGEMENT
SHOWN: 6 HEAT SINKS x 2 CELLS x 2 REDUNDANT = 12 HEAT SINKS, 24 CELLS
TOTAL SYSTEM: 36 HEAT SINK ASMS, 72 CELLS
CONVERTER & CONTROL: 18' LONG, 7' DEEP, 7-1/2' HIGH; 11,000# APPROX.
ISOLATION TRANSFORMER: 5-1/2' LONG, 5' DEEP, 8-1/2' HIGH; 12,000# APPROX.**

Figure 5-12. Cycloconverter

5.11.2 PERFORMANCE

The performance of the MOD-5A model 304.2 was computed from full rotor power coefficients, mechanical and electrical losses, start-up and shutdown losses, and homekeeping energy losses.

The design wind regime is defined as a Weibull distribution with a 32.8 ft. shape factor of 2.29 and a mean coefficient of 7.17 mps. The vertical wind distribution varies exponentially with elevation and the exponent varies with wind speed. At the hub height of 250 ft., the Weibull parameters are 2.75 and 10.46 mps. Hub height parameters were used as full immersion valves and the sub-rated energy capture was later reduced by 4.2% to account for rotor tilt, teeter, and vertical wind variation.

The baseline performance is shown in Figure 5-13 for the design wind at sea level, and at an elevation of 7000 ft. The net output power and wind speed at hub height are plotted against cumulative probability. At sea level, the cut-in wind speed is 14 mph, the rated wind speed is 32 mph and the cut-out wind speed is 60 mph. The predicted annual energy capture, at 96% availability, is 21.2 GWh at sea level, and 17.9 GWh at 7,000 ft.

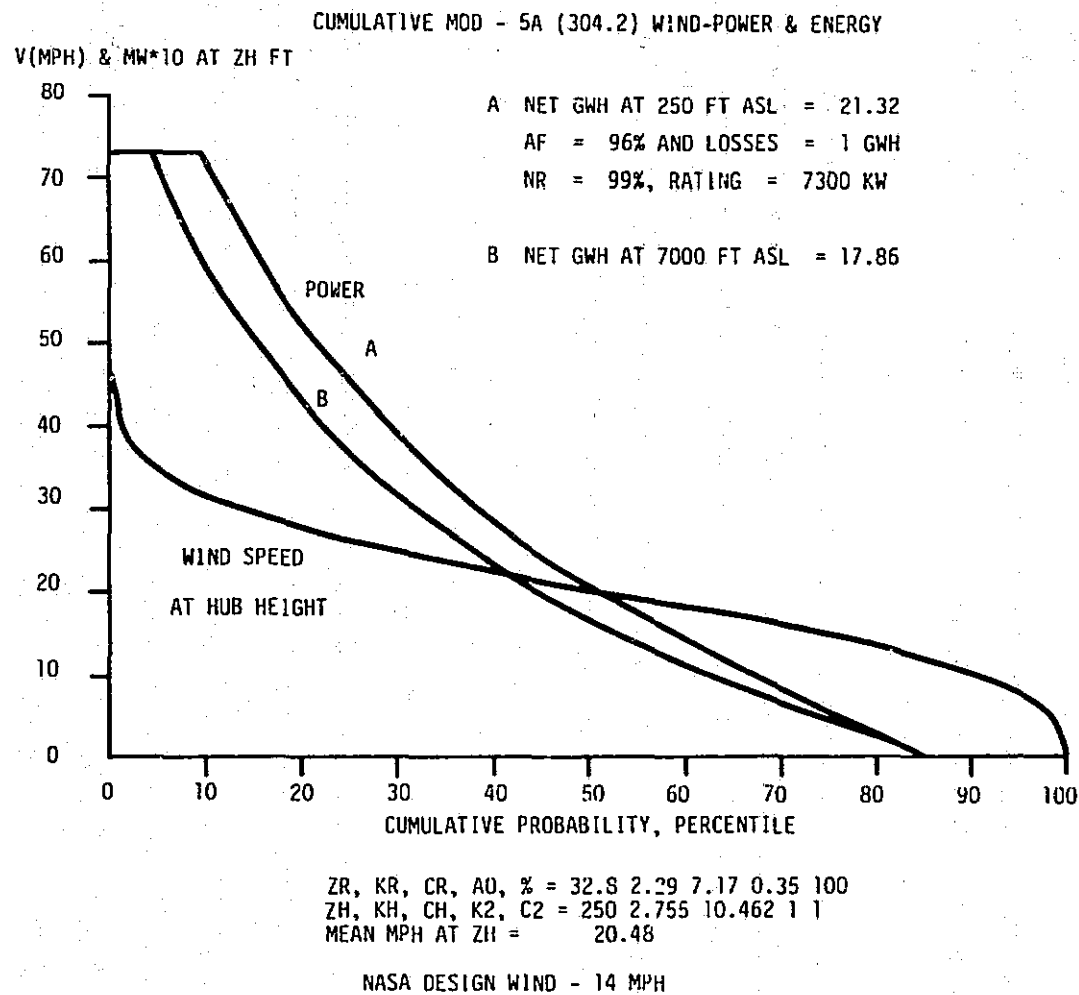
The distribution of energy losses, with respect to the total energy in the wind passing through the rotor disk area, is shown in Table 5-12.

The predicted performance for the wind turbine in Kahuku, Oahu, HI, is shown in Figure 5-14. The strong trade winds in this area provide almost 2.5 times the operating time at the rating provided by the design wind. The predicted annual energy capture at 96% availability is 32.2 GWh.

In the design wind distribution, the 7300 kW rating is based on a relatively high power density, and the plant factor is, therefore, a low value: 33%.

The rotor performance predictions use the automatic control plan, where changes in speed are made while power is being delivered. A low speed range, from 13.2 to 13.8 rpm, and a high speed range, from 16.2 to 16.8 rpm, are used to maintain high rotor efficiency. Start-up and shutdown losses are based on 1100 starts per year, at 15 minutes for each.

C-3



ORIGINAL PAGE IS
OF POOR QUALITY

Figure 5-13 Power and Wind Speed Probability for the Design Wind Regime

Table 5-12 Design Energy Output

Item (Model 304.0)	Energy Loss -GWh/Year	Net Energy Output GWh/Year	Gross % of Wind Energy
Gross Wind Energy (12-60 mph)		72.34	100.0
Not Extractable	29.44		(40.7)
Maximum Theoretical Energy (Betz Limit)		42.90	59.3
Rotor Profile & Degradation	11.60		(16.0)
Rotor Power Limit (Above Rating)	4.57		(6.3)
Rotor Teeter, Tilt, Heading, Misc.	1.44		(2.0)
Rotor Start-up, Shifting Losses	0.29		(0.4)
Rotor Output Energy		25.00	34.6
Transmission Losses	1.06		(1.5)
Generator Losses	0.99		(1.4)
Generator Output Energy		22.95	31.7
Accessory/Auxiliary Losses	0.58		(0.8)
Transformer Losses	0.11		(0.1)
Single Unit Output Energy		22.26	30.8
Interconnection Losses	0.21		(0.3)
Availability Losses	0.86		(1.2)
Net Utility Substation Output Energy		<u>21.19</u>	<u>29.3</u>

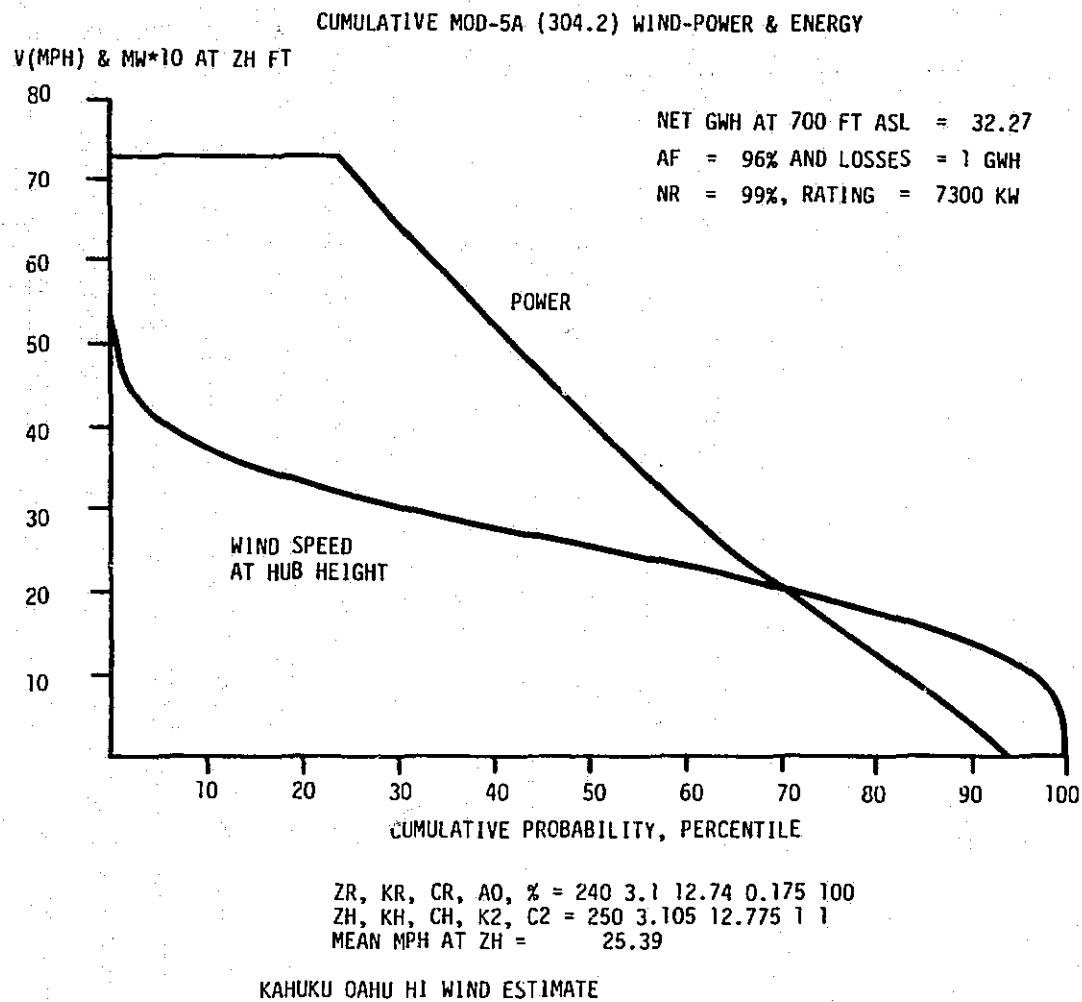


Figure 5-14 Power and Wind Speed Probability for the Wind Regime in Kahuku

5.11.3 WEIGHT SUMMARY

The model 304.2 equipment above ground level weighs 1,803,926 lb. Thirty-five percent of the weight is in the support tower and elevator, and 5% is in the ground electrical equipment. The electrical equipment building structure is not included in the weight breakdown. Nineteen percent of the weight is in the nacelle and yaw structure. Twenty-five percent of the weight is in the rotor, and 14% of the weight is in the drivetrain.

A weight breakdown by major subsystem is shown in Table 5-13.

5.11.4 COST SUMMARY

Cost summaries for the first, second third, the 100th unit in a single installation, and the 100th unit in a cluster installation are shown in Tables 5-14 through 5-18. The costs are in 1980 dollars.

5.11.5 COST OF ENERGY

Cost of energy values are shown in Tables 5-14 through 5-18. The predicted cost of energy for the clustered installation, in volume production, for a design wind regime and mature availability is 3.69 cents/kWh. This cost is below the maximum of 3.75 cents/kWh specified in the Statement of Work.

Table 5-13 Model 304.2 Weight Summary

<u>Subsystem</u>	<u>Item</u>	<u>Weight (lb.)</u>
Rotor	Blades	229,900
	Ailerons	9,760
	Yoke	150,000
	Teeter Bearing Assembly	45,670
	Other	39,140
	Subtotal	474,470
Drivetrain	Low Speed Shaft	66,700
	Gearbox	137,000
	Generator	47,200
	Other	8,736
	Subtotal	259,636
Nacelle	Bedplate, Supports	111,000
	Rotor Support	130,150
	Fairing	6,800
	Yaw	54,400
	Other	26,350
	Subtotal	328,700
Tower	Structure	609,120
	Lift	28,500
	Other	15,500
	Subtotal	653,120
Ground Electrical Equipment		88,000
Total Weight Above Grade		1,803,926

Table 5-14 Cost Summary for the First Unit

SUBSYS. ABBREV.	ITEM NAME ABBREV.	REF. NUM.	WEIGHT # 1ST UNIT	COST (1980) 1ST UNIT	DOLLARS PER LB.	% OF TOTAL WT.	% OF COE	COE CONTRIB. (1990 CENTS)
SITE	FOUNDATION	110		\$362,300.00			2.75	0.329
	GRD EQUIP.	120	88000	\$725,500.00	\$8.24	4.8781	5.50	0.658
	SPECIAL	130		\$180,800.00			1.22	0.146
			88000	\$1,248,400.00	N/A	4.8781	8.47	1.132
TRANSPORT.	TRANSPORT.	240		\$306,854.82			2.33	0.278
ERECTION	INSTALL.	310		\$605,200.00			4.58	0.549
	INTES. & C/O	380		\$1,194,700.00			9.06	1.084
				\$1,799,900.00			13.65	1.633
ROTOR	BLADES	410	228900	\$2,514,758.00	\$11.37	12.7441	18.83	2.372
	ROTOR HYDR.	420	8418	\$47,861.00	\$5.70	0.4868	0.38	0.044
	ATLERNONE	425	9780	\$188,516.00	\$19.35	0.5410	1.43	0.171
	YOKE ASM/BRGS.	430	170582	\$777,877.00	\$4.55	9.4770	5.90	0.706
	TEETER ASM.	440	55430	\$305,528.00	\$5.51	3.0727	2.32	0.277
			474470	\$3,834,970.00	\$8.29	23.2298	29.84	3.569
DRIVE TRAIN	LOW SPEED SFT.	518	86700	\$298,601.00	\$4.48	3.8374	2.26	0.271
	TRANSMIS.	520	138730	\$488,491.00	\$3.50	7.7457	3.70	0.443
	HI SPEED	530	3000	\$17,763.00	\$5.82	0.1863	0.13	0.016
	GEN. & EXCIT.	540	50208	\$320,716.00	\$6.38	2.7831	2.43	0.291
			259636	\$1,125,571.00	\$4.34	6.6468	8.54	1.021
MACELE	ROTOR SUPPORT	605	138150	\$405,891.00	\$2.82	7.7136	3.08	0.368
	BEDPLATE	610	116050	\$338,866.00	\$2.82	6.4330	2.57	0.307
	HYD. SYSTEM	620	8100	\$18,118.00	\$2.27	0.3381	0.14	0.016
	FAIR. & MISC.	646	8800	\$90,326.00	\$13.28	0.3769	0.68	0.082
	SLP. ELEC.	680	2870	\$53,812.00	\$18.15	0.1846	0.41	0.049
	INST. & CON.	670	3270	\$114,752.00	\$35.09	0.1813	0.67	0.104
	YAW SUBSYS.	680	54400	\$354,899.00	\$6.53	3.0156	2.69	0.322
			328740	\$1,376,864.00	\$4.19	18.2232	10.44	1.249
TOWER	TOWER	710	609120	\$681,000.00	\$1.12	33.7656	5.16	0.618
	PERS. LIFT	720	29500	\$88,827.00	\$3.12	1.5799	0.67	0.081
	CABLING	740	15500	\$88,806.00	\$5.73	0.8592	0.67	0.081
			653120	\$858,633.00	\$1.31	36.2047	6.51	0.779
REN. CONT.	LINE MODERN	810		\$728.00			0.01	0.001
	REN. DISP.	820		\$4,776.00			0.04	0.004
				\$5,504.00			0.04	0.005
SAPRES	SAPRES	930		\$117,486.00			0.89	0.107
SPECIAL	PROFIT	1010		\$1,154,827.26			8.76	1.047
	ASM. & TEST	1020		\$774,080.00			5.87	0.702
	GROWTH BUDGET	1030		\$0.00			0.00	0.000
				\$1,928,907.26			14.63	1.750
LAND	MTG LAND	1110		\$0.00			0.00	0.000
	ROAD LAND	1140		\$0.00			0.00	0.000
				\$0.00			0.00	0.000
CLUSTER	SUBSTATION	1240		\$0.00			0.00	0.000
	TRANSM. ETC.	1250		\$0.00			0.00	0.000
				\$0.00			0.00	0.000
O & M	YEARLY O & M	1340		\$43,500.00			3.67	0.438
TOTAL OVERALL (NO O&M)								
REF. NUM. 100-1288			1803966 #	\$12,703,099.88	7.0417	100.0000	100.00	11.960
PREPROFIT COST								
				PRE-PROFIT (1980)	AF	GROSS	GMH/YR#E4	NET
				\$11,548,272.62	0.9	220500		198450

ORIGINAL PAGE IS
OF POOR QUALITY

Table 5-15 Cost Summary for the Second Unit

SUBASS. ABBREV.	ITEM NAME ABBREV.	REF. NUM.	HEIGHT # 2ND UNIT	COST (1980) 2ND UNIT	DOLLARS PER LB.	% OF TOTAL WT.	% OF COE	COE CONTRIB. (1980 CENTS)
SITE	FOUNDATION	110		\$333,318.00			3.08	0.302
	GRO EQUIP.	120	88000	\$687,460.00	\$7.58	4.9781	6.17	0.605
	SPECIAL	130		\$128,480.00			1.18	0.117
			88000	\$1,128,258.00	N/A	4.9781	10.43	1.024
TRANSPORT.	TRANSPORT.	240		\$306,854.52			2.84	0.278
ERECTION	INSTALL.	310		\$486,004.00			4.31	0.423
	INTEG. & C/D	350		\$436,280.00			7.73	0.759
				\$1,302,284.00			12.03	1.181
ROTOR	BLADES	410	228800	\$1,581,058.50	\$6.53	12.7441	18.12	1.778
	ROTOR HYDR.	420	8418	\$43,184.80	\$5.13	0.4868	0.40	0.039
	AILERONS	428	9780	\$141,634.50	\$14.51	0.5410	1.31	0.128
	YOKE ASM/BRGS.	430	170862	\$684,831.75	\$4.00	8.4770	6.32	0.621
	TEETER ASM.	440	85430	\$259,638.80	\$4.69	3.0727	2.40	0.236
			474470	\$3,080,088.45	\$6.51	23.2288	28.55	2.803
DRIVE TRAIN	LOW SPEED SFT.	518	88700	\$238,880.80	\$3.58	3.6874	2.21	0.217
	TRANSMIS.	520	138730	\$439,641.80	\$3.15	7.7487	4.06	0.399
	HI SPEED	530	3000	\$14,210.40	\$4.74	0.1863	0.13	0.013
	GEN. & EXCIT.	540	50206	\$304,680.20	\$6.07	2.7831	2.82	0.276
			259636	\$997,413.30	\$3.84	8.6468	9.22	0.905
NACELLE	ROTOR SUPPORT	605	138150	\$345,007.35	\$2.48	7.7136	3.19	0.313
	BEDPLATE	610	116050	\$281,258.78	\$2.42	6.4330	2.60	0.255
	HYD. SYSTEM	620	6100	\$16,306.20	\$2.67	0.3381	0.15	0.015
	FAIR. & MISC.	645	8800	\$76,777.10	\$11.28	0.3789	0.71	0.070
	SLP. ELEC.	660	2870	\$48,520.80	\$16.34	0.1645	0.45	0.044
	INST. & CON.	670	3270	\$94,056.64	\$28.78	0.1813	0.87	0.085
	YAW SUBSYS.	680	54400	\$312,399.12	\$5.74	3.0156	2.89	0.283
			328740	\$1,174,365.89	\$3.57	16.2232	10.85	1.065
TOWER	TOWER	710	608120	\$626,520.00	\$1.03	33.7656	5.78	0.568
	PERS. LIFT	720	28600	\$79,944.30	\$2.81	1.5789	0.74	0.073
	CABLING	740	15500	\$81,701.52	\$5.27	0.8592	0.75	0.074
			653120	\$788,165.82	\$1.21	36.2047	7.28	0.715
REM. CONT.	LINE MODEM	810		\$684.32			0.01	0.001
	REM. DISP.	820		\$4,793.82			0.04	0.004
				\$5,078.24			0.05	0.005
SPARES	SPARES	830		\$97,521.68			0.90	0.088
SPECIAL	PROFIT	1010		\$344,838.57			8.73	0.857
	ASM. & TEST	1020		\$557,337.80			5.15	0.506
	GROWTH BUDGET	1030		\$0.00			0.00	0.000
				\$1,502,176.37			13.88	1.363
LAND	MTG LAND	1110		\$0.00			0.00	0.000
	ROAD LAND	1140		\$0.00			0.00	0.000
				\$0.00			0.00	0.000
CLUSTER	SUBSTATION	1240		\$0.00			0.00	0.000
	TRANSM. ETC.	1250		\$0.00			0.00	0.000
				\$0.00			0.00	0.000
O & M	YEARLY O & M	1340		\$38,715.00			3.87	0.380

TOTAL OVERALL (IND O&M)

REF. NUM. 100-1299 1803966 \$ \$10,393,224.28 5.7613 100.0000 100.00 8.817

PREPROFIT COST PRE-PROFIT (1980) AF GROSS GMI/YR#E4 NET
\$9,448,366.71 0.8 220500 198450

Table 5-16 Cost Summary for the Third Unit

SUBASS. ABBREV.	ITEM NAME ABBREV.	REF. NUM.	WEIGHT # 3RD UNIT	COST (1980) 3RD UNIT	DOLLARS PER LB.	% OF TOTAL MT.	% OF COE	COE CONTRIB. (1980 CENTS)
SITE	FOUNDATION	110		\$317,050.80			3.29	0.270
	GRD EQUIP.	120	88000	\$634,889.20	\$7.21	4.8781	8.57	0.540
	SPECIAL	130		\$112,380.13			1.18	0.096
			88000	\$1,064,320.13	N/A	4.8781	11.01	0.905
TRANSPORT.	TRANSPORT.	240		\$306,854.62			3.18	0.261
ERECTION	INSTALL.	310		\$398,367.86			4.12	0.339
	INTEG. & C/O	350		\$875,174.03			8.89	0.574
				\$1,073,541.89			11.11	0.913
ROTOR	BLADES	410	228900	\$1,650,173.17	\$7.18	12.7441	17.08	1.403
	ROTOR HYDR.	420	8418	\$40,520.64	\$4.81	0.4886	0.42	0.034
	AILERONS	425	8760	\$118,180.67	\$12.21	0.5410	1.23	0.101
	YOKE ASM/BRGS.	430	170962	\$633,891.17	\$3.71	9.4770	6.56	0.538
	TEETER ASM.	440	55430	\$235,570.71	\$4.25	3.0727	2.44	0.200
			474470	\$2,679,436.35	\$5.65	23.2288	27.73	2.278
DRIVE TRAIN	LOW SPEED SFT.	518	96700	\$208,946.57	\$3.13	3.6974	2.18	0.178
	TRANSMIS.	520	138730	\$412,709.61	\$2.95	7.7457	4.27	0.351
	HI SPEED	530	3000	\$12,428.69	\$4.14	0.1663	0.13	0.011
	GEN. & EXCIT.	540	50206	\$295,446.18	\$5.88	2.7831	3.06	0.251
			259636	\$929,532.05	\$3.58	8.8468	9.62	0.780
NACELLE	ROTOR SUPPORT	605	139150	\$312,953.42	\$2.25	7.7136	3.24	0.266
	BEDPLATE	610	116050	\$251,508.66	\$2.17	6.4330	2.60	0.214
	HYD. SYSTEM	620	5100	\$15,307.28	\$2.51	0.3381	0.16	0.013
	FAIR. & MISC.	646	6800	\$69,643.80	\$10.24	0.3769	0.72	0.059
	SLP. ELEC.	660	2870	\$45,548.43	\$15.34	0.1646	0.47	0.039
	INST. & CON.	670	3270	\$83,533.84	\$25.55	0.1813	0.86	0.071
	YAM SUBSYS.	680	54400	\$289,333.96	\$5.32	3.0156	2.99	0.246
			328740	\$1,067,829.49	\$3.25	18.2232	11.05	0.908
TOWER	TOWER	710	609120	\$595,947.00	\$0.98	33.7656	6.17	0.507
	PERS. LIFT	720	28500	\$75,046.94	\$2.63	1.3789	0.78	0.064
	CABLING	740	15500	\$77,714.64	\$5.01	0.8592	0.80	0.066
			653120	\$748,708.58	\$1.15	36.2047	7.75	0.637
REM. CONT.	LINE MODEN	810		\$659.38			0.01	0.001
	REM. DISP.	820		\$4,178.50			0.04	0.004
				\$4,838.89			0.05	0.004
SPARES	SPARES	830		\$87,203.33			0.80	0.074
SPECIAL	PROFIT	1010		\$841,990.17			8.71	0.716
	ASM. & TEST	1020		\$457,633.53			4.74	0.389
	GROWTH BUDGET	1030		\$0.00			0.00	0.000
				\$1,299,623.70			13.45	1.105
LAND	MTG LAND	1110		\$0.00			0.00	0.000
	ROAD LAND	1140		\$0.00			0.00	0.000
				\$0.00			0.00	0.000
CLUSTER	SUBSTATION	1240		\$0.00			0.00	0.000
	TRANSM. ETC.	1250		\$0.00			0.00	0.000
				\$0.00			0.00	0.000
O & M	YEARLY O & M	1340		\$36,100.50			4.15	0.341

TOTAL OVERALL (NO O&M)

REF. NUM. 100-1289

1803966 #

\$9,261,891.84

5.1341

100.0000

100.00

8.217

PREPROFIT COST

PRE-PROFIT (1980)

\$8,419,901.60

AF

0.96

GROSS

220500

GMH/YR#E4

NET

211680

Table 5-17 Cost Summary for the 100th Unit, Single Installation

SUBASS. ABBREV.	ITEM NAME ABBREV.	REF. NUM.	HEIGHT # 100TH UNIT	COST (1980) 100TH UNIT	DOLLARS PER LB.	% OF TOTAL MT.	% OF COE	COE CONTRIB. (1980 CENTS)
SITE	FOUNDATION	110		\$227,949.83			4.83	0.194
	GRD EQUIP.	120	88000	\$414,989.20	94.72	4.8781	8.87	0.353
	SPECIAL	130		\$39,613.31			0.86	0.034
			88000	\$682,532.44	N/A	4.8781	14.75	0.560
TRANSPORT.	TRANSPORT.	240		\$238,106.35			5.17	0.202
ERECTION	INSTALL.	310		\$145,047.75			3.13	0.123
	INTES. & C/O	350		\$109,500.41			2.37	0.093
				\$254,548.16			5.50	0.216
ROTOR	BLADES	410	228900	\$380,488.88	\$1.86	12.7441	8.22	0.324
	ROTOR HYDR.	420	8418	\$23,678.28	\$2.81	0.4868	0.51	0.020
	AILERONS	425	9780	\$27,480.10	\$2.82	0.5410	0.58	0.023
	YOKE ASM/BRGS.	430	170962	\$330,327.08	\$1.83	8.4770	7.14	0.281
	TEETER ASM.	440	55430	\$102,838.89	\$1.86	3.0727	2.22	0.087
			474470	\$854,811.80	\$1.82	23.2288	18.69	0.735
DRIVE TRAIN	LOW SPEED SFT.	518	88700	\$66,956.72	\$1.00	3.5874	1.45	0.057
	TRANSMIS.	520	138730	\$241,148.73	\$1.73	7.7457	5.21	0.205
	HI SPEED	530	3000	\$3,983.08	\$1.33	0.1863	0.09	0.003
	GEN. & EXCIT.	540	50206	\$227,441.01	\$4.53	2.7831	4.81	0.183
			259636	\$539,527.55	\$2.08	8.6488	11.86	0.459
NACELLE	ROTOR SUPPORT	605	139150	\$136,820.61	\$0.88	7.7136	2.85	0.116
	BEDPLATE	610	116050	\$97,241.40	\$0.84	8.4330	2.10	0.083
	HYD. SYSTEM	620	6100	\$8,844.07	\$1.47	0.3381	0.19	0.008
	FAIR. & MISC.	646	6800	\$30,403.22	\$4.47	0.3783	0.86	0.026
	SLP. ELEC.	660	2870	\$26,614.01	\$9.86	0.1646	0.68	0.023
	INST. & CON.	670	3270	\$30,360.79	\$9.28	0.1813	0.66	0.026
	VAN SUBSYS.	680	54400	\$150,751.29	\$2.77	3.0156	3.26	0.128
			328740	\$480,935.39	\$1.46	18.2232	10.39	0.409
TOWER	TOWER	710	608120	\$447,843.65	\$0.74	33.7656	8.68	0.381
	PERS. LIFT	720	28500	\$43,950.02	\$1.54	1.5789	0.85	0.037
	CABLING	740	15500	\$50,794.98	\$3.28	0.8582	1.10	0.043
			653120	\$542,588.65	\$0.83	36.2047	11.72	0.461
REM. CONT.	LINE MODEM	810		\$480.84			0.01	.000
	REM. DISP.	820		\$2,731.76			0.06	0.002
				\$3,212.70			0.07	0.003
SPARES	SPARES	930		\$75,862.79			1.64	0.065
SPECIAL	PROFIT	1010		\$395,637.86			8.55	0.336
	ASM. & TEST	1020		\$85,686.73			1.85	0.073
	GROWTH BUDGET	1030		\$0.00			0.00	0.000
				\$481,324.59			10.40	0.409
LAND	MTG LAND	1110		\$4,953.00			0.08	0.004
	ROAD LAND	1140		\$954.00			0.02	0.001
				\$5,923.00			0.11	0.004
CLUSTER	SUBSTATION	1240		\$48,708.00			1.05	0.041
	TRANSM. ETC.	1250		\$132,886.00			2.87	0.113
				\$181,594.00			3.82	0.154
O & M	YEARLY O & M	1340		\$24,906.48			5.98	0.235
TOTAL OVERALL (NO O&M)								
REF. NUM. 100-1298			1803966 #	\$4,352,017.52	2.4124	100.0000	100.00	3.935
PREPROFIT COST								
				\$3,956,379.56	0.96	GROSS 220500	GMI/YR#E4	NET 211680

Table 5-18 Cost Summary for the 100th Unit, Clustered Installation

SUBSYS. ABBREV.	ITEM NAME ABBREV.	REF. NUM.	HEIGHT # 100TH UNIT	COST (1980) 100TH UNIT	DOLLARS PER LB.	% OF TOTAL MT.	% OF COE	COE CONTRIB. (1980 CENTS)
SITE	FOUNDATION	110		\$207,227.21			4.76	0.178
	GRD EQUIP.	120	88000	\$414,868.20	84.72	4.8781	9.59	0.353
	SPECIAL	130		\$38,012.10			0.83	0.031
			86000	\$658,208.51	N/A	4.8781	15.22	0.560
TRANSPORT.	TRANSPORT.	240		\$178,816.81			4.16	0.153
ERECTION	INSTALL.	310		\$105,047.76			2.43	0.089
	INTEG. & C/D	380		\$108,500.41			2.53	0.093
				\$214,548.18			4.96	0.182
ROTOR	BLADES	410	228800	\$380,488.88	81.86	12.7441	8.80	0.324
	ROTOR HYDR.	420	8418	\$23,678.26	82.81	0.4886	0.55	0.020
	AILERONS	425	8780	\$27,480.10	82.82	0.5410	0.64	0.023
	YOKE ASM/BRGS.	430	170882	\$330,327.58	81.83	8.4770	7.64	0.281
	TEETER ASM.	440	85430	\$102,838.88	81.86	3.0727	2.38	0.087
			474470	\$864,811.80	81.82	23.2288	18.89	0.735
DRIVE TRAIN	LOW SPEED SFT.	518	88700	\$66,856.72	81.00	3.8874	1.55	0.057
	TRANSMIS.	520	138730	\$241,146.73	81.73	7.7457	5.57	0.205
	HI SPEED	530	3000	\$3,883.08	81.33	0.1863	0.09	0.003
	GEN. & EXCIT.	540	50208	\$227,441.01	84.53	2.7831	5.26	0.193
			258636	\$639,527.55	82.08	8.6468	12.47	0.458
NACELLE	ROTOR SUPPORT	605	138150	\$136,620.61	80.88	7.7136	3.16	0.116
	REDPLATE	610	116050	\$97,241.40	80.84	6.4330	2.25	0.083
	HYD. SYSTEM	620	8100	\$8,944.07	81.47	0.3381	0.21	0.008
	FAIR. & WISC.	646	6800	\$30,403.22	84.47	0.3788	0.70	0.026
	SLP. ELEC.	680	2870	\$26,614.01	88.86	0.1846	0.62	0.023
	INST. & CON.	670	3270	\$30,360.78	88.28	0.1813	0.70	0.026
	YAW SUBSYS.	680	54400	\$150,781.28	82.77	3.0156	3.48	0.128
			328740	\$480,935.38	81.46	18.2232	11.12	0.408
TOWER	TOWER	710	608120	\$389,516.23	80.64	33.7656	8.00	0.331
	PERS. LIFT	720	28500	\$43,850.02	81.54	1.8789	1.01	0.037
	CABLING	740	18500	\$50,784.88	83.28	0.9582	1.17	0.043
			653120	\$484,161.22	80.74	36.2047	11.19	0.412
REM. CONT.	LINE MODEN	810		\$480.84			0.01	.000
	REM. DISP.	820		\$2,731.76			0.06	0.002
				\$3,212.70			0.07	0.003
SPPARES	SPPARES	830		\$33,716.80			0.78	0.028
SPECIAL	PROFIT	1010		\$373,214.27			8.63	0.317
	ASM. & TEST	1020		\$85,686.73			1.88	0.073
	GROWTH BUDGET	1030		\$0.00			0.00	0.000
				\$458,901.00			10.61	0.390
LAND	MTS LAND	1110		\$4,858.00			0.10	0.004
	ROAD LAND	1140		\$964.00			0.02	0.001
				\$5,823.00			0.11	0.004
CLUSTER	SUBSTATION	1240		\$48,708.00			1.13	0.041
	TRANSM. ETC.	1250		\$132,888.00			3.07	0.113
				\$181,594.00			4.20	0.154
O & M	YEARLY O & M	1340		\$19,825.18			5.12	0.188
TOTAL OVERALL (NO O&M)								
REF. NUM. 100-1288			1803966 #	\$4,105,356.82	2.2757	100.0000	100.00	3.678
PREPROFIT COST								
				PRE-PROFIT (1980)	AF	GROSS	GMH/YR#E4	NET
				\$3,732,142.66	0.86	220500		211680

ORIGINAL PAGE IS
OF POOR QUALITY

6.0 SYSTEM DYNAMICS ANALYSIS

6.0 SYSTEM DYNAMICS ANALYSIS

6.1 INTRODUCTION

The objectives of the analysis of the system's dynamics were:

- (1) to place the system's natural frequencies so as to avoid resonances,
- (2) to ensure aeroelastic stability,
- (3) to provide satisfactory control system performance.

The evaluation of the system's natural frequencies used state-of-the-art finite element and modal synthesis techniques. The MOD-1 program (ref. 6-1) provided valuable experience in applying these methods to wind turbine problems. The measured natural frequencies of the MOD-1 agreed with the predictions, thereby instilling confidence in these methods.

The same methods were the basis of the MOD-5A analysis. Fully coupled system dynamic models were used to compute natural frequencies, which provided the initial assessment of potential operational resonances. Any required changes were implemented. The final evaluation of the acceptable frequency placement was based on the analysis of the system's dynamic loads. The details of the frequency analysis are discussed in sections 6.2 and 6.3.

Aeroelastic stability analyses developed during the MOD-1 program provided the foundations for the analysis of the MOD-5A. Extensions for these methods were needed, and developed, to evaluate the aileron system. Details may be found in sections 6.2 and 6.4.

The control system analysis performed on the MOD-5A contains significant extensions to the methods used on the MOD-1. Most notably, the effects of the interaction between the structure and the control system were modelled. Unlike the MOD-5A, the MOD-1 had a stiff tower; its fundamental bending frequency was 3P (P = per revolution). The stiff tower and the control system with a low frequency bandwidth enabled the MOD-1 analysis to be carried out without structural considerations. The MOD-2, which was the first multi-megawatt wind turbine with a soft tower, experienced problems stemming from the control system coupling with the tower. So that similar difficulties would not occur on the MOD-5A, control system dynamics were implemented into

TRAC, the aeroelastic loads analysis code. The code was able to predict the behavior of the MOD-2. Simultaneously SIM-5A, a wind turbine control system analysis code with simplified rotor aeroelasticity, was developed. The code was able to capture all the important structural interaction effects. Because it performed computations faster, it was used for the MOD-5A control system design. The results of the control system analysis are discussed in sections 6.5 and 6.6.

6.2 METHODS OF ANALYSIS

6.2.1 NATURAL FREQUENCY ANALYSIS

The natural modes and frequencies of the MOD-5A wind turbine were calculated from a model of the MOD-5A system. The dynamic mathematical model was made up of models of each substructure, which were unified by the stiffness coupling method of modal synthesis. The MOD-5A wind turbine substructures and their coupling interfaces are shown in Figure 6-1. The substructures were the rotor, the yoke and rotor support, the bedplate and nacelle and their associated hardware, and the tower.

The natural modes and frequencies of each substructure, except the blade, were calculated using NASTRAN or a similar finite element program. The blade modes and frequencies were determined using a proprietary GE program called STRAP (Static Row Analysis Program). STRAP is a finite element beam modelling program that includes the stiffening effects of centrifugal forces.

The stiffness links used to unify the substructures were derived as follows:

- o Rotor to Yoke - The links were derived from stiffness data obtained from the manufacturer of the teeter bearing. The teeter bearing is elastomeric and has stiffness in all 6 degrees of freedom.
- o Rotor Support to Bedplate - The links were calculated by inverting a bedplate flexibility matrix obtained from detailed NASTRAN load cases.
- o Bedplate to Tower - The link was derived from manufacturer's data on the yaw bearing and yaw hydraulics, and from the structural design of the upper yaw housing (the lower yaw housing was included in the tower finite element model). A scalar spring element was created from yaw bearing stiffnesses in 5 degrees of freedom and yaw brake stiffness (or yaw hydraulic stiffness depending on the case investigated) in the yaw degree of freedom. This scalar spring was then added in series with a beam model of the upper yaw housing.

SCAMP (Stiffness Coupling Approach Modal-synthesis Program), a proprietary GE computer program, unified the substructures. This modal synthesis method has been used extensively at the General Electric Space Division for spacecraft analysis. The method uses the free substructure vibration modes and

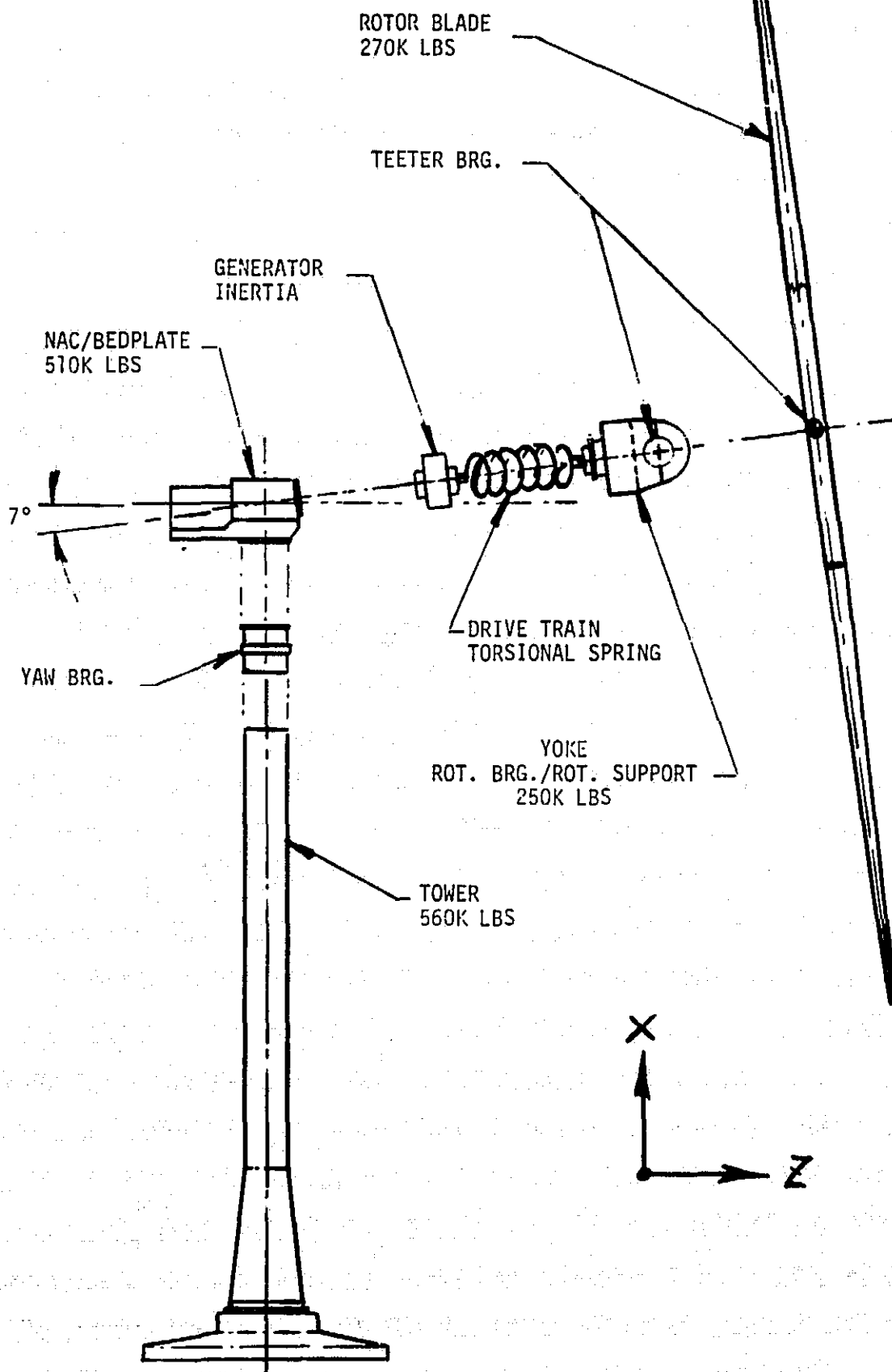


Figure 6-1 Wind Turbine Model Substructures

frequencies to determine the modes of the entire system. These substructures, as defined by the stiffness coupling method, have no common degrees of freedom and are coupled together by the stiffness links that relate the free attachment coordinates of the substructures.

In some methods of modal synthesis, the stiffness coupling method yields an approximate solution in which high frequency modes are truncated; however, the dynamic transformation includes modes that would be truncated in these methods. This transformation relates the high-frequency modes to the low-frequency modes at a selected system frequency. Then the transformation reduces the generalized mass and stiffness matrices that describe the dynamic behavior of the coupled system. The details of the dynamic transformation used in SCAMP are documented in ref. 6-2.

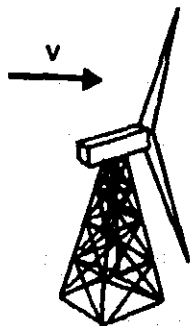
6.2.2 AEROELASTIC STABILITY

During the design of the MOD-1, GE developed a comprehensive rotor and tower aeroelastic stability analysis computer program called GETSTAB. Its features are depicted in Figure 6-2. The program analyzes blade flap-lag-pitch instability, classical flutter, divergence, whirl flutter, and other instabilities that may occur because of rotor/tower coupling. The elastic degrees of freedom of the blade are represented by fully-coupled, three-dimensional natural modes. The blades may have arbitrary twist, taper, and chordwise center of gravity distributions. The program also analyzes modes, such as teetering, that correspond to general root boundary conditions, in which the motions of two separate blades are coupled. The analysis uses quasi-steady aerodynamic strip theory, incorporating the Theodorsen unsteady aerodynamic terms with $C(k)=1$. Aerodynamic coefficients (C_L , C_D , C_M) are obtained from a table as a function of the angle of attack. Tables corresponding to the airfoil characteristics at various radial stations may be supplied as inputs, thereby allowing airfoil thickness taper distributions. The solutions are for perturbations from a trim condition. The use of stallable airfoil tables allows the stability for fully or for partially-stalled trim conditions to be estimated. The program can be used for isolated blade studies or a two-bladed rotor coupled to a flexible tower. (The latter would be represented by general three-dimensional natural modes.)

The program can also analyze non-rotating conditions, for example, with the blades parked in hurricane winds.

The equations of motion are expressed as linear equations. An eigenvalue solution is used to determine the stability of an isolated blade. Floquet theory is used to extract exponential decay rates for the coupled rotor/tower case because periodic coefficients arise for two-bladed rotors.

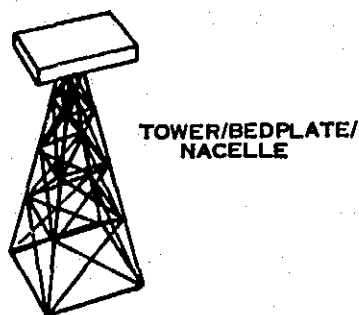
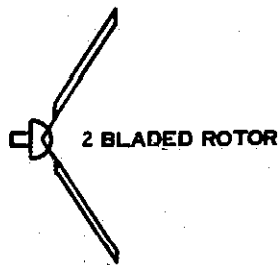
The GETSTAB code does not contain aileron dynamics or aerodynamics. In order to determine the stability of the aileron blades, a simpler, three degree of freedom analysis, called AILSTAB, was developed. The features of AILSTAB are shown in Figure 6-3. This code extracts eigenvalues for a system with three degrees of freedom, consisting of: (1) a blade flapwise mode, (2) a blade torsional mode, and (3) an aileron torsional mode. Mode shapes are supplied as inputs, and the aileron can be specified over an arbitrary length of the blade span and chord. Quasi-steady aerodynamic strip theory is used to compute aerodynamic derivatives of the blade-aileron combination as a function of spanwise position. The program yields rotating blade stability boundaries for torsional divergence, classical flutter (bending/torsion) and wing/aileron flutter.



COUPLED ROTOR TOWER AEROELASTIC STABILITY ANALYSIS

ORIGINAL PAGE IS
OF POOR QUALITY

COMPONENTS



MODEL

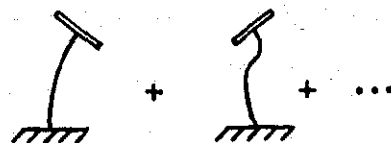
$$\Omega \left(\text{---} + \text{---} + \text{---} + \dots \right)$$

ROTOR COLLECTIVE MODES

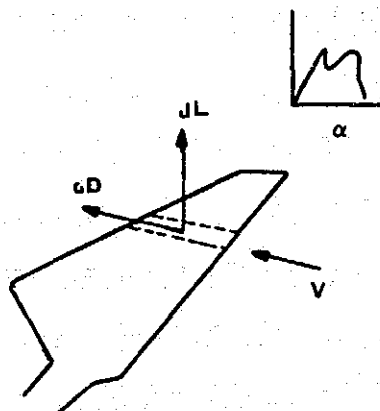
$$\Omega \left(\text{---} + \text{---} + \dots \right)$$

ROTOR CYCLIC MODES

- UP TO 12 FULLY COUPLED ROTOR MODES
- ARBITRARY BLADE INITIAL DEFLECTIONS
- EASY TO VARY Ω , C.G., INITIAL DEFLECTION



UP TO 15 3-DIMENSIONAL MODES



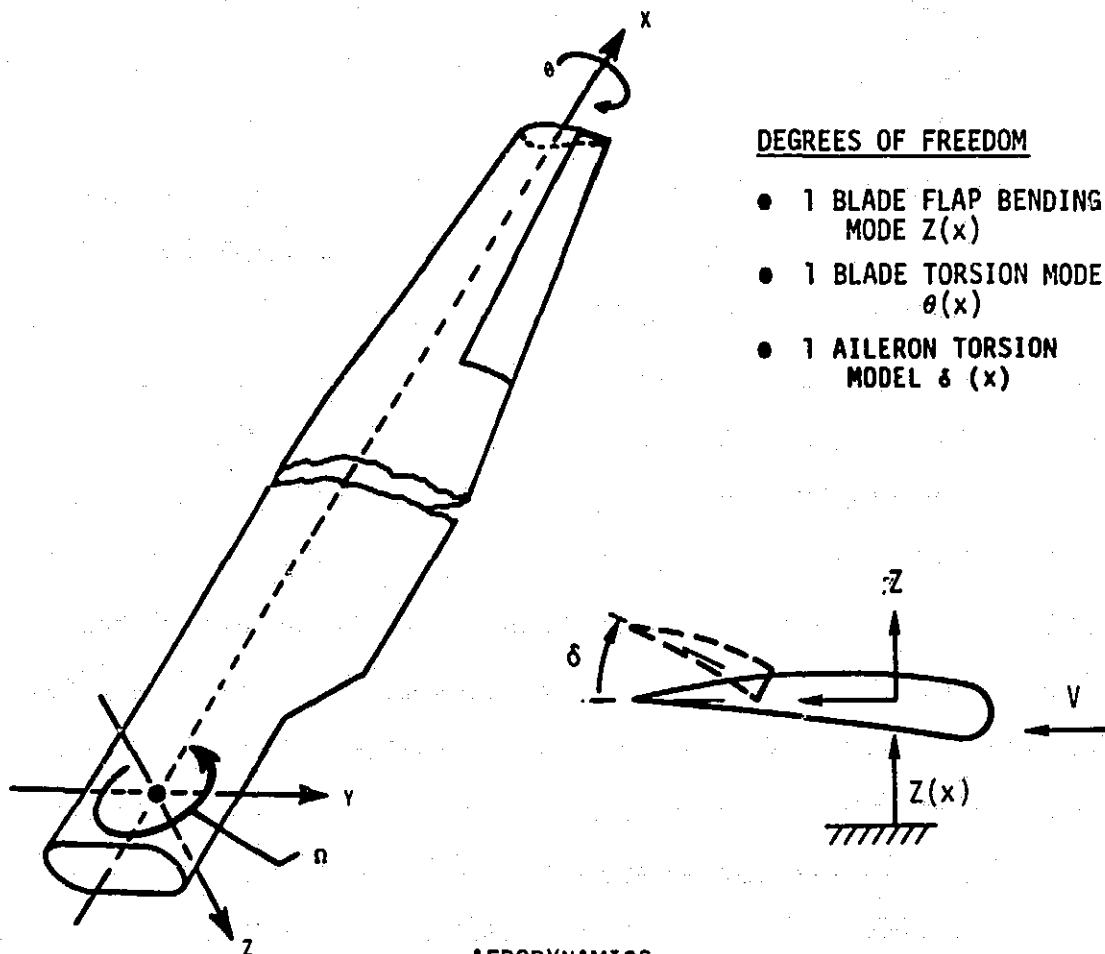
SOLUTION

- EIGENVALUES OF LINEAR PERTURBATION EQUATIONS FLOQUET THEORY

AERODYNAMICS

- TABLE LOOKUP C_L , C_D , C_M
- ARBITRARY TWIST, TAPER
- NO RESTRICTIONS ON $V/\Omega R$ (HANDLES $\Omega \rightarrow 0$)
- QUASI-STATIC, ANGLE OF ATTACK @ 3/4 CHORD $\Rightarrow C(k) = 1$

Figure 6-2 Features of Aeroelastic Program, GETSTAB



PROGRAM CAN ANALYZE CLASSICAL BENDING TORSION ($Z-\theta$) FLUTTER AS WELL AS BLADE/AILERON FLUTTER

Figure 6-3 Features of Aeroelastic Program, AILSTAB

6.3 SYSTEM MODES AND NATURAL FREQUENCIES

6.3.1 BASELINE DESIGN - MODEL 304.2

6.3.1.1 Model Description

The structural dynamic model used for model 304.2 is summarized in this section. All section, mass and coupling stiffness properties necessary to reconstruct the model are included.

Tables 6-1 through 6-4 contain stiffness and mass properties for the tower, bedplate, yoke and rotor support, and blade. The following comments should be noted:

1. All units are in inches and pounds.
2. Stiffness properties for the bedplate are not included because only rigid body modes were used.
3. The coordinate systems for the various substructures do not have a common zero, because modes and eigenvalues were calculated for each substructure independently, and then assembled through modal synthesis.

Figure 6-4 is included to help clarify the geometry of the yoke and low speed shaft model and its connection to the blade. The various substructures and their connections are shown in Figure 6-1.

Table 6-5 contains the stiffness properties and geometry for the yaw bearing and the upper yaw adapter. This stiffness element was used to couple the bedplate to the tower. The teeter bearing stiffness element, which was used to attach the blade to the yoke and rotor support model, is in Table 6-6. The full 12 x 12 stiffness element used to attach the yoke and rotor support model to the nacelle is in Table 6-7. This stiffness element was derived from a bedplate flexibility matrix that was obtained from the finite element stress model of the bedplate.

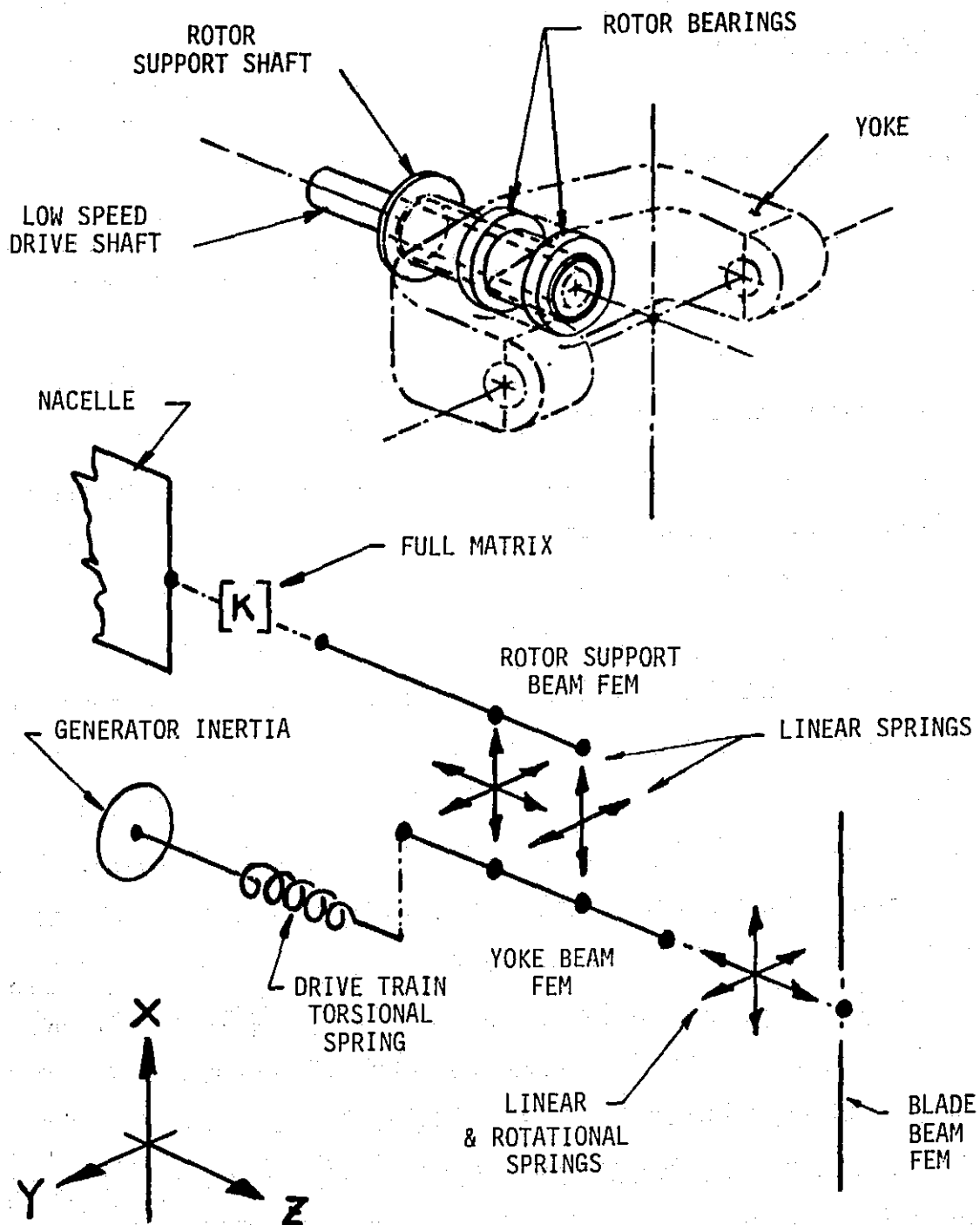


Figure 6-4 Rotor/Yoke Finite Element Model

Table 6-1 Tower Model Data

Element Properties

Station (in)	GJ (lb-in ²)	EI (lb-in ²)	EA (lb)	Cumulative Weight (kips)
2705.0	3.415x10 ¹³	4.442x10 ¹³	1.184x10 ¹⁰	8.53
2632.0	3.010	3.915	1.042	20.66
2514.1	3.281	4.266	1.137	33.89
2396.1	3.550	4.617	1.231	48.22
2278.2	3.775	4.909	1.309	63.47
2160.2	4.043	5.258	1.404	79.82
2042.3	4.356	5.665	1.513	97.50
1924.4	4.668	6.070	1.623	116.4
1806.4	4.929	6.475	1.733	136.6
1688.5	5.290	6.879	1.842	158.1
1570.5	5.555	7.224	1.936	180.7
1452.6	5.864	7.626	2.045	204.6
1334.6	6.129	7.970	2.139	229.6
1216.7	6.436	8.370	2.248	255.8
1098.8	6.699	8.712	2.342	283.2
980.8	6.962	9.053	2.435	311.7
862.9	7.267	9.451	2.544	341.5
744.9	7.529	9.791	2.638	372.3
627.0	9.258	1.204x10 ¹⁴	3.173	389.3
573.0	9.453	1.229	2.827	421.4
458.4	1.171x10 ¹⁴	1.523	2.903	454.3
343.8	1.419	1.846	2.962	487.9
229.2	1.701	2.213	3.031	522.3
114.6	2.028	2.637	3.121	557.6

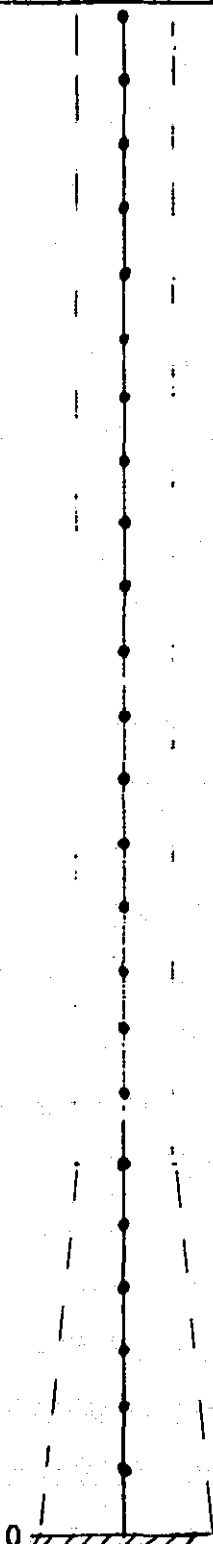
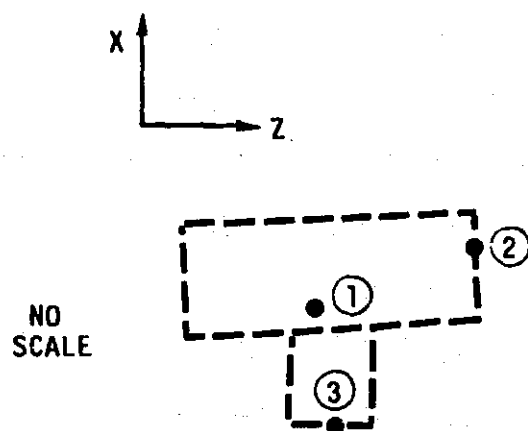
0  No Scale

Table 6-2 Rigid Body Bedplate Model

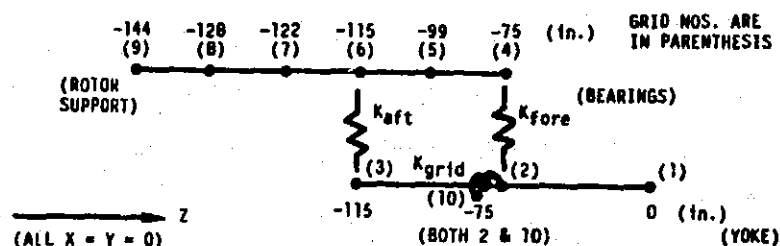


NODE	COORDINATE		WEIGHT/INERTIA
1	X	165.2 in.	509470 lb.
	Y	0.	509470 lb.
	Z	-28.4	509470 lb.
	θ_x	-	4.89×10^9 lb-in ²
	θ_y	-	7.01×10^9
	θ_z	-	2.79×10^9
2	X	225.6	-
	Y	0.	-
	Z	145.0	-
	θ_x	-	-
	θ_y	-	-
	θ_z	-	-
3	X	0.	-
	Y	0.	-
	Z	0.	-
	θ_x	-	-
	θ_y	-	-
	θ_z	-	-

Table 6-3a Rotor Support/Yoke Model

ORIGINAL PAGE IS
OF POOR QUALITY

δJ (lb-in ²)	EI_{xx} (lb-in ²)	EI_{yy} (lb-in ²)	ELEMENT
7.70×10^{13}	1.00×10^{14}	1.00×10^{14}	8-9
3.97×10^{13}	5.16×10^{13}	5.16×10^{13}	7-8
2.56×10^{13}	3.33×10^{13}	3.33×10^{13}	6-7
2.56×10^{13}	3.33×10^{13}	3.33×10^{13}	5-6
2.23×10^{13}	2.90×10^{13}	2.90×10^{13}	4-5



ELEMENT	δJ (lb-in ²)	EI_{xx} (lb-in ²)	EI_{yy} (lb-in ²)
2-3	4.44×10^{12}	9.90×10^{11}	4.10×10^{11}
1-2	2.5×10^{13}	3.00×10^{13}	3.00×10^{13}

Table 6-3b

Bearings and Electrical Grid, Point to Point
Stiffness Elements

	X (lb/in)	Y	Z	θ_x (in-lb/rad)	θ_y	θ_z
Kfore	1.5×10^8	1.5×10^8	-	-	-	-
Kaft	1.0×10^8	1.0×10^8	2.5×10^8	-	-	-
Kgrid	-	-	-	-	-	5.04×10^9

Yoke and Rotor Support Weights and Inertias

Grid No.	X (lb)	Y	Z	θ_x (lb-in ²)	θ_y	θ_z
1	70,092	70,092	70,092	1.0×10^6	1.0×10^6	1.13×10^9
2	70,092	70,092	70,092	1.0×10^6	1.0×10^6	4.60×10^8
3	70,092	70,092	70,092	1.0×10^6	1.0×10^6	4.60×10^8
4	11,710	11,710	11,710	1.0×10^6	1.0×10^6	3.00×10^7
6	14,264	14,264	14,264	1.0×10^6	1.0×10^6	1.12×10^7
9	11,775	11,775	11,775	1.0×10^6	1.0×10^6	1.72×10^7
10	-	-	-	-	-	2.50×10^{10}

Table 6-4 Blade Properties

A-MASS PROPERTIES

\bar{X}	CHORD (IN)	W1' (LBM/IN)	WTOT' (LBM/IN)	X-CG (IN)	Y-CG (IN)	I-FLAP LBM-IN ² /IN	I-CHORD LBM-IN ² /IN	THETA-P (DEG)
0.	300.0	117.6	117.6	89.96	0.00	0.1355E 06	0.4520E 06	0.
0.100	300.0	90.59	92.63	98.56	0.24	0.1040E 06	0.3721E 06	0.00
0.200	300.0	70.33	72.37	107.21	0.74	0.7216E 05	0.2588E 06	0.00
0.250	300.0	61.22	63.05	110.55	0.64	0.5957E 05	0.2096E 06	0.00
0.300	284.9	54.75	56.37	104.34	1.65	0.4688E 05	0.1655E 06	0.00
0.400	254.6	48.33	49.65	92.17	2.85	0.3110E 05	0.1101E 06	0.00
0.500	224.3	42.93	43.94	80.46	3.67	0.2002E 05	0.7079E 05	0.00
0.600	194.1	33.54	37.49	74.32	3.74	0.1112E 05	0.4869E 05	-0.00
0.700	163.8	24.08	28.28	64.69	3.66	5355.	0.2771E 05	-0.00
0.800	133.5	13.26	16.98	55.65	2.96	1700.	0.1188E 05	-0.00
0.900	103.3	5.420	7.690	45.52	2.05	313.3	3357.	-0.00
1.000	73.0	2.660	4.020	33.22	1.35	48.71	878.8	-0.00

TOTAL WT = 0.1117E 06LB NON-STRUCT. MASS = 5484. LB
 1ST MOMENT = 0.8584E 08LB-IN I = 0.2670E 09LB-SEC²-IN

B - ELASTIC PROPERTIES

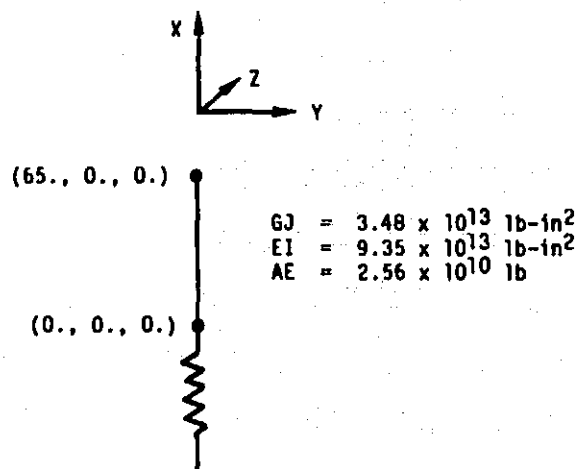
\bar{X}	EI-FLAP	EI-CHORD	EA	GJ	NEUTRAL AXIS ELASTIC AXIS				THETA-P
					X-NA	Y-NA	X-EA	Y-EA	
0.	0.1220E 14	0.4068E 14	0.1058E 11	0.1937E 13	90.0	0.0	88.4	0.4	0.0
0.100	0.9361E 13	0.3076E 14	0.8153E 10	0.1546E 13	95.9	0.2	97.8	1.2	0.0
0.200	0.6504E 13	0.2092E 14	0.6330E 10	0.1138E 13	104.0	0.8	111.7	2.7	-0.0
0.250	0.5365E 13	0.1687E 14	0.5510E 10	0.9186E 12	107.3	0.7	120.4	2.0	-0.0
0.300	0.4221E 13	0.1328E 14	0.4928E 10	0.7224E 12	101.3	1.7	114.4	2.4	-0.0
0.400	0.2799E 13	0.8835E 13	0.4350E 10	0.4734E 12	89.6	2.9	102.6	3.1	-0.0
0.500	0.1802E 13	0.5725E 13	0.3864E 10	0.2970E 12	78.5	3.8	90.8	3.7	-0.0
0.600	0.9951E 12	0.3149E 13	0.3019E 10	0.1563E 12	67.8	4.2	77.8	4.0	0.0
0.700	0.4757E 12	0.1593E 13	0.2168E 10	0.7438E 11	56.8	4.3	64.5	4.0	0.0
0.800	0.1518E 12	0.5760E 12	0.1194E 10	0.2326E 11	46.2	3.8	51.0	3.4	-0.0
0.900	0.2709E 11	0.1397E 12	0.4878E 09	0.4218E 10	35.6	2.9	38.1	2.5	0.0
1.000	0.4095E 10	0.3351E 11	0.2394E 09	0.6877E 09	25.2	2.0	28.2	1.7	0.0

\bar{X} = FRACTION OF BLADE RADIUS (2400 IN.)
 THETA - P = PRINCIPLE AXIS ANGLE

E = 2.25×10^6 PSI
 G = 150,000 PSI

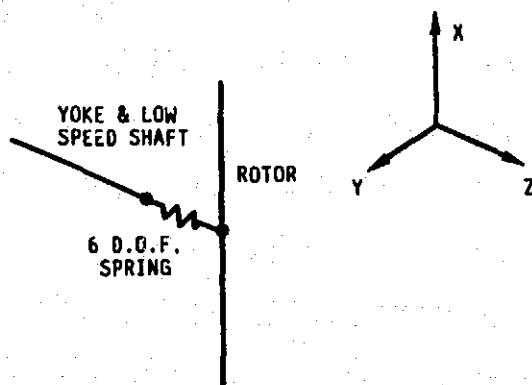
X IS MEASURED FROM NOSE TOWARD TAIL
 Y IS MEASURED FROM PRESSURE SURFACE TOWARD SUCTION SURFACE

Table 6-5
Yaw Bearing and Upper Yaw Adapter



X lb/in	Y	Z	θ_x in-lb/rad	θ_y	θ_z
$K = 1.08E/9 \times 10^9$	$2.5E/8 \times 10^8$	$2.5E/8 \times 10^8$	1.5×10^{10}	4.44×10^{12}	4.44×10^{12}

Table 6-6
Teeter Bearing



X lb/in	Y	Z	θ_x in-lb/rad	θ_y	θ_z
$K = 4.0E/6 \times 10^6$	$8.0E/6 \times 10^6$	$4.0E/6 \times 10^6$	4.5×10^{10}	5.7×10^2	4.5×10^{10}

Table 6-7 Yoke/Rotor Support to Nacelle Coupling Stiffness

ORIGINAL PAGE IS
OF POOR QUALITY

*OUTPUT MATRIX SPRING (12 x 12)		(1)	(2)	(3)	(4)	(5)	(6)	(7)	(8)	(9)	(10)
NUM	COL	(1)	(2)	(3)	(4)	(5)	(6)	(7)	(8)	(9)	(10)
1	1	2.5768E 07	4.9375E 02	1.4237E 07	2.1623E 04	-2.4944E 08	-6.0214E 04	-2.5768E 07	-4.9375E 02	-1.4237E 07	-2.1623E 04
1	11	2.4944E 08	6.0214E 04								
2	1	4.9375E 02	1.0076E 07	9.7537E 02	2.9984E 08	5.2066E 04	-1.5468E 09	-4.9375E 02	-1.0076E 07	-9.7537E 02	-2.9984E 08
2	11	-5.2066E 04	1.5468E 09								
3	1	1.4237E 07	9.7537E 02	1.9460E 07	3.0965E 04	6.4480E 08	-1.4973E 05	-1.4237E 07	-9.7537E 02	-1.9460E 07	-3.0965E 04
3	11	-6.4480E 08	1.4973E 05								
4	1	2.1623E 04	2.9984E 08	3.0965E 04	9.5277E 10	1.3957E 06	-6.3893E 10	-2.1623E 04	-2.9984E 08	-3.0965E 04	-9.5277E 10
4	11	-1.3957E 06	6.3893E 10								
5	1	-2.4944E 08	5.2066E 04	6.4480E 08	1.3957E 06	1.0475E 11	-7.7398E 06	2.4944E 08	-5.2066E 04	-6.4480E 08	-1.3957E 06
5	11	-1.0475E 11	7.7398E 06								
6	1	-6.0214E 04	-1.5468E 09	-1.4973E 05	-6.3893E 10	-7.7398E 06	4.1777E 11	6.0214E 04	1.5468E 09	1.4973E 05	6.3893E 10
6	11	7.7398E 06	-4.1777E 11								
7	1	-2.5768E 07	-4.9375E 02	-1.4237E 07	-2.1623E 04	2.4944E 08	6.0214E 04	2.5768E 07	4.9375E 02	1.4237E 07	2.1623E 04
7	11	-2.4944E 08	-6.0214E 04								
8	1	-4.9375E 02	-1.0076E 07	-9.7537E 02	-2.9984E 08	-5.2066E 04	1.5468E 09	4.9375E 02	1.0076E 07	9.7537E 02	2.9984E 08
8	11	5.2066E 04	-1.5468E 09								
9	1	-1.4237E 07	-9.7537E 02	-1.9460E 07	-3.0965E 04	-6.4480E 08	1.4973E 05	1.4237E 07	9.7537E 02	1.9460E 07	3.0965E 04
9	11	6.4480E 08	-1.4973E 05								
10	1	-2.1623E 04	-2.9984E 08	-3.0965E 04	-9.5277E 10	-1.3957E 06	6.3893E 10	2.1623E 04	2.9984E 08	3.0965E 04	9.5277E 10
10	11	1.3957E 06	-6.3893E 10								
11	1	2.4944E 08	-5.2066E 04	-6.4480E 08	-1.3957E 06	-1.0475E 11	7.7398E 06	-2.4944E 08	5.2066E 04	6.4480E 08	1.3957E 06
11	11	1.0475E 11	-7.7398E 06								
12	1	6.0214E 04	1.5468E 09	1.4973E 05	6.3893E 10	7.7398E 06	-4.1777E 11	-6.0214E 04	-1.5468E 09	-1.4973E 05	-6.3893E 10
12	11	-7.7398E 06	4.1777E 11								

* First 2 columns contain row and column number of element directly to the right of them

Degrees of Freedom 1-6 connect to node 9 on yoke/low speed shaft

Degrees of Freedom 7-12 connect to node 2 on bedplate

6.3.1.2 Natural Modes and Frequencies

The system modes and frequencies were calculated with the blades in the vertical and horizontal positions. Typical mode shapes with the rotor in a vertical position are shown in Figure 6-5. The drivetrain and teetering modes are simply rigid body rotations of the rotor about the drive shaft and teeter pin, with little or no motion of the other system elements. The fundamental tower bending mode, shown for the direction normal to the axis of rotation, has a small yaw rotation caused by the offset center of gravity of the nacelle. The tower bending mode in the direction of the drive shaft axis is not shown, but it has nearly the same natural frequency, and considerably more blade elastic deflection in the softer flapwise direction. The final elastic mode shape displays collective flapwise bending of the blades. The mode shape plots are used to provide insight into the response of the system.

Table 6-8 contains a summary of the system natural frequencies for the baseline design. The calculations were made with the blades in vertical and horizontal positions at 13.8 and 16.8 rpm. Frequencies are shown in Hz and P. The numbers in parentheses denote P values at the 13.8 rpm. The last column earmarks the harmonics that should be avoided in each mode. E stands for even, and O, for odd. For example, fixed system modes of the tower must avoid even integers of rotor speed with a two-bladed rotor, while rotor cyclic modes must avoid odd integers. Figure 6-6 depicts frequency placement of model 304.2 graphically. The hatched areas indicate frequency ranges that should be avoided, to preclude resonant excitation. Symbols connected by horizontal lines indicate that the frequency changes in going from a vertical to horizontal blade position.

All system frequencies are well placed with the possible exception of the first flap collective, which is at 4.2P. The blade design, however, is compatible with the loads predicted for this blade. Furthermore, dominant blade fatigue stresses were due to chord bending loads, which are not affected by this frequency. There is still reason for concern, though, because of the uncertainty in some variables used in the load calculations. The variable most in question is the amount of 4P turbulence in the wind at the chosen

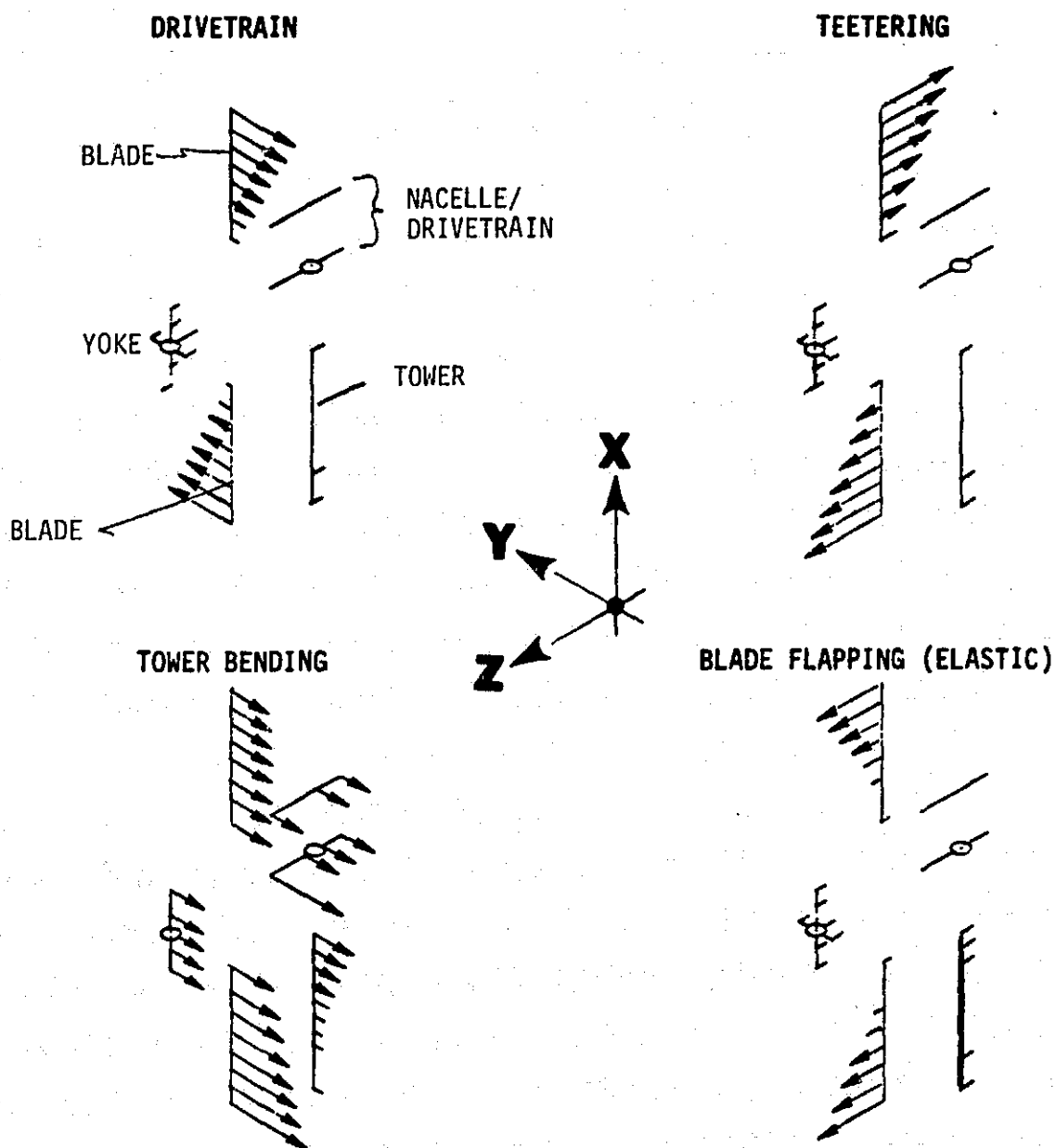


Figure 6-5 Coupled Mode Shapes

Table 6-8. MOD-5A Model 304.2 System Natural Frequencies

	VERTICAL		HORIZONTAL		HARMONICS TO AVOID
	Hz	P	Hz	P	
1) DRIVE TRAIN	0.		0.		E
2) TEETER	.28 (.23)	1. (1.)	.28 (.23)	1. (1.)	-
3) TOWER Z	.340	1.21 (1.48)	.340	1.21 (1.48)	E
4) TOWER Y	.341	1.22 (1.48)	.344	1.23 (1.50)	E
5) FLAP COLLECTIVE	1.17	4.18 (5.00)	1.17	4.18 (5.00)	E
6) DRIVE TRAIN	1.33	4.75 (5.78)	1.33	4.75 (5.78)	E
7) CHORD CYCLIC	1.60	5.71 (6.96)	1.84	6.57 (8.00)	0
8) FLAP CYCLIC	2.37	8.46 (10.3)	2.3	8.25 (9.96)	0
9) TOWER AND TORSION	2.24	8.00 (9.74)	1.80	6.43 (7.83)	E
10) TOWER Z (2nd)	3.03	10.8 (13.2)	3.23	11.7 (14.0)	E
11) FLAP COLLECTIVE (2nd)	3.14	11.2 (13.6)	3.11	11.1 (13.4)	E
12) CHORD COLLECTIVE	4.08	14.6 (17.7)	4.08	14.6 (17.7)	E
13) TOWER Y (2nd)	4.18	14.9 (18.2)	4.18	14.9 (18.2)	E
14) FLAP CYCLIC (2nd)	4.56	16.3 (19.7)	4.56	16.3 (19.7)	0

* P values in parenthesis are for 13.8 rpm

E = even

0 = odd

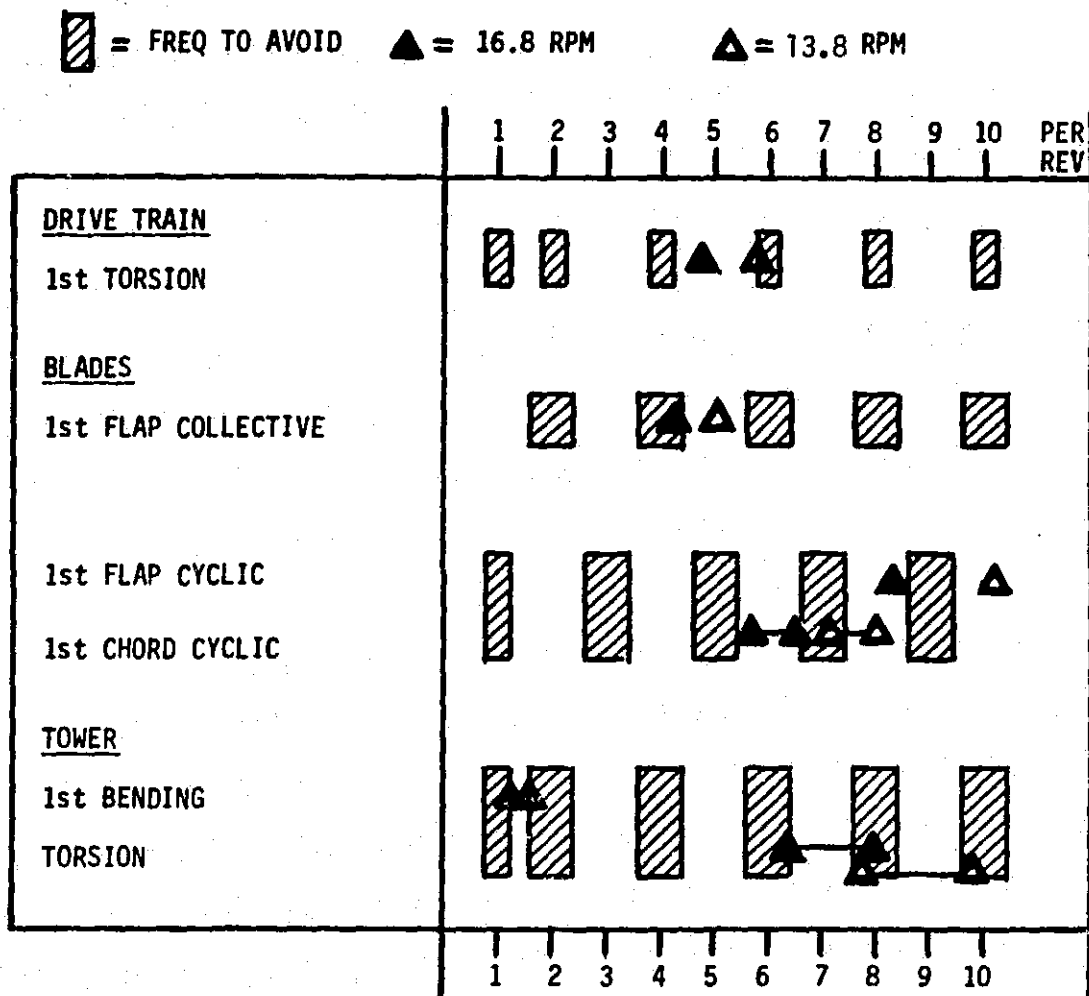


Figure 6-6 MOD-5A Frequency Placement Model 304.2

site. The loads would be sensitive to this turbulence, since the blade resonance is near the excitation frequency. To eliminate this risk, methods for raising or lowering the flapwise frequency were investigated near the end of final design. Three feasible avenues were identified:

1. Structural modification - (blade thickness, chord, or both).
2. Addition of ballast weight to the outboard blade (the earlier, heavier, partial span control configuration had a desirable 3P frequency, which increased to 4.2P when the lighter ailerons were substituted).
3. Change operating speed (this change could be made in the field, because of the variable speed generator).

Were the MOD-5A to be built, it is likely that one of these modifications would be implemented to minimize risk.

6.3.2 SENSITIVITY STUDIES

6.3.2.1 Tower Frequency Sensitivity to Foundation Stiffness

A parametric study of foundation stiffness assessed the effect of the foundation flexibilities on the tower's natural frequencies. Using NASTRAN, tower bending frequencies were determined for six values of foundation stiffness, ranging from 1×10^{11} in.-lb./rad. to 5×10^{12} in.-lb./rad. These stiffnesses correspond to moduli of elasticity of the soil between 1,000 and 50,000 psi. Cantilevered frequencies were also calculated. The tower design used in this analysis was that of November 9, 1982. A figure from a data sheet prepared by Chicago Bridge & Iron (CBI) is presented in Figure 6-7, with a stick figure depicting the NASTRAN model. The NASTRAN model consisted of 25 nodes with six degrees of freedom for the tower, and one node with six degrees of freedom at the center of gravity of the nacelle and rotor, and one node with six degrees of freedom representing the center of gravity of the foundation. CELAS2 scalar spring elements were used to tie the foundation mass to ground in all six degrees of freedom. The weight of the tower model was 498 kips. The nacelle and rotor weight was 813.6 kips, and the foundation weight was 3474 kips. This study was performed before the final design, hence the physical properties noted above differ from those reported in section 6.3.1 for the final configuration-model 304.2. The fundamental tower bending frequency was .4 Hz for the model used in this study, as opposed to .34 Hz for model 304.2. Since this parametric study intended to define trends, the difference is not important.

The basic equation used to relate the foundation rotational stiffness to soil properties was taken from ref 6-3. It is:

$$K_{\theta y} = K_{\theta z} = \frac{33GD^3}{1-\nu} = C_{\phi} I_{\theta y} = C_{\phi} I_{\theta z}$$

$$C_{\phi} = \frac{6.723G}{(1-\nu)D}$$

where: D = foundation diameter (72 ft. and 8 in.)

ν = Poisson's Ratio (assumed to be .3)

G = torsional rigidity of soil = $E/2(1+\nu)$

I_{θ} = area bending inertia of foundation = $\frac{\pi D^4}{64}$

215'-5" TOWER (X) 11/9/82

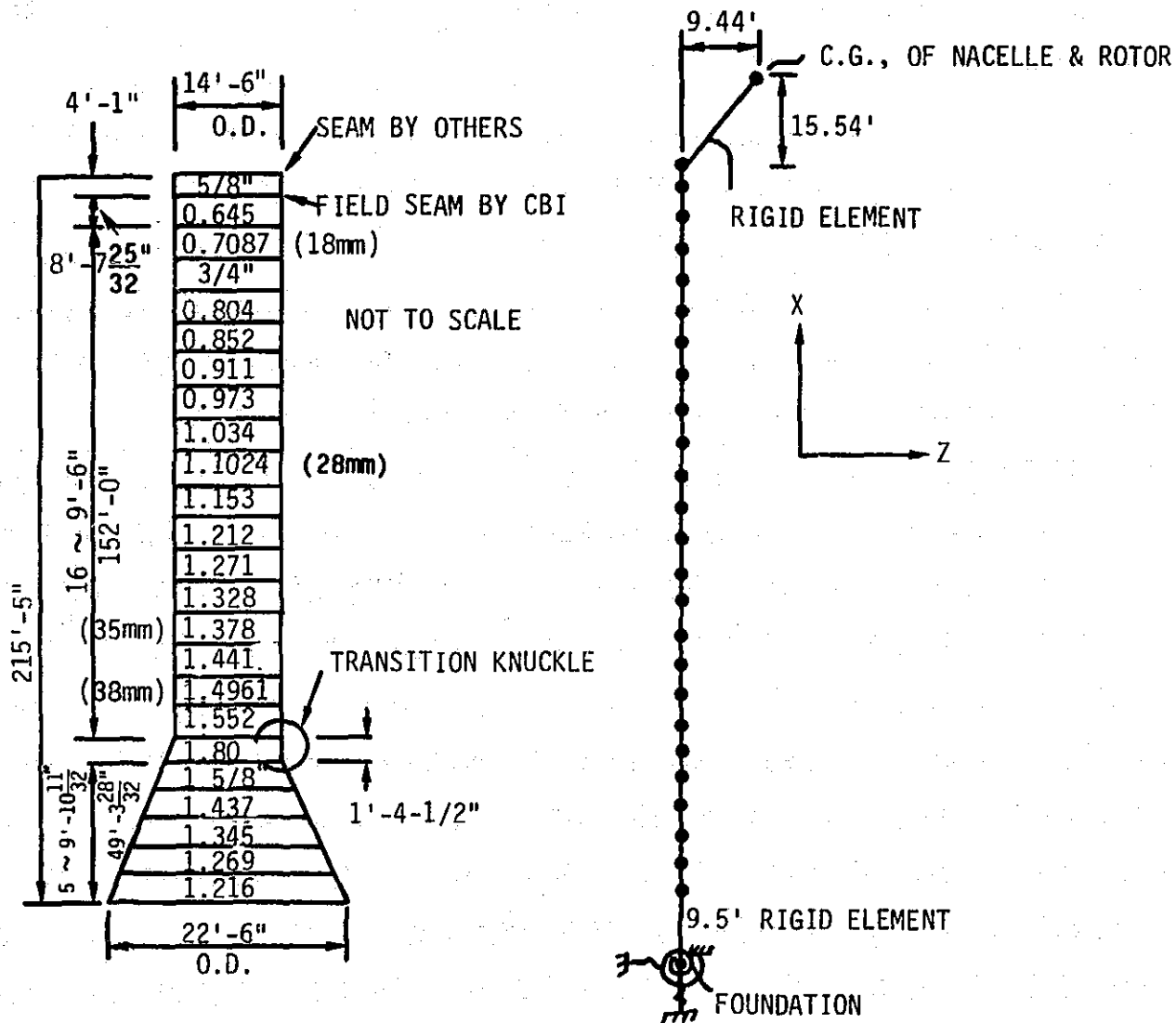


Figure 6-7 Tower Frequency Model

To determine the other components of stiffness, the following relations from ref. 6-4 were used.

$$\begin{aligned} C_{\phi}/C_u &= 1.5 & K_x^* &= C_u A = \frac{3.53GD}{(1-\nu)} \\ C_{\phi}/C_{\tau} &= 1.92 & K_y &= K_z = C_{\tau} A = \frac{2.75GD}{(1-\nu)} \\ C_{\phi}/C_{\psi} &= 1.28 & K_{\theta x} &= C_{\psi} I_{\theta x} = \frac{.51GD^4}{(1-\nu)} \end{aligned}$$

where: A = cross sectional area of foundation

$$I_{\theta x} = \text{polar area inertia of foundation} = \frac{\pi D^4}{32}$$

* The equation derived for C_u in ref. 6-3 gives K_x equal to $\frac{2.0GD}{(1-\nu)}$ rather than the above.

The relations are empirical and a range of values is given in the reference. In addition, the equations consider only the soil beneath the foundation. Contributions from the overburden and soil to the sides of the foundation are not included. For these reasons it is possible for the actual stiffnesses to be as much as two times higher than those computed from the formulas.

The preceding equations were used to set the ratios between the rotational and translational foundation stiffnesses. The natural frequency parametric study was conducted using stiffnesses that were calculated for the soil's moduli of elasticity, ranging from 1,000 to 50,000 psi.

The resulting frequencies are plotted against the rotational stiffness ($K_{\theta y}$, $K_{\theta z}$) in Figures 6-8 and 6-9. Figure 6-8 contains frequencies of the coupled y bending and torsion modes, and Figure 6-9 is a plot of the frequencies of the coupled z bending and axial modes. A scale of elastic moduli is included above the stiffness scale in these figures. A primary concern is to avoid resonances below 10P, which is approximately 3 Hz on the MOD-5A. For soil moduli greater than 10,000 psi, only the fundamental bending and tower torsion modes fall in this frequency range. Furthermore, the variation of natural frequency is small for elastic moduli above 10,000 psi. At the Hawaiian site the soil modulus was estimated to be between 10,000 and 25,000 psi. Hence, it was concluded that the MOD-5A would not be sensitive to foundation stiffness at this location.

At sites with lower soil moduli, the design would have to be reassessed. A secondary concern is to avoid resonances at the generator speed, which is rated at 20 Hz. Figures 6-8 and 6-9 indicate that modes near this frequency are completely insensitive to tower foundation stiffness, because at higher frequencies the concrete foundation inertial impedance is much larger than any stiffness effects. Therefore, a tower with satisfactory high frequency placements at one site will have satisfactory high frequencies at all other sites.

ORIGINAL PAGE IS
OF POOR QUALITY

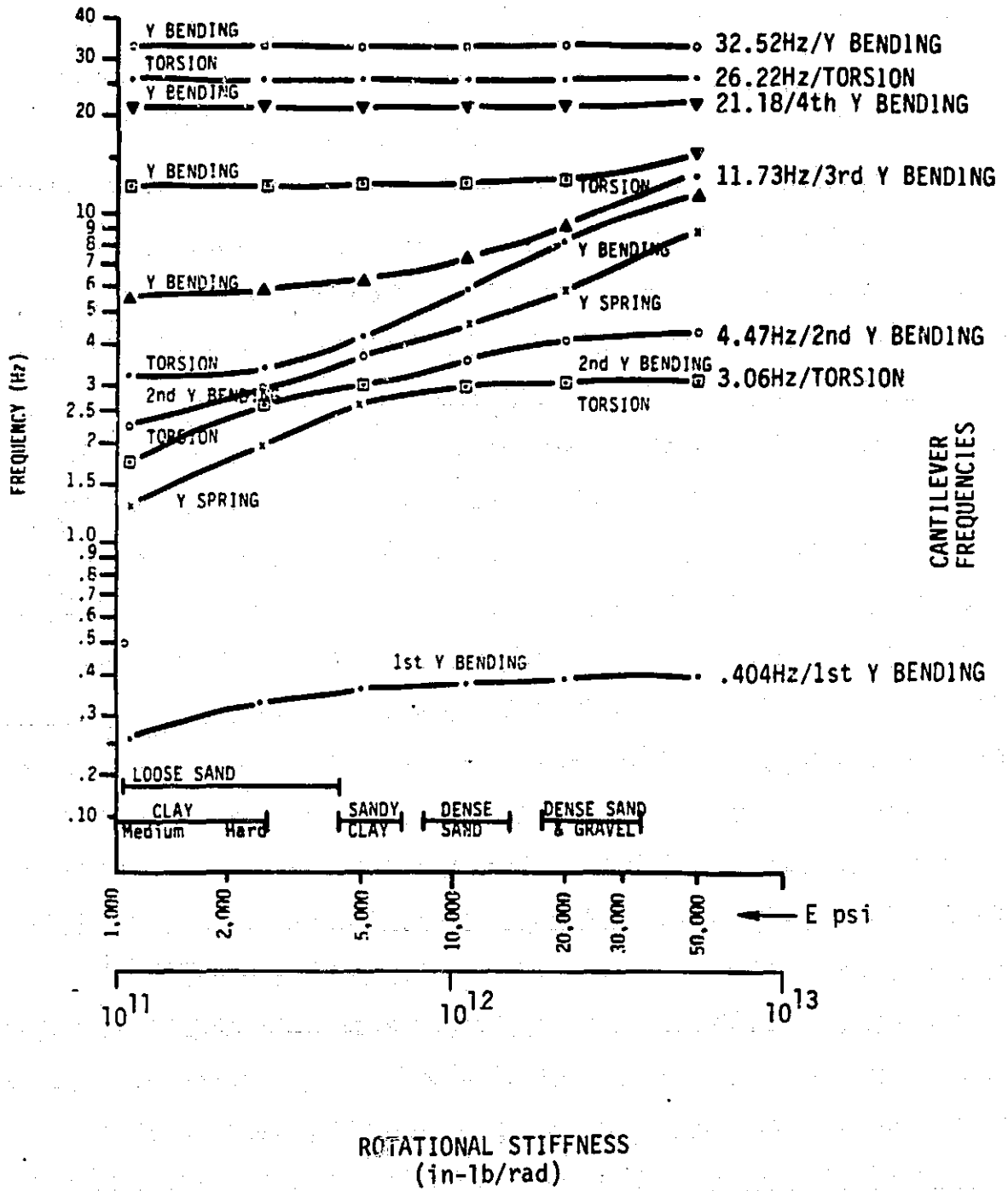


Figure 6-8 Tower Y Bending and Torsion Frequencies vs Rotational Foundation Stiffness

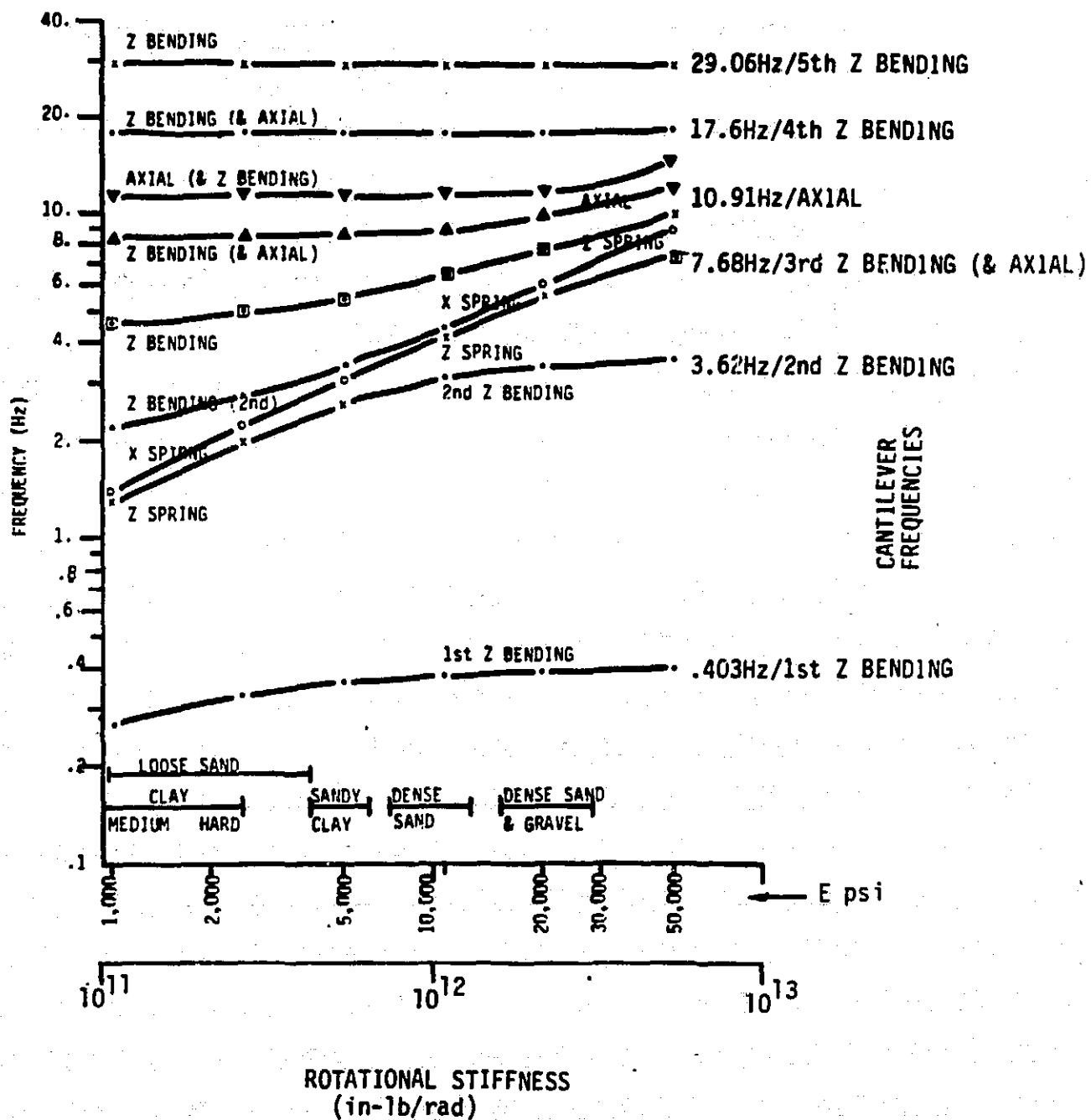


Figure 6-9 Tower Z Bending and Axial Frequencies vs Rotational Foundation Stiffness

6.3.2.2 Sensitivity of Tower Loads to Tower Fundamental Frequency

Steady state loads were calculated for the tower, using natural frequencies of .35, .39, and .43 Hz. Loads were calculated and histograms prepared for the yaw bearing and tower base interfaces for each of the tower frequencies. The loads calculations include the variable speed generator, airfoil tables based on Ohio State University's test data, and an active control system. The blade and nacelle properties were not those of the final design, but the load trends indicated by the study are not influenced by variations in the blade or nacelle properties. The tower frequency is a far more important factor.

The Weibull wind spectrum from the Statement of Work was divided into 6 bins, as shown in Table 6-9. Steady state loads were calculated for winds at 14 and 24 mph with a rotor speed of 13.75 rpm and for winds at 24, 31.7, 45, and 60 mph with a rotor speed of 16.8 rpm. These runs were made for tower frequencies of .35, .39 and .43 Hz, and fatigue load histograms were generated.

Tower fatigue load distributions are shown for the three natural frequencies in Figures 6-10 and 6-11. Significant increases in load level were noted as the tower natural frequency increased toward 2P, which is equal to .46 Hz at the lower speed. The curves for Mz in Figure 6-11 show a distinct jump in load magnitude near the 50th percentile. The higher loads to the right of the jump are due to operation at the low speed, which is nearer to 2P. The My bending loads in Figure 6-10 do not jump since the fore-aft tower mode is less sensitive to resonance because of its higher aerodynamic damping. Root-mean-cubed load levels, which serve as an indication of fatigue severity in steel, are summarized in Table 6-10 and plotted versus tower frequency in Figure 6-12. The loads rise rapidly as the frequency approaches the 2P low rotor speed forcing frequency of .46 Hz. It is clear that the tower frequency should be kept as low as possible.

As a result of this study, the MOD-5A tower height was raised from 235 ft. to 245 ft., to achieve a very favorable natural tower frequency equal to .34 Hz.

Table 6-9 Weibull Distribution from Statement of Work

BIN	ROTOR SPEED	BIN RANGE (MPH)	BIN MID SPEED	# HRS/30 YR	% TOTAL TIME	# 2P CYCLES	#TYPE IIA	# TYPE II GUSTS (T=50 s)
1	13.75	14-19	16.5	56,230	29.4	9.27×10^7	3.65×10^5	4.05×10^6
2	13.75	19-24	21.5	56,655	29.6	9.35×10^7	3.68×10^5	4.08×10^6
3	16.8	24-28	26.0	35,370	18.5	7.13×10^7	2.30×10^5	2.55×10^6
4	16.8	28-35	31.5	32,968	17.2	6.65×10^7	2.14×10^5	2.37×10^6
5	16.8	35-45	40.0	9,511	5.0	1.92×10^7	6.18×10^4	6.85×10^5
6	16.8	45-60	52.5	426	.2	8.59×10^5	2769	3.07×10^4
TOTAL				191,160	99.9	34.41×10^7	12.42×10^5	13.77×10^6

SOW NASA DISTRIBUTION

AT 240 FT AGL

K = 2.74

C = 23.13 MPH

BASED ON $A_0 = 0.35$, $V_H = 67$ MPS

Table 6-10 Root Mean Cubed Tower Load Comparison

f_n (hz)	YAW BEARING (ft-lb x 10 ⁻⁶)			TOWER BASE (ft-lb x 10 ⁻⁶)		
	RMC M_y	RMC M_z	RMS	RMC M_y	RMC M_z	RMS
.35	.667	.478	.821	5.02	3.93	6.38
.39	.756	.730	1.05	6.27	6.99	9.39
.43	1.19	1.68	2.06	12.1	18.0	21.7

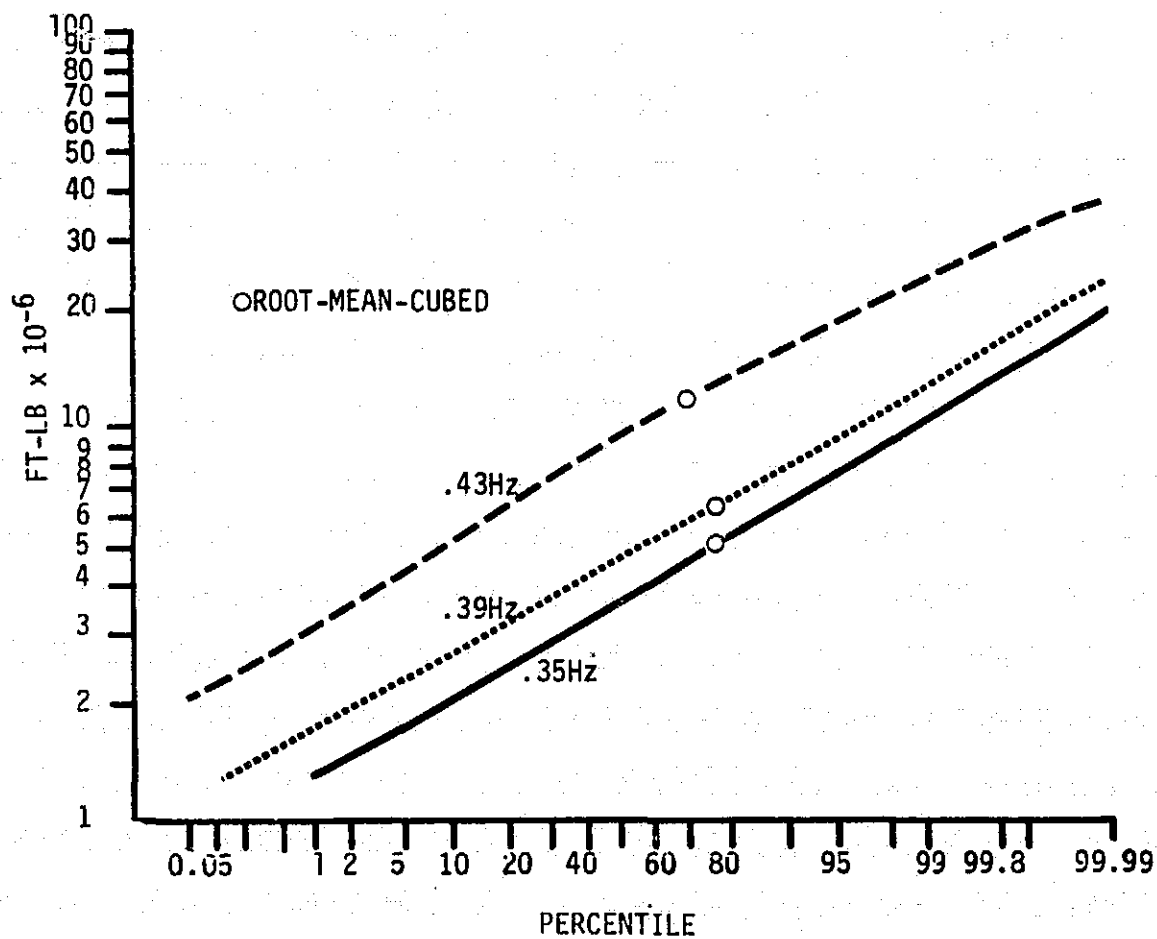


Figure 6-10 Probability Distribution for Tower Base Bending Moment
My-Alternating

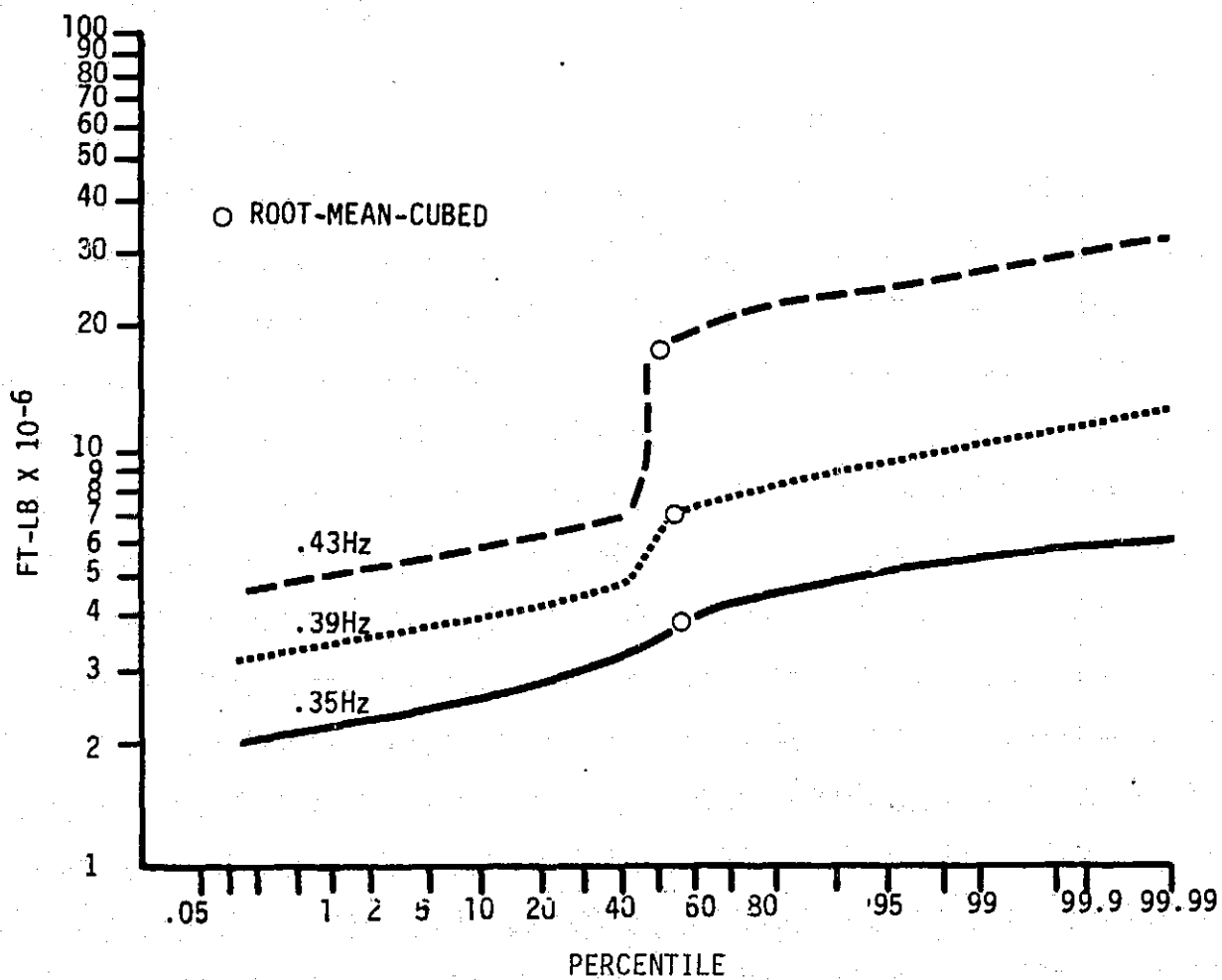


Figure 6-11 Probability Distribution for Tower Base Bending Moment
Mz-Alternating

NOTE: MOMENTS SHOWN ARE THE RESULTANT OF ROOT-MEAN-CUBED
CYCLIC BENDING LOADS

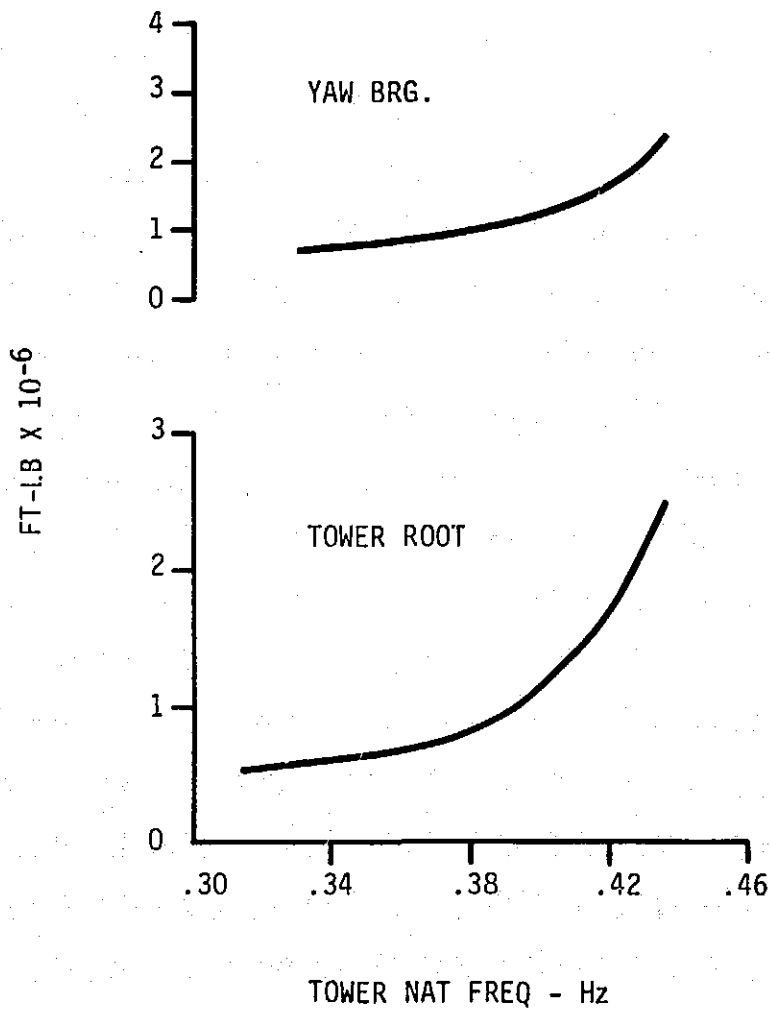


Figure 6-12 Variation of Tower Fatigue Moments with Natural Frequency

6.3.2.3 System Frequency Sensitivity to Bearing and Yaw Drive Stiffness

Stiffness elements representing the teeter bearings, rotor bearings, and yaw bearing, including the yaw drive, were varied from their baseline rated values to determine their effect on system frequencies.

The rated stiffnesses for each of the three bearing interfaces are listed below. The stiffness axes on all plots were normalized to these values. All are given in their local coordinate systems, as shown in Figure 6-13. The units are lb/in. and in.-lb./rad.

	X	Y	Z	Θ_x	Θ_y	Θ_z
Teeter Bearing	4.E6	8.E6	4.E6	4.5E10	5.7E7	4.5E10
Yoke Bearing (Fore)	1.5E8	1.5E8	0	0	0	0
(Aft)	1.0E8	1.0E8	2.5E8	0	0	0
Yaw Bearing	1.08E9	2.5E8	2.5E8	3.0E10	4.44E12	4.44E12

All values are the minimum required except for Θ_y , which is a maximum. The yoke bearing stiffnesses are estimates. The yaw bearing stiffnesses are from a letter from Rotek dated April 8, 1983. The yaw drive stiffness ($\Theta_x = 3.0 \times 10^{10}$) used for this parametric study was based on an early estimate of the structural stiffness with the yaw drive locked. A more accurate estimate, based on the final configuration finite element model, is 1.5×10^{10} in.-lb/rad.

The modal synthesis program, called SCAMP, was used to assemble models of the system with values of bearing stiffness varied about the rating. The resulting frequencies were tabulated, and those that were significantly affected by the changing stiffness were plotted. All runs in this study were made with the blades in a vertical position.

Figure 6-14 shows the effect of blade teetering stiffness (Θ_y) on the teeter frequency, which approaches the tower bending frequency as the stiffness exceeds ten times the rating. This stiffness should be held as low as possible to minimize loads. Figures 6-15 and 6-16 show the effect of radial

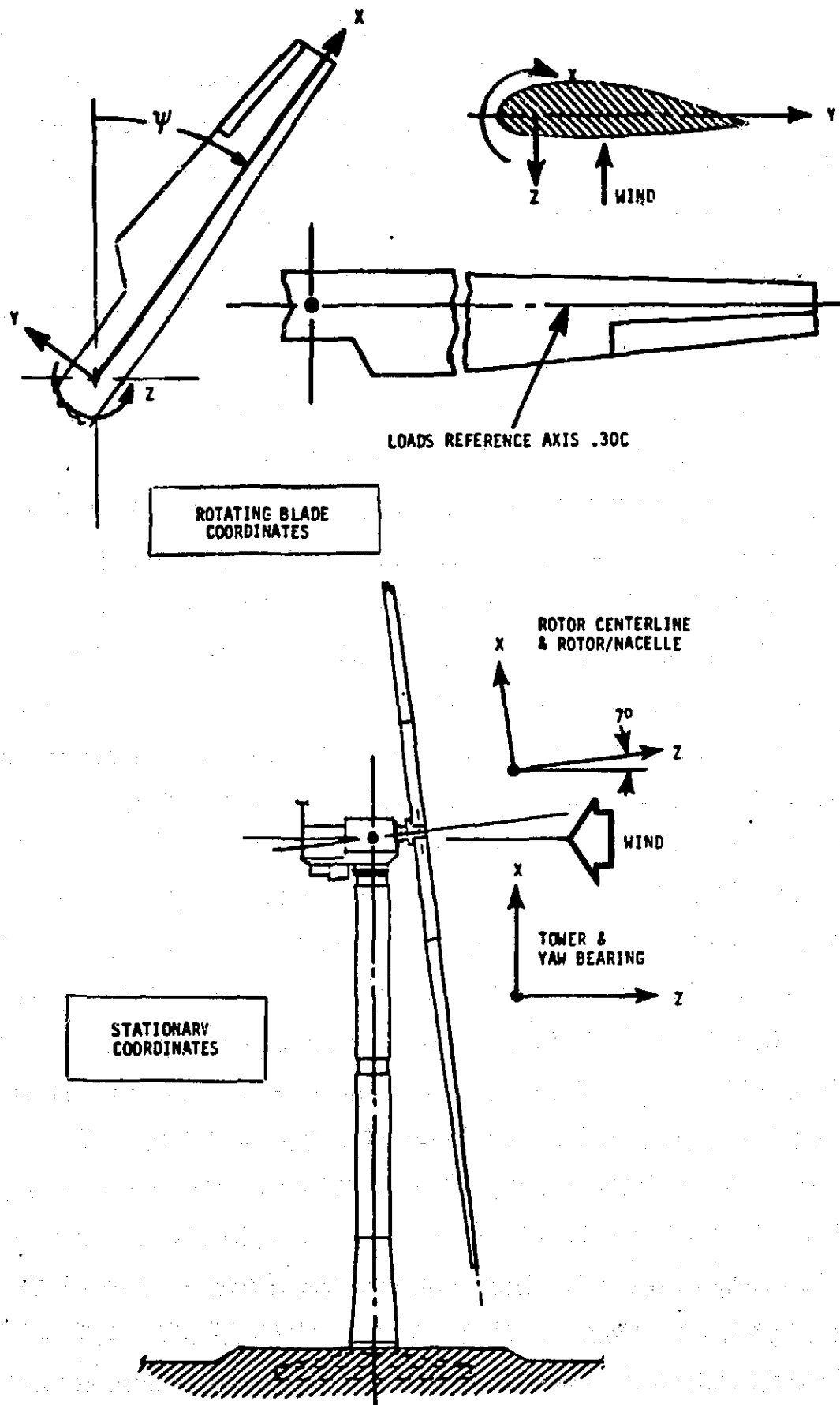


Figure 6-13 Sign Conventions

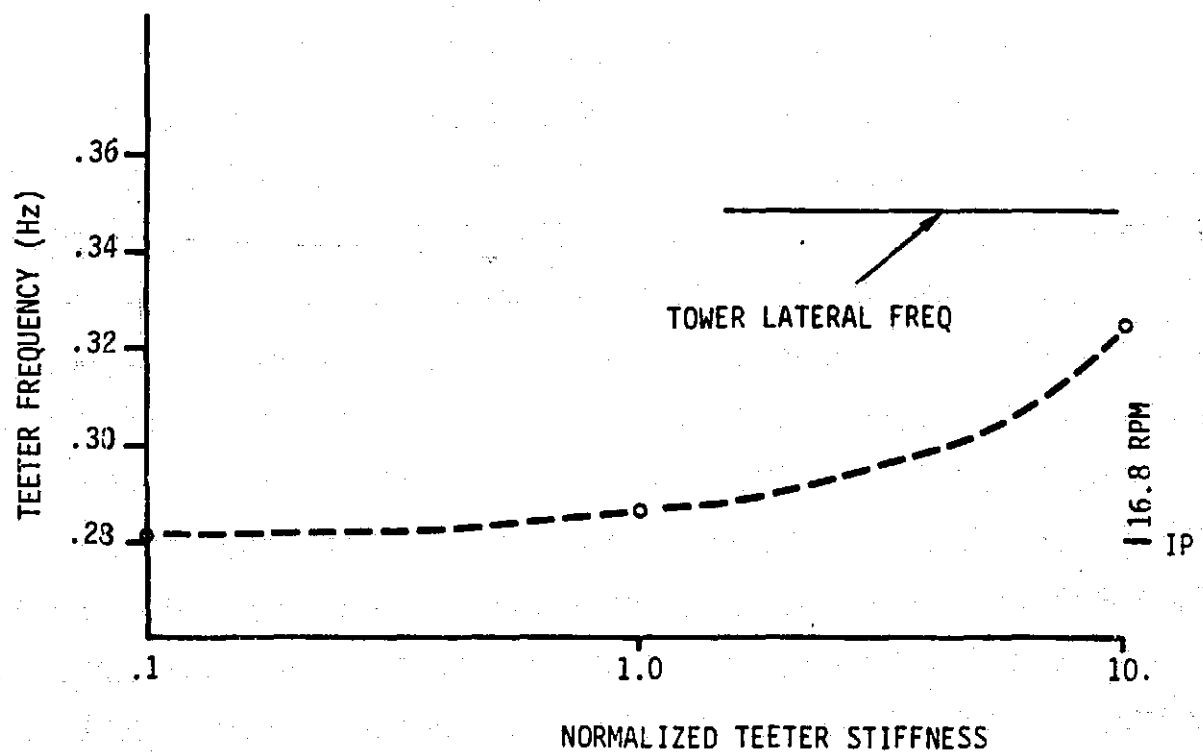


Figure 6-14 Effect of Rotor Teetering Stiffness on Teeter Frequency

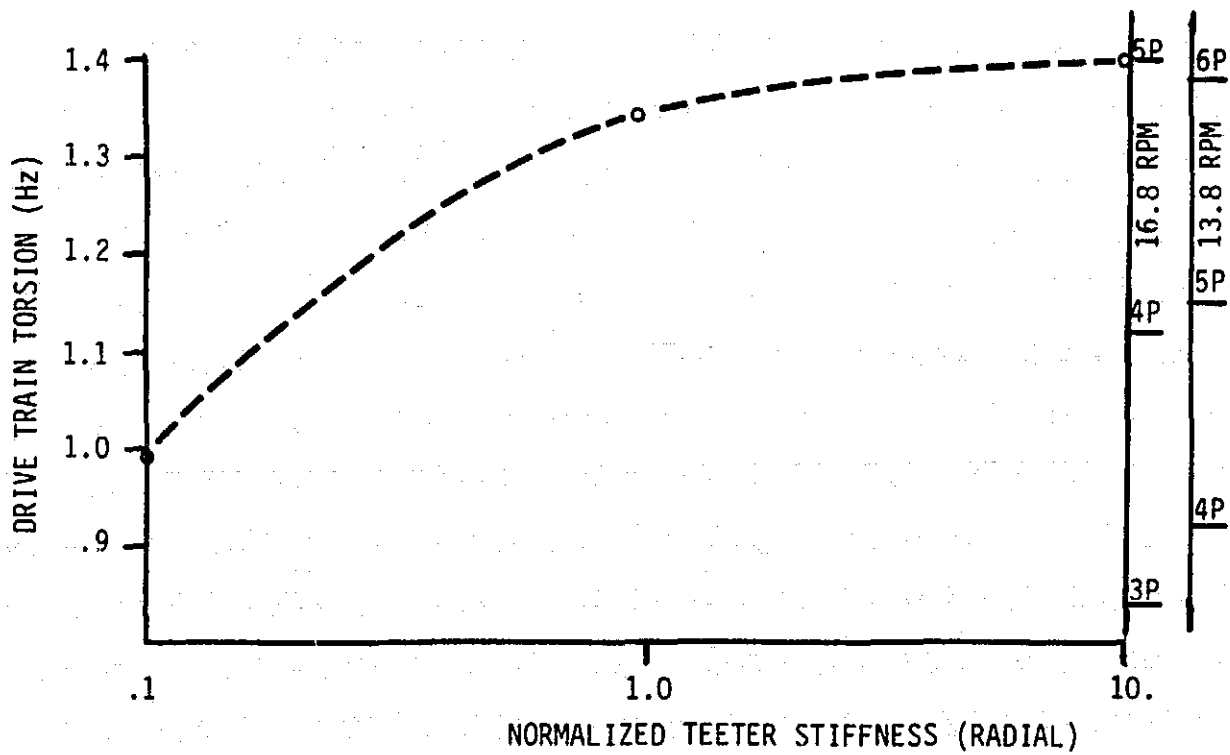


Figure 6-15 Effect of Radial Teeter Bearing Stiffness on Drive Train Frequency

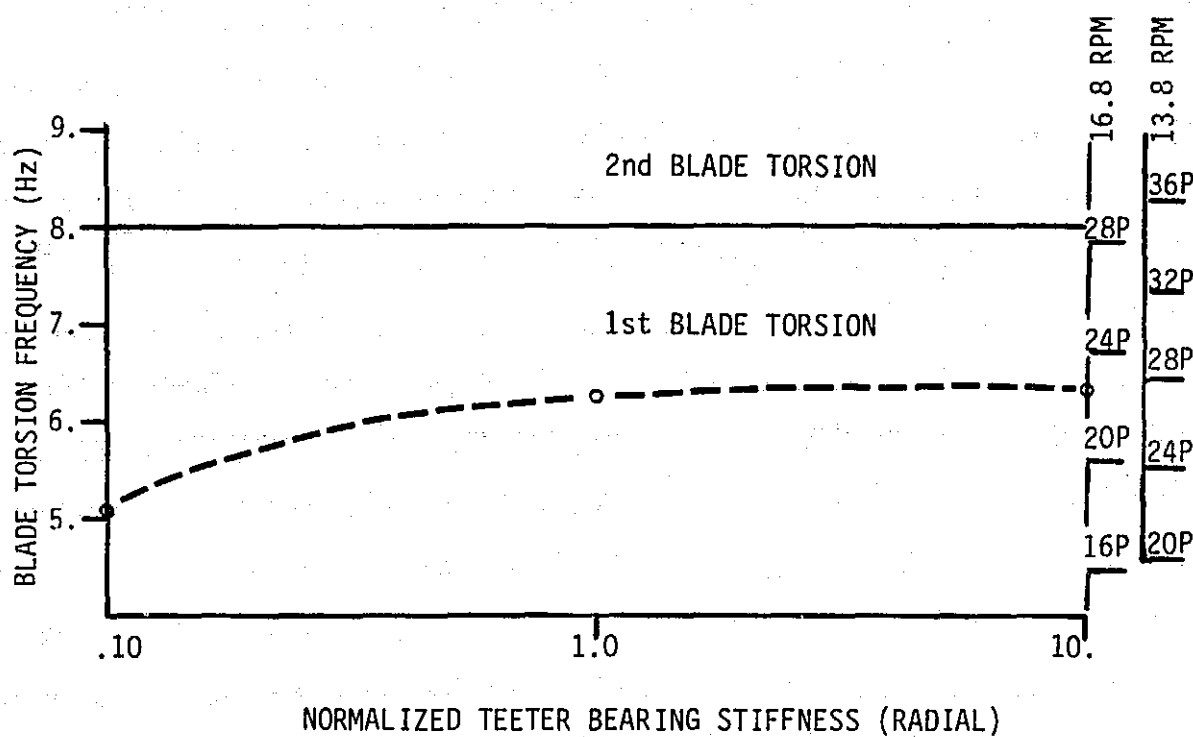


Figure 6-16 Effect of Radial Teeter Bearing Stiffness on Blade Torsional Frequency

(X & Z) stiffness on drivetrain and blade torsional frequencies. It is obvious from these plots that the radial stiffness should not be significantly reduced from the rating, since the drivetrain torsion should not drop near 4P (1.12 Hz).

The effects of yoke bearing stiffness on the tower torsion and second lateral (Z) bending is shown in Figure 6-17. Large decreases in stiffness are required to significantly lower the system frequencies.

In Figure 6-18, tower fundamental frequency is plotted against normalized yaw bearing stiffness. The effect is small for stiffness changes between .1 and 10 times the rating. Figure 6-19 shows the change in tower torsion and chord cyclic frequencies with changes in yaw stiffness. As the plot shows, these modes are highly coupled. Near the rated stiffness it is impossible to label the modes exactly, but the trend shows a small increase in the blade's cyclic frequency with decreasing yaw stiffness, while the torsional frequency decreases very significantly. One tenth of the rated yaw stiffness is approximately the lower limit of the present yaw drive design. The rated stiffness on this plot is twice the current estimate for the yaw brake. The yaw stiffness must not be further reduced. Note that during a yaw maneuver the torsional stiffness is near zero because the dominant stiffness elements in the system are the gas bladders of the hydraulic accumulators. This situation should not produce a resonance problem.

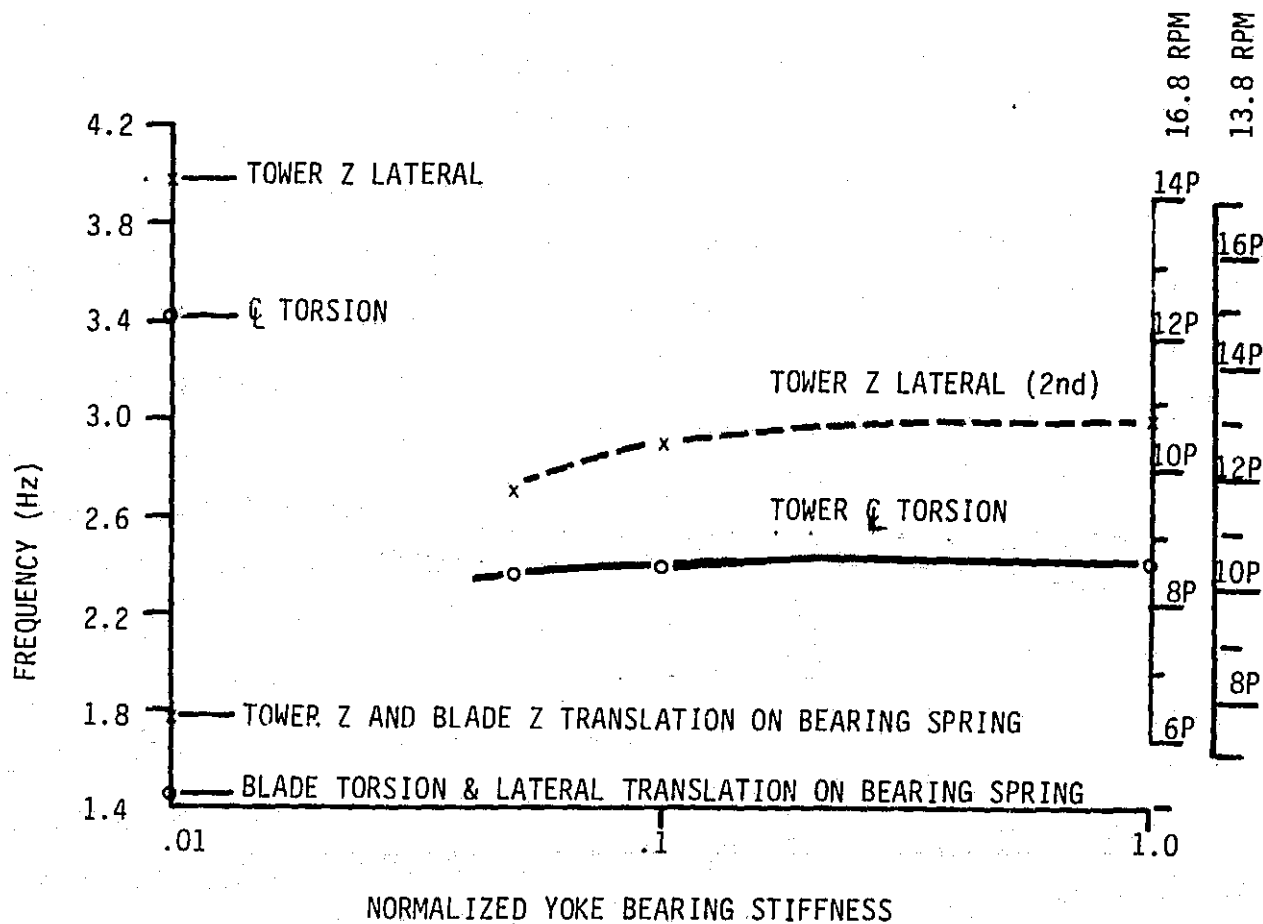


Figure 6-17 Effect of Yoke Bearing Stiffness on Tower Torsion and Second Lateral Bending Frequencies

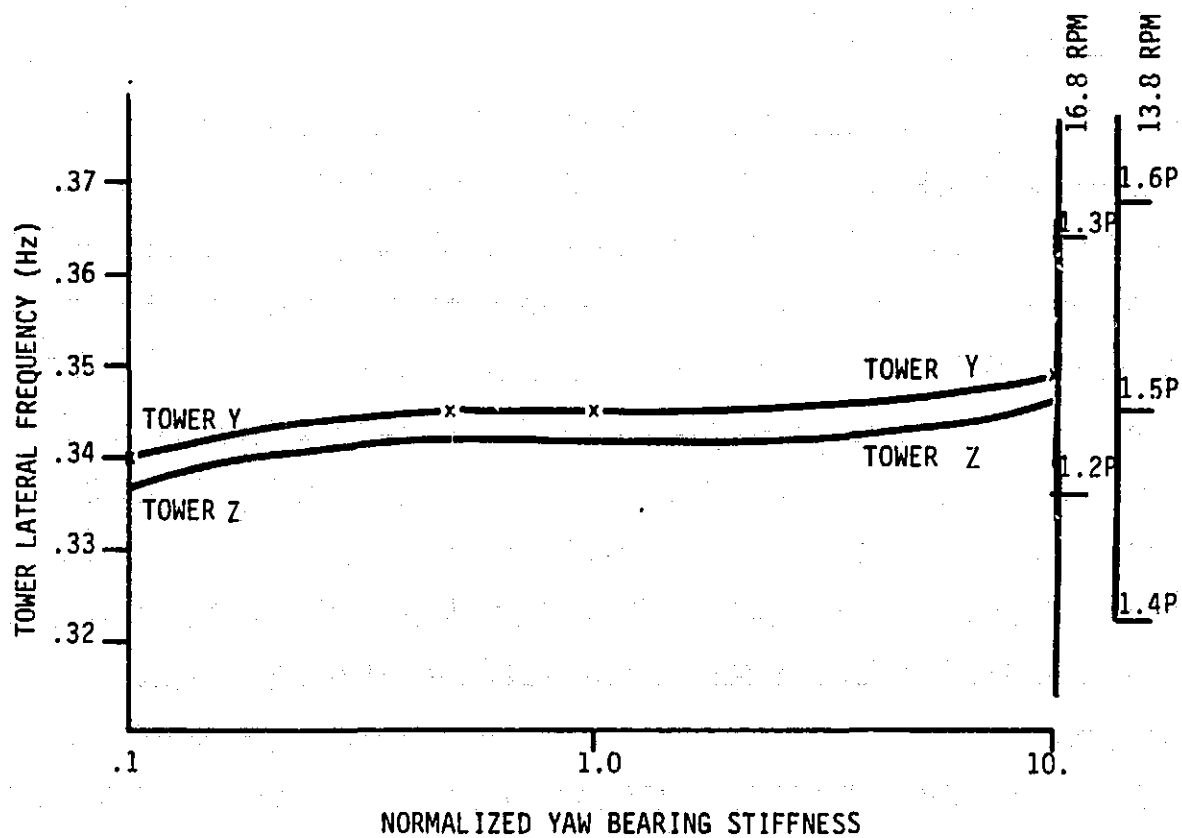
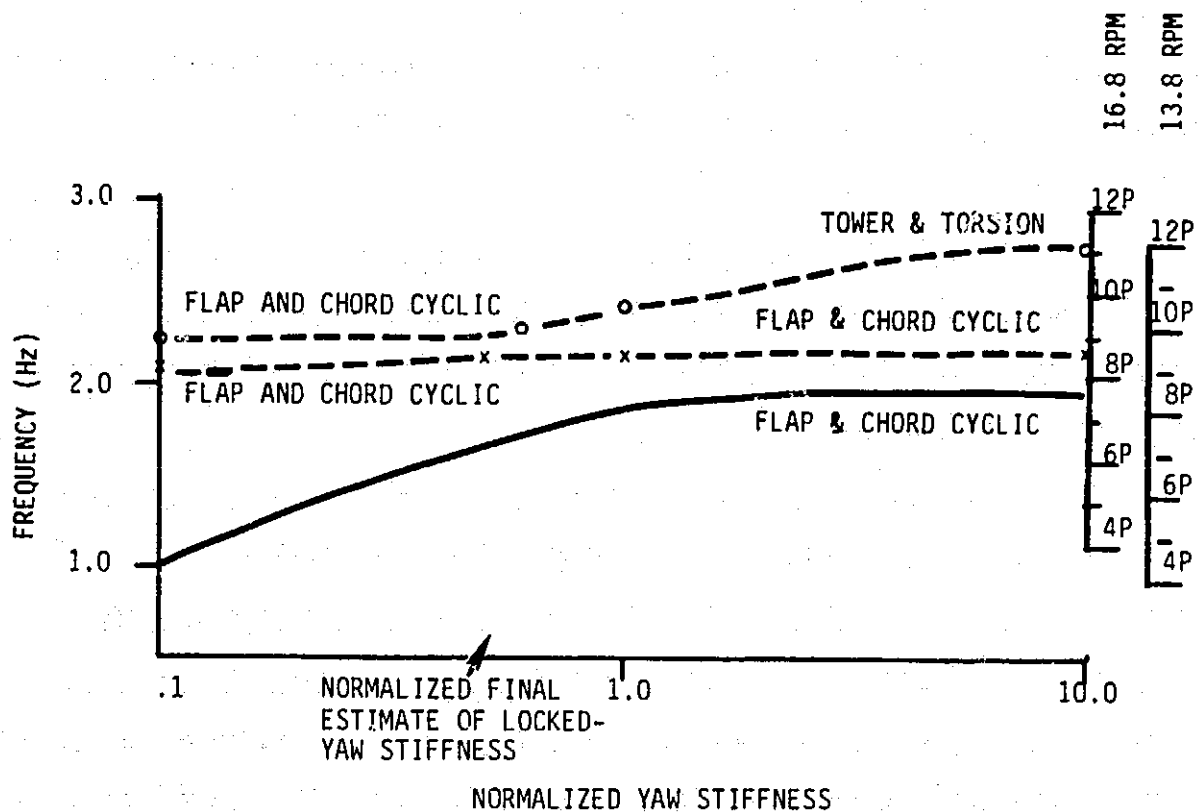


Figure 6-18 Effect of Yaw Bearing Stiffness on Tower Fundamental Frequency



* NOTE: THE BLADE USED IN THESE STUDIES WAS NOT THE FINAL MODEL, SO THE BLADE FREQUENCIES ARE NOT IDENTICAL TO THOSE DESCRIBED IN SECTION 6.3.1. THIS DIFFERENCE WILL NOT, HOWEVER, HAVE ANY QUALITATIVE EFFECT ON THE RESULTS OF THESE PARAMETRIC STUDIES.

Figure 6-19 Effect of Yaw Stiffness on Chord Cyclic and Tower Torsion Frequencies

6.4 AEROELASTIC STABILITY

Analyses have shown that the MOD-5A will not encounter aeroelastic instability. Although several types of rotor instability are possible, the dynamic characteristics of modern wind turbines preclude most of them. One concern for the MOD-5A was the stability of the aileron system, which was a point of departure from previous large wind turbines. Other potential instabilities are classical flutter/divergence, blade flap-lag and pitch instability, coupled rotor/tower instabilities, and blade stall flutter.

A brief discussion of each of these appears in this section. This section also includes a more comprehensive treatment of blade/aileron flutter.

6.4.1 CLASSICAL FLUTTER AND DIVERGENCE

Rotor blades are subject to classical bending-torsion flutter and torsional divergence, similar to that experienced by an airplane wing. The key structural parameters are torsional stiffness and chordwise center of gravity, while the important operating parameter is rotor speed. Most wind turbine blades are not mass-balanced, and they have a destabilizing, aft center of gravity. They are stable, however, because of relatively high torsional stiffness, and more importantly, the low operational tip speeds, which are about half that of a typical helicopter blade.

The computer code GETSTAB was used to assess flutter and divergence on the early MOD-5A with a partial span control. In this design, it was necessary to ensure that the stiffness of the partial span control was sufficient to preclude flutter. In the current configuration with ailerons, the main blade structure no longer has a potentially soft torsional link. Flutter speeds above 50 rpm were computed using the computer code, AILSTAB.

6.4.2 BLADE FLAP-LAG-PITCH INSTABILITY

Many recent studies (ref. 6-5) identified rotor instabilities caused by coupling between blade flap, lag or chord, and pitch motions. The mechanisms of instabilities are varied and often complex. They usually depend on rotor thrust and blade natural frequency placements. In particular, there is a strong potential for instability when the fundamental flapwise and chordwise

natural frequencies nearly coincide. This situation does not exist on the MOD-5A blades. GETSTAB indicated that the MOD-5A blade with partial span control was free of any of these problems. It is unlikely that the changes associated with ailerons would alter these conclusions. It would be desirable, however, to analyze the final design before actual operation.

6.4.3 COUPLED ROTOR AND TOWER INSTABILITIES

Coupling between the rotor and tower modes can produce instabilities, such as whirl flutter. These couplings depend on the relative natural frequencies of the rotor and tower, which should not be close. Whirl flutter generally involves the blade fundamental flapwise mode and rotational modes of the tower, pitch and yaw. Whirl flutter is not likely to occur on wind turbines, because of the wide separation usually found between these frequencies. The MOD-5A is no exception. Furthermore, there were no such problems on the MOD-2, which is a similar design and there were no indications of instability in the transient loads analyses performed for the MOD-5A. These loads analyses, conducted with the TRAC code described in Section 7.2, model the modes in question.

Nonetheless, it would be desirable to perform a final analysis before operation. This could be done either with GETSTAB or NASA's code, ASTER-5.

6.4.4 BLADE STALL FLUTTER

Stall flutter is characterized by limit cycle oscillations of the blade in its first torsional mode. The aerodynamics are non-linear and difficult to quantify, as the blades are oscillating into and out of a stalled state. The airfoil type, torsional damping and the reduced frequency of the first torsional mode are the key parameters. Reduced frequency is a non-dimensional parameter defined as the product of semi-chord times torsional natural frequency divided by resultant velocity or $b\omega_0/V$. Because of their relatively low tip speed and high torsional stiffness, wind turbine blades generally have a high reduced frequency, which is important for avoiding stall flutter. The MOD-5A has a reduced frequency greater than .60 over 75% or more of the blade for all operating conditions, including 50% overspeed. Therefore, no problems are expected in this area.

6.4.5 BLADE/AILERON FLUTTER

The stability of the blade and aileron system was investigated using the AILSTAB code. The blade's natural modes were determined for cantilevered and pinned end conditions. The model was constructed before the final design, so some of the natural frequencies reported in this section may differ slightly from those of the final blade. However, the system's stability is relatively insensitive to such changes, so the conclusions are also valid for the final configuration.

Three model sets, shown below, were analyzed.

<u>Set</u>	<u>Flapwise Mode</u>	<u>Blade Torsion</u>	<u>Aileron Torsion</u>
1	Teeter (1P)	1st Torsion	Rigid Body, f_n varies
2	1st Collective	1st Torsion	Rigid Body, f_n varies
3	1st Cyclic	1st Torsion	Rigid Body, f_n varies

Higher flapwise modes were also analyzed, but were not found to be critical. The blade flapwise collective (cantilever) and cyclic (pinned) frequencies were 7, and 13.8 rad/sec respectively. The blade torsion frequency is 51 rad/sec. By comparison, the ailerons are essentially rigid in torsion with cantilevered frequencies above 400 rad/sec. For all practical purposes, the aileron natural frequencies are dominated by the control system stiffness and oscillate as a rigid body. Rather than attempting to model the actual aileron torsional natural mode, the frequency, or equivalently the actuator stiffness was varied, to determine the minimum requirements. In this way failure mode conditions, such as loss of actuator hydraulic stiffness, are fall-outs of the analysis. In addition to aileron frequency sweeps, variations in aileron torsional damping and mass-balancing were considered. The MOD-5A aileron's center of gravity is aft of the 60% chord hinge line. The aft center of gravity has a destabilizing effect.

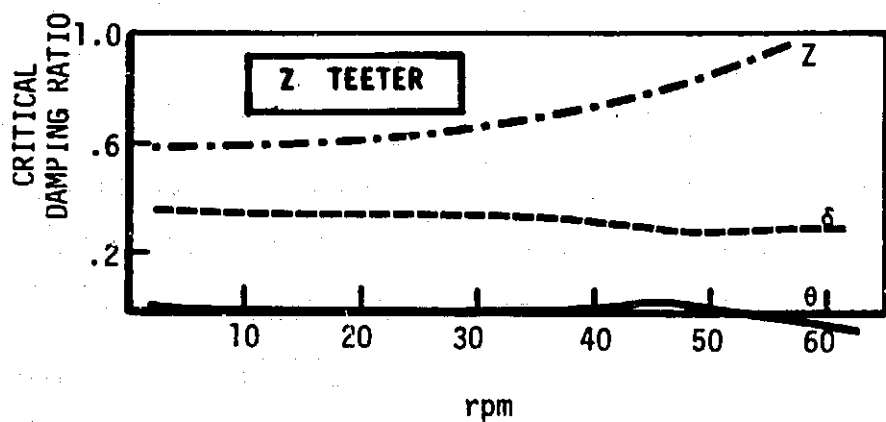
The output of the AILSTAB computer program is given in eigenvalues, and eigenvectors if desired, as a function of rotor speed. Critical damping values were computed at each rotor speed and were plotted to determine the

stability. The symbol Z in these plots refers to the blade's flapwise degree of freedom, the symbol θ refers to the blade torsion, and δ to the aileron torsion. Each figure contains three plots, one for each of the blade flapwise modes investigated.

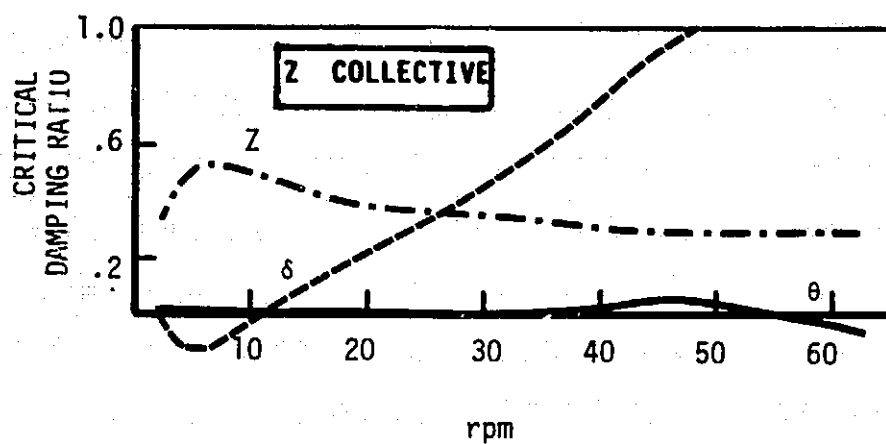
The most critical condition occurs when the root torsional stiffness provided by the actuators is lost and the ailerons are free to rotate about their hinges. This cannot happen under normal circumstances, so it represents a system failure. Figure 6-20 shows damping vs. rotor speed for the blade with a free unbalanced aileron. (The aileron torsion frequency of 1P is due to centrifugal stiffening). Only coupling with the 4P collective mode causes an instability in the range of interest. The instability at 60 rpm is classical bending-torsion flutter of the main blade. The free ailerons are unstable in the region of low rotor speed, 3-12 rpm, which is typical of wing and aileron systems with an unbalanced mass. In particular, there is the possibility of instability when the aileron torsional frequency is less than the flapwise frequency. The system in Figure 6-20 becomes stable again at 12 rpm, because the torsional aerodynamic spring increases the aileron frequency beyond that of the first flapwise mode. The system is not unstable in higher flapwise modes because of the modal weighting. Analogous problems exist on small, low-speed airplanes, in which stick-free ailerons with unbalanced mass can encounter flutter over a range of relatively low forward speeds. A common solution is to mass-balance the ailerons.

An identical analysis was conducted for a mass-balanced system. The results, shown in Figure 6-21, indicate a stable system. The variation of minimum damping in the aileron mode is shown for different degrees of balance in Figure 6-22. The system becomes stable with 85% balance (the center of gravity is still aft of the hinge). However, a 5% stability margin ($\xi_f = .05$) was imposed on the final design, to compensate for possible inaccuracies in the analysis.

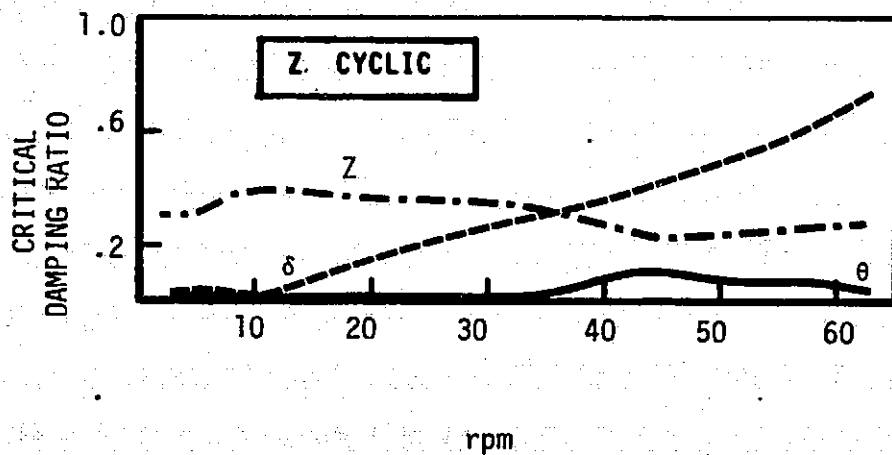
The stability of the baseline aileron, which is unbalanced, but with a torsional spring that produces an 8 rad/sec natural frequency, is shown in Figure 6-23. This configuration is stable for all three mode sets. Similar



$$\begin{aligned}\Omega_Z &= 1p \\ \Omega_\theta &= 51 \text{ rad/s} \\ \Omega_\delta &= 1p \\ c &\approx e = .2\end{aligned}$$



$$\Omega_Z = 4p$$



$$\Omega_Z = 7p$$

Figure 6-20 Stability with Free, Unbalanced Aileron

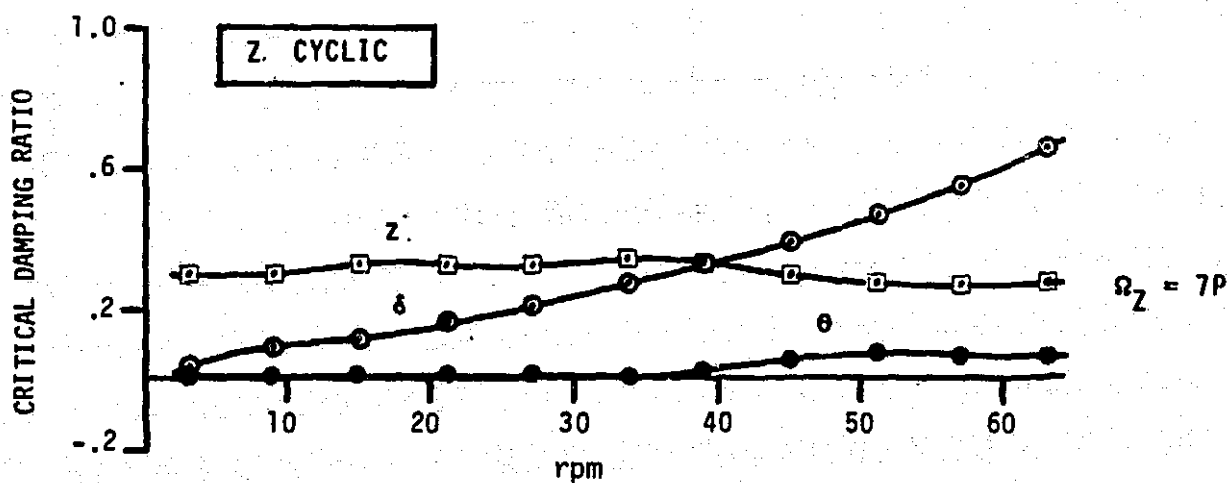
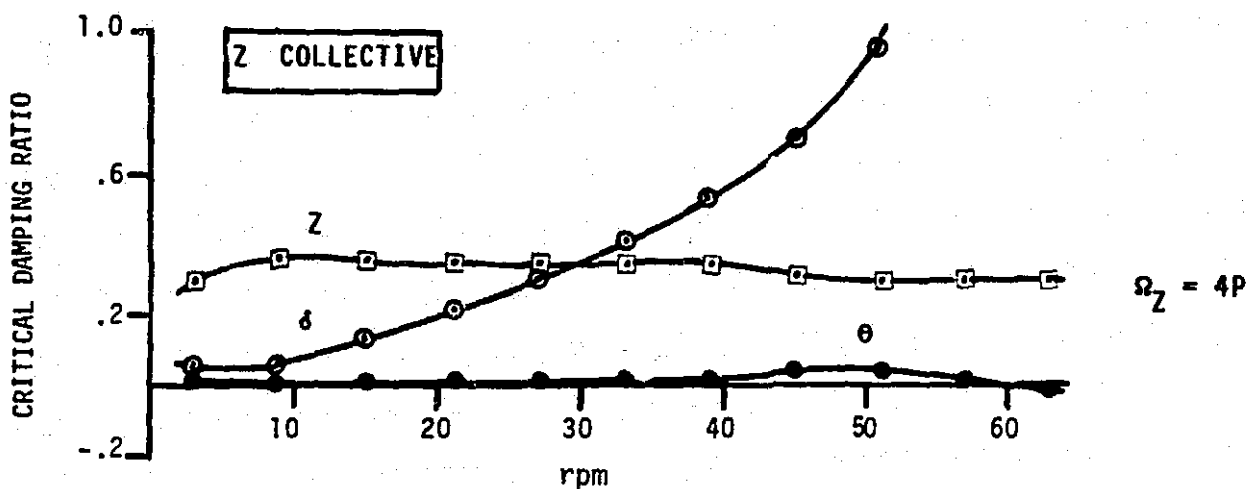
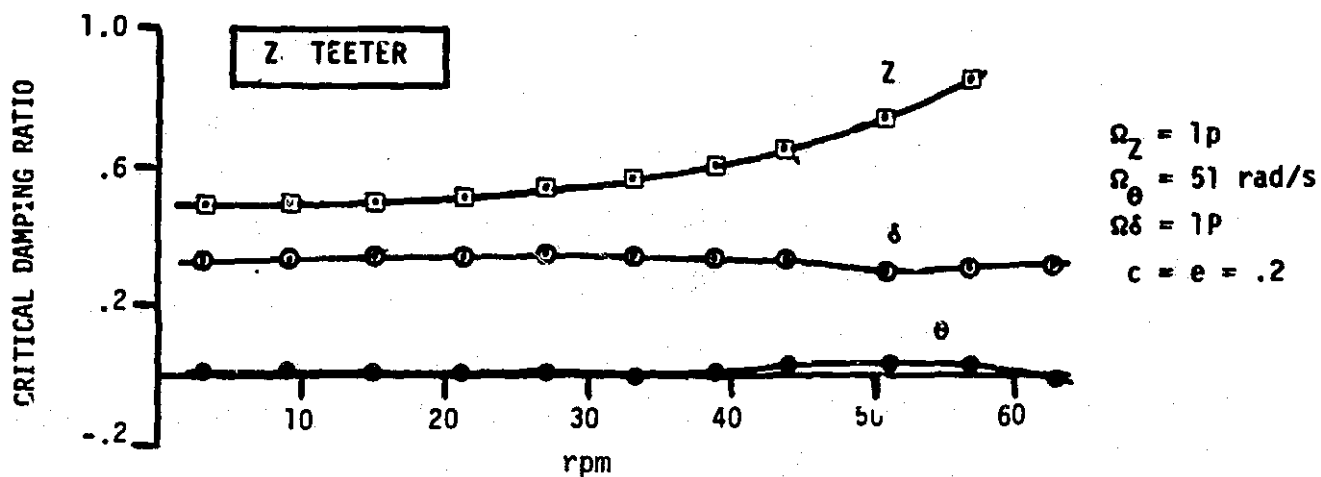


Figure 6-21 Stability with Free, Mass-Balanced Aileron

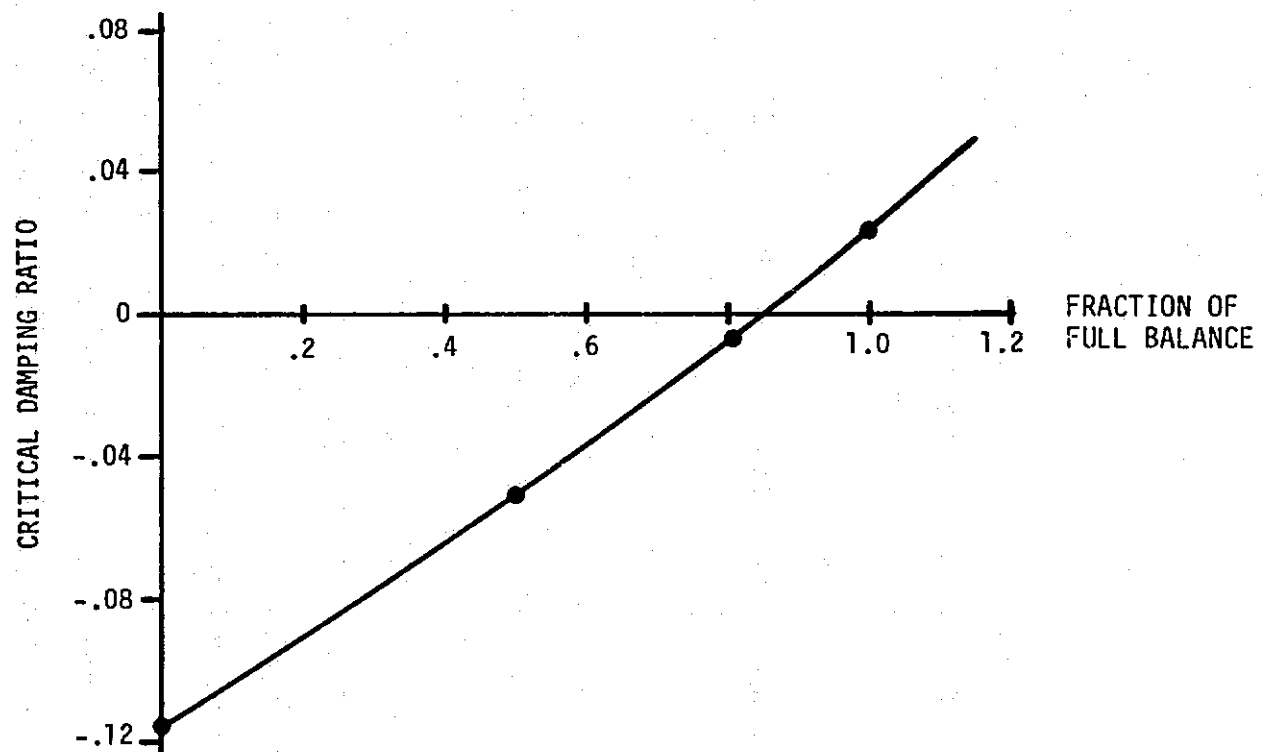


Figure 6-22 Free Aileron Stability at 6 rpm vs. Mass Balance

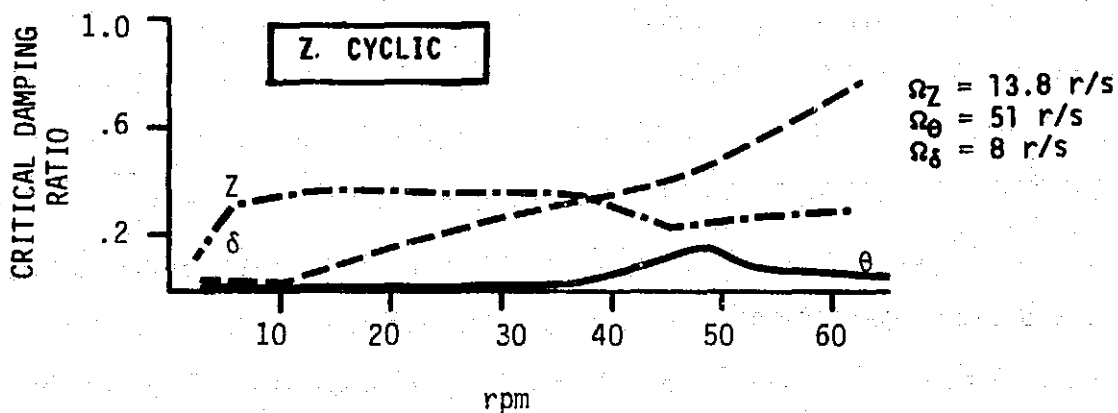
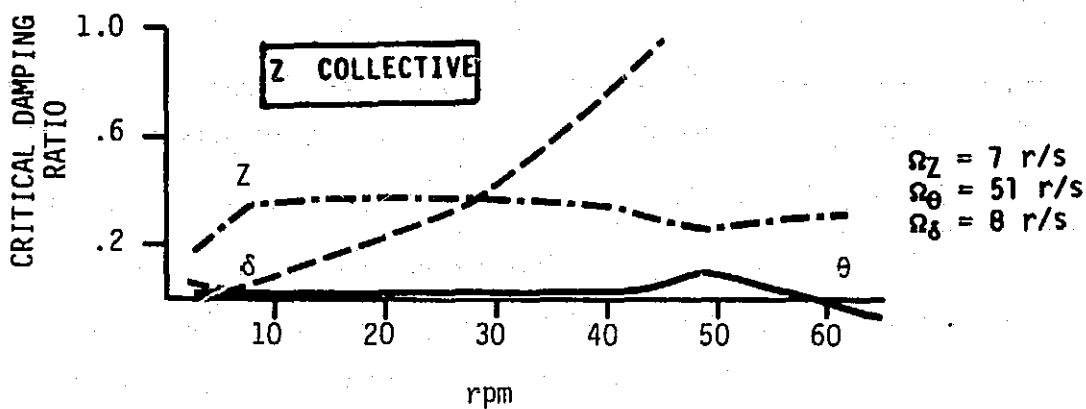
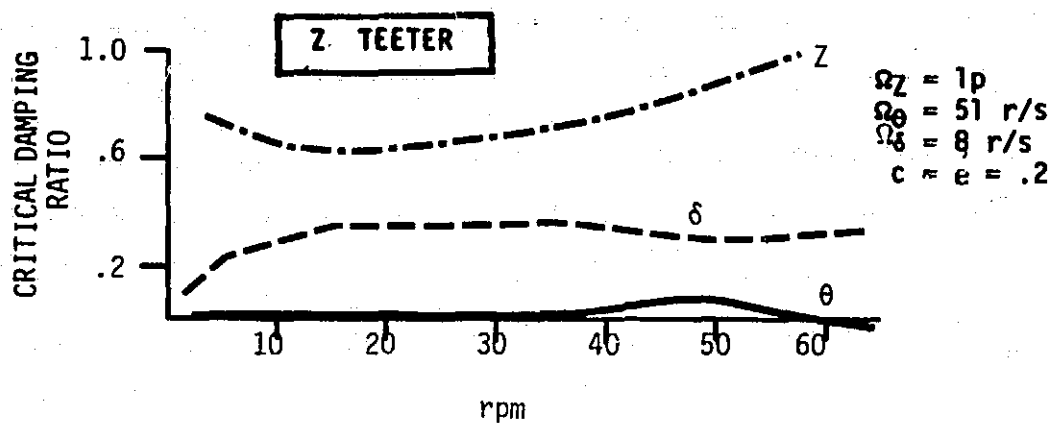


Figure 6-23 Stability of an Unbalanced Aileron System with Torsional Hinge Stiffness. Aileron Torsional Frequency = 8 rad./sec.

runs were made for other spring rates in order to develop the stability boundary shown in Figure 6-24. It is apparent that for the system to be stable at all rotor speeds, the torsional natural frequency of the ailerons must exceed 7.7 rad/sec. Under normal circumstances, this condition is easily satisfied. It is necessary, however, to protect the system in the event of an actuator failure, in which case the natural frequency is 0. This protection may be provided by mass-balancing, as discussed earlier, or by incorporating dampers at the hinges. It should be noted that analysis has shown that even if only one of the six actuators on the rotor fails, the system will be unstable unless this protection is provided.

Figure 6-25 shows the MOD-5A stability boundary as a function of torsional damping rate for the free, unbalanced aileron. The system is stable at all rotor speeds, provided the damping rate is 2,700 ft.-lb.-sec/rad or more. In order to achieve a 5% margin above neutrally stable conditions, the rate must be 7,000 ft.-lb.-sec/rad. Because the MOD-5A has three distinct aileron sections per blade, the total damping must be divided amongst the ailerons. The division is done in proportion to the respective torsional inertias. The results are summarized below (R is the radius of the blade):

	<u>Damping Rate</u>
Inner Aileron (.60-.725R)	4,430 ft.-lb.-sec/rad
Mid Aileron (.725-.85R)	1,925 ft.-lb.-sec/rad
Outer Aileron (.85R-TIP)	<u>645 ft.-lb.-sec/rad</u>
Total	7,000

The forces produced by these damping rates are negligible in comparison to normal operating pitching moments for which the aileron actuators are designed. Therefore, the dampers can be operative at all times without hurting the system's performance.

The comparison of stiffness and damping requirements is an interesting sidelight to the stability problem. The damping rate, multiplied by the flutter frequency gives the effective impedance, in stiffness units, of the damper. Figure 6-26 contains plots of impedance vs. flutter damping ratio at 6 rpm for both spring and damper systems. The system's stability is largely a function of the aileron torsional impedance whether it be derived from a

spring or a damper. This conclusion is strengthened by Figure 6-27, which shows the stability boundaries in terms of impedances. The approximate equivalence of spring and damper impedance effects is an important consideration during dynamic conditions, such as pitch change, in which the hydraulic actuator impedance has both spring and damper characteristics.

In summary, the MOD-5A blade and aileron system can be stabilized for all operating environments by either providing a sufficiently high impedance about the aileron hinge axis, or by mass-balancing of the ailerons.

The basic actuator system provides the necessary impedance during normal operation. To protect the system if an actuator fails, torsional dampers were incorporated into the MOD-5A design rather than mass-balancing the ailerons. These dampers are passive elements in the sense that they will always be operative.

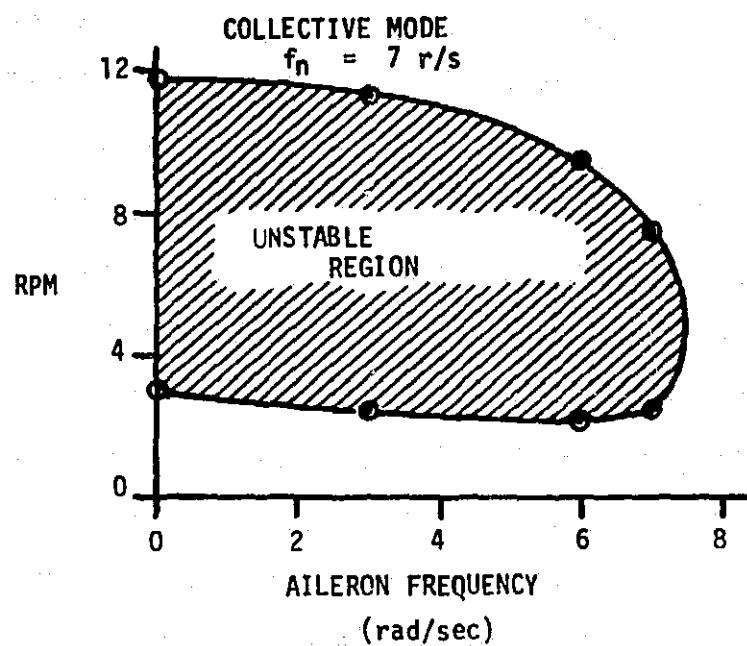


Figure 6-24 Unbalanced Aileron Stability Boundary
with Control System Stiffness

ORIGINAL PAGE IS
OF POOR QUALITY

FLAP COLLECTIVE MODE

$$f_n = 7 \text{ r/s}$$

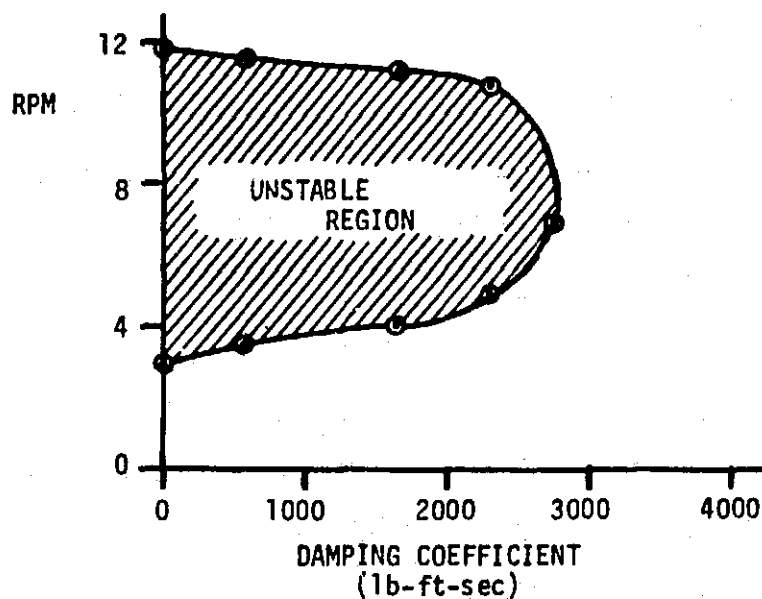


Figure 6-25 Unbalanced Aileron Stability Boundary
with Hinge Dampers and Free Aileron

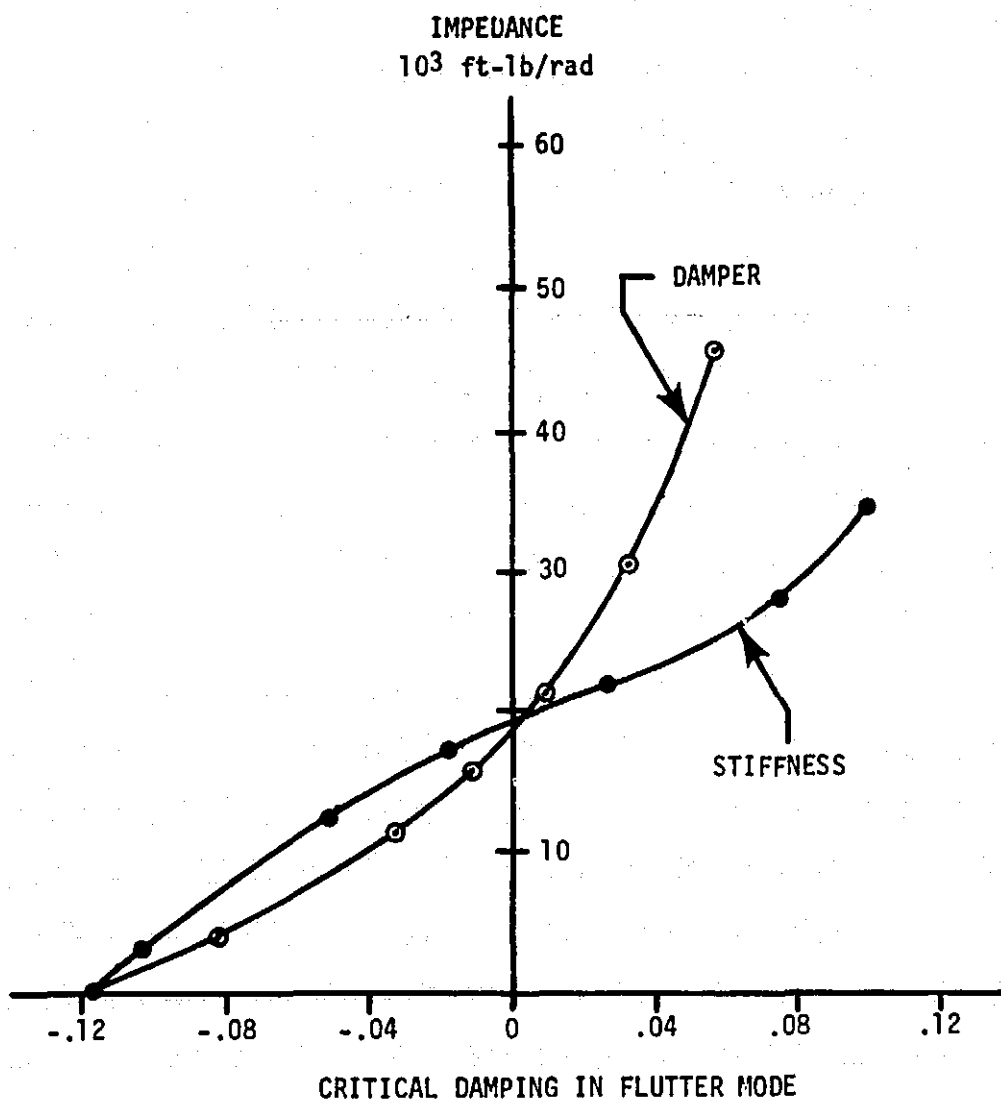


Figure 6-26 Comparative Effects of Stiffness and Damping Impedance on Aileron Stability

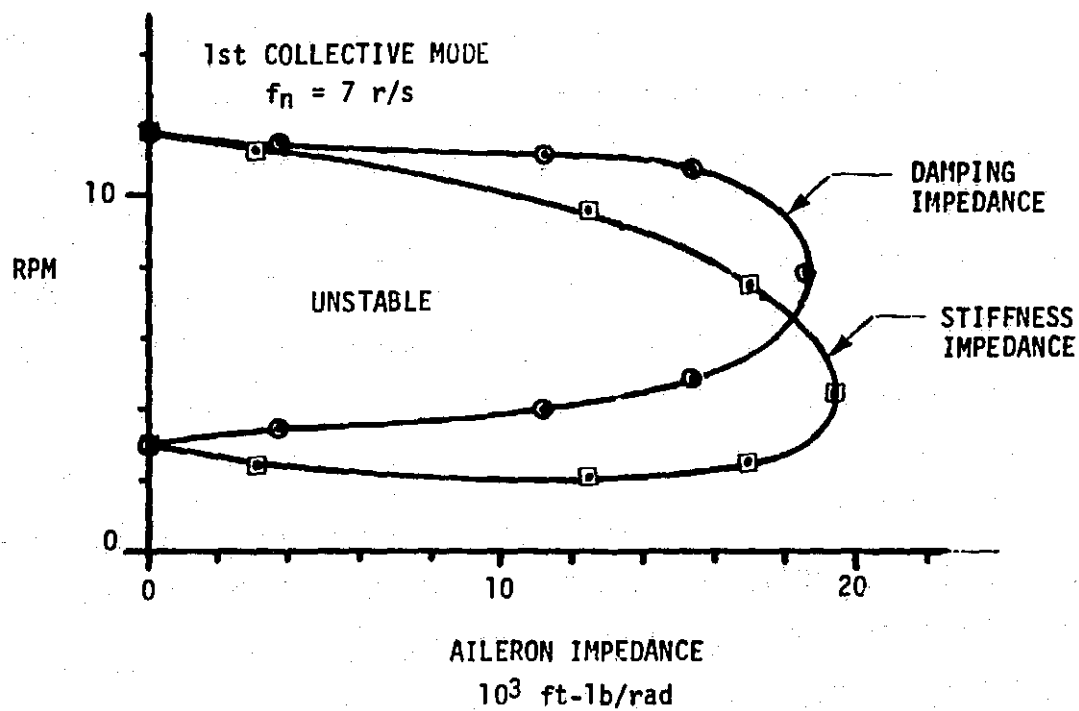


Figure 6-27 MOD-5A Flutter Boundary
 Shown in Terms of Aileron Root Impedance

6.5 CONTROL SYSTEM

6.5.1 OVERVIEW

The control system for the MOD-5A is defined in detail in the Control System Specification. The system comprises the components and assemblies shown in Figure 6-28. The functions of the control are to:

1. control the yaw orientation
2. control the rotor speed using the ailerons
3. control the rotor position
4. control the rotor brake
5. control the teeter brake
6. monitor and control the hydraulic and lubricating system pressure, heating, and cooling
7. control the electrical power output (generator, converter, bus/utility tie)
8. control the emergency shutdown
9. control the operator interface (site, remote dispatch, manual operations)
10. display operating data

From the standpoint of dynamics, the key function of the control system is speed control, which is provided by the joint operation of functions #2 and #7. A rotor speed control loop and a generator speed control loop are used, as shown in Figure 6-29.

The regions of operation during power generation are shown on Figure 6-30. In subrated power or low wind conditions the generator speed will be controlled. Regulation of generator air gap torque by the variable speed generator subsystem provides speed control. Either a low speed or a high speed operating region will be automatically selected for the most efficient use of the wind and the rotor. The low speed region occurs when the average power is less than 4.5 MW, at average wind speeds between 14 and 25 mph. When the average power is greater than 4.5 MW, the generator and rotor speed references are automatically moved upward by 3 rpm to the high speed region, at a rate such that approximately 1/7th of the input torque is used to accelerate the rotor. The transition from the high speed region to the low speed region is made when the average power drops below 3 MW, at average winds below 22 mph.

At the rated power, when the wind speed is greater than 32 mph, the rotor speed control loop regulates the aileron positions to maintain the average

ORIGINAL PAGE IS
OF POOR QUALITY

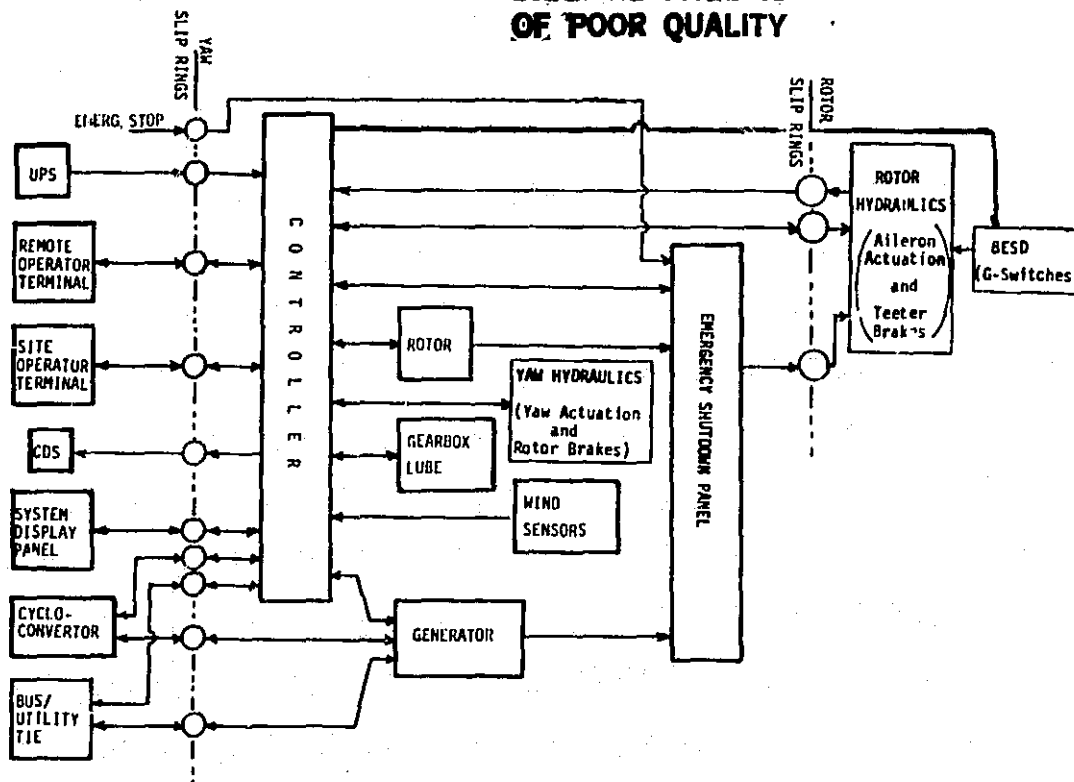


Figure 6-28 General Control System Block Diagram

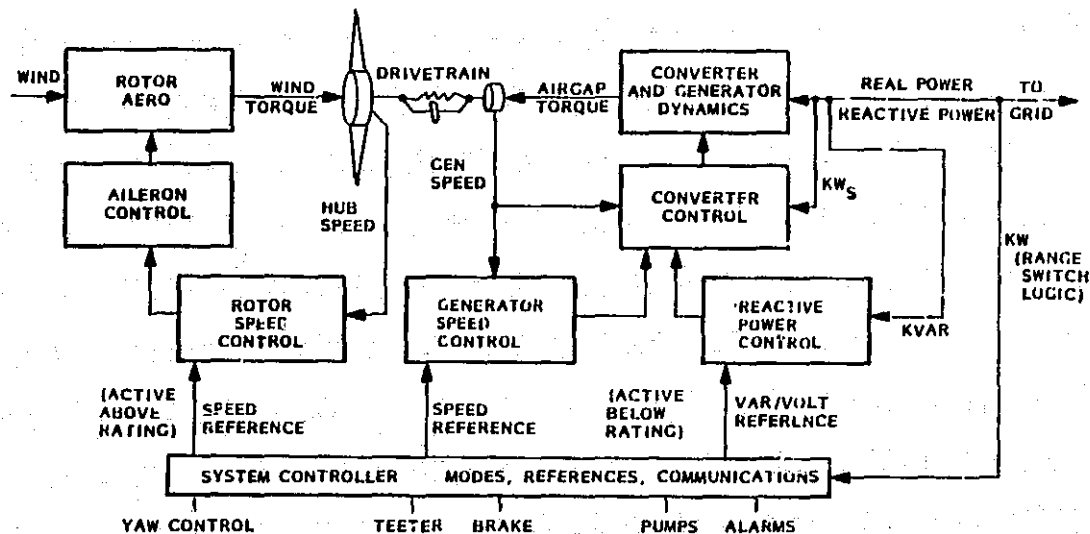


Figure 6-29 System Control Plan

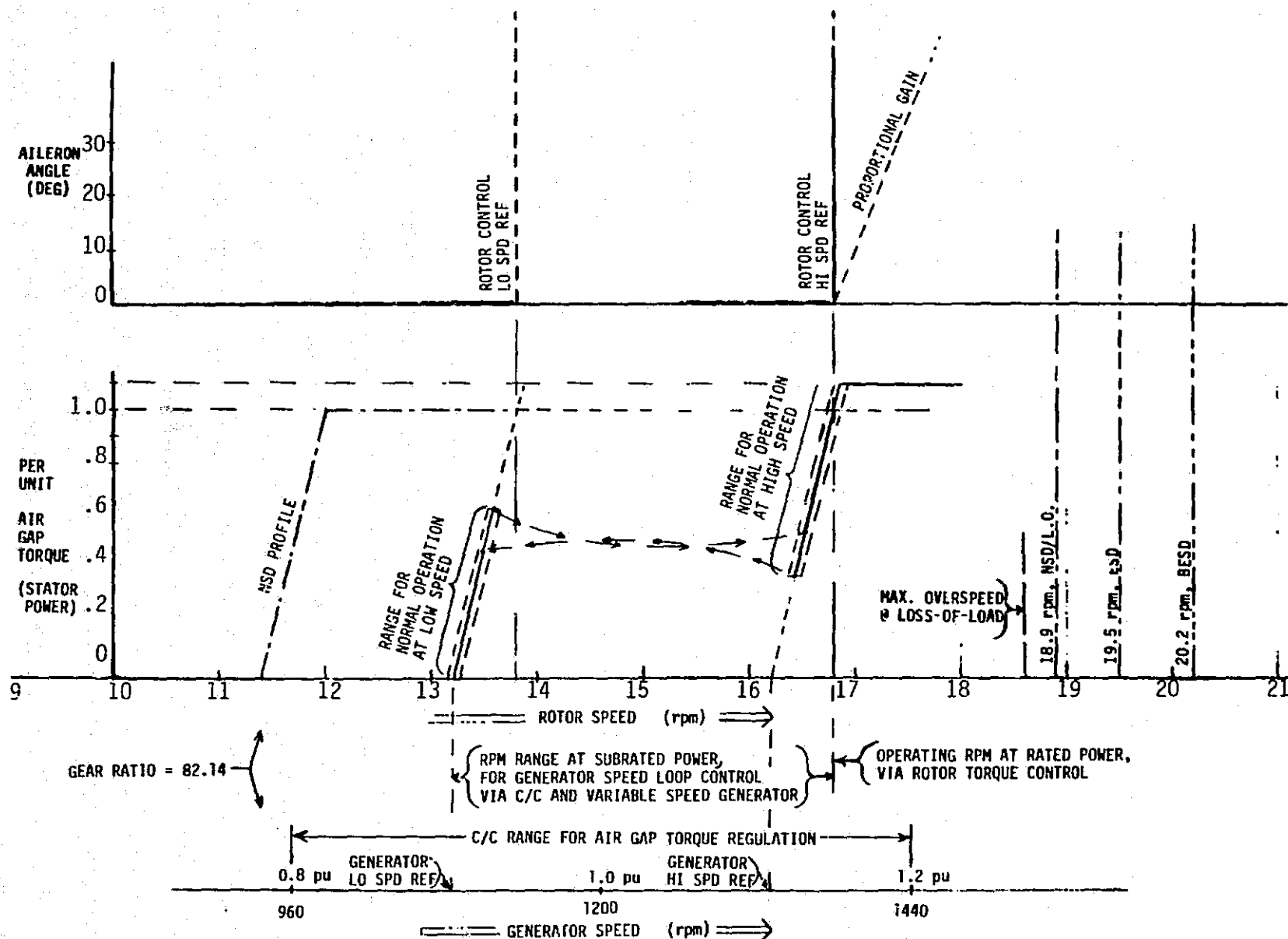


Figure 6-30 Power Generation Operation Regions

rotor speed at 16.8 rpm. As shown in Figure 6-30, the generator speed loop functions at 16.8 rpm, but a generator air gap torque limit of 1.1 per unit is imposed if wind gusts result in a transient rotor speed greater than 16.9 rpm. Negligible interaction between the two-speed control loops is due to a wide difference in bandwidth. The rotor speed loop has a low bandwidth of 1 rad/sec and the generator speed loop has a wide bandwidth of 17 rad/sec. The frequency response characteristics are discussed in Section 6.5.2.1. The time response characteristics are discussed in Section 6.5.2.2.

6.5.2 CONTROL SYSTEM FREQUENCY AND TIME RESPONSE

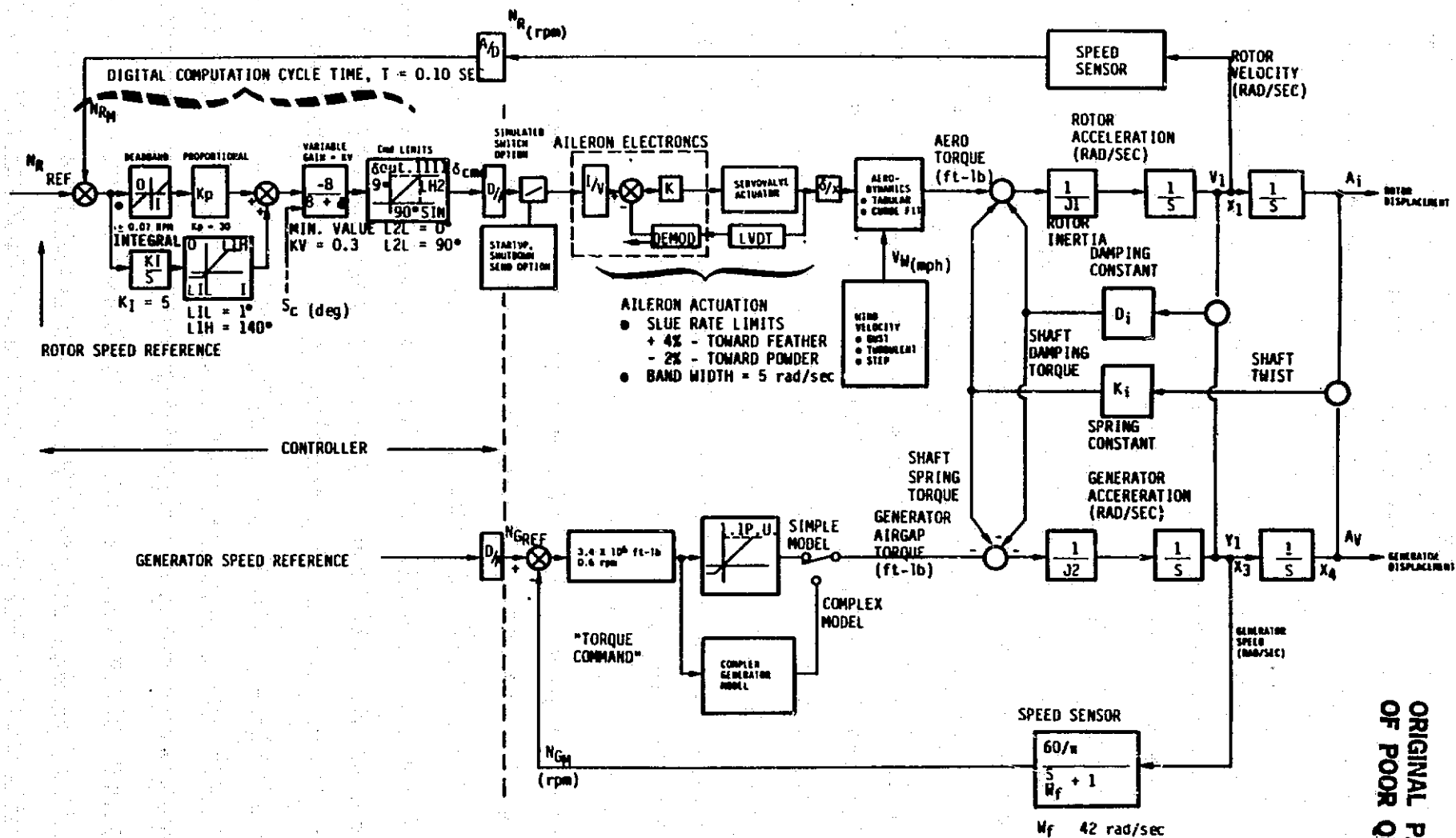
The model definition and response characteristics for frequency response, and time response of the control system are discussed in this section. A simplified mathematical model of the rotational dynamics of the rotor speed and generator speed control loops is shown on Figure 6-31. The translational dynamics for tower bending and blade flap motions were included in the control simulations, but are not shown in the figure. The mass property values used for the analysis and simulation of Model 304.2 are listed in Table 6-11.

6.5.2.1 Frequency Response

The frequency response characteristics of the rotor speed and generator speed control loops were analyzed as non-interacting control loops. A linearized mathematical model is shown in Figure 6-32.

The rotor speed control loop controls the rotor speed during ramp-up, power generation at wind speeds above 32 mph, and shutdown. This loop is functional, but effectively inactive during subrated power generation with the ailerons in the maximum power positions. In this condition, the generator air gap torque is regulated by the converter to control the generator speed. A detailed definition of the hardware and software associated with this control loop is given in the Control Systems Specification. The gain/phase characteristic of a linearized analog representation with an ideal speed sensor and no computational delays is given in Figure 6-33.

The variable gain term, $K_v = \frac{-8}{8 + \delta}$, is a programmed adaptive gain that was



ORIGINAL PAGE IS
OF POOR QUALITY

Figure 6-31 Control System Rotational Dynamics

Table 6-11 Model 304.2 Control System Parameter Definition

J1 = Rotor Inertia	$40 * 10^6 \text{ slug-ft}^2$
J2 = Generator and High Speed Shaft Inertia (Reflected to Rotor)	$(745+30)(82.14)^2 = 5.2*10^6 \text{ slug-ft}^2$
J3 = Tower Mass	$2.9 * 10^4 \text{ slug}$
J4 = Blade Flap Mass	$1.06 * 10^3 \text{ slug}$
K1 = Drivetrain Spring Constant Gearbox and Shaft (Reflected to Rotor)	$3.38 * 10^8 \text{ ft-lb/rad}$
K2 = Tower Spring Constant	$1.674 * 10^5 \text{ lbs/ft}$
K3 = Blade Flap Spring Constant	$3.370 * 10^4 \text{ lbs/ft}$
D1 = Drivetrain Damping Coefficient Gearbox and Shaft (Reflected to Rotor)	$3.0 * 10^6 \text{ ft-lb/(rad/sec)}$
D2 = Tower Damping Coefficient	6968 lb/(ft/sec)
D3 = Blade Flap Damping Coefficient	3785 lb/(ft/sec)

$$W_1 = \sqrt{\frac{K1}{J1}} = 2.9 \text{ rad/sec}$$

$$W_2 = \sqrt{\frac{K1}{J2}} = 8.1 \text{ rad/sec}$$

$$W = \sqrt{\frac{K1(J1 + J2)}{J1, J2}} = 8.6 \text{ rad/sec}$$

$$\xi_1 = \frac{D_1}{2J_1 W_1} = 0.013$$

$$\xi_2 = \frac{D_1}{2J_2 W_2} = 0.036$$

$$\xi = \frac{D_1(J_1+J_2)}{2J_1 J_2 W} = 0.038$$

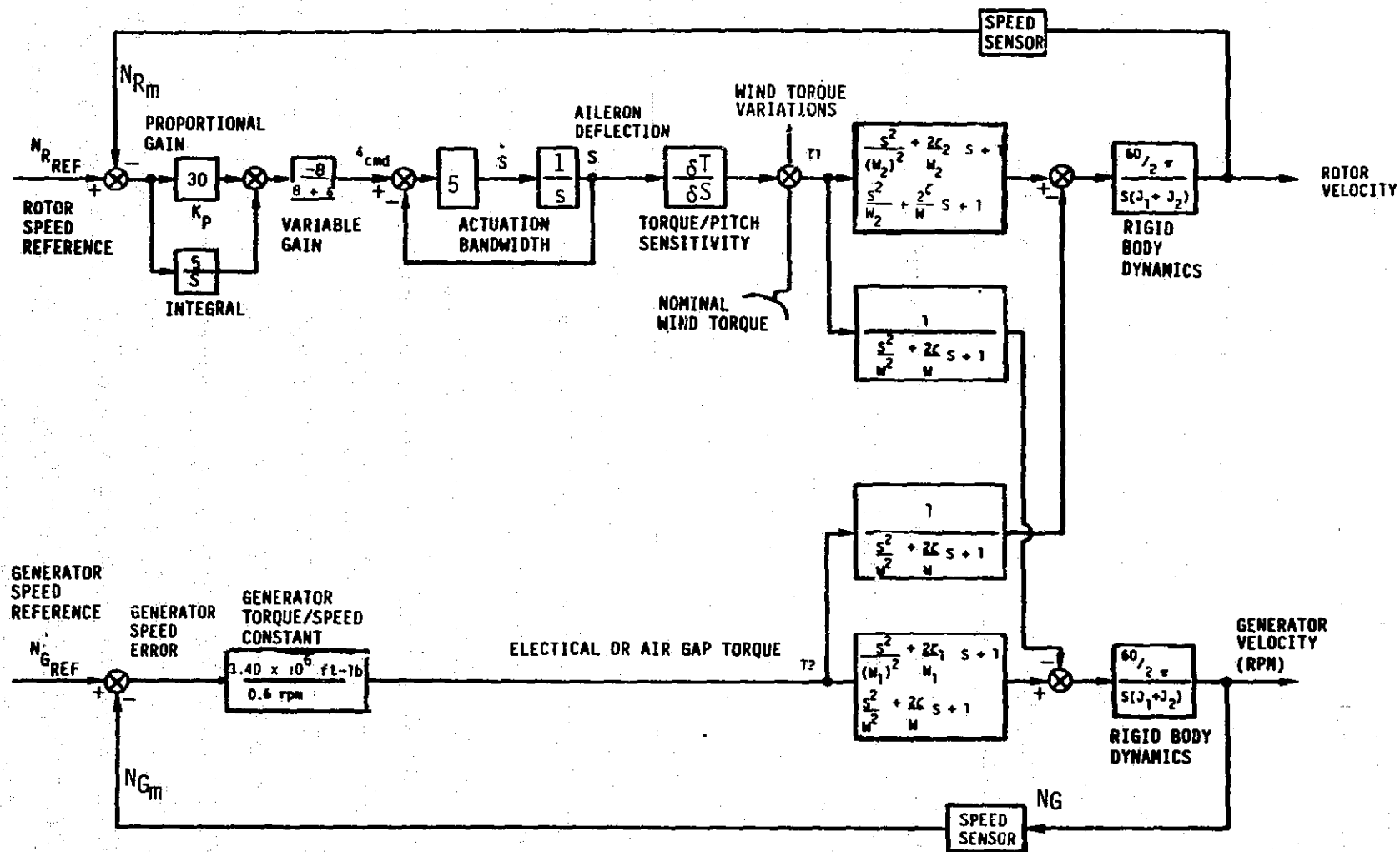


Figure 6-32 Linear Model of Speed Control Loops

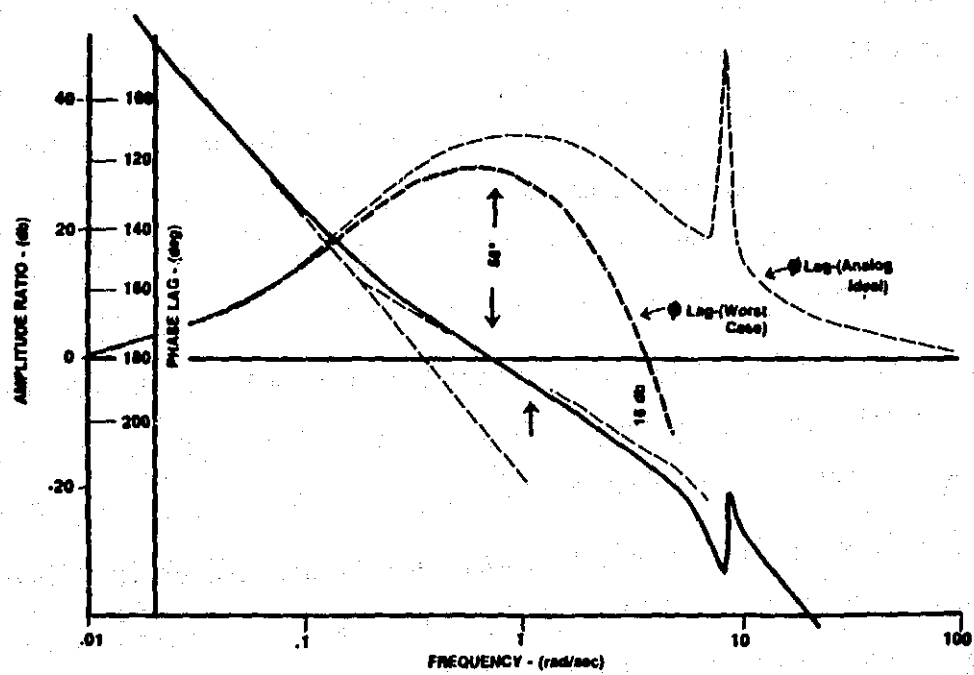


Figure 6-33 Open Loop Gain/Phase Characteristics of Rotor Speed Loop

selected to yield a product of K_V and aerodynamic gain, $\partial T / \partial \delta$, which remains relatively constant for average wind speeds greater than 32 mph, as shown in the following table:

V_{wind} (mph)	δ_{trim} ($^{\circ}$)	K_V (unitless)	$\frac{\partial T}{\partial \delta}$ (ft-lb/ $^{\circ}$)	$K_V * \frac{\partial T}{\partial \delta}$ (ft-lb/ $^{\circ}$)
32	0	-1	-0.06×10^6	$.06 \times 10^6$
35	7.3	-.52	-0.21×10^6	$.11 \times 10^6$
40	10.8	-.43	-0.24×10^6	$.10 \times 10^6$
50	15.0	-.35	-0.31×10^6	$.11 \times 10^6$
60	21.0	-.30	-0.29×10^6	$.09 \times 10^6$

The K_V term is limited to a minimum absolute value of 0.3 when aileron deflections are large, because of start-up and shutdown considerations. The phase lag characteristics for the "analog ideal" case, as shown in Figure 6-33, are used to establish a bounding condition for comparison with actual hardware characteristics. A block diagram that is more representative of the hardware and that shows system time delays is given in Figure 6-34. The gain curve for this case is the same as shown for the ideal analog case, but there is a significant increase in phase lag, which limits the bandwidth. The contributions to this phase lag are:

- (1) a 100 msec computation cycle time between updates of the aileron command signals,
- (2) a 50 msec rotor speed sensor delay for data accumulation and averaging computation,
- (3) a 0 to 80 msec rotor speed sensor output delay, because of an 80 msec output cycle that is not synchronized with the analog to digital conversion cycle rate,
- (4) a 10 msec delay while the analog speed input is converted to a digital signal,
- (5) a 0 to 50 msec delay of the digital value available at the start of the controller's computation, since the conversion cycle and the controller's computation cycle are not synchronized. The speed signal is an input to two channels of the analog to digital converter, so that updates can be obtained at every 50 msec rather than every 100 msec,

ORIGINAL PAGE IS
OF POOR QUALITY

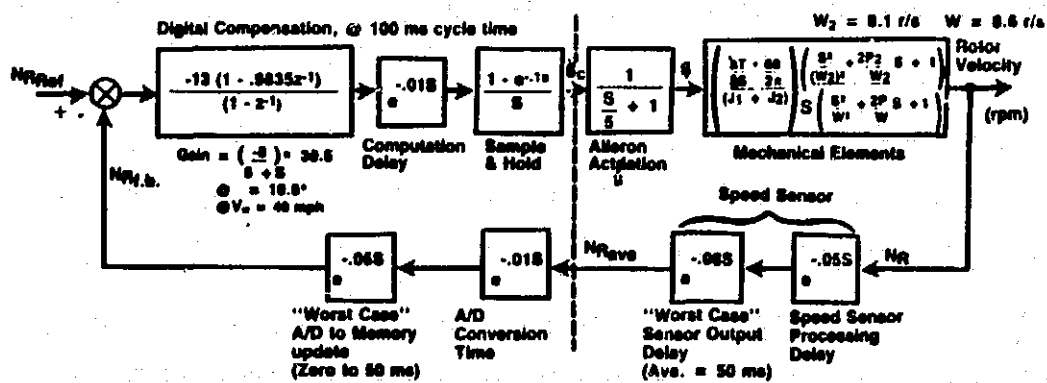


Figure 6-34 Rotor Speed Loop Hardware Implementation Representation

- (6) 10 msec, the computation time in the controller for aileron command generation and output.

The phase lag for the combination of these conditions that yields the worst case is shown in Figure 6-33. The gain and phase margins for this case are approximately 16 db and 58° , respectively. This loop should be stable, even if the system parameters vary significantly. The bandwidth of this rotor speed control loop is approximately 1 rad/sec. Time response simulations show that this value is adequate for this high inertia system in normal operation and loss of load conditions. Limiting this bandwidth results in a decrease in the amplitude of the tower oscillation, which is an advantage. Large tower oscillations require a stronger tower, as discussed in section 6.6.

The frequency response of the generator speed control loop was represented by the simplified mathematical model shown in Figure 6-35. The model is a linearized LaPlace representation, with the rotor side of the gearbox as the reference. The gear ratio is 82.14:1. The open loop gain/phase characteristic of this loop is shown in Figure 6-36. The bandwidth of the loop is approximately 20 times that of the rotor speed loop, minimizing loop interaction when the loops are functioning simultaneously, during wind speeds above 32 mph. Also, only proportional control is used in the generator speed loop, whereas proportional and integral control are used in the rotor speed loop control. As shown, this control loop was closed by analog circuitry that is not part of the digital controller, since stability would be greatly reduced by the additional phase lag resulting from the controller's computation cycle time. An unacceptable 50° of extra phase lag would occur at the bandwidth frequency when the cycle time is 100 msec. The "break frequencies" for the converter and generator speed sensor are shown at the minimum expected values. An adequate gain and phase margin should be assured for the generator speed control loop, even for significant variability in the system parameters.

6.5.2.2 Time Response

The control system time response characteristics during power generation are shown in Figures 6-37 through 6-38 for the Model 304.2 wind turbine generator. The characteristics of these five cases are given on Table 6-12.

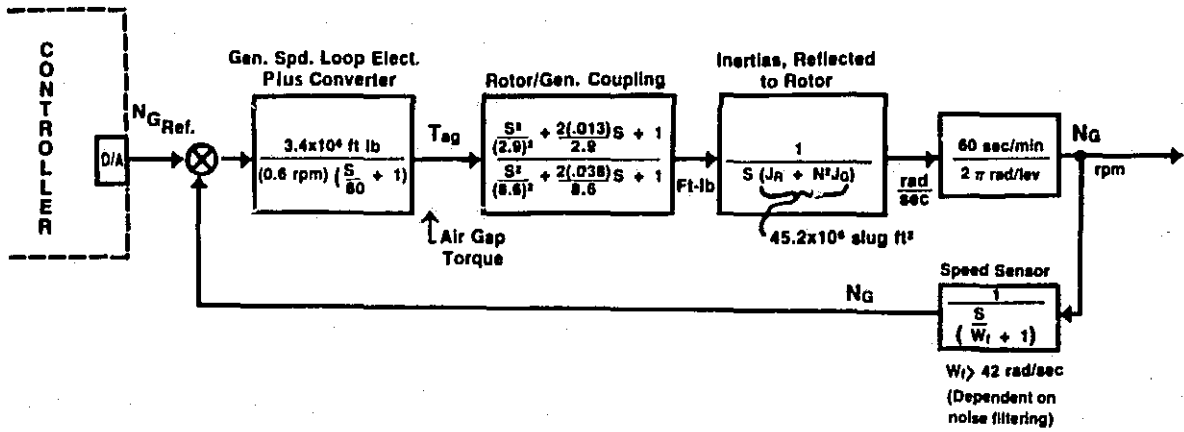


Figure 6-35 Generator Speed Loop LaPlace Representation

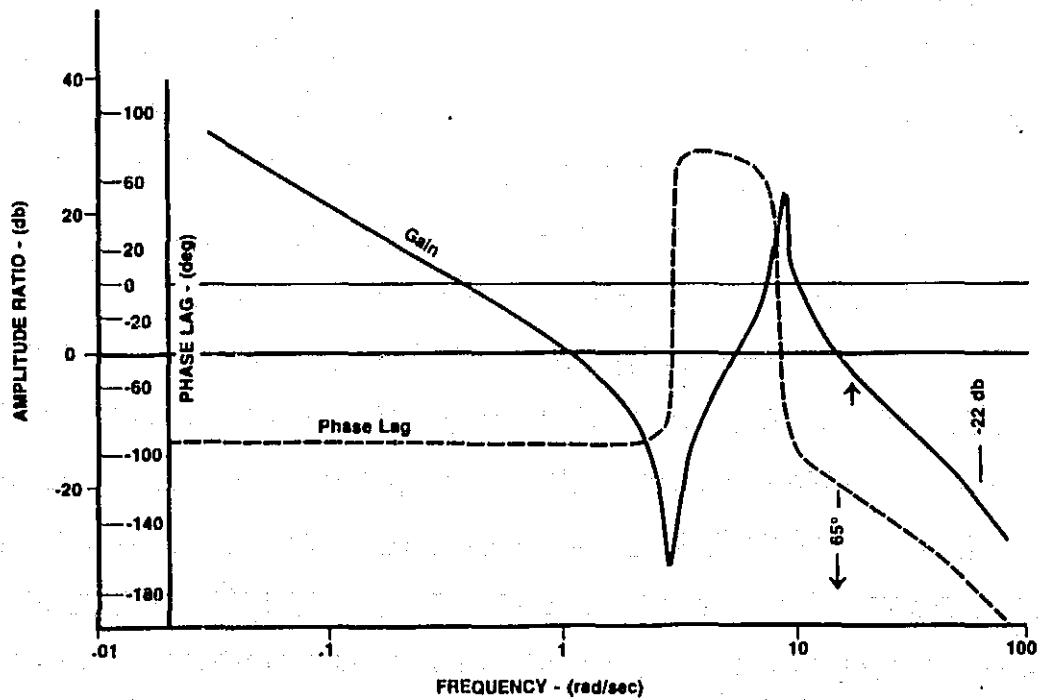


Figure 6-36 Time Response for Step Wind Change at $V_W = 45$ mph

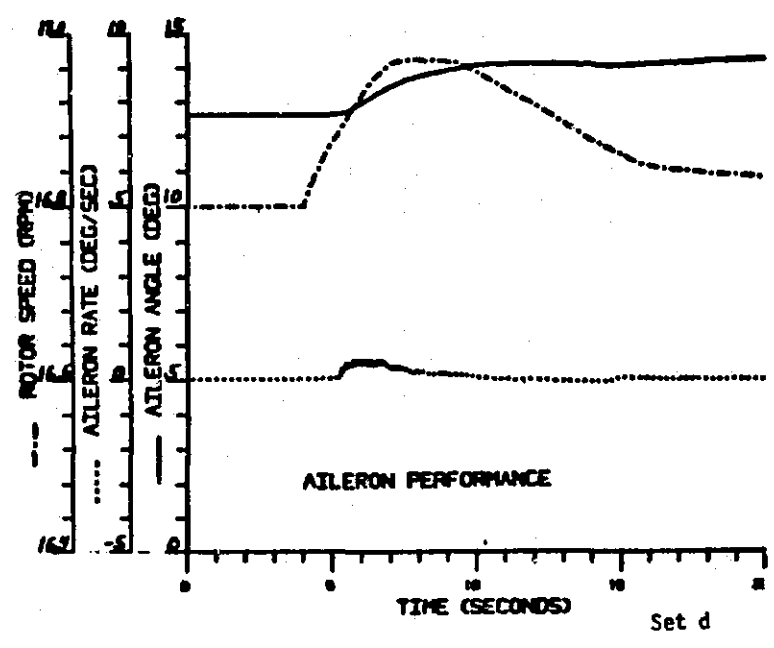
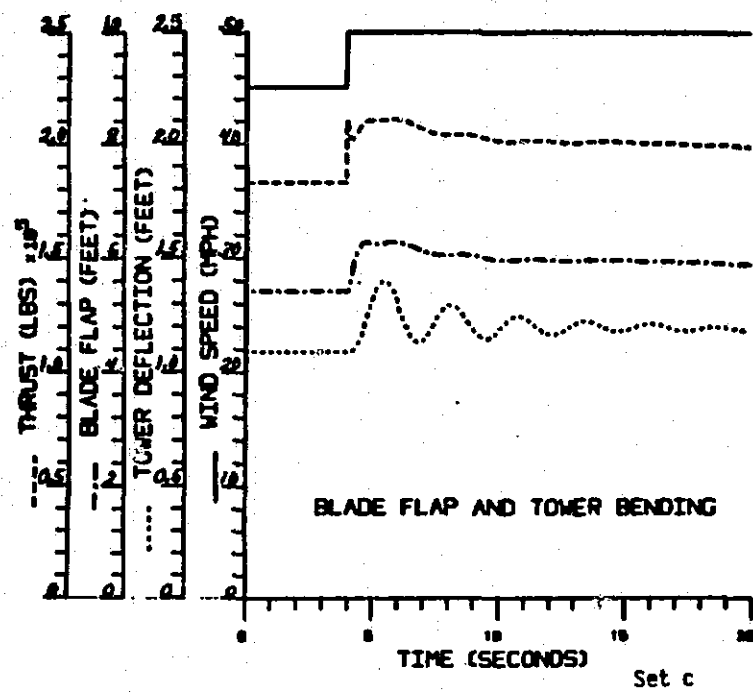
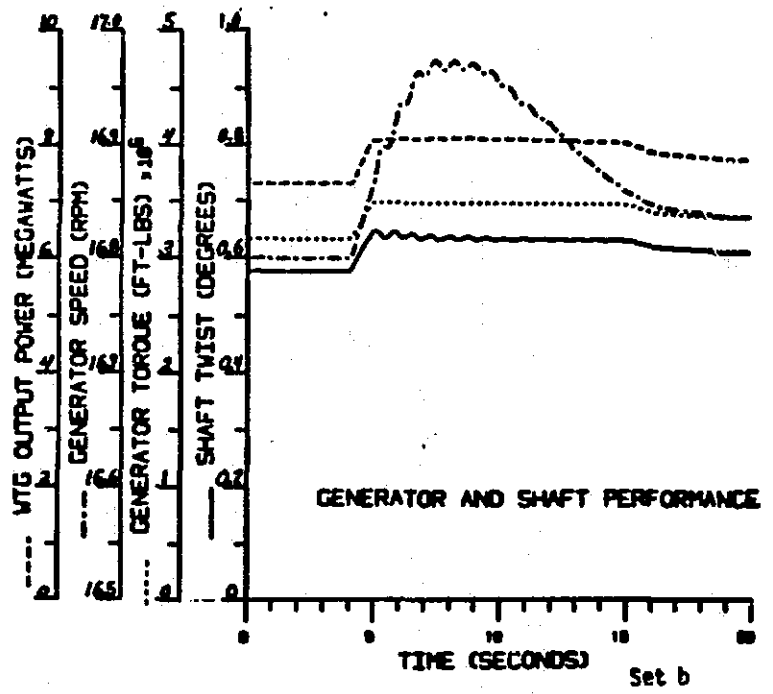
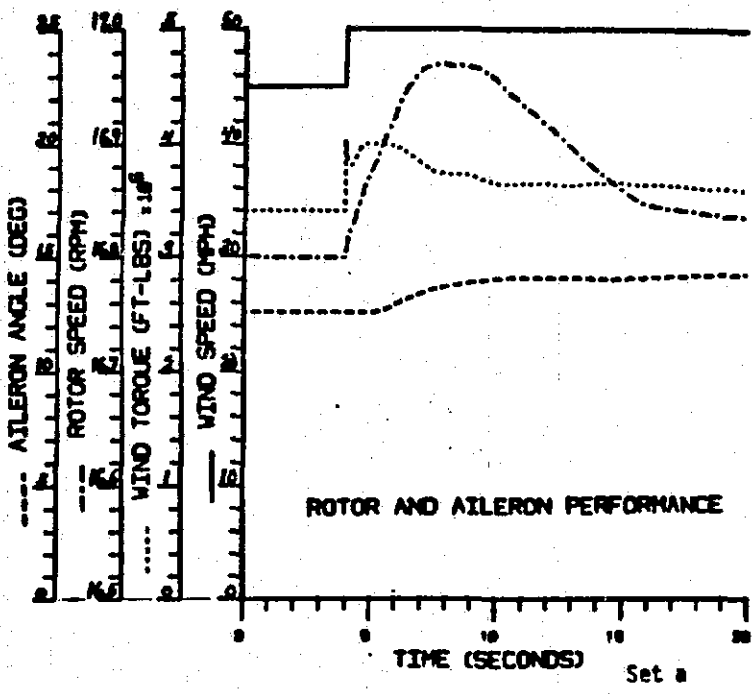
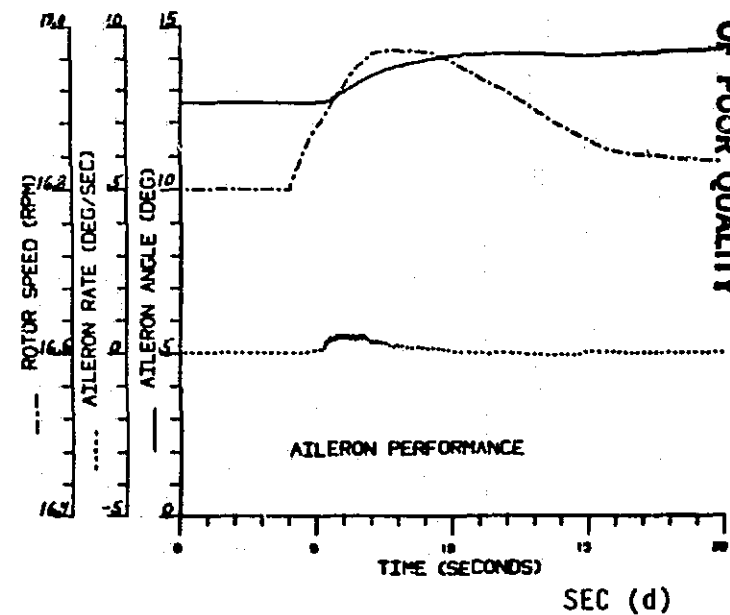
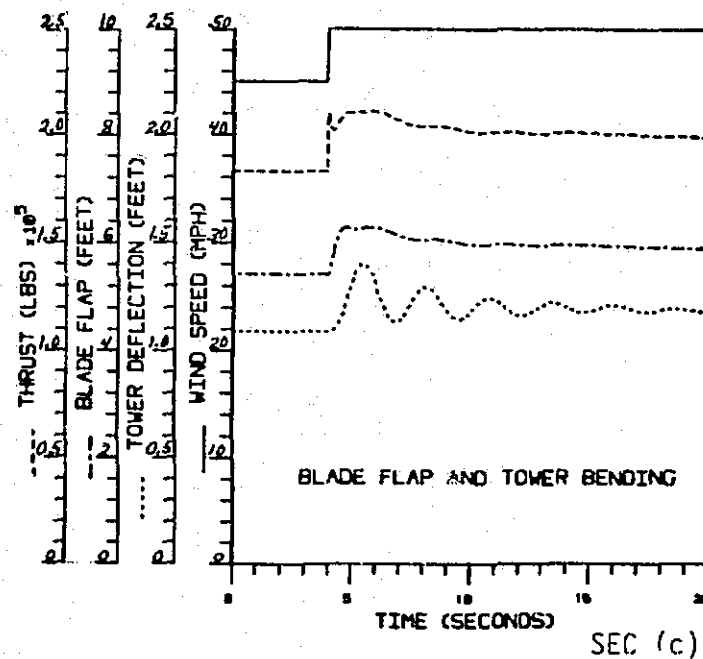
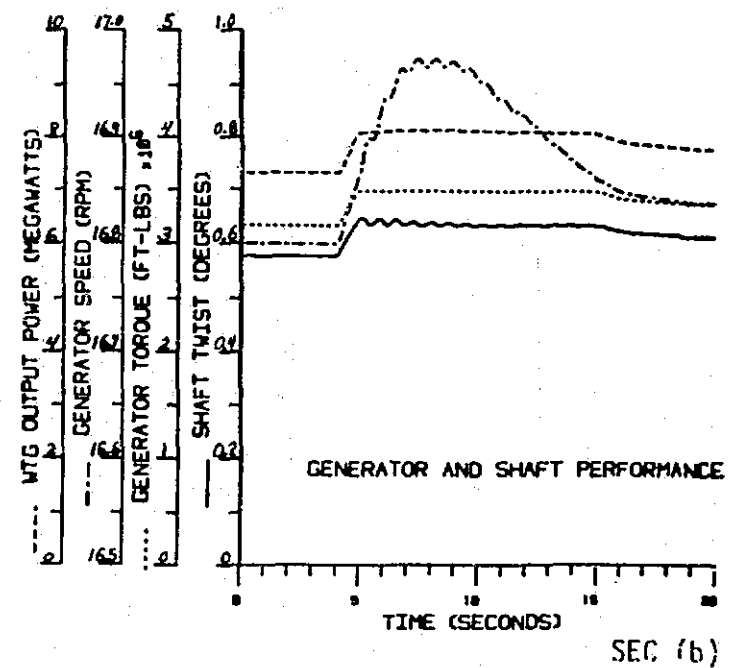
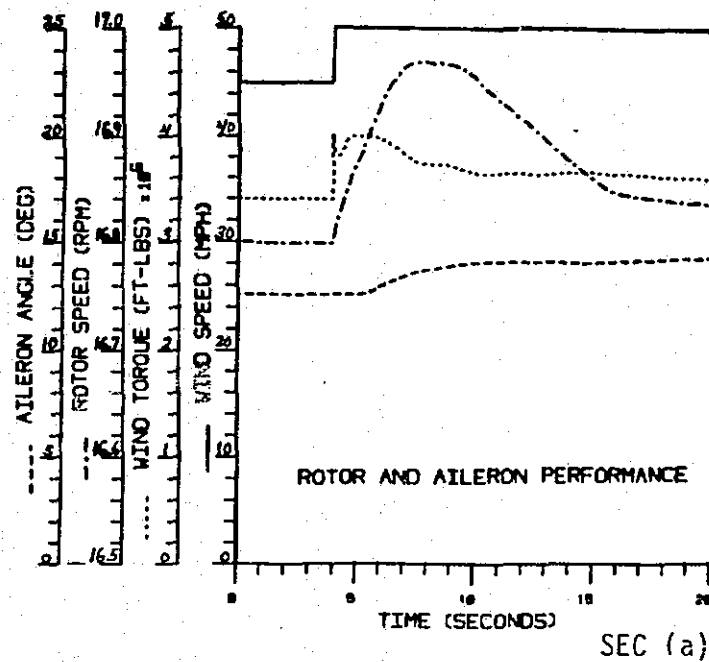


Figure 6-37 Time Response For Step Wind Change at $V_W = 45$ mph



ORIGINAL PAGE IS
OF POOR QUALITY

Figure 6-38 Time Response for Wind Gust at $V_w = 32$ mph

Table 6-12 Time Response Simulation Run Listing

CASE #	FIGURE #	WIND VELOCITY (MPH)	WIND-GUST (1-COS) AMP, DURATION	WIND TURBULENCE	COMMENTS
1	6.5-10	45	-	-	System response for a 5 mph step wind change
2	6.5-11	32	+20%/12 sec	-	At rated conditions, with ailerons near their minimum gain position
3	6.5-12	45	+20%, 12 sec	-	At rated conditions, base runs for Case 4
4	6.5-13	45	-	IN	Worst case wind turbulence case (per turbulence model defined by NASA)
5	6.5-14	32	-	-	Shutdown at loss-of-load condition

Table 6-13 Time Response Plot Identification

<u>ITEM</u>	<u>COMMENT</u>
Set (a) Rotor and Aileron Performance	
1. Wind speed (mph)	Full rotor wind - steady, gust, turbulence
2. Wind torque (ft.-lb.)	From aerodynamic data table
3. Rotor speed (rpm)	Main rotor speed
4. Aileron angle ($^{\circ}$)	Rotor torque control position
Set (b) Generator and Shaft Performance	Values in rotor speed reference frame
1. Shaft twist ($^{\circ}$)	Deflection of gearbox and shaft in torsion
2. Generator torque (ft.-lb.)	Airgap reaction torque on generator
3. Generator speed (rpm)	Generator rotor speed
4. Output power (MW)	Based on generator torque and speed losses
Set (c) Blade Flap and Tower Bending	
1. Wind Speed (mph)	Same as set (a)-1
2. Tower Deflection (ft.)	Nacelle translation caused by thrust on tower
3. Blade Flap (ft.)	Tip deflection from first elastic blade mode
4. Thrust (lbs.)	From aerodynamic data table
Set (d) Aileron Performance	
1. Aileron angle ($^{\circ}$)	Same as set (a)-4
2. Aileron rate ($^{\circ}/\text{sec}$)	Determined by controller with +5, -2 $^{\circ}/\text{sec}$ limits
3. Rotor speed (rpm)	Same as set (a)-1

The cases are a representative sample selected from the many conditions examined during the design of the control system. A description of the plot values and arrangement is given in Table 6-13.

The wind step responses illustrated by case 1 are well behaved. The rotor speed control loop and generator speed control loop stop acceleration in 3 seconds and reduce the speed error to less than the proportional "deadband" value in 12 seconds. The tower motion is acceptable and is not excited by control action. The generator air gap torque is limited to the designed transient 10% overload condition without any objectionable oscillations.

The response to a severe wind gust during normal wind conditions is shown by case 2. Response amplitudes are larger than the step response amplitudes observed in case 1 because the simulated wind disturbance was larger. The system speed has a typical overshoot-undershoot pattern caused by the gust shape and time. Initial rotor control action reduces the torque-producing acceleration. This action continues as long as the rotor speed exceeds the reference value, with the result that the rotor speed falls below the reference value. This is because of the lag in the control response and the return of the wind to initial conditions. All response characteristics are acceptable.

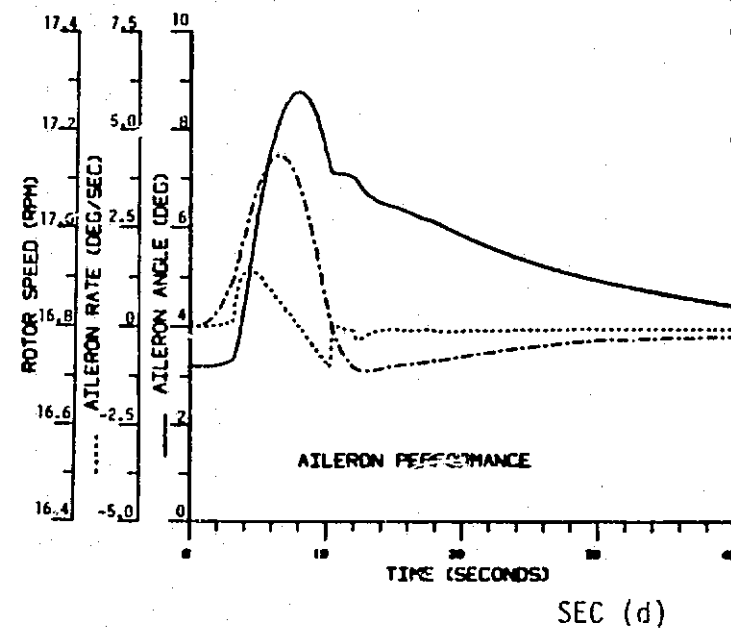
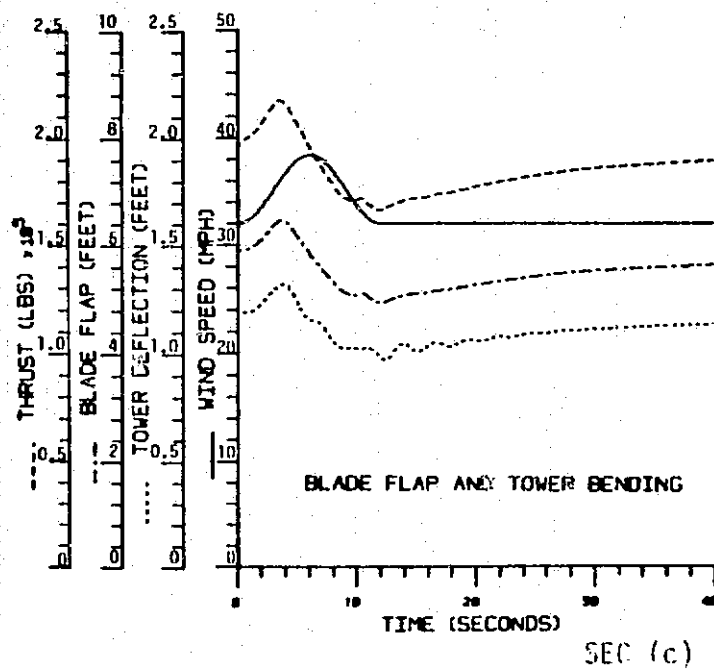
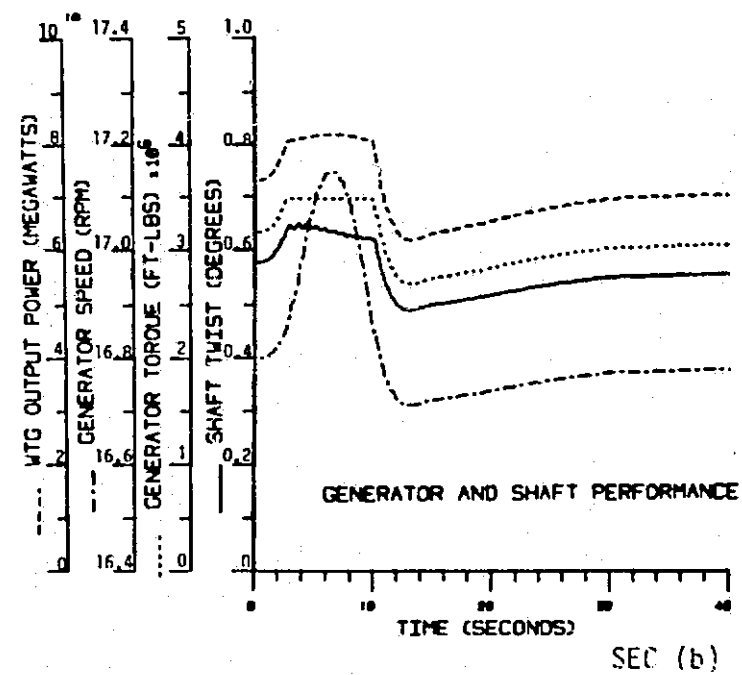
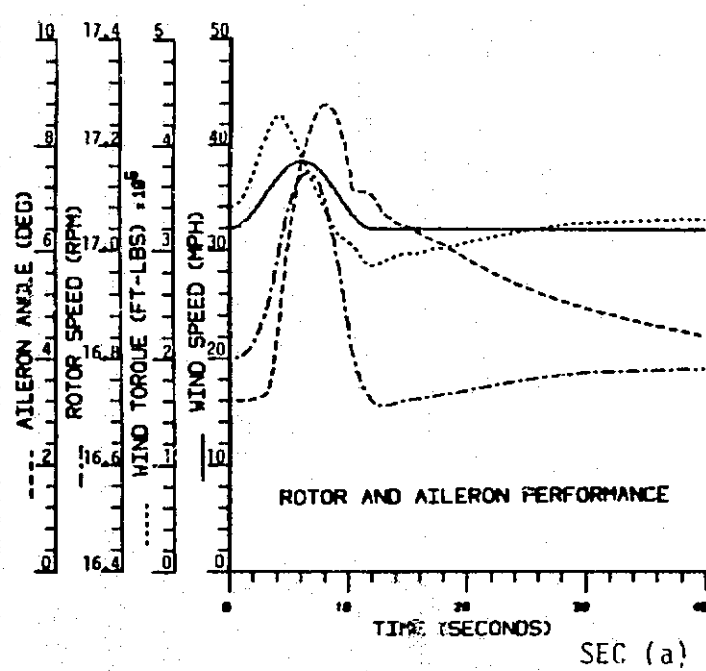
The result of a severe wind gust during operation at high wind speeds is illustrated by case 3. The response characteristics are similar to those observed in case 2, but the aileron deflection is less, because of the variable gain term in the controller. Speed fluctuations are slightly greater than in case 2, but are acceptable.

A turbulent wind excitation was added to the conditions of case 3 to obtain case 4. This excitation simulates the torque fluctuations that would be experienced by a two-bladed rotor through the addition of a series of harmonic fluctuations to the steady wind and smooth gust. The aileron position responds to this fluctuation when the speed error exceeds the deadband imposed on the proportional control. This oscillation would not be acceptable during

steady operation and the satisfactory operation of the deadband is shown at the start and end of the aileron rate and angle curves.

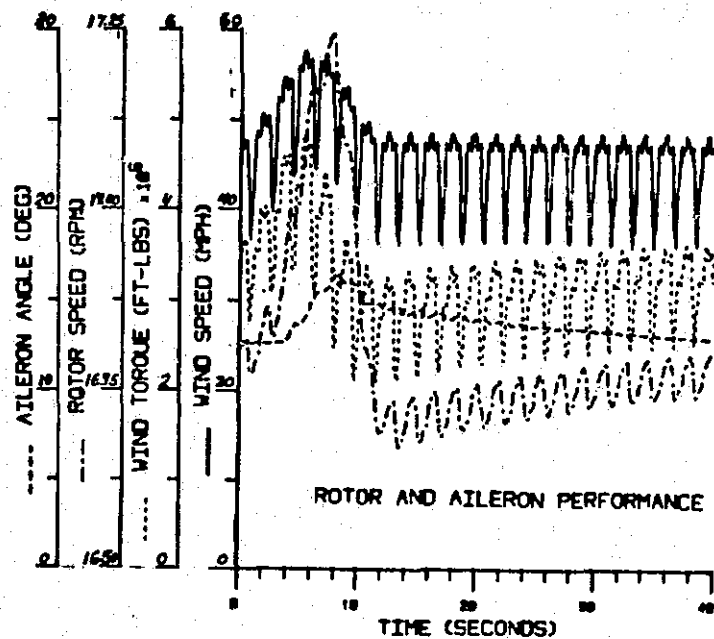
A loss of load condition is illustrated by case 5. This condition would occur rarely, but the system must be protected from it. The load is lost if the protective switch gear for the generator or utility operates. The sudden unbalanced torque accelerates the rotor at a rate that causes the maximum aileron control speed, 5° /second. The limiting rate is a simulated value, to reflect the flow rate limits of the aileron control valves. The response motions of this case are large, but within acceptable limits. The maximum rotor speed does not reach the overspeed trip point and the normal rotor speed control action is satisfactory. The sudden unloading of the drivetrain produces a lightly damped oscillation of the generator inertia, but the amplitudes are not too large.

The speed control time response results were acceptable for all the conditions that were analyzed. These results confirm the acceptable small signal characteristic results of the frequency analysis.

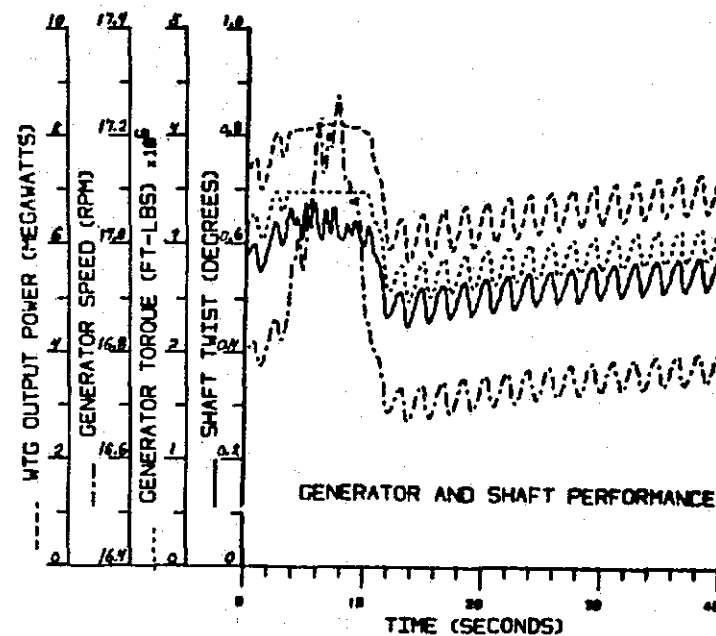


ORIGINAL PAGE IS
OF POOR QUALITY

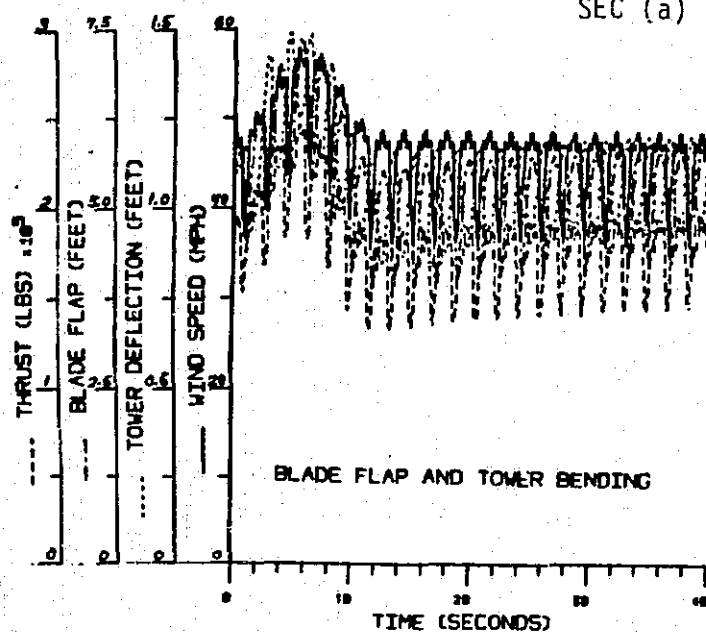
Figure 6-39 Time Response for Wind Gust at $V_w = 45$ mph



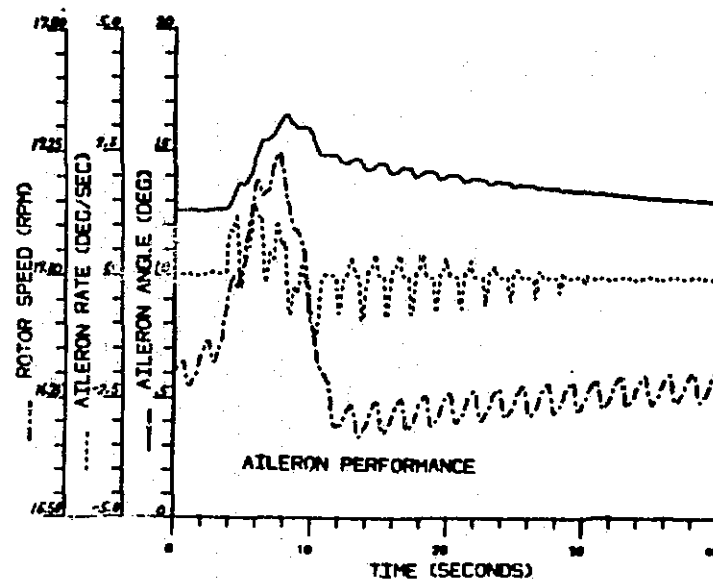
SEC (a)



SEC (b)



SEC (c)



SEC (d)

Figure 6-40 Time Response for Wind Gust, Plus Turbulence
6-77

ORIGINAL PAGE IS
OF POOR QUALITY

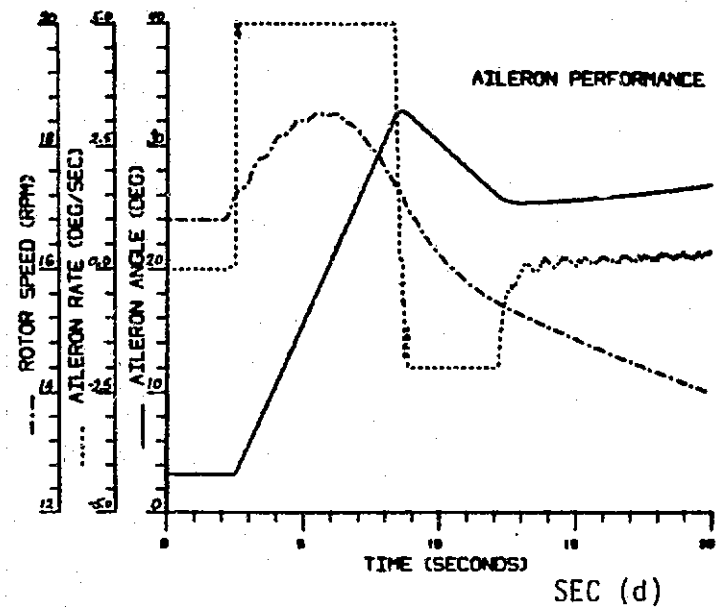
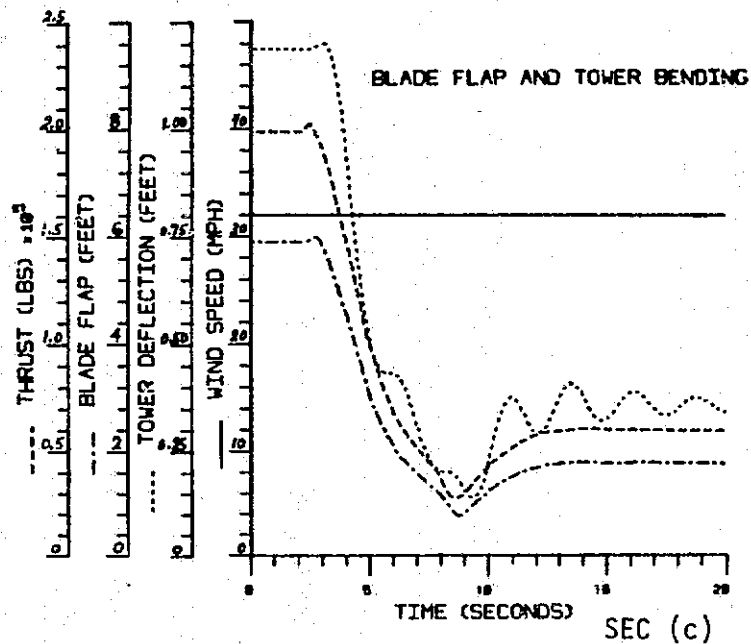
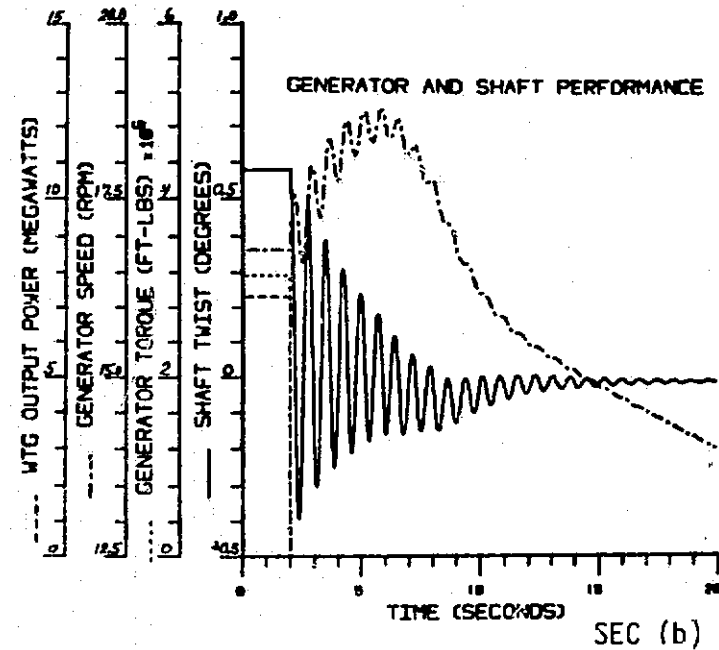
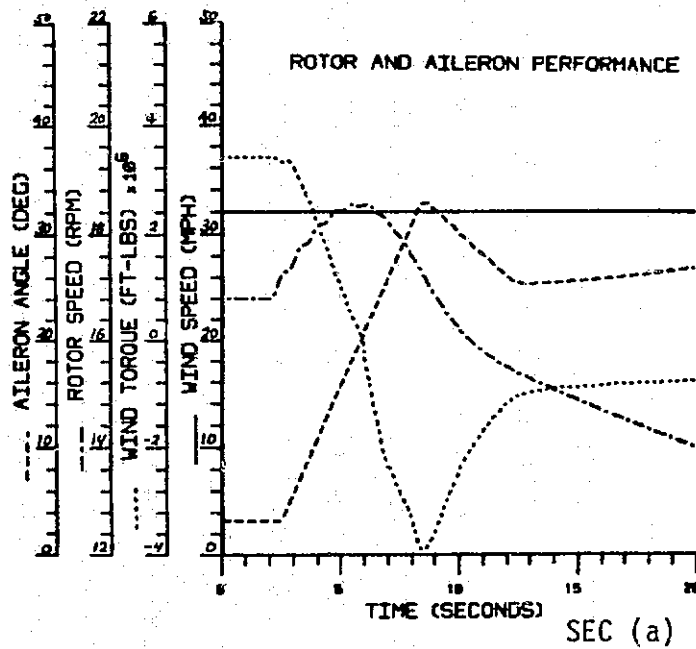


Figure 6-41 Time Response for Loss-of-Load Shutdown

6.6 STRUCTURE/CONTROL SYSTEM INTERACTION

6.6.1 BACKGROUND

The effect of the control system on structural responses was studied because of problems encountered in the MOD-2 system. The MOD-2's problem originated in the form of large alternating rotor torques caused by a lack of drivetrain damping. To remedy this problem, damping was added to the drivetrain by adding rotor speed error feedback to the control loop. This remedy resulted in larger tower responses. It was necessary for GE's computer codes to predict these problems, so that they would be avoided on the MOD-5A machine.

6.6.2 SENSITIVITY STUDIES WITH TIP CONTROLLED WTG

GE developed the Transient Rotor Analysis Code (TRAC) to investigate the coupling of the structure and control systems on the MOD-5A wind turbine. To verify that TRAC could predict these interactions, the TRAC predictions were correlated with Boeing's MOD-2 test data. Since the mode shapes of the MOD-2 substructures were not readily available, the physical properties of the MOD-2 were scaled to the size of the MOD-5A and used with the MOD-5A mode shapes. Table 6-14 contains the MOD-2 model parameters, both unscaled and scaled to a 400-ft. rotor diameter. The last two columns list the MOD-5A parameters used in the analysis, and a comparison by ratio of the MOD-2 and MOD-5A. The most important numbers to note are:

1.) Drivetrain Damping

- The MOD-2 has no significant passive damping in its control system, while MOD-5A has 22% of critical passive damping.

2.) Tower Frequency

- The MOD-2 scaled tower frequency is lower than the MOD-5A tower frequency, so it required a lower control system bandwidth to avoid interaction.

3.) Rate Gain

- The MOD-2 rate gain is nearly 10 times the MOD-5A rate gain.

Table 6-14 Significant Model Parameters

	PARAMETER	SCALE* FACTOR	MOD-2	SCALED MOD-2	MOD-5A	RATIO SCALED MOD-2 MOD-5A
GEOMETRY	R XPSC CHORD	L 1.0 L	150'	200'	200'	1.0
			.7	.7	.75	
			X = 0 C = 11.3	X = 0 C = 15.1	X = 0 C = 16.67	
			.3 11.3 .75 7.07 1.0 4.71	.3 15.1 .75 9.42 1.0 6.28	.25 16.67 .75 9.61 1.0 6.08	.98
DYNAMIC	FREQUENCY DAMPING INERTIA STIFFNESS	L ⁻¹ 1.0 L ⁵ L ³	.14 Hz / .48P	.105 Hz / .48P	.15 Hz / .54P	.77/.89
			.02	.02	.22	.09
			21.5E6 lb-sec ² -ft	90.6E6 lb-sec ² -ft	57.E6 lb-sec ² -ft	1.59
			16.7E6 ft-lb/rad	39.6E6 ft-lb/rad	50.E6 ft-lb/rad	.79
TOWER	FREQUENCY DAMPING MACELLE WT.	L ⁻¹ 1.0 L ³	.368 Hz / 1.26P	.275 Hz / 1.26P	.38 Hz / 1.27P	.72
			.02	.02	.02	1.0
			175.6 K-lb	416 K-lb	378 K-lb	1.10
ROTOR	FREQUENCY DAMPING (STR) RPM V _{TIP} WEIGHT	L ⁻¹ 1.0 L ⁻¹ 1.0 L ³	.963 Hz / 3.3P	.72 Hz / 3.3P	.58 Hz / 1.93P	1.24 / 1.71
			.03	.03	.075	.40
			17.5	13.1	17.9	.73
			275 fps 180 K-lb	275 fps 426 K-lb	375 fps 300 K-lb	.73 1.42
CONTROL	PROD. GAIN	L ⁻²	7.5 deg/MW	4.22 deg/MW	.5 deg/MW	8.44
	RATE GAIN	L	3533 deg/Rad S	4711 deg/Rad S	500 deg/Rad S	9.42
	INTEGRAL GAIN	L ⁻³	1.0 deg/MW S	.422 deg/MW S	.32 deg/MW S	1.32
	PITCH SERVO, T	L	.667s	.889s	.1s	8.89
	POWER SENSOR, T	L	-	-	.1s	"
	RATED POWER	L ²	2500 KW	4444 KW	7300 KW	.61

* L = Length Mod-5A = 1.33
Length Mod-2

4.) Pitch Servo Time Constant

- The MOD-2 time constant is nearly 9 times the MOD-5A time constant, which produces a 57° phase lag in pitch input at the natural frequency of the tower, compared to a 13° lag on the MOD-5A.

Figure 6-42 is a schematic of the MOD-5A control system at the time of this study. Two changes were made for the MOD-2 simulation. Since a time constant for the MOD-2 power sensor was not available, the power sensor loop in the upper left corner was bypassed. Also, the MOD-2 has no deadband in rate feedback, so the $\Delta\Omega$ switch tolerance (.008 for MOD-5A) was set equal to 0. Note that the MOD-2 control loop added a tower frequency notch filter, to avoid large tower motions. This filter was not used in this analysis.

The effect of the differences between the MOD-2 and MOD-5A control systems is exemplified in Figures 6-43a and b. These two runs were for identical conditions of 30 mph wind, 4,444 kW power set point, 0° inflow and an initial tip angle of 2° toward feather. The tip angle of the MOD-5A is very stable, with excursions of less than .05° after 40 seconds, while the tip angle on the scaled MOD-2 system varied by $\pm 12^\circ$. Similar observations were made on the tower acceleration response and hub torques, which are shown in Figures 6-44a and b.

Integral, proportional, and rotor speed gains, and the pitch servo time constants were all varied between the MOD-2 and MOD-5A baseline values to determine the effect of each on system responses. Varying the integral and proportional gains within the range of baseline values had little effect on the results. Variations in the rotor speed gain and the pitch servo time constant, however, had significant effects. The effects of these two variables are shown in Figure 6-45a and b. Tower g's varied nearly linearly with rate gain, while servo constant had little affect. The alternating tip angle varied linearly with rate gain, with the smaller MOD-5A servo time constant giving about half the excursions of the larger MOD-2 servo time constant.

Note that the effective servo loop gain depends on both the rate gain and the time constant. That is,

$$\text{Effective gain} = \text{rate gain} / (1 + T\omega)$$

$$\text{Rate gain} = 4711$$

$$\begin{array}{l} \text{Effective gain} \\ \text{at } \omega_{\text{tower}} \end{array} = (4711) (.394) = 1856 \text{ (T = .89), MOD-2}$$

$$\begin{array}{l} \text{Effective gain} \\ \text{at } \omega_{\text{tower}} \end{array} = (4711) (.853) = 4018 \text{ (T = .1), MOD-5A}$$

Thus, if Figure 6-45 were plotted against the effective loop gain (at the tower's natural frequency), the system with the higher time constant would appear much worse, as it should, because of the undesirable phase lag that is introduced.

The TRAC analysis with the scaled MOD-2 model parameters predicted qualitatively the interaction between the control system and the structure that Boeing experienced. The high rate gain is the main offender, with the pitch servo time constant a significant contributor. This high rate gain was needed on MOD-2 to provide damping to the drivetrain. However, drivetrain damping is obtained passively on the MOD-5A design.

The output tower g's, and other loads were not in close agreement with MOD-2 measurements. The reason for this was that the tower notch filter in the control system was not simulated.

The run using the MOD-5A control system parameters showed no unfavorable coupling between control system and structure, for two reasons. First, the passive drivetrain damping in the MOD-5A drivetrain allows a much smaller rate gain than in the MOD-2 design. Second, the MOD-5A tower is stiffer than the dynamically scaled MOD-2 tower.

6.6.3 APPLICABILITY TO CURRENT MOD-5A CONTROL SYSTEM DESIGN

All subsequent analyses on the MOD-5A with the updated control system models showed that the system is stable. In addition, a deadband was added to the

system before the pitch servo, to eliminate dither caused by small excitations from atmospheric turbulence.

There is another important difference between the current and the tip-controlled MOD-5A designs. The constant speed generator was replaced by a variable speed generator and cycloconverter. This substitution has no effect on the stability of the control system since the numerical value of damping (in the form of a controlled back torque) provided by the cycloconverter was designed to be better than that of the earlier design.

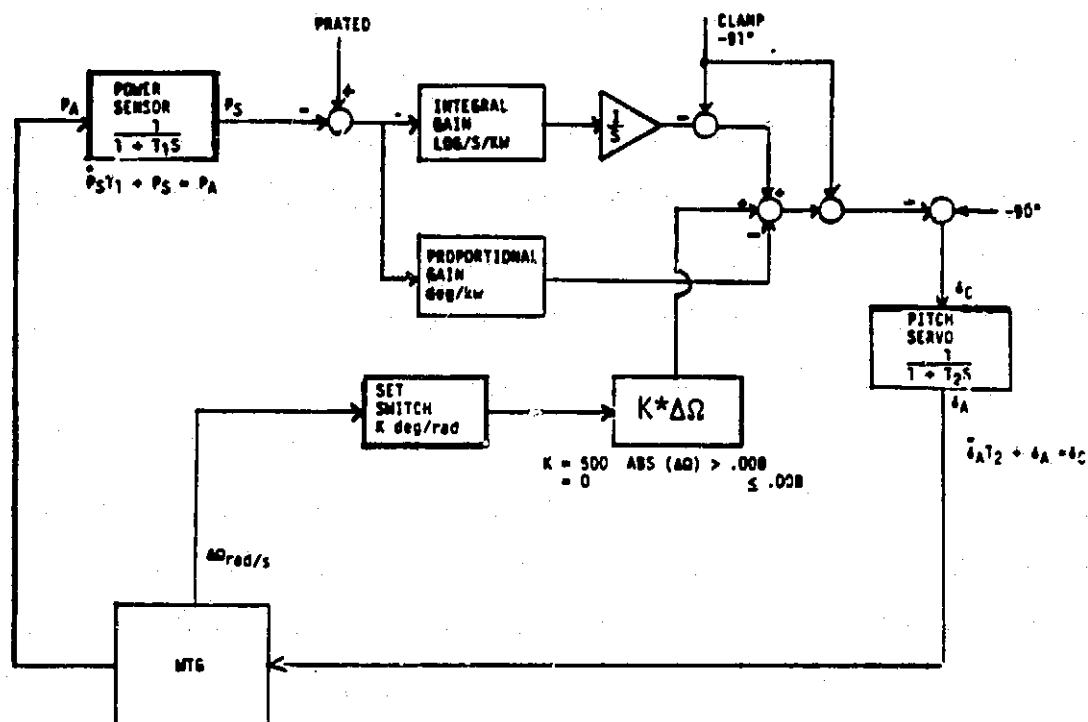


Figure 6-42 MOD-5A Control System Schematic

ORIGINAL PAGE IS
OF POOR QUALITY

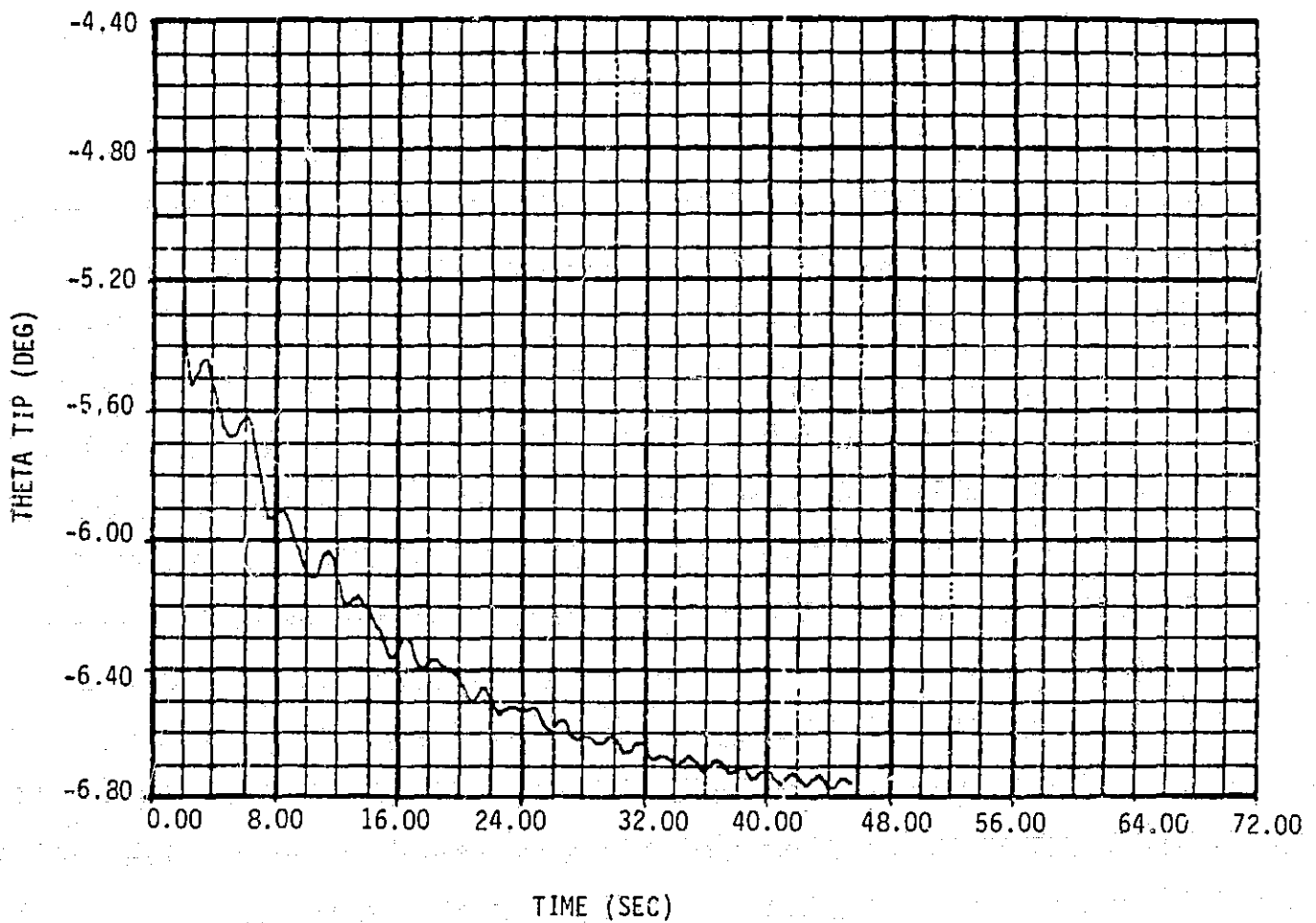


Figure 6-43a Tip Angle Response - GE Baseline

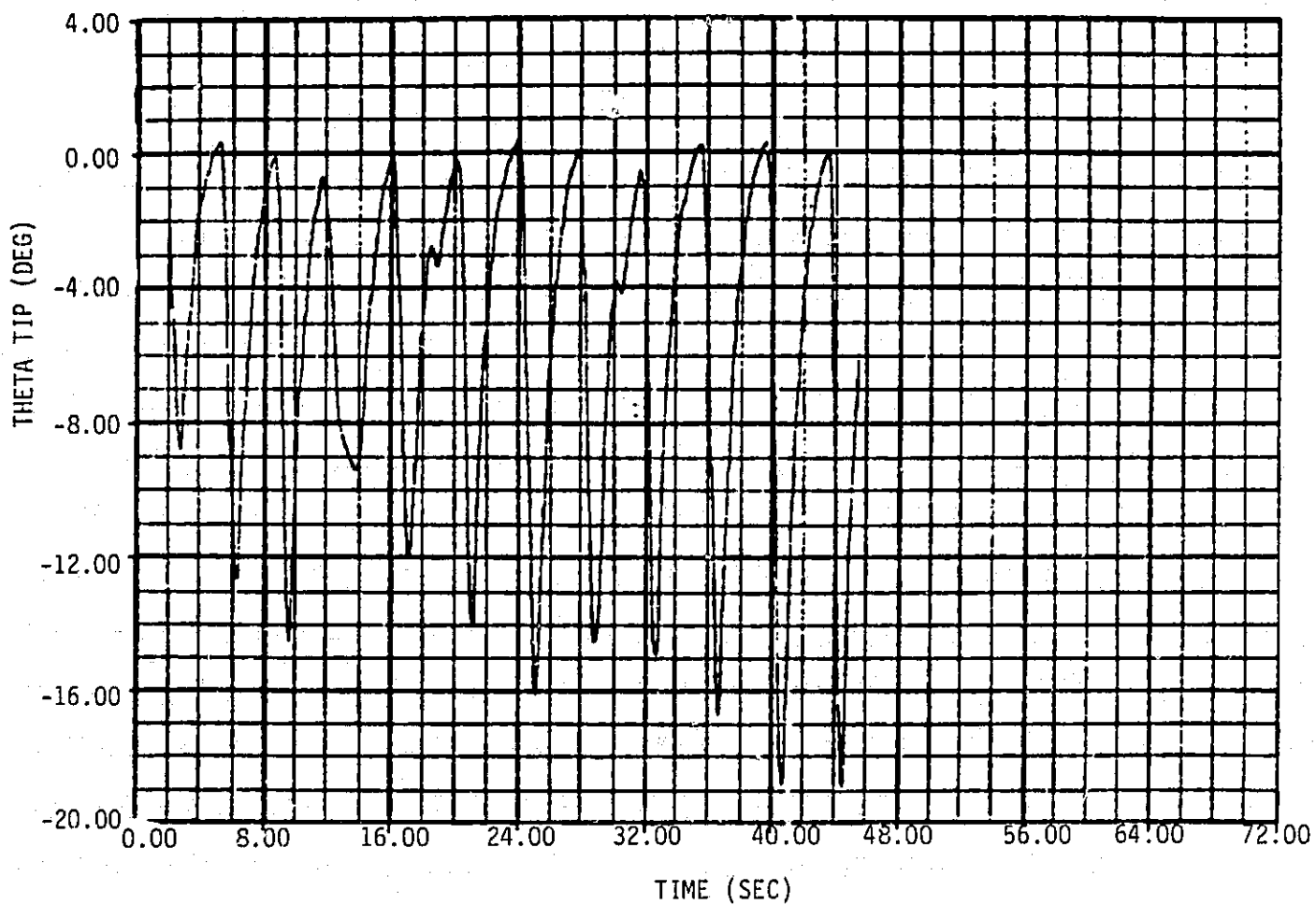


Figure 6-43b Tip Angle Response - Boeing Baseline

ORIGINAL PAGE IS
OF POOR QUALITY

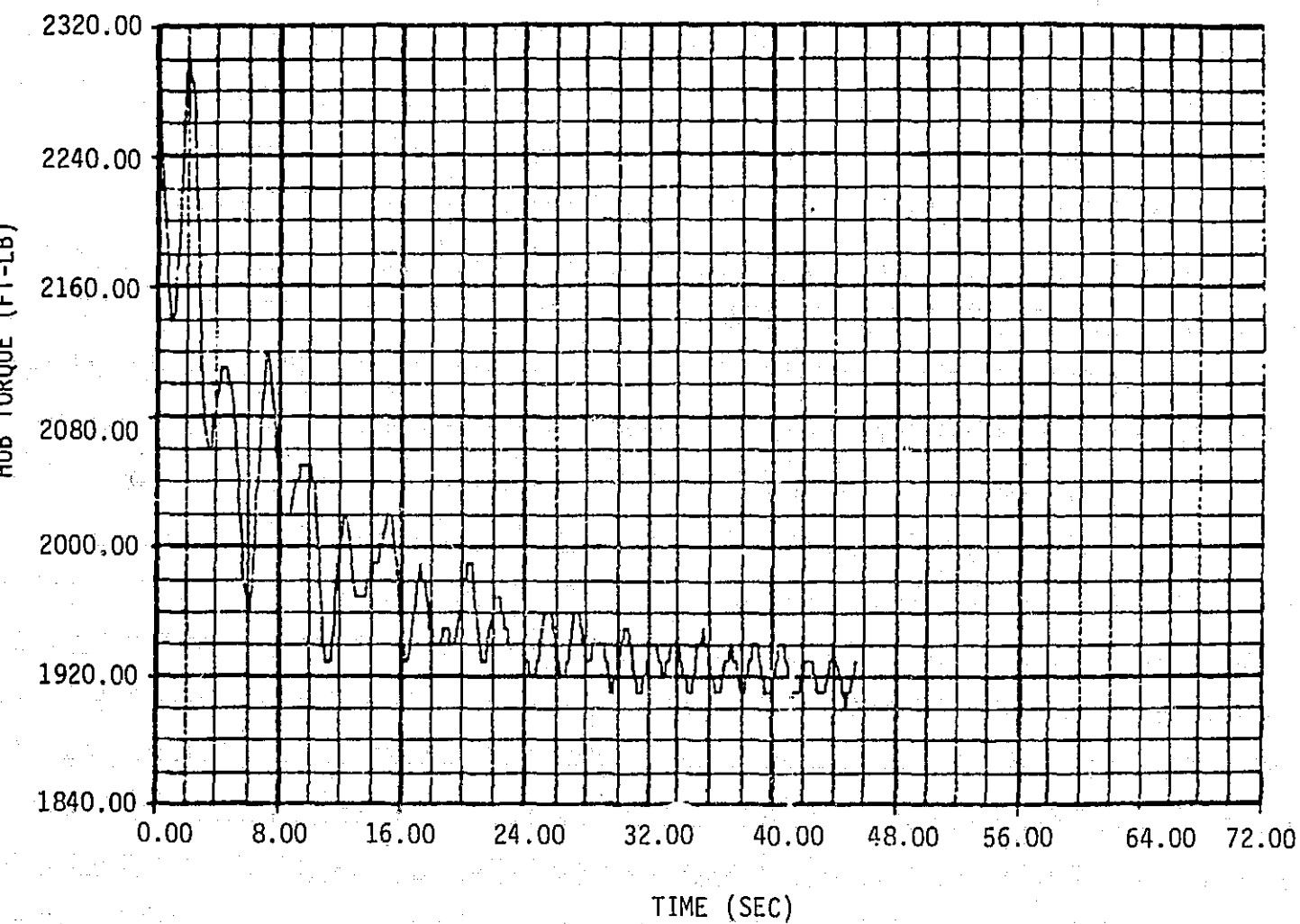


Figure 6-44a Hub Torque Response - GE Baseline

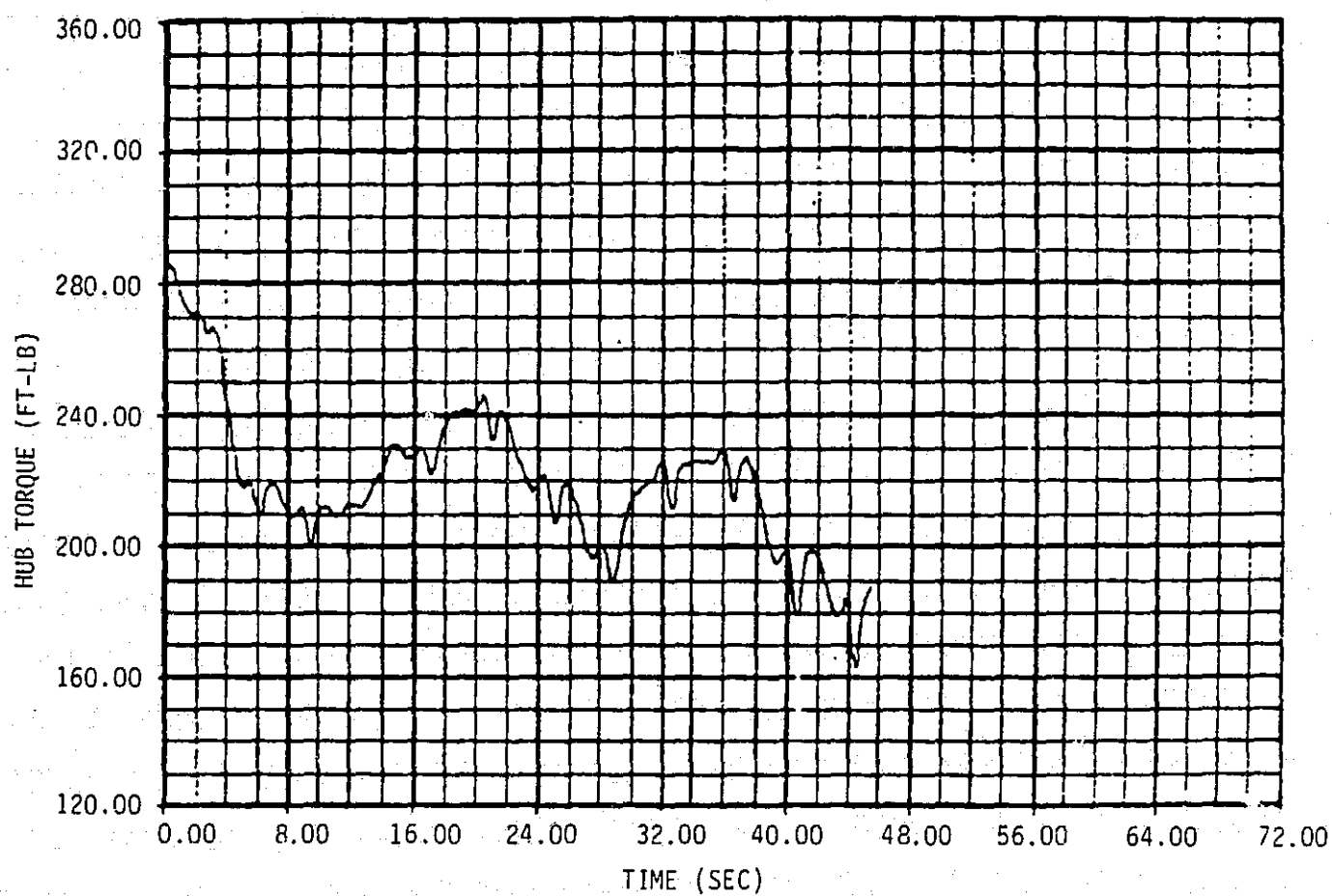


Figure 6-44b Hub Torque Response - Boeing Baseline

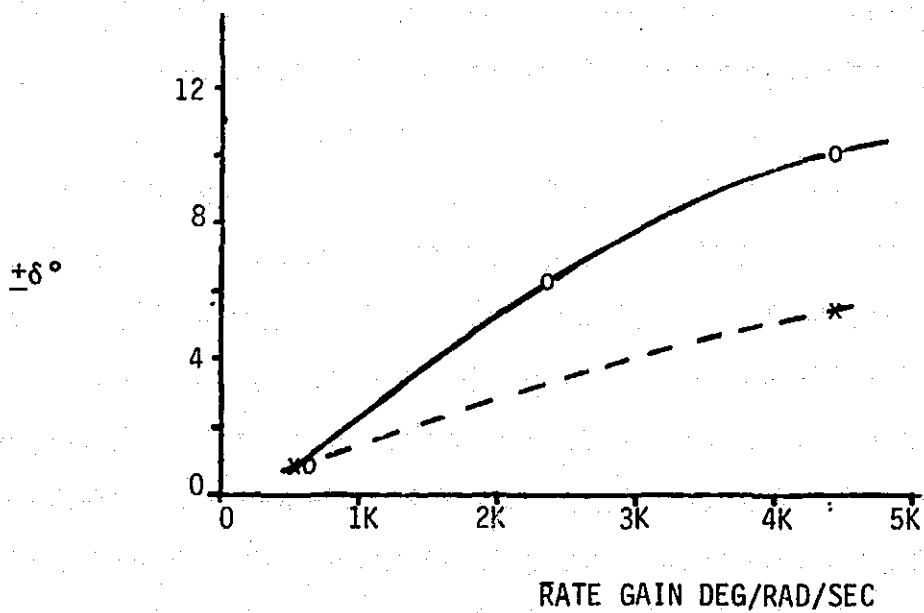
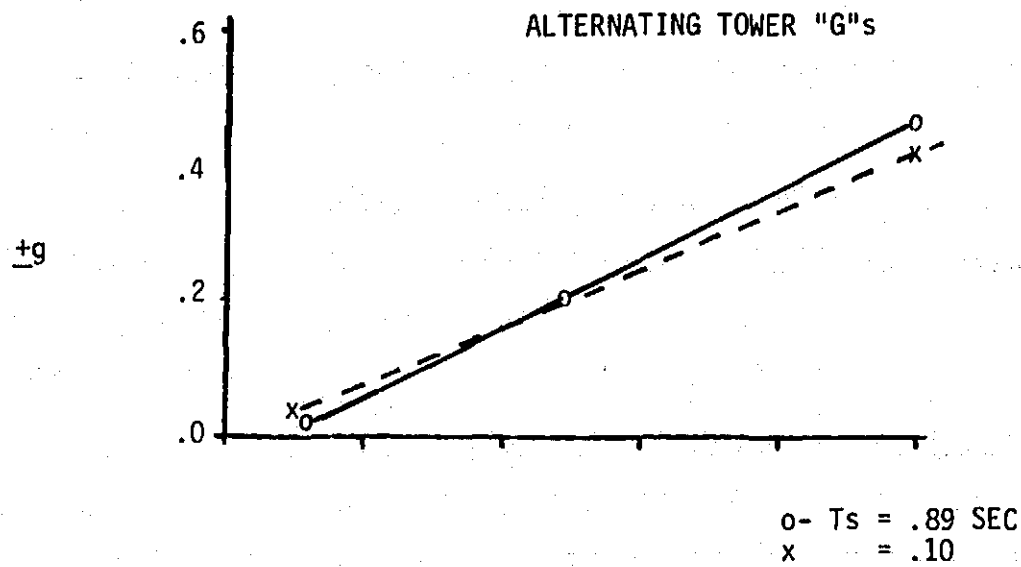


Figure 6-45 Effect of Rotor Speed Gain and Pitch Servo Time Constant on Response

References

- 6-1 MOD-1 Wind Turbine Generator Analysis and Design Report, Vol. 1, DOE/NASA/0058-79/2, NASA CR-159495, May 1979.
- 6-2 Kuhar, E.J., "Selected System Modes Using the Dynamic Transformation with Modal Synthesis", Shock and Vibration Bulletin, August 1974, pp. 91-102.
- 6-3 Yee, Suey T.; Change, Tse-Yung P.; Scavuzzo, R.J.; Timmerman, D.H.; Fenton, J.W.; "Vibration Characteristics of a Large Wind Turbine Tower on Non-rigid Foundations", NASA TMX 73670, May 1977.
- 6-4 Barkan, D.D. "Dynamics of Bases and Foundations", McGraw-Hill, 1962.
- 6-5 Loewy, R., "Review of Rotary-Wing V/STOL Dynamic and Aeroelastic Problems", Journal of the American Helicopter Society, July, 1969.

ORIGINAL PAGE IS
OF POOR QUALITY

7.0 SYSTEM LOADS ANALYSIS

7.0 SYSTEM LOADS ANALYSIS

7.1 INTRODUCTION

The objective of the system loads analysis was to determine design loads consistent with those that the MOD-5A will experience over its 30-year life. The analysis was also used to:

- (1) specify the system's dynamic properties, such as the teeter brake characteristics and yaw rate requirements,
- (2) determine the control system procedures and characteristics that minimize shutdown and normal operating loads,
- (3) verify the safe operation within the operating envelope.

The experience gained, and methods developed during the MOD-1 program served as a cornerstone for the MOD-5A analysis. Extensive correlation studies and code verification exercises were conducted before and during the MOD-5A program using test data drawn from the MOD-0, MOD-1 and MOD-2 wind turbines. GE's loads prediction capabilities were enhanced during the MOD-5A program, particularly in the areas of transient analysis, wind modelling and load statistics. These topics are discussed in Section 7.2. The final design loads are defined in sections 7.3 through 7.5.

7.2 METHODS OF ANALYSIS

7.2.1 AEROELASTIC CODES

Two aeroelastic codes were used to predict design loads for the MOD-5A: GETSS, General Electric Turbine System Synthesis and TRAC, Transient Rotor Analysis Code.

GETSS - GETSS was developed during the MOD-1 program and was used to predict the MOD-5A's fatigue loads during the preliminary design phase. The code was verified by NASA during the MOD-1 program, by correlating its predictions with MOD-0 test data. It provided excellent load estimates for MOD-1 and was verified against MOD-0 soft tower and teetering rotor configurations during the MOD-5A contract.

The GETSS analysis flow is shown in Figure 7-1. The system's structural dynamics are approximated by piecewise linear models of the entire system, in which natural modes are input for discrete rotor positions. As the blades

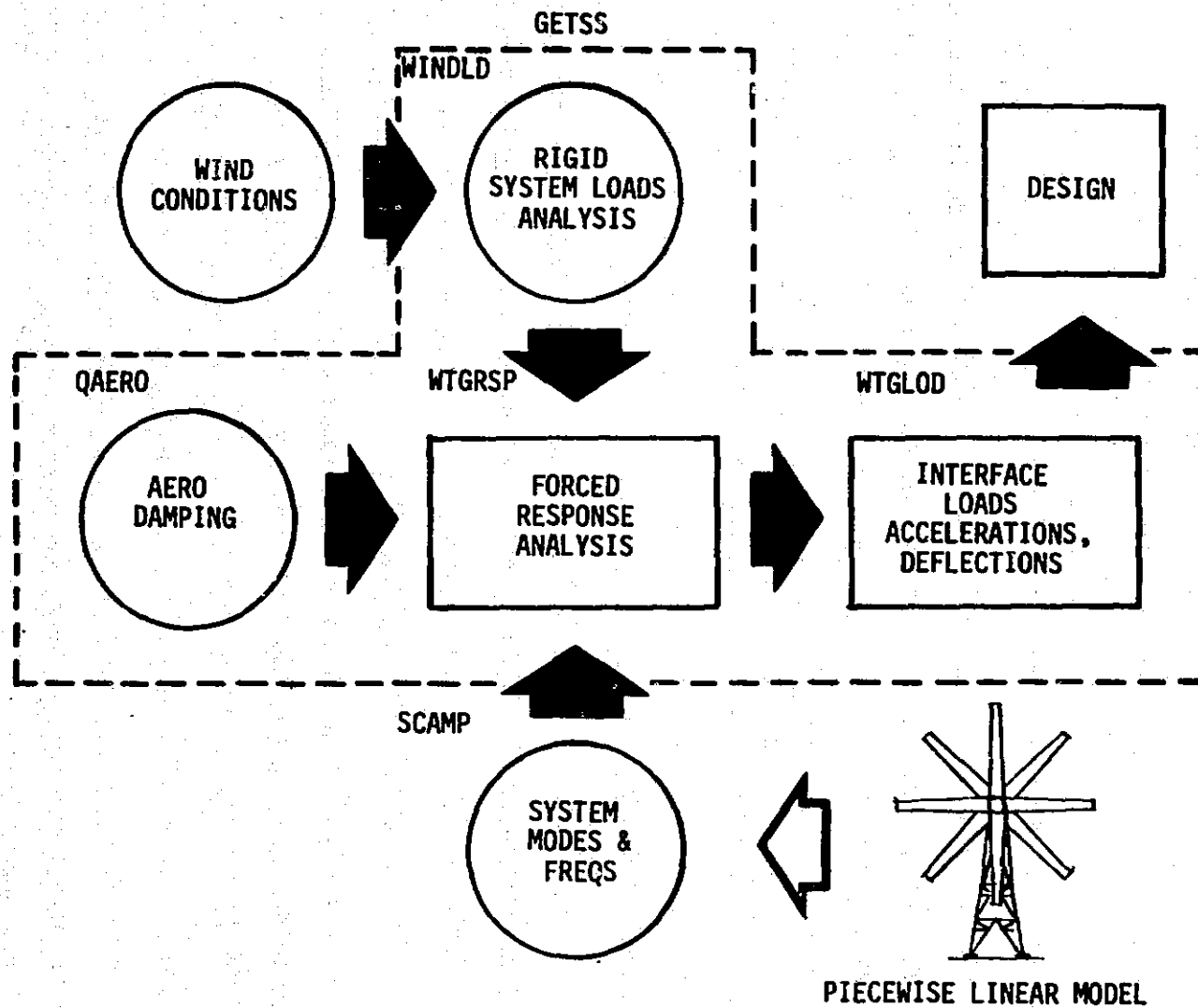


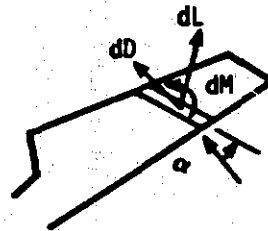
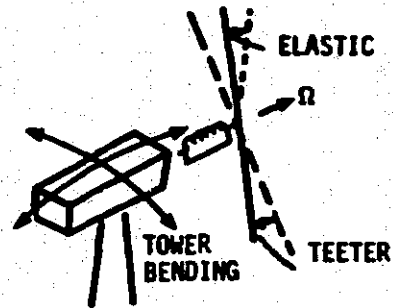
Figure 7-1 GETTS Analysis Flow

rotate, the dynamical equations switch from one model to the next. A time history solution is determined over as many revolutions as are required to produce a steady-state response. The last rotor cycle is used to compute steady-state fatigue loads. Aerodynamic and gravitational forces are computed as a function of the rotor position by the computer code, WINDLD, before the time history calculations, and are applied to the right side of the modal equations. Aeroelastic coupling comes from aerodynamic modal damping coefficient calculations computed by the computer code, QAERO, before the time history calculations. Finally, interface design loads are computed from the modal response. The code can handle a large number of system modes at relatively low computational cost, because the modal equations are decoupled, linear, second-order equations, for which there are very efficient numerical integration algorithms. More detailed code descriptions may be found in the MOD-1 preliminary and final design reports (ref. 7-1, 7-2).

TRAC - TRAC was developed during the MOD-5A program to predict transient loads. It was successfully correlated against measured MOD-1 shutdown loads. Recently, steady-state results were shown to correlate with MOD-1 operational fatigue loads. The program was checked, using steady-state loads calculated by the GETSS code as a benchmark. The verification provided confidence in the calculations made by both programs. TRAC also agreed qualitatively with MOD-2 on the subject of interactions between the structure and the control system. TRAC was used to compute all the MOD-5A's final design loads.

The self-explanatory features of the TRAC code are illustrated in Figure 7-2. It does not use piecewise-linear modal inputs, as GETSS does. Rather, separate inputs are provided for rotating and fixed system modes. Complete inertial and aerodynamic coupling between the degrees of freedom was retained in the development. Furthermore, non-linear inertia terms, caused by finite elastic deflections of the blade, are included. As such, the equations are highly coupled. A Runge-Kutta numerical integration was used to obtain solutions. Loads are calculated after each time step using the "modal acceleration" technique, which is superior to basing loads on elastic deflections (modal deflection technique). When the rotor speed varies during a transient solution, the blade stiffness terms are adjusted using Southwell coefficients, which are computed within the program. NASA's interim turbulence model was incorporated into the code for fatigue load computation,

TRANSIENT ROTOR ANALYSIS CODE



FREEDOM

- TEETER
- ROTOR SPEED
- 3 ELASTIC FLAP MODES/BLADE
- TOWER BENDING 2-DIRECTION
- CONTROL SYSTEM
- GENERATOR

AERODYNAMICS

- TABLE LOOKUP, C_L , C_D , C_M , vs α
- AIRFOIL TABLES AS F'N OF SPAN
- ARBITRARY TWIST, TAPER
- QUASI-STEADY AERODYNAMICS
- STALL DELAY AS F'N OF α
- MOMENTUM THEORY DOWNWASH
 - SEPARATE CALCULATIONS FOR TIP AND INNER BLADE
 - TIME LAG IN V_i FOR TRANSIENTS

SPECIAL FEATURES

- V , YAW ψ , CONTROL δ vs TIME INPUTS
- DESYNCH @ PRESCRIBED TIME OR POWER LEVEL
- TEETER BRAKE/STOPS DYNAMICS
- NACELLE TILT
- BLADE ELASTIC CHORD BENDING DUE TO GRAVITY
- WIND SPEED VARIATIONS AT ROTOR HARMONICS TO SIMULATE TURBULENCE

OUTPUT

TIME HISTORIES OF LOADS AND MOTIONS

Figure 7-2 Features of the TRAC Code

however, the capability of analyzing only wind shear or tower shadow, or both, was retained. A comparison of TRAC's theoretical predictions with measured loads is given in section 7.2.4.

7.2.2 LOAD STATISTICS

Fatigue loads for the MOD-5A were expressed as probability distributions (or histograms) to be applied for the 30-year life of the machine. This section describes the methodology used in deriving the fatigue load statistics. (Limit loads were computed for critical design conditions, which are covered in Section 7.2.5). Fatigue loads were segregated into three categories, shown in Figure 7-3, the same categories used in previous wind turbine generator programs. The Type I loads represent the alternating loads, which occur at 1 or 2P (P stands for per revolution). For design purposes, all load components were conservatively assigned an occurrence rate of 2P. The Type II loads stem from gusts, which cause a shift in mean load during the gust. This mean shift, and the normally occurring alternating loads were used to compute a cycle of fatigue loading for each gust occurrence. Similar Type IIA loads, which stem from longer shifts in mean wind speed, are not shown in the figure. The Type III loads represent the "ground to air to ground" cycle and have a frequency of occurrence equal to the number of start-stop cycles. Type III loads were computed from the delta loads between normal operation and shutdown to the parked state. Note that shutdown transients can produce wider deltas in some load components than simply considering the normal operating and parked conditions. The number of Type I, II, IIA, and III cycles expected over 30 years are 3.5×10^6 , 1.4×10^7 , 1.5×10^6 and 35,000, respectively.

The first step in determining the life cycle fatigue loads was to obtain the mean wind statistics of the site. The wind specification in the Statement of Work was used for MOD-5A. The operation of the wind turbine was separated into discrete wind bins, as illustrated in Figure 7-4. The total number of Type I cycles, which was based on the number of rotor cycles, and Type II cycles, which was based on the number of gusts, were computed for each bin.

In the second step, mean and alternating steady-state loads were computed from cut-in to cut-out speeds, using TRAC. The wind speeds analyzed did not

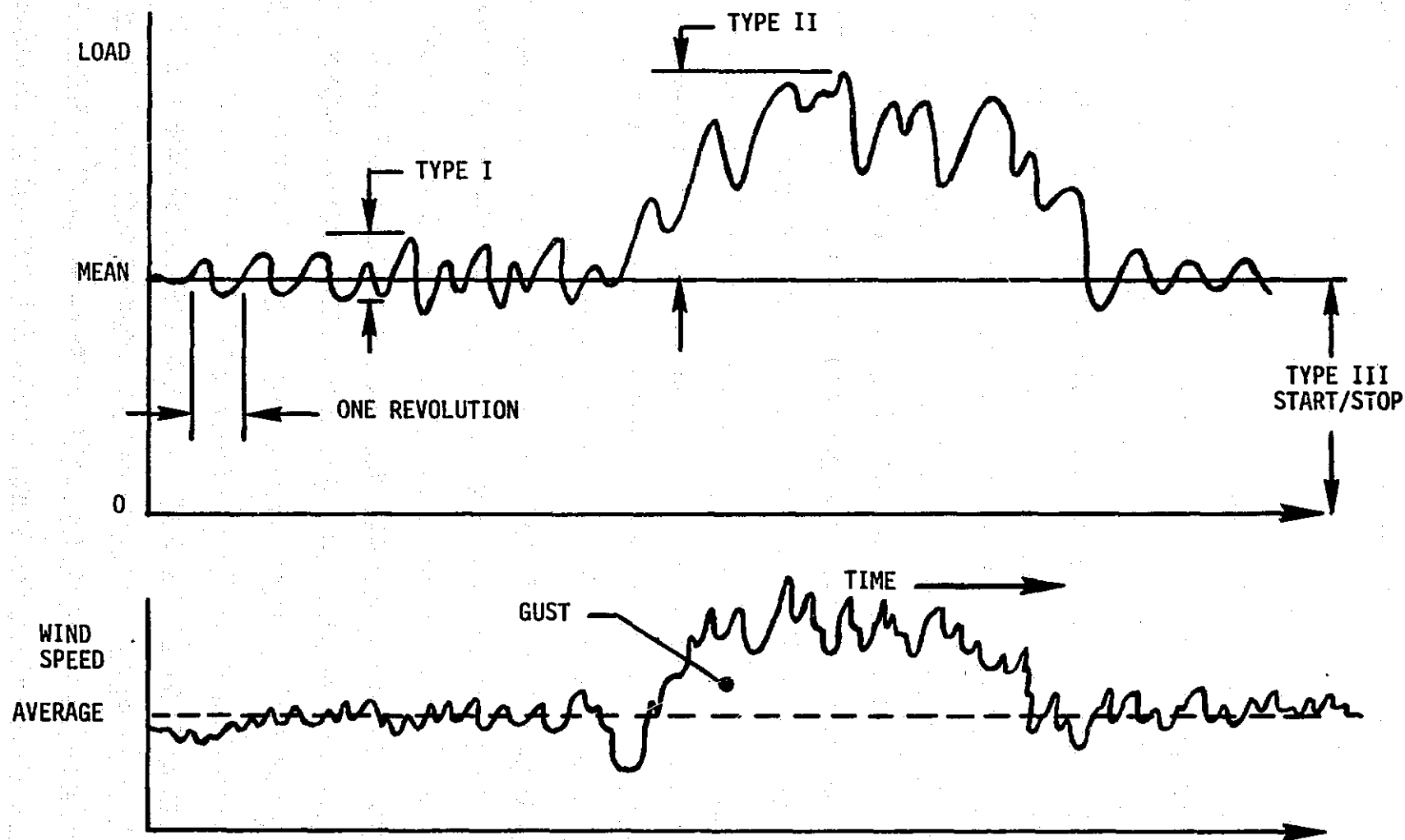
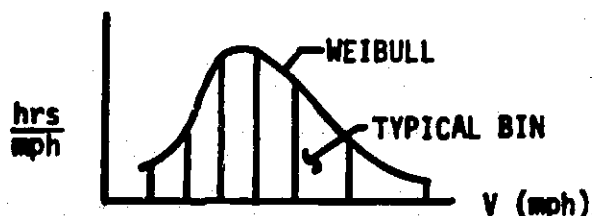


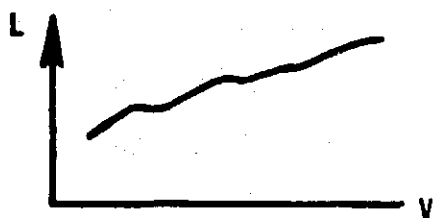
Figure 7-3 Fatigue Load Types

STEP 1. WIND PROFILE

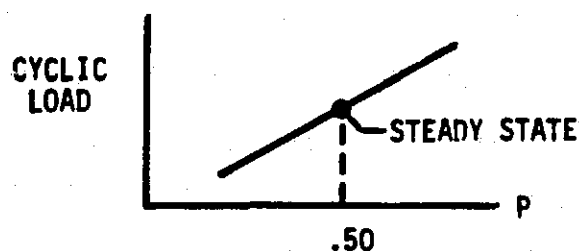


- SEPARATE OPERATION INTO WIND BINS
- DETERMINE # ROTOR CYCLES AND GUSTS PER BIN

STEP 2. COMPUTE STEADY-STATE LOADS VS. V



STEP 3. DETERMINE TYPE I LOADS (EACH BIN)



- LOG-NORMAL DISTRIBUTION
- SLOPE BASED ON TEST DATA

STEP 4. DETERMINE TYPE II LOADS (EACH BIN) - ALSO TYPE II A

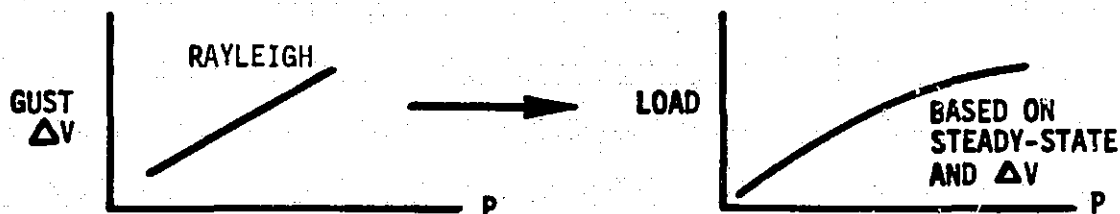


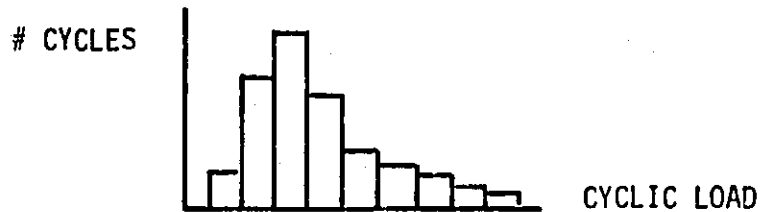
Figure 7-4 Procedure for Determining Life Cycle Fatigue Loads (Sheet 1 of 2)

STEP 5. DETERMINE TYPE III LOADS

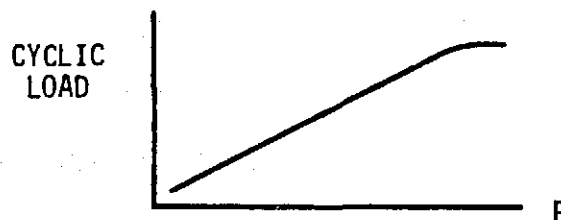
ESTIMATE NUMBER OF START/STOP CYCLES ~ 35,000

COMPUTE DELTA LOAD FROM POWER TO SHUTDOWN EXTREME

STEP 6. COMPOSITE LOAD HISTOGRAM (ALL TYPES/ALL BINS)



-OR-



+ STATISTICS OF CORRESPONDING
MEAN LOADS

TO DESIGNERS

Figure 7-4 Procedure for Determining Life Cycle Fatigue Loads (Sheet 2 of 2)

necessarily correspond to the bin mean wind speeds; instead a sufficient number of wind speeds was chosen to construct smooth curves of load versus wind speed. In this way, the data could be applied to wind sites other than the one selected. The steady-state loads were computed using the root mean square wind speed harmonic variations given by NASA's Interim Turbulence Model. The third step determined the distribution of Type I loads for each bin. First the steady-state loads data were converted to 50th percentile values on the basis of a Rayleigh distribution. Data measurements from existing wind turbines indicated that Type I loads were well fitted by a log-normal distribution and so this distribution was used to compute loads at other percentiles. The slope of the distribution was based on existing teetered rotor test data. It is believed that the log-normal distribution stems from the sum of a constant (or deterministic) load level and stochastic loads with a Rayleigh distribution. This premise was supported by the MOD-1 fatigue load correlation study reported in section 7.2.4, in which loads were computed for various turbulence amplitude percentiles and were compared to measured values. Both the measurements and predictions appeared to be log-normal.

In the fourth step of Figure 7-4, the procedures used to obtain Type II and Type IIA loads are summarized. A probability distribution of gust amplitude was constructed on the basis of the wind turbulence model. Mean and alternating loads were used to determine the Type II loads corresponding to a sufficient number of discrete gust amplitudes. The load probabilities were equal to the gust probabilities from which they were derived. The 0th percentile load (no gust) was equal to the steady-state, 50th percentile load. Note that the Type II load distribution was not assumed to follow any prescribed probability law; instead it was constructed directly from the wind turbulence model and associated response load. Type II calculations were further refined to account for the dynamic action of the control system causing load amplification during a gust.

Type III loads were determined from the differential load encountered in the transition between normal operation and the parked state.

Finally, in the sixth step, composite fatigue histograms were constructed from all the data. These histograms define the total fatigue loading that is projected to occur over 30 years. The cyclic loads are presented in the form of a histogram as shown, or equivalently as a cumulative probability. These loads, along with statistics of the corresponding mean loads, were supplied to the designers. The procedure was computerized, for rapid turnaround and to allow life cycle loading for various wind sites to be generated with little effort.

7.2.3 WIND MODELS

The wind models used to compute design loads are classified in Table 7-1. Wind models used for (A) limit and (B) fatigue load calculations appear separately. The same large gust model is used in each case (Model A.2 and Model B.3). Models B.2, B.3, and B.4 will be described in this section. The other models appearing in the table are self-explanatory.

Mean Wind Variations (Model B.2) - These variations produce shifts in mean load levels that must be considered as fatigue cycles. For example, if the machine is operating in a 20 mph wind and during 10 minutes the wind shifts to 30 mph and returns to 20 mph, a fatigue cycle results from the difference in load levels at 20 and 30 mph. The load shift, which can be viewed as a "DC" phenomenon, is referred to as a Type IIA load. In order to quantify the variation in mean wind speed, data taken over four months at Amarillo, TX by PNL-Battelle was statistically analyzed. Figure 7-5 outlines the analysis and the results. In addition to mean wind shift statistics, the data was used to compute the number of start-stop cycles that would be experienced by a MOD-5A. It might be added that the yearly wind speed distribution at Amarillo is quite similar to the specification in the MOD-5A Statement of Work.

Large Gusts (Models A.2 and B.3) - Figure 7-6 summarizes the large gust model used for the MOD-5A design. The power spectral density (PSD) for the Statement of Work wind was integrated to determine the root mean square gust value. The cut-off frequency of .02 Hz, used in the integration, was based on

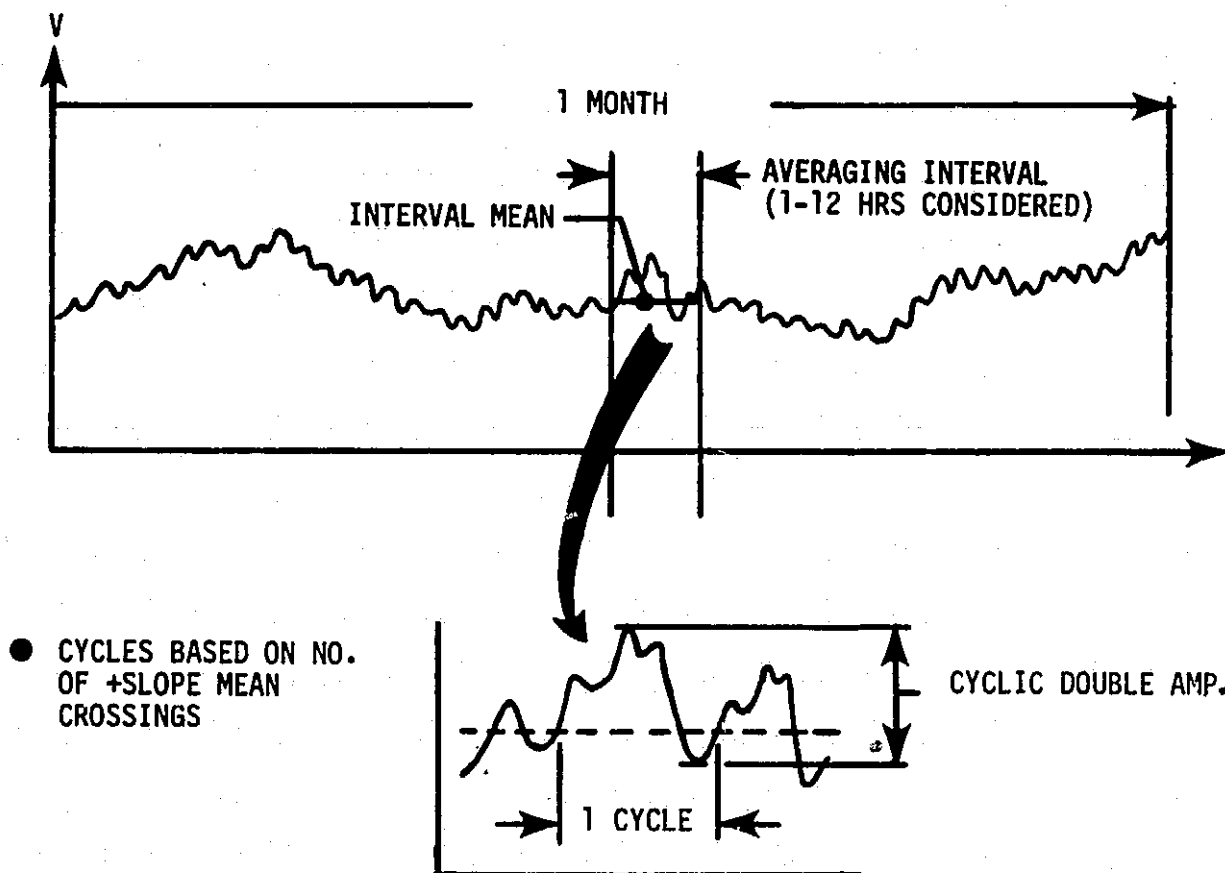
Table 7-1 Classification of Wind Models

A WIND MODELS FOR LIMIT LOADS

1. Hurricane - per MOD-5A SOW
2. Large Rotor Enveloping Gusts (99.99th percentile)
3. Yaw Misalignments
4. Wind Shear - per MOD-5A SOW

B WIND MODELS FOR FATIGUE LOADS

1. Yearly Mean Wind Distribution - Weibull per MOD-5A SOW
 2. Mean Wind Variations
 3. Large Rotor Enveloping Gusts (Up to 99.9%ile)
Note: Same as Model A.2.
 4. Local Turbulence ~ per NASA Interim Turbulence Model
 5. Tower Shadow ~ per Potential Flow Theory for Upwind Rotor
 6. Wind Shear ~ per MOD-5A SOW
-
-



RESULTS

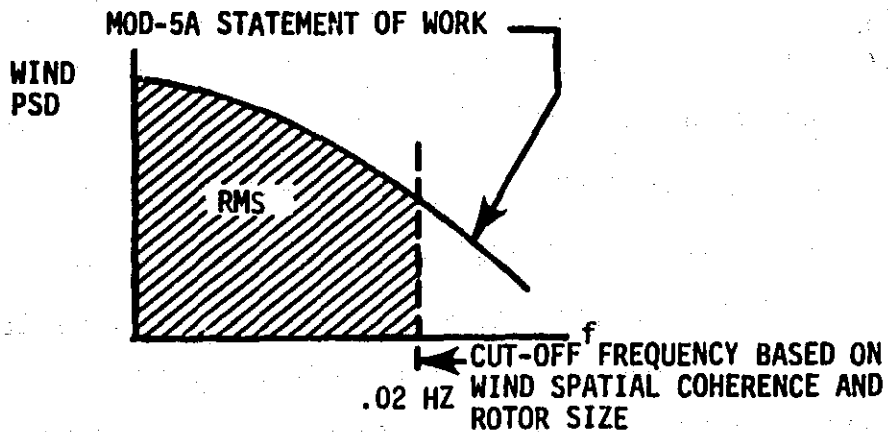
- AVERAGE PERIOD ≈ 10 MIN ($1.5 \times 10^6 \sim 30$ YRS)
- RMS DOUBLE AMP. $\approx 0.16 V_{\text{mean}}$
- PROBABILITY DISTRIBUTION \approx RAYLEIGH
- NO OF START/STOPS = 35,000 PER 30 YRS

BASIS

- ANALYSIS OF 4 MONTHS DATA - AMARILLO, TX

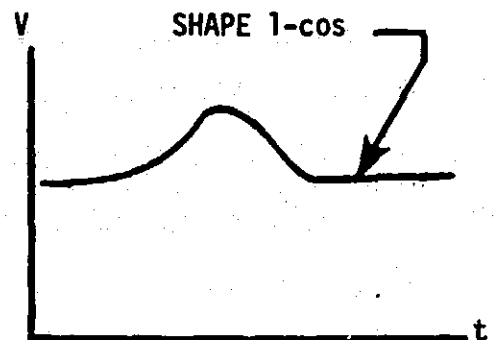
Figure 7-5 Development of Mean Wind Variation Model

ORIGINAL PAGE IS
OF POOR QUALITY



RESULTS

- AVERAGE PERIOD ≈ 50 SEC (13 E6 \sim 30 YRS)
- RMS AMP $\approx .11 V_{\text{mean}}$
- DISTRIBUTION - RAYLEIGH
- SHAPE 1-cos



BASIS/CONFIRMATION

- MOD-5A SOW
- PNL-BATTELLE GUST MEASUREMENTS
- MOD-2 LOADS DATA SUPPORTS MODEL

Figure 7-6 Development of Large Rotor-Enveloping Gust Model

a spatial coherence model developed during MOD-2, and used in conjunction with the MOD-5A rotor diameter. The relevant formula for the coherence, COH, appears below:

$$\text{COH} = \exp(-fxdK_y)$$

where:

f = cut-off frequency (Hz).

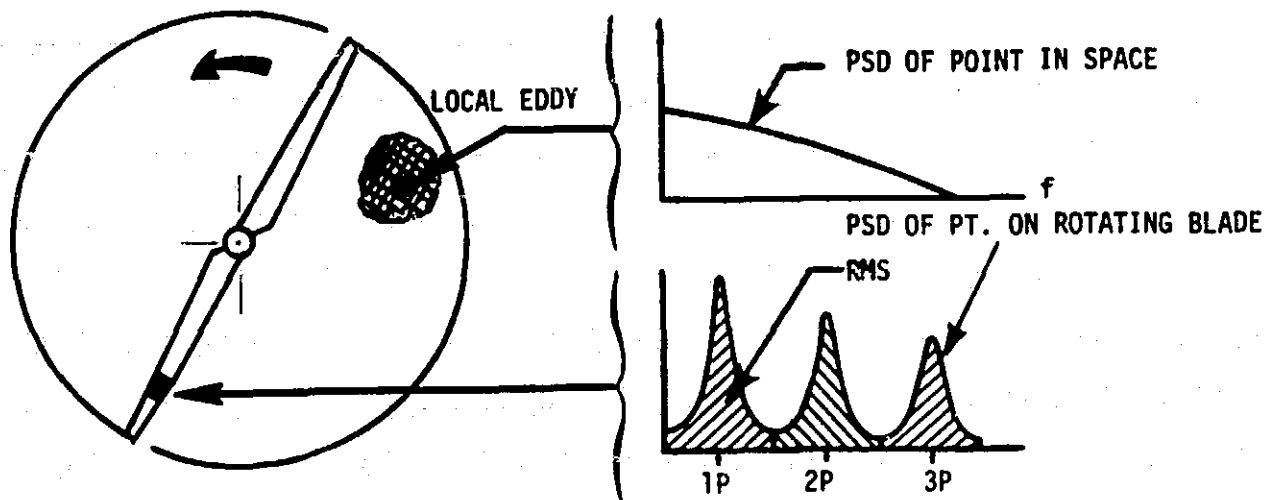
x = fraction of rotor disc for which the coherence is sought.
A value of 1.0 (or the whole disc) was used.

d = rotor diameter (m)

$K_y = .37 - .005V$, V = wind speed (m/s)

Gusts with a coherence equal to or greater than 0.50 were conservatively treated as rotor encompassing gusts. This formula leads to a cut-off frequency of .018 Hz at 25 mph and .022 Hz at 50 mph. An average of .02 Hz was used for all wind speeds. This cut-off frequency implies an average gust period of 50 seconds, which is supported by MOD-2 test measurements discussed in Section 7.2.4. A Rayleigh distribution was selected for the gust amplitudes on the basis of PNL-Battelle's "Gust-0" measurements reported in ref. 7-3. The gust model in Figure 7-6 is used to compute Type II (see Section 7.2.2 for definition) fatigue loads and limit loads. The MOD-2 loads data analysis covered in Section 7.2.4 appears to support the gust amplitudes we have used.

Local Turbulence (Model B.4) - Gusts smaller than the rotor diameter produce variations in the apparent wind speed experienced by the rotating blades at harmonics of the rotor speed. The situation is illustrated in Figure 7-7. This harmonic forcing produces fatigue loads that occur every rotor cycle (Type I). Measurements and data analysis conducted by PNL-Battelle began to quantify the magnitudes of these turbulent inputs. NASA developed an "Interim Turbulence Model" from this data, which conveniently expresses the root mean square values of the harmonic forcing for rotors of different sizes. The formulas are summarized in Table 7-2. GE adopted NASA's model for MOD-5A fatigue load calculations. GE assumed the probability distribution of the random harmonic coefficients was Rayleigh, as would be the case for a narrow-band process. The Rayleigh assumption also seems to be supported by the ratios of 99.9th percentile to 50th percentile loads generally found in flap bending moment test data. The correlation with MOD-1 loads appears in section 7.2.4.



RESULTS

- RANDOM FORCING @ ROTOR HARMONICS
- RMS AMP - VARIES WITH HARMONIC & V
- DISTRIBUTION - ASSUMED RAYLEIGH

BASIS

- PNL BATTELLE MEASUREMENTS
- NASA ANALYSIS

Figure 7-7 Development of Local Turbulence Wind Model

Table 7-2 Formulas for the MOD-5A Wind Turbulence Model

$$V_{\text{TURB}}(X, \psi, P) = X \sum_{i=1}^6 V_{\text{RMS}i} \cos i(\psi + \phi_i) \sqrt{-2 \ln(1-P)}$$

where

V_{TURB} = Wind speed variation caused by turbulence

X = Non-dimensional blade spanwise station

P = Probability that turbulence input is less than or equal to V_{TURB}

$V_{\text{RMS}i}$ = RMS of turbulence velocity at the i^{th} rotor harmonic, per NASA Interim Turbulence Model

i = Rotor harmonic

ψ = Rotor blade angular position

ϕ_i = Phase of i^{th} harmonic (set = constant for MOD-5A analysis - theoretically random)

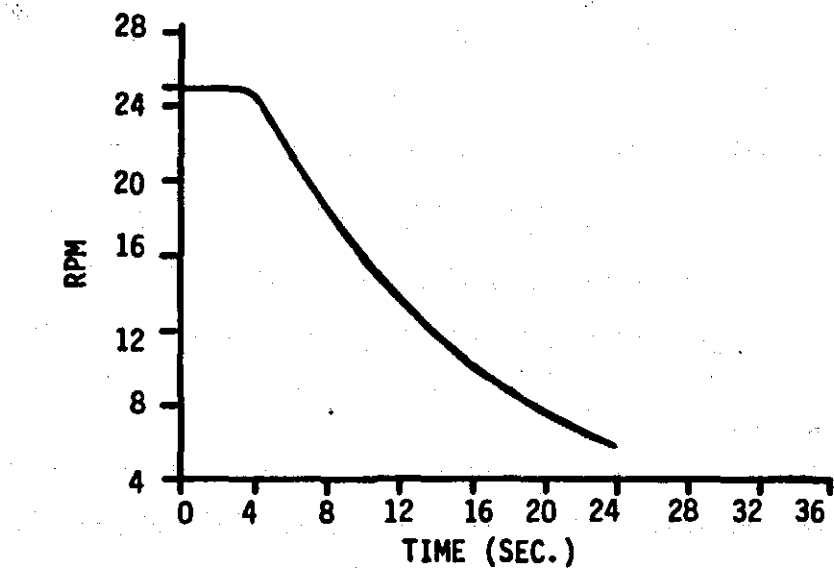
$$V_{\text{RMS}i} = \frac{\Delta V_S}{2\sqrt{2}} \frac{1}{i + .75}$$

ΔV_S = Difference in wind speed between the highest and lowest points in the rotor disc as predicted by the wind shear model in the MOD-5A Statement of Work.

7.2.4 VERIFICATION OF CODES AND MODELS

The GETSS code was correlated with MOD-0 data supplied by NASA during the MOD-1 program and during the conceptual design of the MOD-5A. These validation results will not be repeated here. Rather, this section focuses on substantiating the wind models that were adopted, and the loads predicted by the TRAC code. Specifically, it will cover shutdown transients, Type I load probability distributions and Type II loads. Shutdown testing performed during the MOD-1 check was simulated using the TRAC code. Figure 7-8 shows a typical simulation, in which rotor speed, pitch angle, and blade flap bending moment at .35R (where R is the radius), are plotted versus time. Following about 3 seconds of steady-state operation at 25 rpm, the blades were feathered at 8°/sec for 1.5 seconds followed by a 2°/sec pitch rate for the remainder of the shutdown. (The dual feather rate was used on MOD-1 to guard against high loads). The time histories show that the rotor speed decreased continuously after feather, while the flap bending moment reached a peak at about 5 seconds. Similar analyses were conducted for shutdowns from other initial rotor speeds and the peak flap bending loads were recorded. Figure 7-9 compares theoretically predicted loads with test measurements made at two blade stations. Here, peak moments were plotted against the rotor speed at which the shutdown was initiated. There was excellent agreement between the test and the theory.

Probability distributions of MOD-1 flap-bending moments measured at three blade radial stations are compared with theoretical predictions in Figure 7-10. These represent Type I cyclic (1/2 peak-peak) loads. A band of measured data is shown along with discrete test points taken on a typical day of operation. The theoretical loads were computed using NASA's Interim Turbulence Model with the TRAC code. Points at three percentiles were generated by ascribing turbulence disturbance amplitudes according to a Rayleigh distribution. Tower shadow was also included in the model. The results indicated excellent agreement between test and theory at mid-span, while predictions were at the top and bottom of test scatter for outboard and inboard locations, respectively. In view of the contingency factors of 15-25%, which were applied to all MOD-5A load predictions, the turbulence model was considered to be satisfactory for design purposes.



SIMULATED MOD-1 SHUTDOWN
FROM 25 RPM

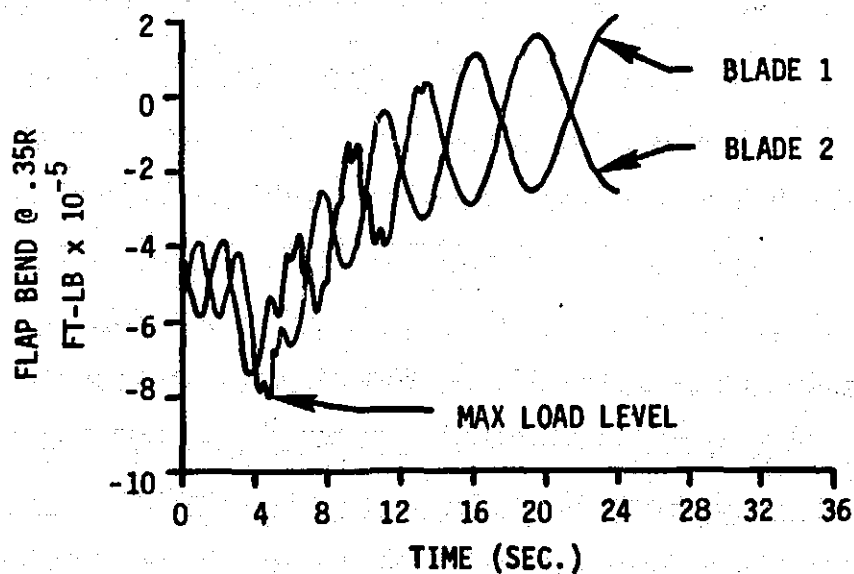
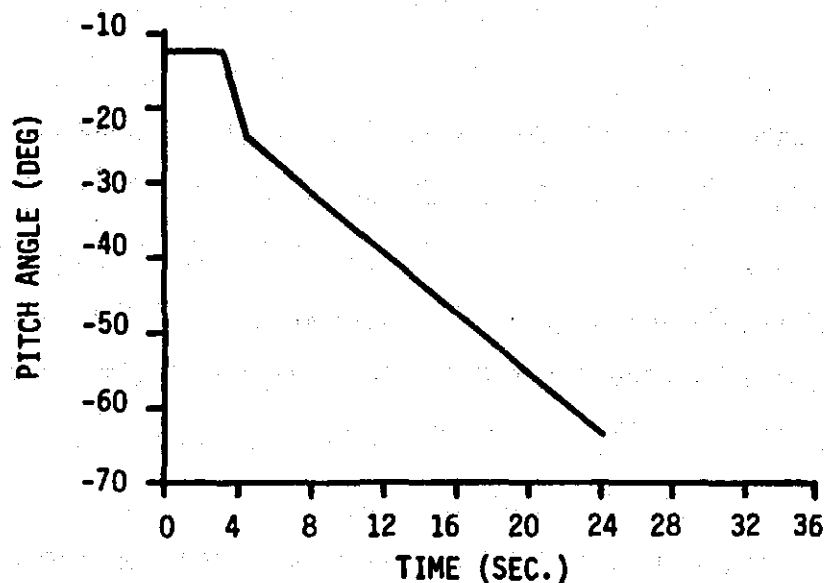


Figure 7-8 Simulation of MOD-1 Shutdown, Using the Trac Code

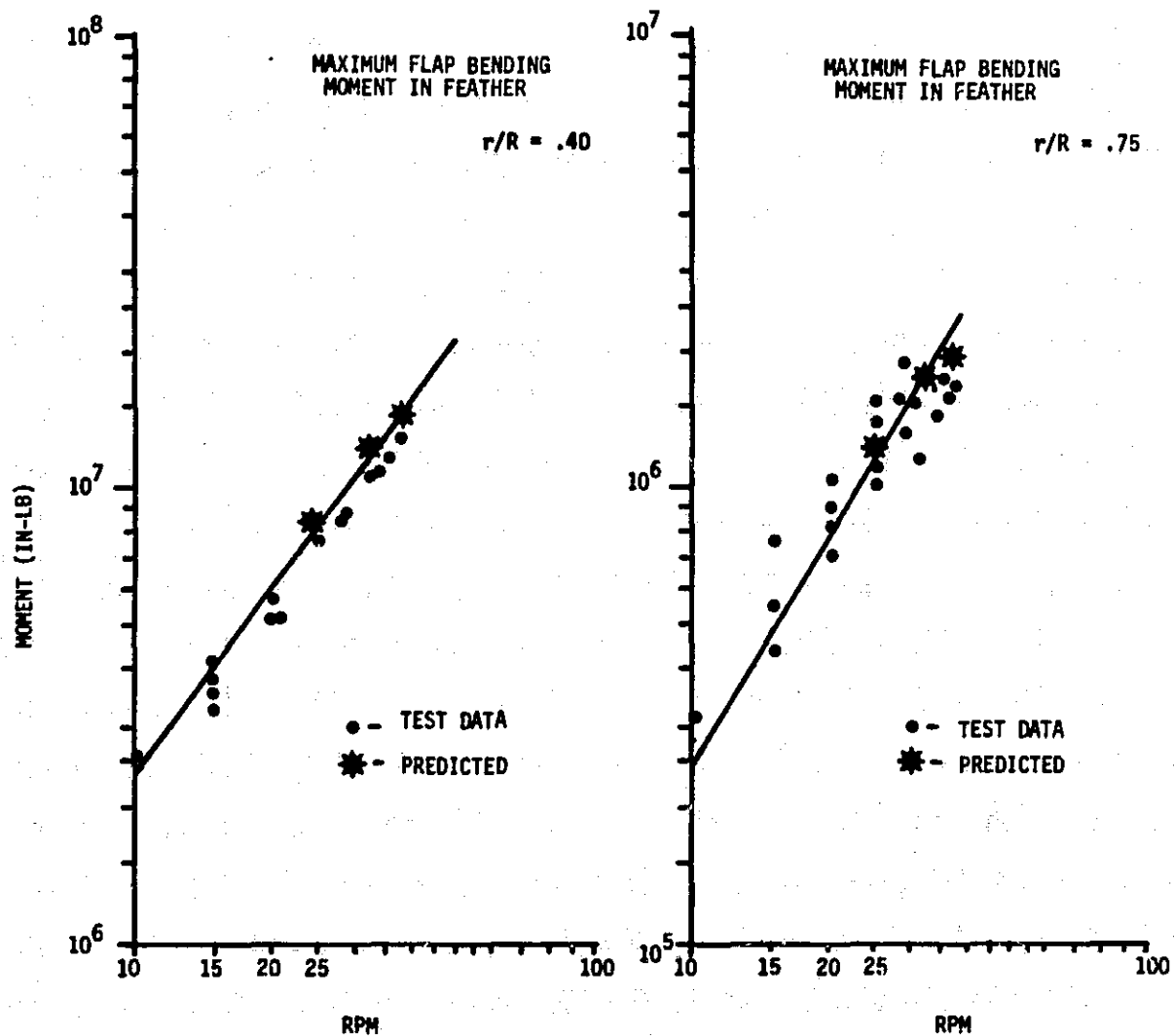


Figure 7-9 Comparison of MOD-1 Shutdown Test Blade Loads with Theoretical Predictions

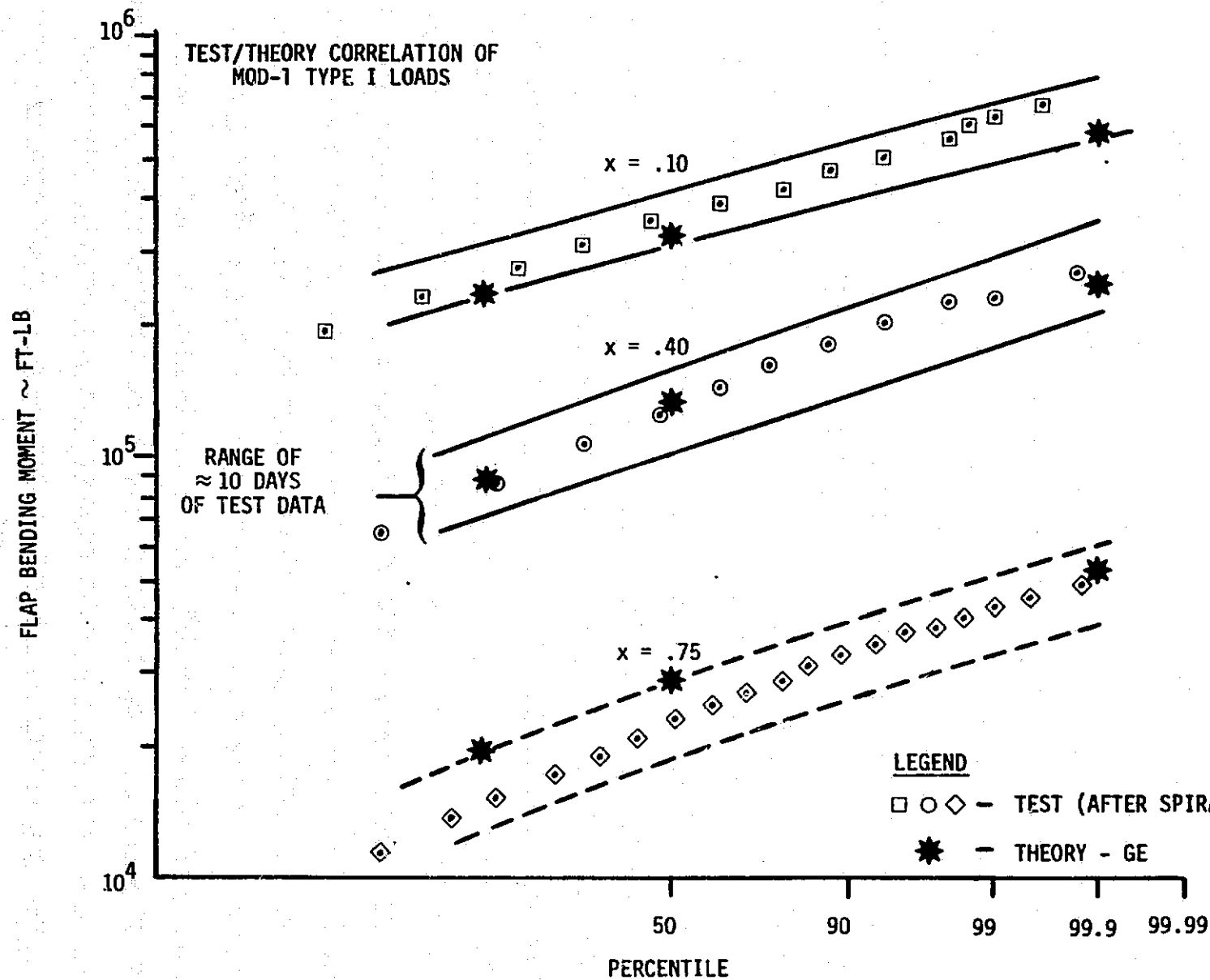


Figure 7-10 Test and Correlation with Theory of MOD-1 Type I Fatigue Loads

Type II loads were extracted from MOD-2 data tapes supplied by NASA. Occurrences were counted according to positive slope crossings of the mean load versus time. Figure 7-5 shows the similar procedure, used for wind data. Figure 7-11 contains a table of the frequency of Type II load occurrences along with the number of wind speed shifts. Note that there are more cycles of the wind speed point measurement (81.9/hr.) than of the loads (55-61/hr.), which makes sense because all the shifts in wind speed may not be spatially large enough to cause a change in mean rotor loads. Below the table, a scattergram of Type II load magnitude is plotted against load period. Higher loads correspond to higher periods, as would be expected because the large rotor enveloping gusts have longer periods. About a 50 second period, or more, was needed to produce peak load levels. The average frequency of MOD-2 loads (55-61/hr.) agreed well with what was modelled for the MOD-5A (65/hr.). If anything, the MOD-5A would be expected to have a lower frequency because of its increased size, so this analysis was slightly conservative.

Type II load probability distributions are plotted in Figure 7-12. MOD-5A predictions for similar wind conditions are also shown. The MOD-5A predictions were in line with the scaled test data, if not somewhat conservative. This analysis provided confidence in the modelling of Type II loads on the MOD-5A.

7.2.5 DESIGN OPERATING CONDITIONS

The MOD-5A loads were based on cut-in and cut-out wind speeds of 14 mph and 60 mph, respectively, at the hub height. Fatigue cycles for 30 years of operation were computed for the MOD-5A Statement of Work Wind Duration Curve, which is defined and illustrated in section 4.2. The wind bins used to generate the fatigue data are summarized in Table 7-3, along with the numbers of Type I, II, and IIA cycles for each bin. Gust and mean wind shift amplitudes at the bin mean wind speeds are contained in Table 7-4. Gust amplitudes up to and including the 99.9th percentile were used to predict the fatigue loads. The 99.99th percentile gust was used to compute limit loads.

# CYCLES/HOUR			
HOUR	V @ 195	FLAP BENDING	
		.20R	.65R
1	76	40	63.8
2	81.5	86.5	64.5
3	78.1	46.5	53.1
4	78.1	59.4	87.7
5	95.6	42.1	36.6
AVG	81.9	54.9	61.1

MOD-5A
Prediction
65 Cycles/Hr

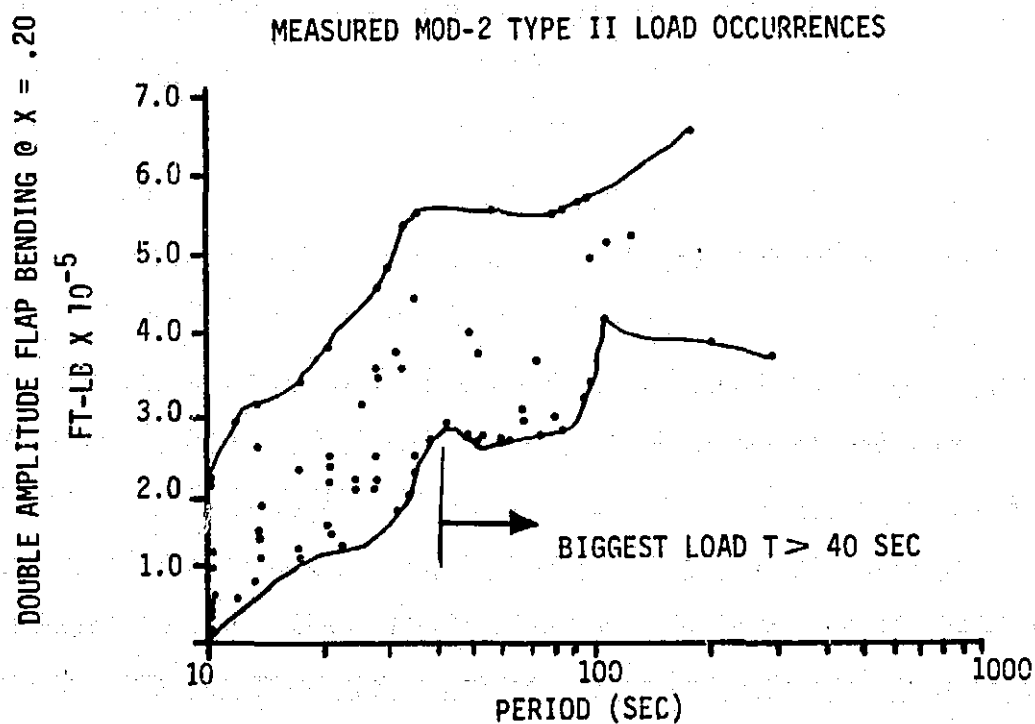


Figure 7-11 Frequency of Occurrence of MOD-2 Type II Load Measurements

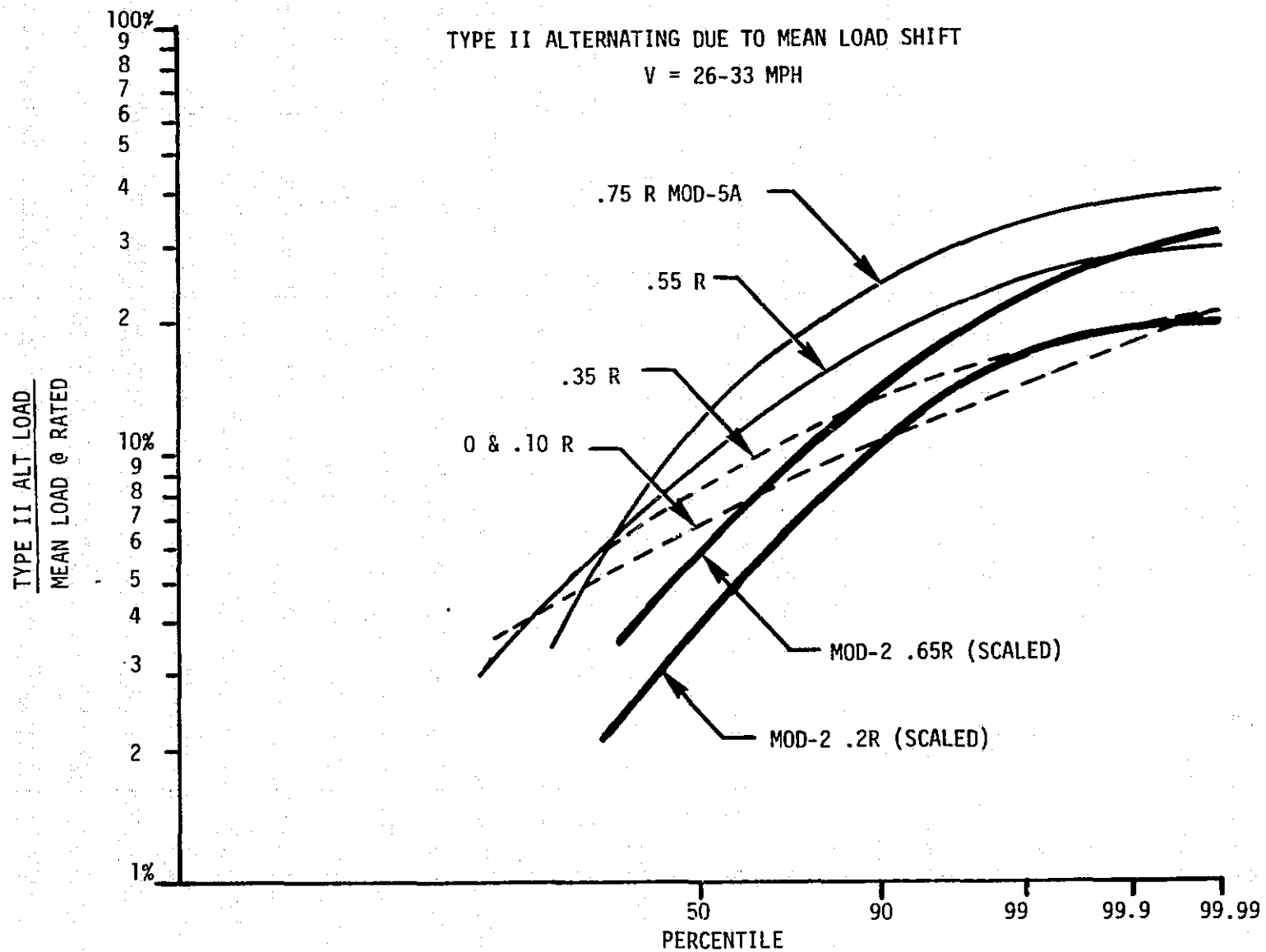


Figure 7-12 Comparison of MOD-5A Type II Load Predictions with Scaled MOD-2 Measurements

Table 7-3 MOD-5A Wind Bin and Fatigue Cycle Summary

BIN	MID-POINT (MPH AT HUB)	RANGE (MPH)	ROTOR SPEED (RPM)	NO. OF FATIGUE CYCLES PER 30 YEARS			
				TYPE I	TYPE II	TYPE IIA	TYPE III
1	16.5	14 - 19	13.8	92.7E6	4.05E6	.365E6	---
2	21.5	19 - 24	13.8	93.5E6	4.08E6	.368E6	---
3	26.0	24 - 28	16.8	71.3E6	2.55E6	.230E6	---
4	31.5	28 - 35	16.8	66.5E6	2.37E6	.214E6	---
5	40.0	35 - 45	16.8	19.2E6	.68E6	.062E6	---
6	52.5	45 - 60	16.8	.86E6	.03E6	2800.	---
TOTAL				344.E6	13.8E6	1.24E6	35000.

NOTES: FATIGUE CYCLES BASED ON .96 AVAILABILITY
TYPE I CYCLES BASED ON 2P OCCURRENCE RATE

Table 7-4 Gust Amplitudes Used for the MOD-5A Fatigue Loads Analysis
(a) Amplitude of Large Rotor Enveloping Gusts Used for Type II and Limit Loads

BIN	V_{MEAN} (MPH)	$\Delta V = \text{TOTAL GUST MAGNITUDE (MPH) FOR PERCENTILE}$				
		40%	86%	99%	99.9%	99.99%
1	16.5	1.83	3.60	5.51	6.75	7.79
2	21.5	2.39	4.69	7.18	7.79	10.2
3	26.0	2.89	5.67	8.68	10.6	12.3
4	31.5	3.50	6.87	10.5	12.9	14.9
5	40.0	4.45	8.73	13.4	16.4	18.9
6	52.5	5.84	11.45	17.5	21.5	24.8

$$\Delta V = .11 V_{\text{MEAN}} \sqrt{-2 \ln (1-P)} \quad , \quad P = \%/100$$

V RANGE = V_{MEAN} TO $(V_{\text{MEAN}} + \Delta V)$ FOR UPGUSTS

V RANGE = $(V_{\text{MEAN}} - \Delta V)$ TO V_{MEAN} FOR DOWNGUSTS

(b) Amplitudes of Mean Wind Shifts Used for Type IIA Loads

BIN	V_{MEAN} (MPH)	$\Delta V = \pm \text{SHIFT MAGNITUDE (MPH) FOR PERCENTILE}$			
		40%	86%	99%	99.9%
1	16.5	1.33	2.62	4.01	4.91
2	21.5	1.74	3.41	5.22	6.39
3	26.0	2.10	4.12	6.31	7.73
4	31.5	2.55	5.00	7.65	9.37
5	40.0	3.23	6.35	9.71	11.9
6	52.5	4.25	8.33	12.8	15.6

$$\Delta V = .08 V_{\text{MEAN}} \sqrt{-2 \ln (1-P)}$$

V RANGE = $(V_{\text{MEAN}} - \Delta V)$ TO $(V_{\text{MEAN}} + \Delta V)$ FOR ALL SHIFTS

Critical operating conditions used to compute limit loads are summarized in Table 7-5. The system was designed to withstand the first four conditions without damage. The last case represented an extreme condition, which the MOD-5A could withstand without a catastrophic failure, such as losing a blade. Table 7-6 summarizes additional events that were analyzed, but were not critically important for the MOD-5A.

7.3 INTERFACES AND COORDINATE AXES

The design loads were calculated at the locations listed in Table 7-7. A full set of shear and moment loads (V_x , V_y , V_z , M_x , M_y , M_z) are given at these points. The sign conventions for the main blade and the fixed system are shown in Figure 7-13. Note that the reference axis for the shear loads on the blade is the 30% chord. Also, the coordinate directions lie on principal axes and twist with the cross-sections of the blade airfoil.

The coordinate system used to define loads on the aileron is illustrated in Figure 7-14. Again, the axes are fixed to the structure and rotate with the aileron. Unlike other load components, local aileron loads are defined by running shears (V_x , V_y , V_z in lb/ft) and a running hinge moment (M_x in ft-lb/ft) as a function of the blade span. The reference line for inertial shear loads is the aileron's center of gravity. The reference line for aerodynamic shear loads is the hinge line. It should be noted that the main blade loads include the local loads generated by the ailerons.

The dimensions of the system and the locations of the non-blade interfaces are shown in Figure 7-15. One-g interface loads are listed in Table 7-8.

Table 7-5 Critical Limit Load Conditions

<u>CONDITION</u>	<u>COMMENTS</u>
1. HURRICANE (130 MPH AT HUB)	TOWER BENDING AND FOUNDATION CRITICAL
2. CONTROL HARDWARE FAILURE (60 MPH, 0° AILERON ANGLE)	INBOARD BLADE/ROTOR CRITICAL
3. 99.99TH PERCENTILE GUST AT RATED WIND SPEED, 25% OVERSPEED, DESYNCRONIZATION AND SHUTDOWN	OUTBOARD BLADE CRITICAL
4. SHUTDOWN AT CUT-OUT WIND SPEED WITH YAW ERROR	SETS DESIGN REQUIRE- MENTS FOR TEETER BRAKES
5. 50% OVERSPEED, HIGH WIND ADVERSE AILERON SETTING	SURVIVAL CONDITION, SYSTEM DESIGNED TO PREVENT CATASTROPHIC FAILURE

Table 7-6 Additional Transient Events Analyzed

<u>CONDITION</u>	<u>COMMENTS</u>
1. GUSTS/SHUTDOWNS AT WIND SPEEDS OTHER THAN RATED	GUST AT RATED WIND SPEED PRODUCED LARGEST LOADS
2. ONE SET OF AILERONS STUCK (i.e MISMATCH BETWEEN THE 2 BLADES)	<ul style="list-style-type: none"> o LOADS NOT CRITICAL BECAUSE OF TEETERING RELIEF o SUFFICIENT ROTOR/TOWER CLEARANCES o SUFFICIENT BRAKING TORQUE ON ONE BLADE FOR SHUTDOWN
3. 180° SHIFT IN WIND DIRECTION WITHIN 10 SECONDS	LOADS/MOTIONS NOT CRITICAL
4. START UP/SHUTDOWN THROUGH TOWER RESONANCE	MOD-5A CONTROL SYSTEM AVOIDS DWELL AT RESONANCE. LOADS NOT CRITICAL

Table 7-7 System Interfaces

<u>Reference</u>	<u>Location</u>	<u>Comment</u>
1	.90R	
2	.80R	
3	.70R	
4	.60R	Main Blade Station
5	.50R	
6	.40R	
7	.30R	
8	.25R	
9	.20R	
10	.10R	
11	.0R	
12	Teeter Bearing	Rotating System
13	Rotor - CL	Center of Teeter Bearing
		Non-rotating
14	Rotor/Nacelle	
15	Yaw Bearing	
16	Tower 185	(Feet Above ground)
17	Tower 117	
18	Tower 51	(Tower knuckle)
19	Tower base	
20	Ailerons	Load/span from .60R to .99R

Table 7-8 One-G Interface Loads (Model 304.2)

INTERFACE	Vx	Vy	Vz	Mx	MY	Mz
	lb	lb	lb	ft-lb	ft-lb $\times 10^{-6}$	ft-lb $\times 10^{-6}$
BLADE .90R	+1465.	+1465.	-180.	0.	.00168	+ .0138
.80R	+4600.	+4600.	-560.	0.	.00876	+ .0719
.70R	+10330.	+10330.	-1260.	0.	.0268	+ .220
.60R	+18600.	+18600.	-2270.	0.	.0620	+ .509
.50R	+28690.	+28690.	-3500.	0.	.122	+1.00
.40R	+40160.	+40160.	-4890.	0.	.208	+1.71
.30R	+53120.	+53120.	-6470.	0.	.324	+2.66
.25R	+60400.	+60400.	-7360.	0.	.395	+3.24
.20R	+68640.	+68640.	-8370.	0.	.475	+3.90
.10R	+88680.	+88680.	-10807.	0.	.668	+5.48
OR	+133940.	+133940.	-16320.	0.	.906	+7.44
TEETER BRGS.	+.268E6	+.268E6	-32650.	0.	0.	0.
ROTOR CL	-.268E6	0.	-32650.	0.	0.	0.
ROTOR/NACELLE	-.514E6	0.	-62650.	0.	-4.39	0.
YAW BEARING	-1.03E6	0.	0.	0.	-9.44	0.
TOWER 185	-1.10E6	0.	0.	0.	1.06	0.
TOWER 117	-1.24E6	0.	0.	0.	1.06	0.
TOWER 51	-1.41E6	0.	0.	0.	1.06	0.
TOWER BASE	-1.59E6	0.	0.	0.	1.06	0.

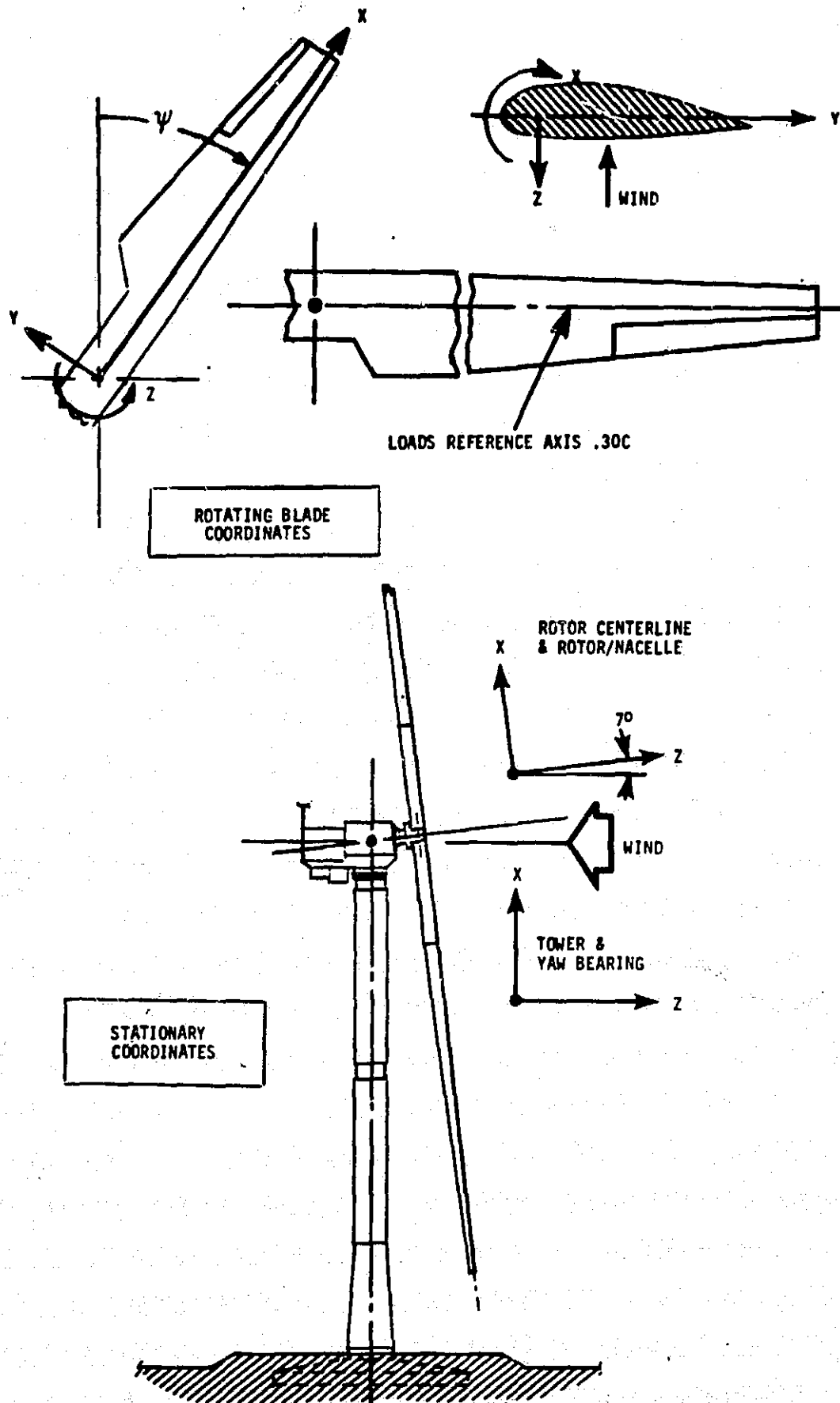


Figure 7-13. Sign Conventions

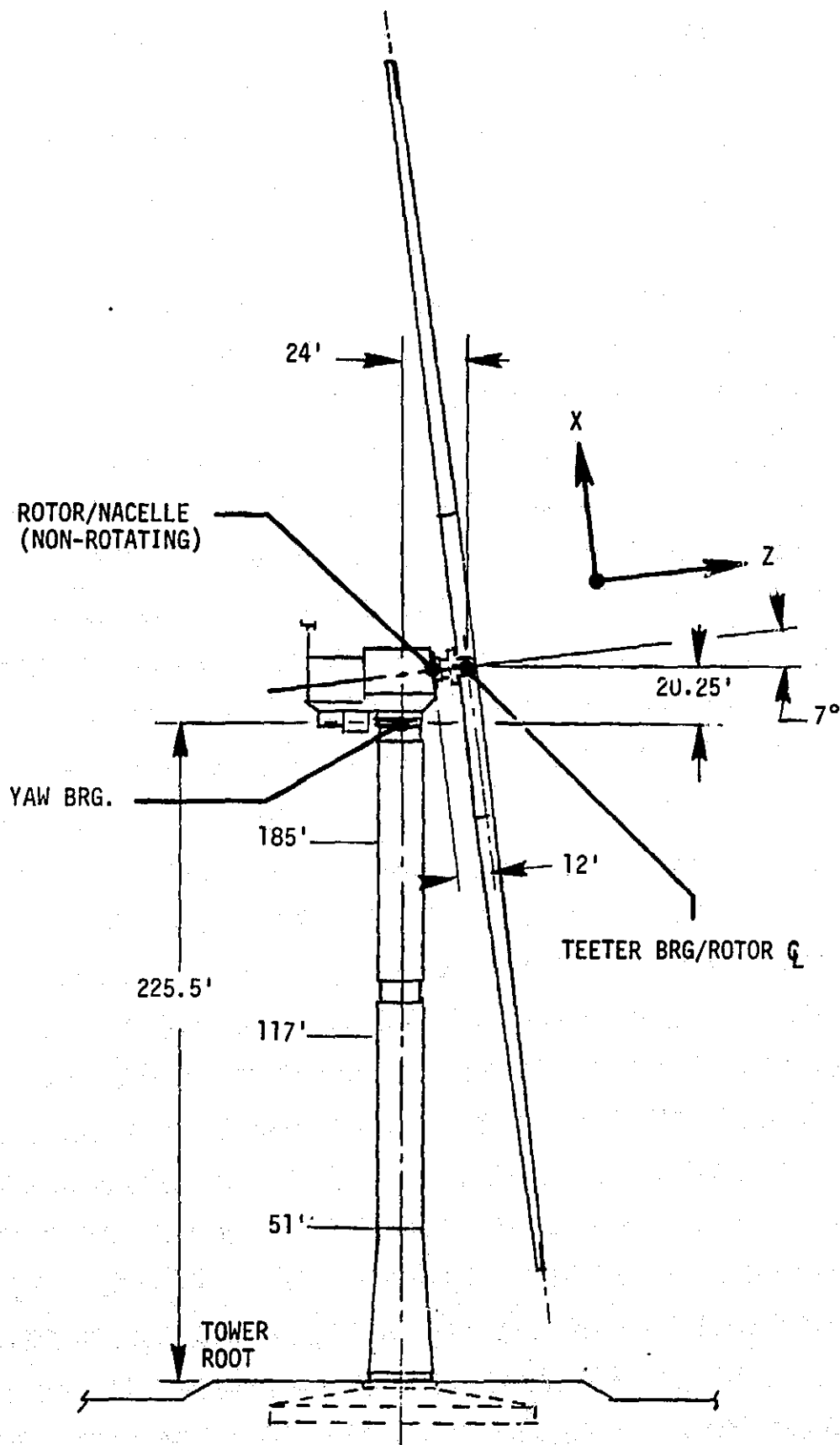


Figure 7-15 System Dimensions and Interfaces

7.4 INTERFACE DESIGN LOADS

The interface design loads are specified in three sets of tables:

- (1) histograms combining Type I, Type II, and Type IIA fatigue loads (359×10^6 cycles in 30 years)
- (2) Type III fatigue loads (35,000 cycles in 30 years)
- (3) limit loads for each critical operating condition

Because of the volume of this data, the complete set of tables has been relegated to Appendix B. Highlights are presented in this section.

A sample histogram is displayed in Table 7-9. Each row corresponds to a bar of the histogram. Columns 1 and 2 provide the number of cycles in and the cumulative probability associated with each bar. The range of cyclic loads for each bar, the bar width, is defined in columns 3 and 4. Columns 5 and 6 are these same dimensional loads divided by the maximum cyclic value. Columns 7 and 8 are also non-dimensionalized by the 50th percentile cyclic load at the rated wind speed. The remaining columns provide statistics of the mean, or mid-range, load for each bar of the histogram. Included below the table are the root-mean-cubed value of all cyclic load occurrences and the average mean load for 30 years of operation. The table formats for Type III fatigue loads and limit loads are self-explanatory and are not illustrated.

Probability distributions of alternating blade flap bending moments are shown in Figure 7-16 for three radial stations. The load magnitudes have been divided by the mean flap-bending moment at the rated wind speed, 32 mph, to allow comparison with data from other wind turbines. The curves display a slight increase in slope above the 99.9th percentile, which is caused by Type II load occurrences. Type III fatigue levels, indicated by horizontal lines, are slightly greater than the maximum Type I and II values. To lend credence to the predictions, scaled test data from the Boeing MOD-2 and Hamilton Standard SVU2 wind turbines are included on the plot. This data suggests that MOD-5A predictions are appropriate, and even somewhat conservative. Figure 7-17 contains probability distributions of the alternating blade chord bending moment, normalized by the one-g moments. Here the loads are dominated by gravity, so there is only a slight increase between the 50th and 99.99th percentile. This trend was also true for MOD-2 test results, which are not shown.

Table 7-9 Typical Load Histogram Presentation

CUMULATIVE FATIGUE HISTOGRAM OUTPUT

TOWER BASE MZ													
I HALF-RANGE FATIGUE LOADS I CORRESPONDING MID-RANGE LOAD DISTRIBUTION													
I I I I I I I I I I I I I I I													
NO. CYCLES	CUM PROB	LOAD LEVELS			NORMALIZED			LOAD/50% AT RATED		MEAN	STANDARD	MAXIMUM	MINIMUM
IN 30 YEARS	-----				LOAD LEVELS						DEVIATION		
(TYPES 1+2)													
0.	0.	I	0.	- 0.178E 06	0.	- 0.03	0.	- 0.08	I	0.	0.	0.	0.
0.	0.	I	0.178E 06	- 0.357E 06	0.03	- 0.07	0.08	- 0.15	I	0.	0.	0.	0.
0.	0.	I	0.357E 06	- 0.535E 06	0.07	- 0.10	0.15	- 0.23	I	0.	0.	0.	0.
0.	0.	I	0.535E 06	- 0.713E 06	0.10	- 0.14	0.23	- 0.31	I	0.	0.	0.	0.
0.	0.	I	0.713E 06	- 0.891E 06	0.14	- 0.17	0.31	- 0.38	I	0.	0.	0.	0.
0.	0.	I	0.891E 06	- 0.107E 07	0.17	- 0.20	0.38	- 0.46	I	0.	0.	0.	0.
0.	0.	I	0.107E 07	- 0.125E 07	0.20	- 0.24	0.46	- 0.54	I	0.	0.	0.	0.
0.	0.	I	0.125E 07	- 0.143E 07	0.24	- 0.27	0.54	- 0.62	I	0.	0.	0.	0.
0.	0.	I	0.143E 07	- 0.160E 07	0.27	- 0.30	0.62	- 0.69	I	0.	0.	0.	0.
0.784E 06	0.00213	I	0.160E 07	- 0.178E 07	0.30	- 0.34	0.69	- 0.77	I	-0.317E 07	0.480E 06	-0.192E 07	-0.335E 07
0.516E 07	0.01650	I	0.178E 07	- 0.196E 07	0.34	- 0.37	0.77	- 0.85	I	-0.307E 07	0.574E 06	-0.192E 07	-0.347E 07
0.171E 08	0.06416	I	0.196E 07	- 0.214E 07	0.37	- 0.41	0.85	- 0.92	I	-0.295E 07	0.649E 06	-0.192E 07	-0.347E 07
0.320E 08	0.15338	I	0.214E 07	- 0.232E 07	0.41	- 0.44	0.92	- 1.00	I	-0.282E 07	0.698E 06	-0.192E 07	-0.347E 07
0.482E 08	0.28771	I	0.232E 07	- 0.254E 07	0.44	- 0.48	1.00	- 1.10	I	-0.269E 07	0.733E 06	-0.131E 07	-0.347E 07
0.390E 08	0.39639	I	0.254E 07	- 0.277E 07	0.48	- 0.53	1.10	- 1.20	I	-0.248E 07	0.798E 06	-0.457E 06	-0.347E 07
0.278E 08	0.47380	I	0.277E 07	- 0.300E 07	0.53	- 0.57	1.20	- 1.29	I	-0.196E 07	0.905E 06	-0.457E 06	-0.347E 07
0.302E 08	0.55802	I	0.300E 07	- 0.322E 07	0.57	- 0.61	1.29	- 1.39	I	-0.134E 07	0.743E 06	-0.457E 06	-0.347E 07
0.377E 08	0.66305	I	0.322E 07	- 0.345E 07	0.61	- 0.66	1.39	- 1.49	I	-0.105E 07	0.560E 06	-0.457E 06	-0.347E 07
0.414E 08	0.77822	I	0.345E 07	- 0.368E 07	0.66	- 0.70	1.49	- 1.59	I	-0.937E 06	0.486E 06	-0.337E 06	-0.347E 07
0.364E 08	0.87972	I	0.368E 07	- 0.391E 07	0.70	- 0.74	1.59	- 1.69	I	-0.793E 06	0.441E 06	-0.135E 06	-0.347E 07
0.228E 08	0.94334	I	0.391E 07	- 0.413E 07	0.74	- 0.78	1.69	- 1.78	I	-0.703E 06	0.419E 06	-0.155E 06	-0.347E 07
0.117E 08	0.97582	I	0.413E 07	- 0.436E 07	0.78	- 0.83	1.78	- 1.88	I	-0.659E 06	0.384E 06	0.394E 05	-0.347E 07
0.537E 07	0.99078	I	0.436E 07	- 0.459E 07	0.83	- 0.87	1.88	- 1.98	I	-0.613E 06	0.347E 06	-0.284E 06	-0.347E 07
0.217E 07	0.99679	I	0.459E 07	- 0.481E 07	0.87	- 0.91	1.98	- 2.08	I	-0.575E 06	0.309E 06	-0.457E 06	-0.347E 07
0.797E 06	0.99901	I	0.481E 07	- 0.504E 07	0.91	- 0.96	2.08	- 2.17	I	-0.569E 06	0.303E 06	-0.457E 06	-0.347E 07
0.322E 06	0.99990	I	0.504E 07	- 0.527E 07	0.96	- 1.00	2.17	- 2.27	I	-0.457E 06	0.453E 02	-0.457E 06	-0.457E 06

TOTAL CYCLES = 0.359E 09

ROOT MEAN CUBED IS 0.322E 07

AVERAGE MEAN IS -0.172E 07

ORIGINAL PAGE IS
OF POOR QUALITY

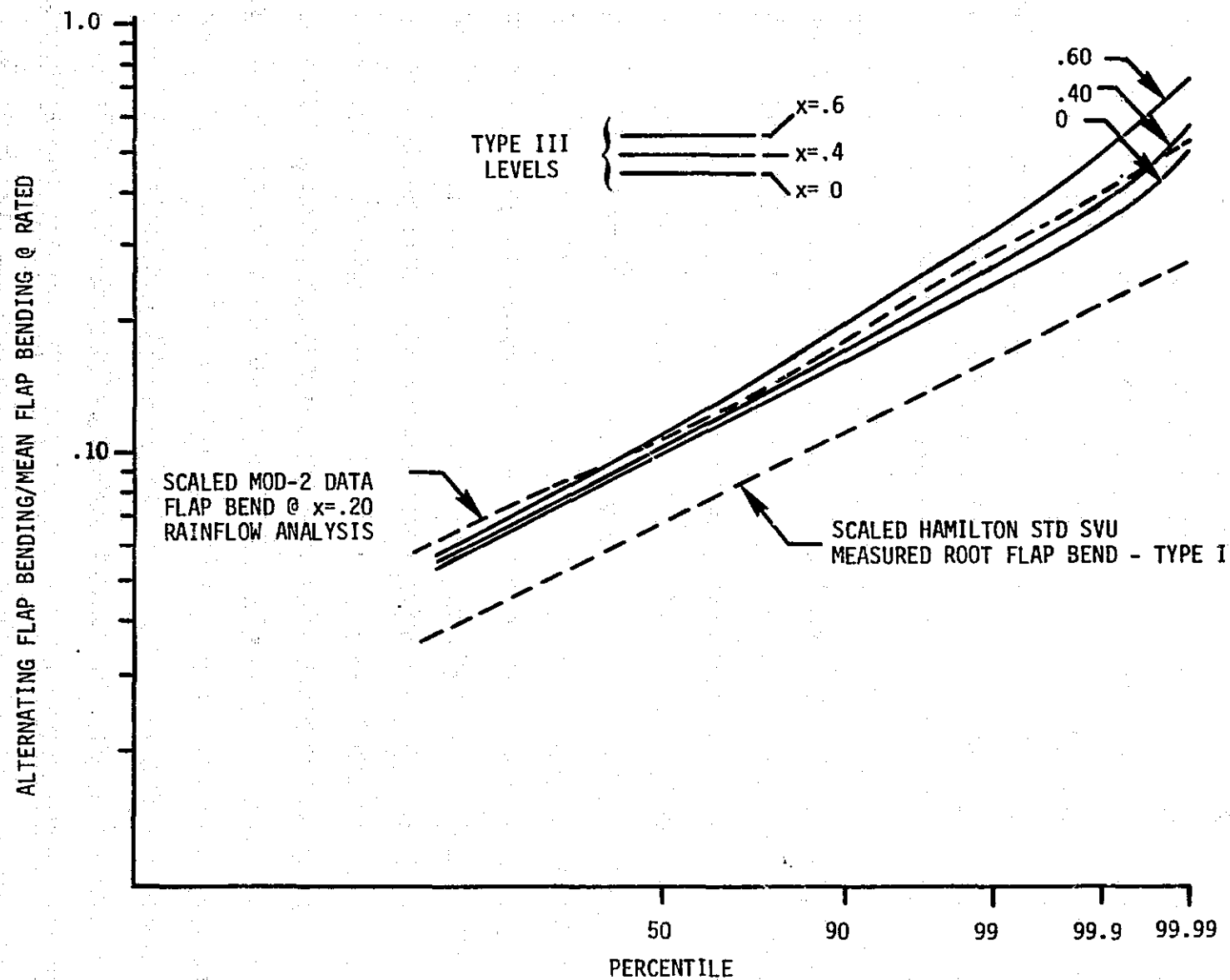


Figure 7-16 Blade Flapwise Bending Moment Probability Distributions

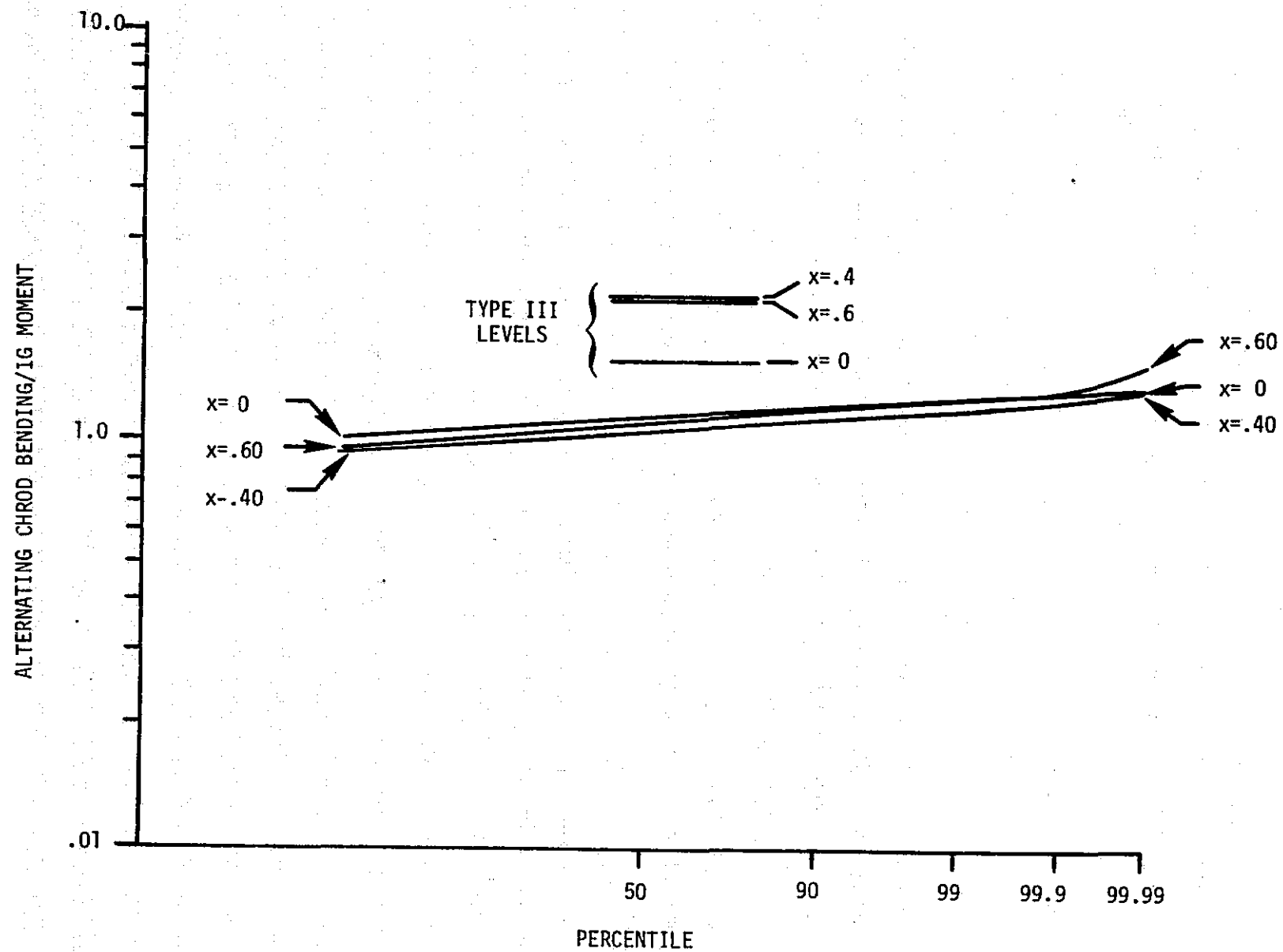


Figure 7-17 Blade Chordwise Bending Moment Probability Distributions

Tower fatigue bending moment distributions are plotted in Figure 7-18. In this case the alternating moments at the base of the tower have been normalized by the mean bending moment created by the rotor aerodynamic thrust at rated wind speed. The alternating thrust moment (M_y) is far more sensitive to gusts than M_z , which accounts for the differences in the probability distributions. The MOD-5A predictions appear to be consistent with MOD-2 data, which is also included in the figure. The earlier MOD-2 data, in the upper curve, was taken before improvements were made to the control system, so it exhibits higher loads.

Vibratory rotor torques are plotted in Figure 7-19. Alternating torque levels and power levels, are below 10% of rated torque for over 90% of the operating time. The pronounced increase in load above the 98th percentile is due to Type II gusts and shifts in mean wind speed. Curves of yaw bearing moments and drive torque are included in Figure 7-20. Probability distributions for other system interfaces may be constructed from the data in Appendix B.

Normalized blade limit loads are summarized in Figure 7-21. The flap bending moments are 2.25 to 3 times the mean moment at rated wind speed. Chord bending moments are about 2 g's at the root, where gravitational effects are greatest. They increase to about 9 g's at the tip, where the aileron drag forces far exceed the 1 g loads. Normalized fixed system limit loads are reported at selected interfaces in Table 7-10. The complete set of dimensional loads may be found in Appendix B.

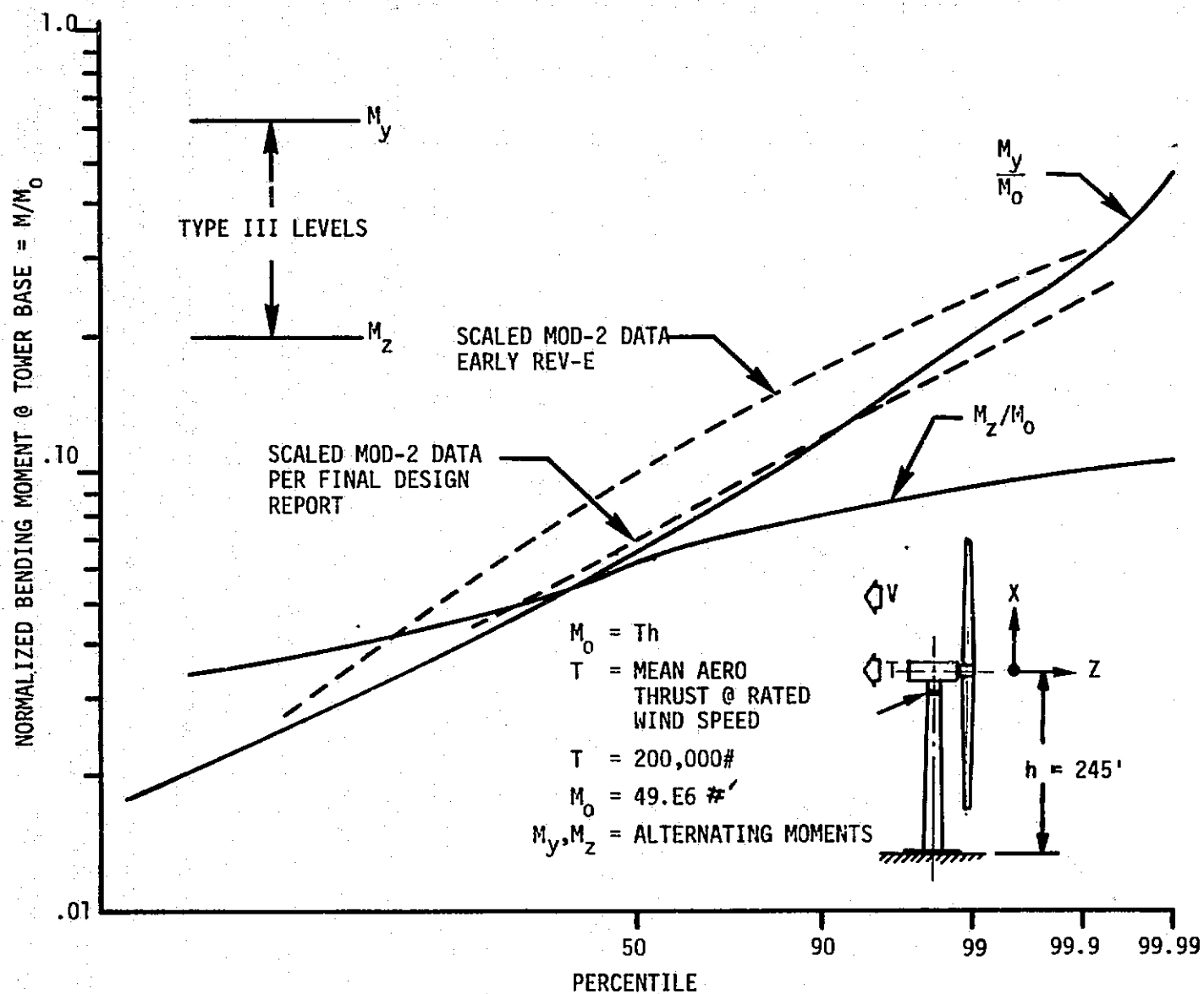


Figure 7-18 Tower Root Bending Moment Probability Distributions

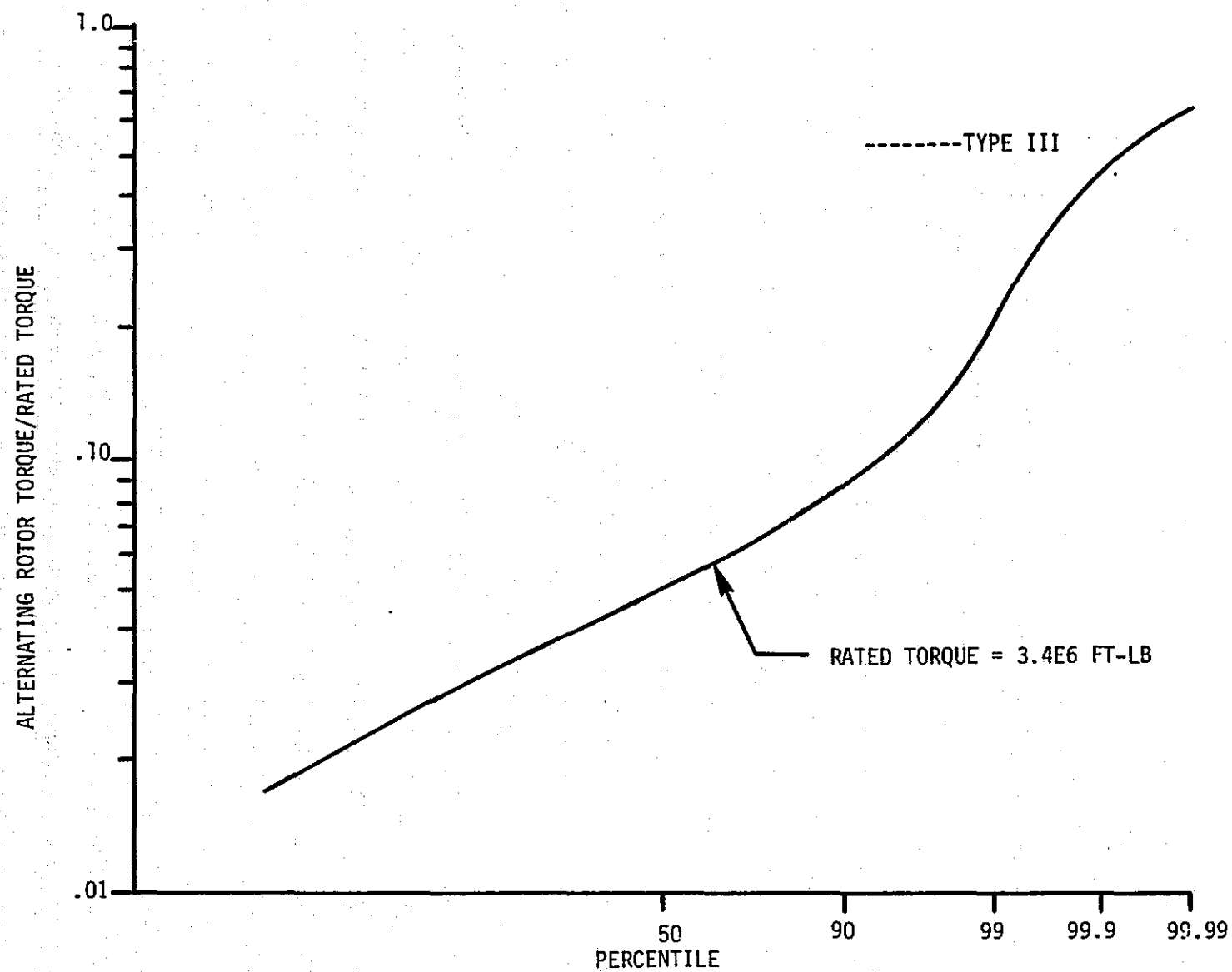


Figure 7-19 Rotor Torque Probability Distribution

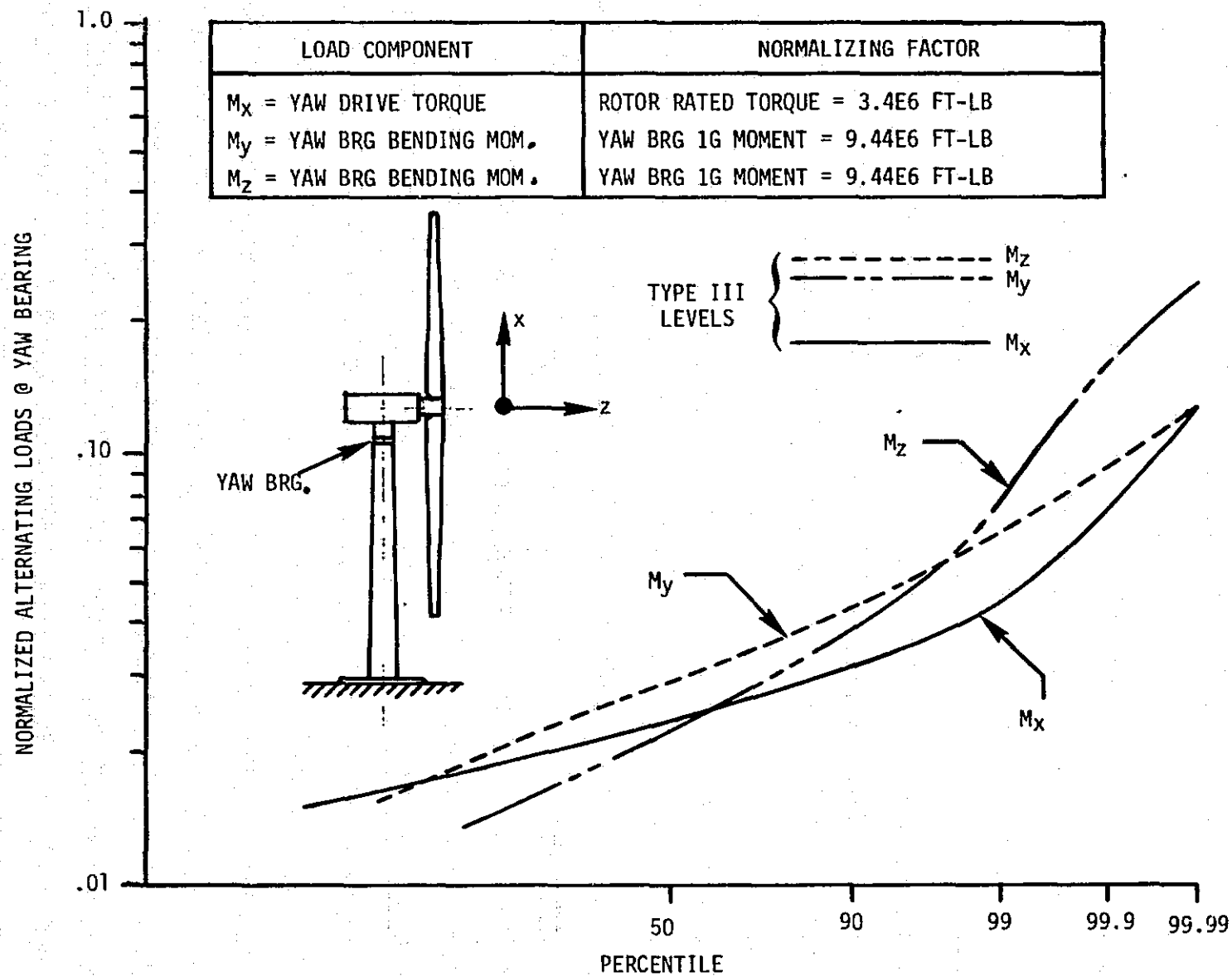


Figure 7-20 Yaw Bearing Bending Moment and Drive Torque Probability Distributions

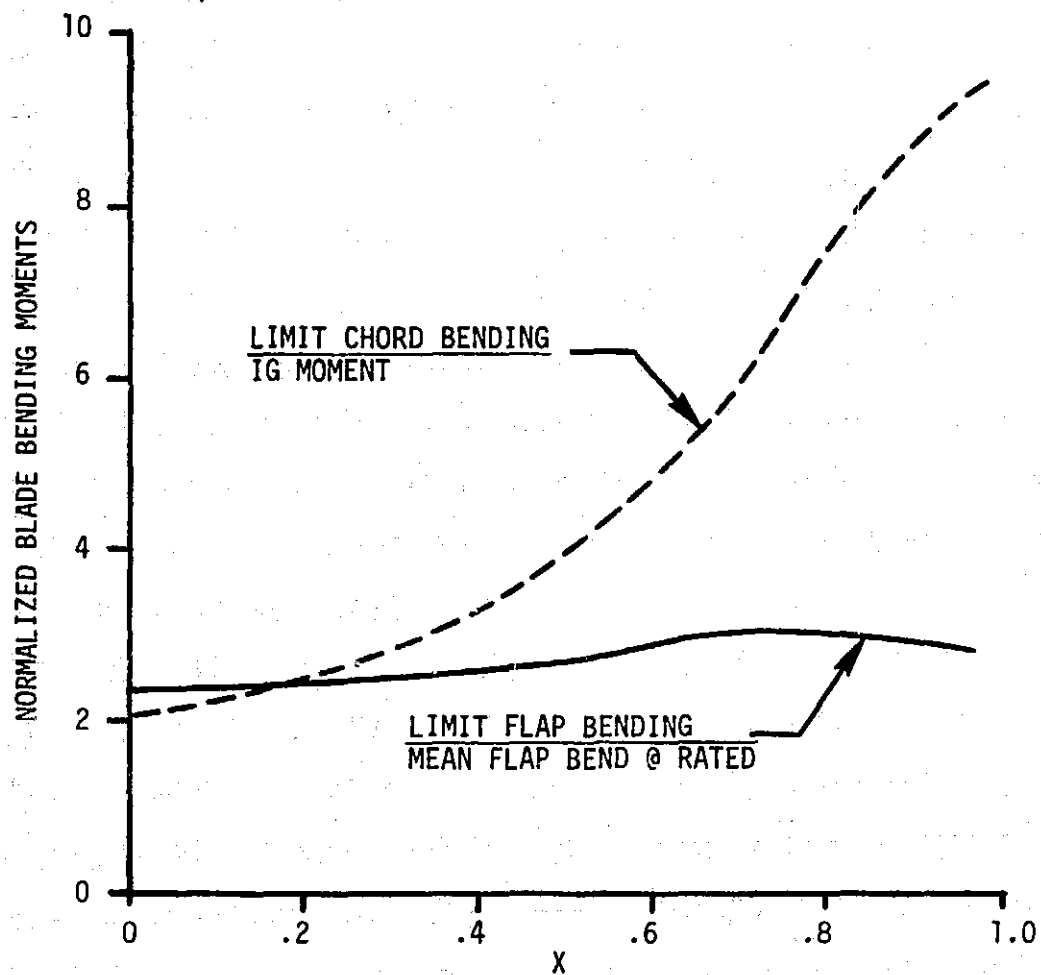


Figure 7-21 Blade Limit Loads

Table 7-10 Normalized Fixed System Limit Load Summary

CONDITION	ROTOR TORQUE	RESULTANT BENDING/1G		RESULTANT
	RATED TORQUE	ROTOR/NACELLE	YAW BEARING	BENDING AT TOWER BASE*
HURRICANE	---	1.0	1.80	2.35
CONTROLS FAILURE AT 60 MPH	1.39	1.57	.60	1.91
99.99% GUST AT RATING	1.26	1.44	.60	1.93
SHUTDOWN AT CUT-OUT WITH YAW ERROR	NOT CRITICAL	1.85	1.22	NOT CRITICAL
CYCLOCONVERTER MISHAP	1.73	---	---	---

* Normalized by bending moment because of rotor aerodynamic thrust at rated wind speed.

7.5 COMPONENT DESIGN LOADS

The design loads and dynamic requirements for components of the MOD-5A are presented in this section. The loads, for the most part, were derived from the interface load resultants discussed in section 7.4. The dynamic requirements were developed from dynamic response parametric studies. The magnitudes and requirements of some loads are quoted from the component specifications prepared for the subcontractors. These loads are often higher than those defined by the interface loads because in many cases the specifications were written for an earlier MOD-5A model. The higher load specifications should not cause problems, and should result in a final design that is conservative in some areas.

Rotor system, drivetrain system and yaw system components are addressed in the following subsections. The tower and nacelle design loads are defined explicitly in the interface load definitions, so they will not be repeated here.

7.5.1 AILERONS

Aileron loads are specified as continuous functions of the blade span, from the start of the aileron at .60R to the outmost section at .99R. Load/unit span, rather than stress resultants were used, so that the hinge locations and their end conditions could be varied during the design without changing the external loads. Furthermore, aerodynamic and inertial loads are specified separately, so that the inertia loads could be made consistent with the actual final design weight by using appropriate g factors.

General formulas that combine the aerodynamic and inertial contributions of the running shears (V_x , V_y , V_z) and hinge moment (M_H) are given in Table 7-11. These formulas must be integrated with respect to span, to determine the hinge reactions and the six stress resultants at a given cross-section. Geometry and sign conventions were defined in section 7.3, Figure 7-14.

Table 7-11 Formulas Needed to Combine Aileron Aerodynamics and Inertial Loads

- (1) $V_X = W \cdot G_X$
- (2) $V_Y = W \cdot G_Y + V_{YA}$
- (3) $V_Z = W \cdot G_Z + V_{ZA}$
- (4) $M_H = -\bar{Z} \cdot W \cdot G_Y + \bar{Y} \cdot W (G_Z - G_X \sin \Lambda_H)$
 $+ K I_{OH} + M_{HA}$

Where:

V_X, V_Y, V_Z	= Running design shears that are a function of spanwise position x (lb/ft)
M_H	= Running design hinge moment (torsion) function of x (lb-ft/ft)
V_{YA}, V_{ZA}, M_{HA}	= Aerodynamic loads - functions of x
G_X, G_Y, G_Z, K	= Design g factors - functions of x
W	= Aileron running weight (lb/ft) to be determined as a function of x for the actual design being analyzed
\bar{Y}, \bar{Z}	= Center of gravity of aileron structure that rotates about hinge (ft). See Figure 7-14. To be determined as a function of x for actual design.
I_{OH}	= Aileron running mass moment of inertia about hinge (slug - ft ² /ft).
Λ_H	= Inclination of hinge axis in X-Z plane (see Figure 7-14).

It is likely that concentrated masses will exist at certain points in the structure (e.g. actuators, fittings, etc.). Concentrated loads should be applied at these points using equations (1)-(4) with W being replaced by the concentrated weight (lb) and the aerodynamic contributions set to zero, (\bar{Y} and \bar{Z} in Equation (4) should be replaced by the concentrated weight's center of gravity).

Limit Loads

(1) Hurricane (130 mph)

(a) Blades Horizontal (Aileron in Line with Main Blade)

$V_{ya} = 0$ for all X
 V_{za} vs X in Figure 7-22
 M_{ha} vs X in Figure 7-22
 $G_x = 0$ for all X
 $G_y = +1$ for all X or -1 for all X
 $G_z = -.18$ for all X
 $K = 0$ for all X

(b) Blades Vertical (Aileron Pitched 90°)

V_{ya} vs X in Figure 7-23
 V_{za} vs X in Figure 7-23
 M_{ha} vs X in Figure 7-23
 $G_x = +1$ for all X or -1 for all X
 $G_y = .018$ for all X
 $G_z = 0$ for all X
 $K = 0$ for all X

(2) Overspeed Condition (Aileron Pitched 45°)

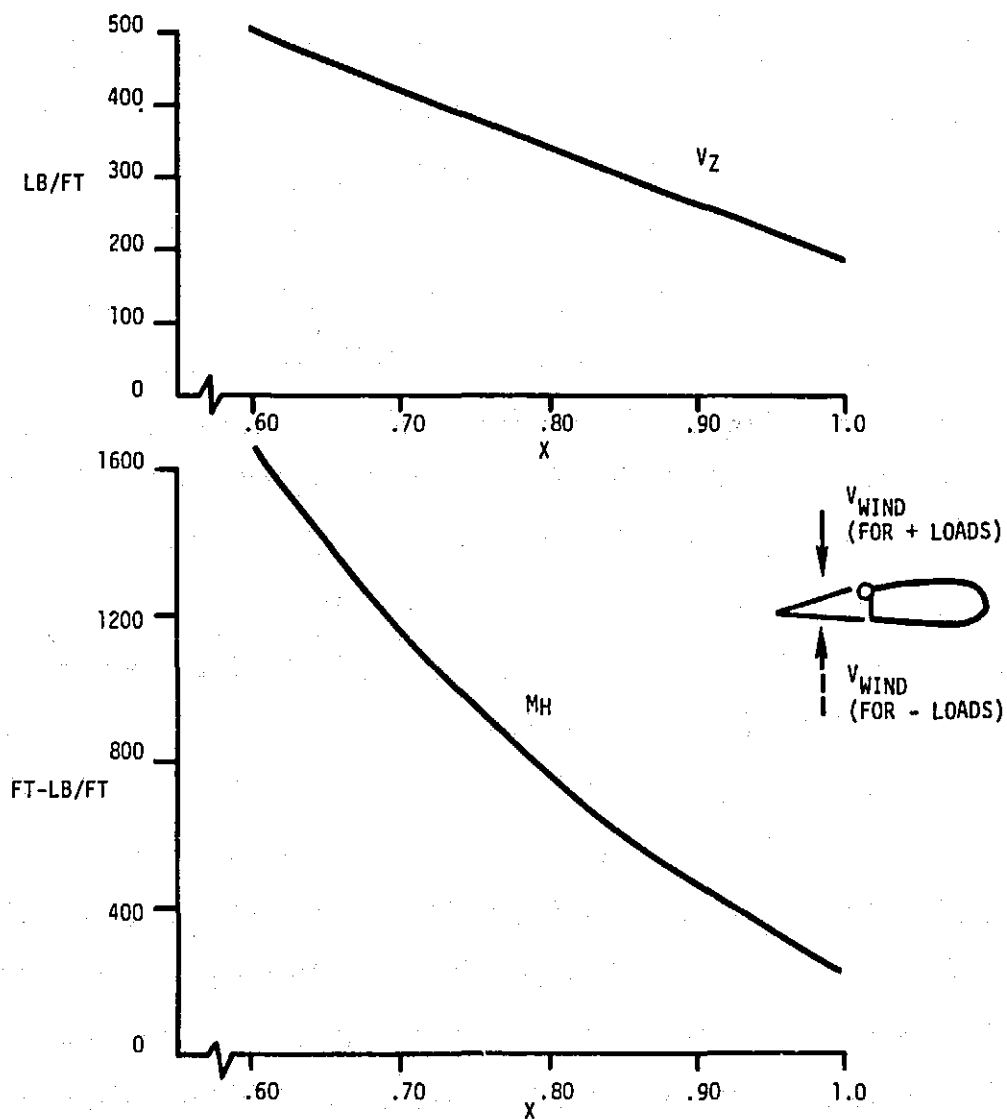
V_{ya} vs X in Figure 7-24
 V_{za} vs X in Figure 7-24
 M_{ha} vs X in Figure 7-24
 G_x vs X in Figure 7-25
 G_y vs X in Figure 7-25
 G_z vs X in Figure 7-25
 $K = 1.7$ for all X

Fatigue Loads

A mean and alternating load component was used to define each fatigue cycle. The same mean loads are conservatively applied to all fatigue cycles, and probability distributions are assigned to the alternating loads. The total number of fatigue cycles for the 30-year life of the machine is 400×10^6 .

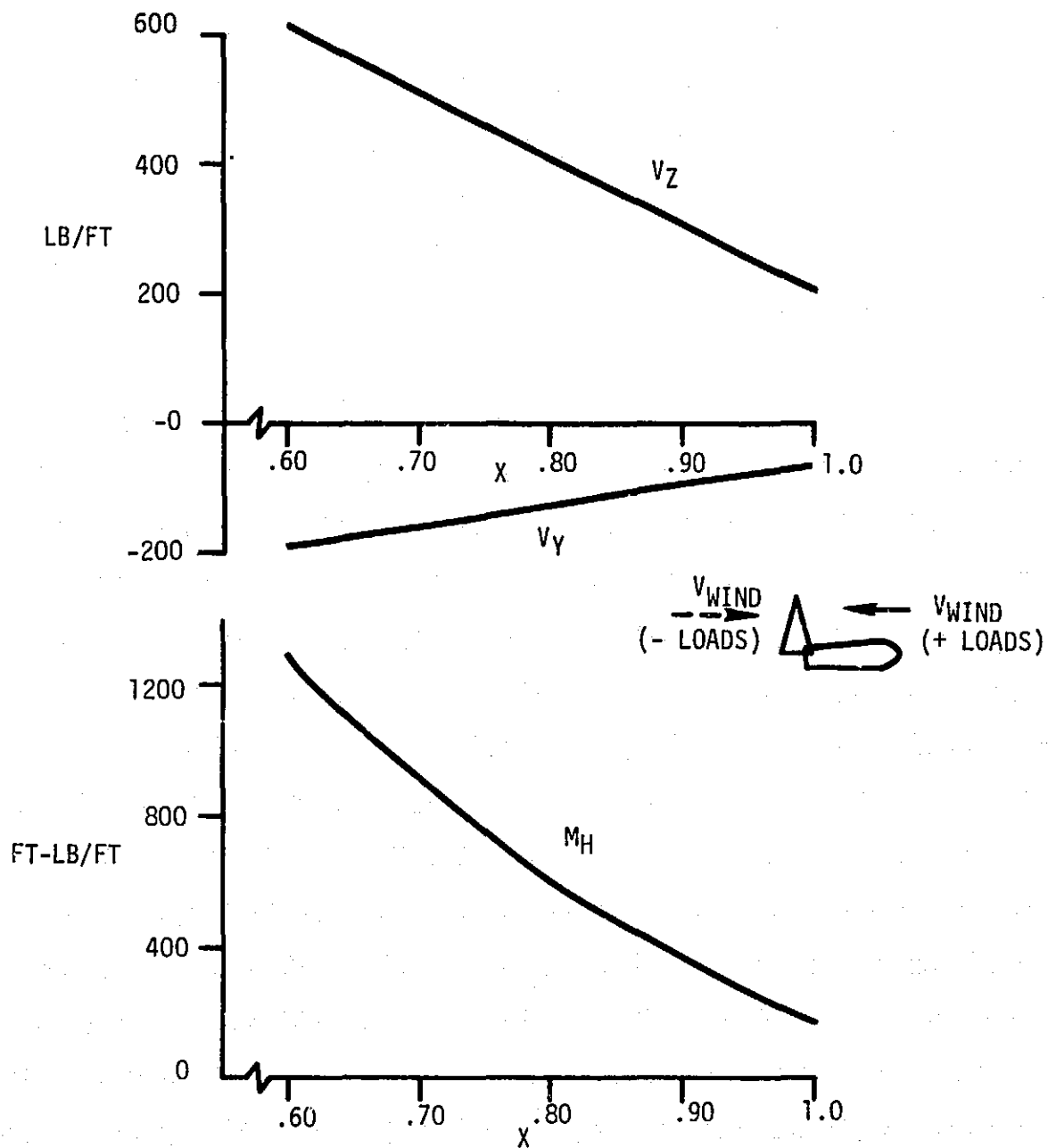
Mean Loads

V_{ya} vs X in Figure 7-26
 V_{za} vs X in Figure 7-26
 M_{ha} vs X in Figure 7-26
 G_x vs X in Figure 7-27
 G_y vs X in Figure 7-27
 G_z vs X in Figure 7-27
 $K = .55$ for all X



NOTE: V_z & M_H HAVE SAME SIGN BUT LOAD MAGNITUDES ABOVE MAY BE \pm .

Figure 7-22 Aileron Aerodynamic Loads for Hurrican Conditions with the Blades Horizontal, and the Ailerons Undeflected



NOTE: V_Z & M_H HAVE THE SAME SIGN BUT LOAD MAGNITUDES MAY BE ±.

Figure 7-23 Aileron Aerodynamic Loads for Hurrican Conditions with the Blades Vertical and the Ailerons Deflected 90°

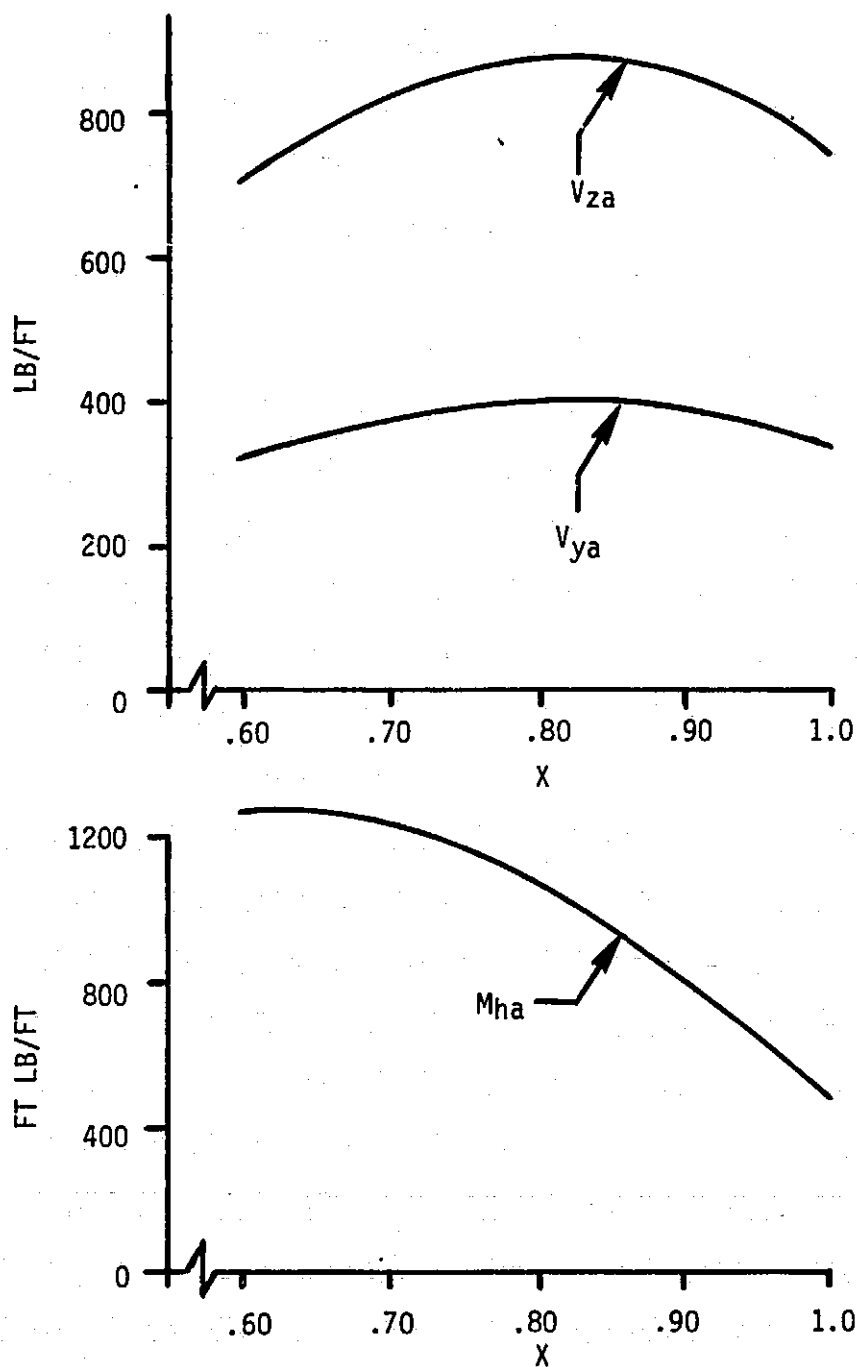


Figure 7-24 Aileron Aerodynamic Limit Loads for a 25% Overspeed Condition, with the Ailerons Deflected 45°

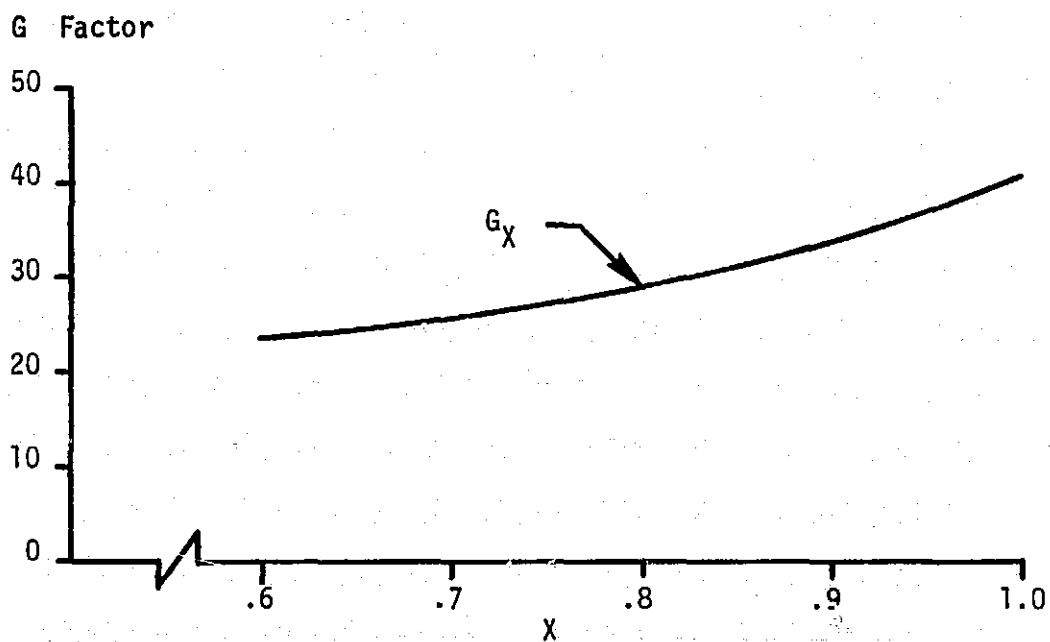
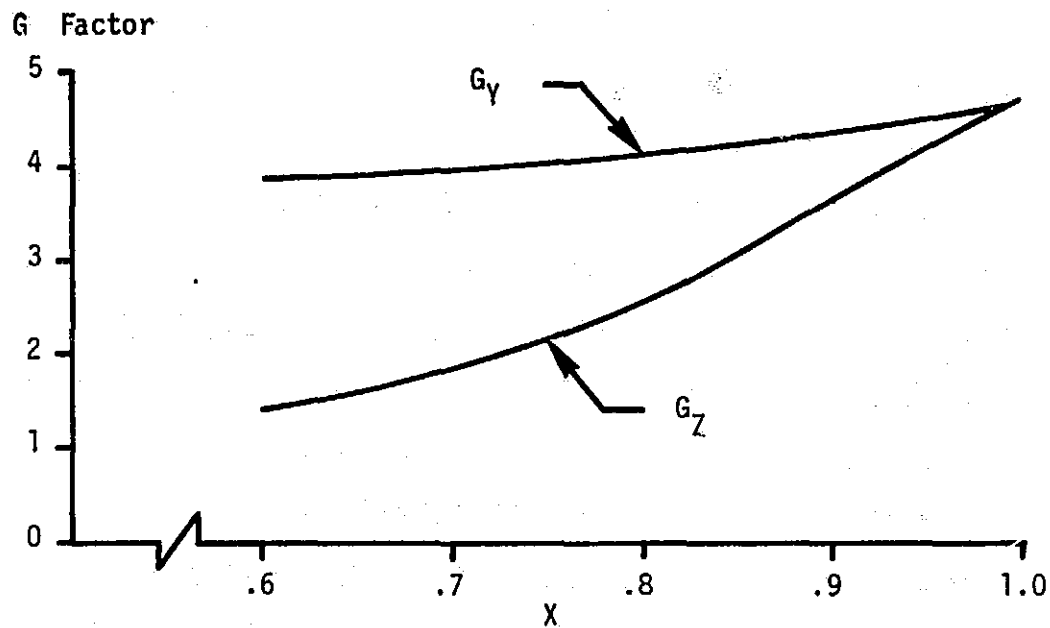


Figure 7-25 Aileron Inertial Limit Loads for a 25% Overspeed Condition with the Ailerons Deflected 45°

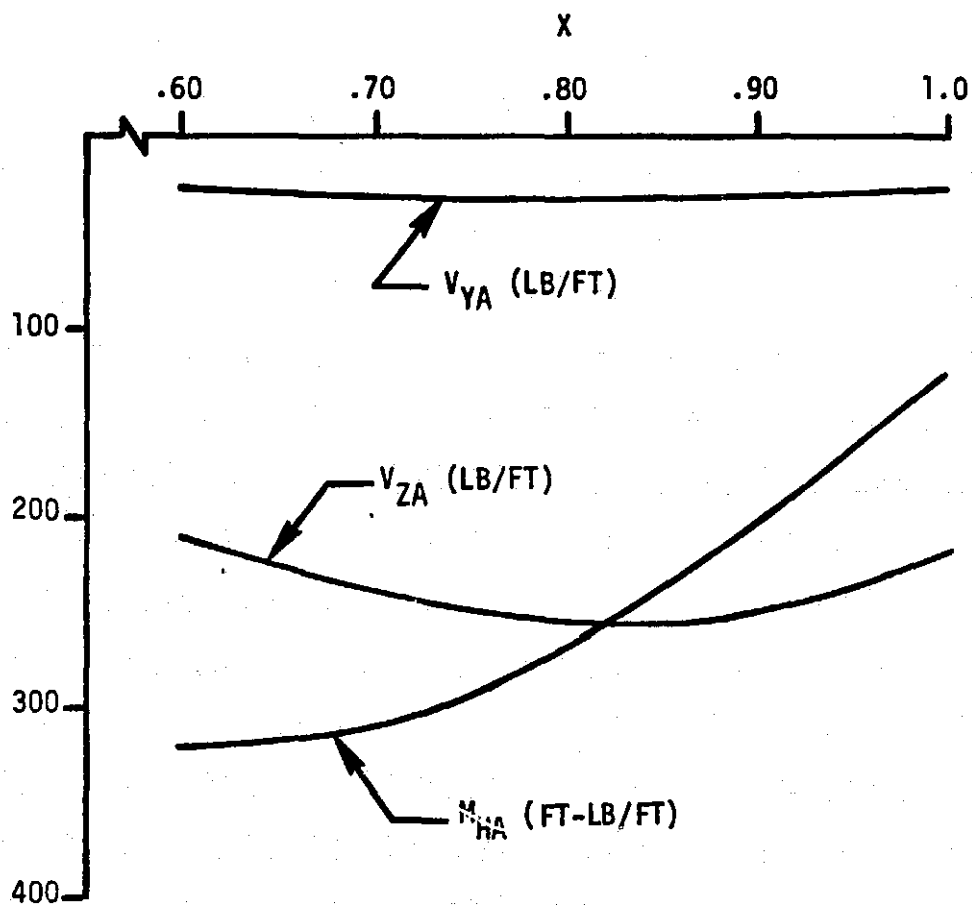


Figure 7-26. Mean Aerodynamic Aileron Loads at Rated Wind Speed,
50th Percentile Cyclic Loads are 15% of Shown Mean Loads

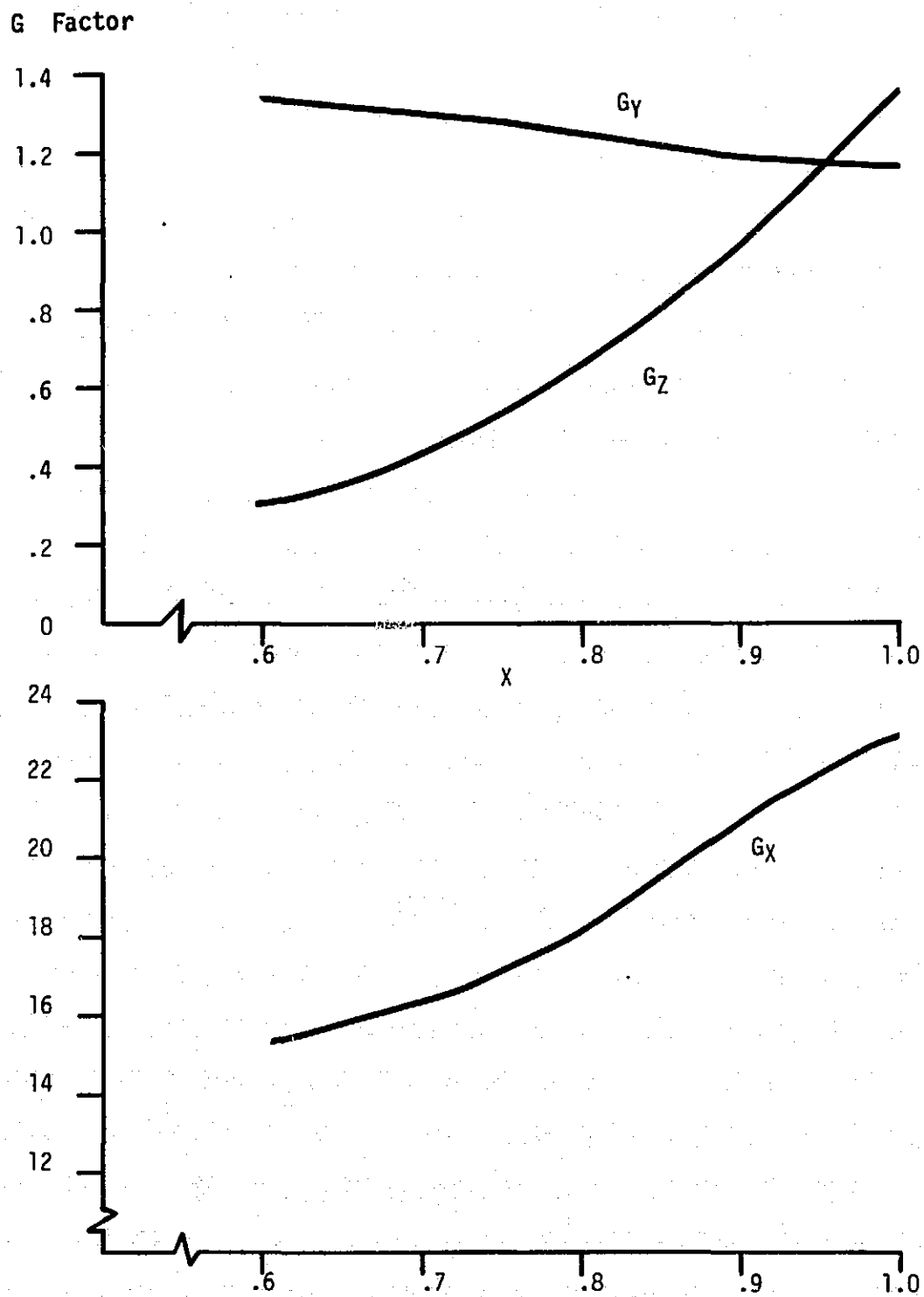


Figure 7-27 Mean Aileron Inertial Factors (G_x , G_y , G_z)

Alternating Loads

The load probability distribution of each load component is determined by multiplying the corresponding normalized probability distribution (NPD) and the load magnitude given below. The same NPD applies to all X stations.

V_{ya} NPD in Figure 7-28
 magnitude = .15 * values in Figure 7-26

V_{za} NPD in Figure 7-28
 magnitude = .15 * values in Figure 7-26

M_{ha} NPD in Figure 7-28
 magnitude = .15 * values in Figure 7-26

G_x NPD in Figure 7-29
 magnitude = 1.15 for all X

G_y NPD in Figure 7-29
 magnitude = 1.15 for all X

G_z NPD in Figure 7-28
 magnitude vs X in Figure 7-30

$K = 0$ (No Contribution)

Because the design for the ailerons was not as mature as other system components, these structural loads were developed conservatively. This approach was adopted to ensure a safe configuration on the first design. The particulars of the loads derivation are summarized:

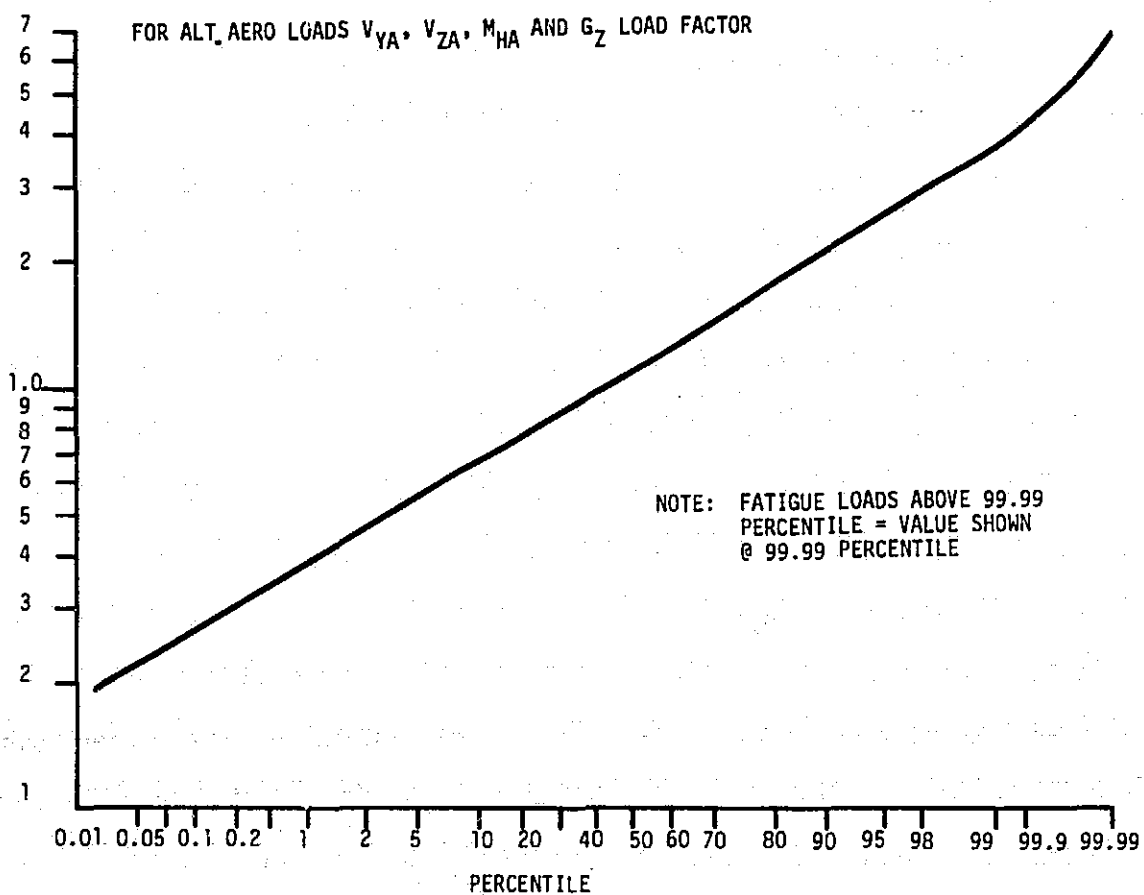


Figure 7-28 Aileron Normalized Fatigue Load Probability Distribution. Used for all Aerodynamic Loads, and Inertial Normal Force (G_z)

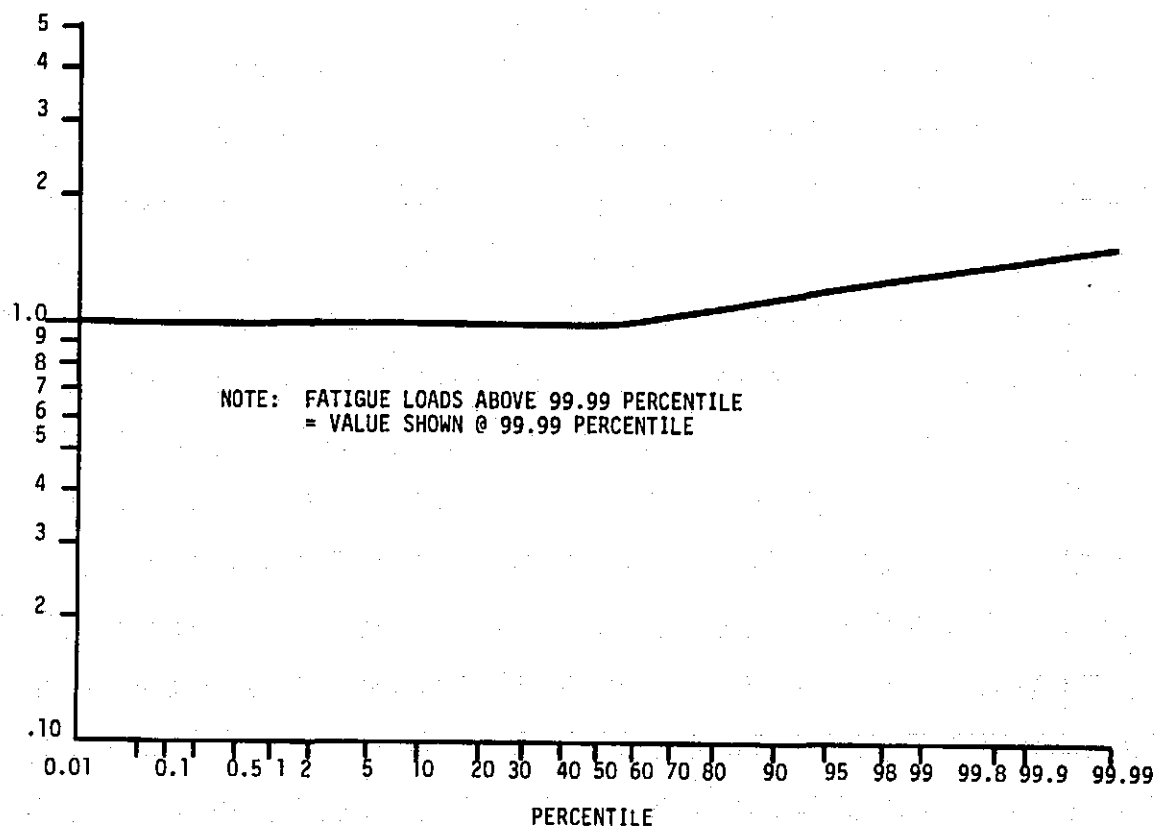


Figure 7-29 Aileron Normalized Fatigue Load Probability Distribution. Used for Radial and Lateral Inertial Loads (G_x & G_y)

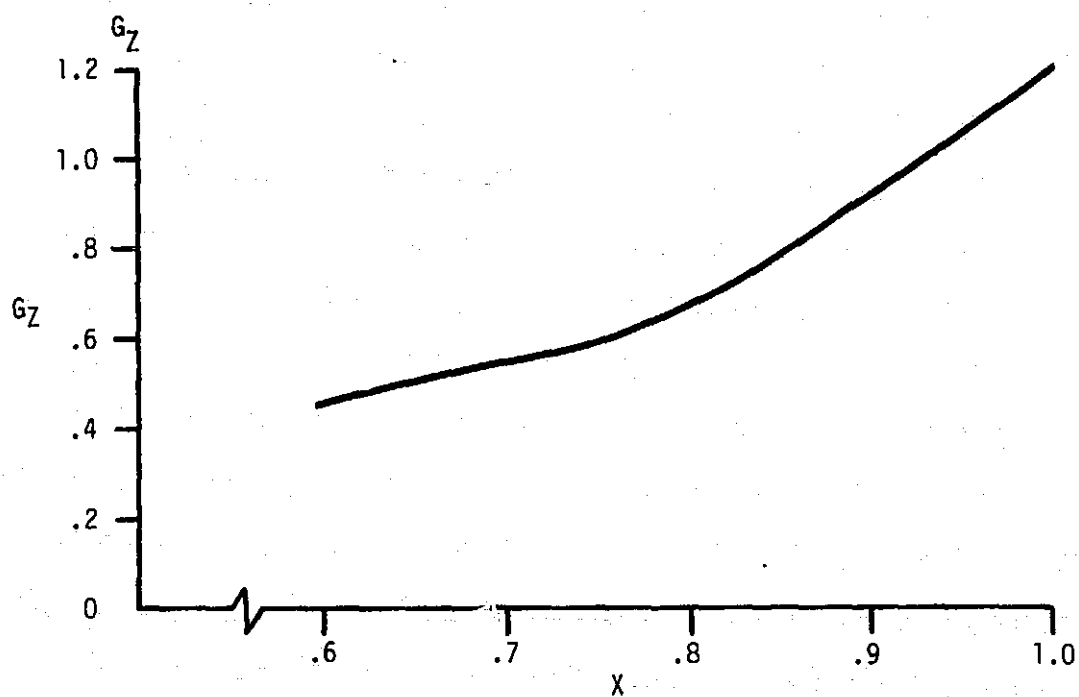


Figure 7-30 Aileron Normal Force Inertial Factor (G_z)
50th Percentile Cyclic Values

Mean Fatigue

Aerodynamics - The maximum normal operating condition, or the rating, was specified for all cycles, with a contingency factor of 1.2

G - Steady-state values at the rated wind speed, with contingency factors between 1.15 to 1.25, depending on the wind direction

Alternating Fatigue

Aerodynamics -. 50% Load = 15% of the mean load, with a contingency factor of 1.2

(Note - outboard main blade is 11% of mean)

99.9% load = 4.2 times 50% of the mean load (based on main blade).

The distribution is log-normal to 99.99%. This definition covered all possible Type II and Type III occurrences.

G- 50% = steady-state TRAC with contingency factors between 1.15 to 1.25. Distribution is log-normal (similar to aero in flap direction).

Limit loads were estimated for the hurricane and for 25% overspeed. For the latter, TRAC accelerations were used and airloads were based on an aileron deflection of 45°. Less than 45° would be needed to stop the machine, and lower angles produce lower loads. A 20% contingency was applied to the limit loads. It was assumed that g-loads and airloads were phased to add directly in both limit and fatigue conditions.

Weight could probably be trimmed from the final aileron design, using refined loads and less conservatism.

7.5.2 BLADES

7.5.2.1 Primary Bending Loads

Stress resultants acting on the main blade structure were defined at a sufficient number of interfaces to determine the size of the primary structure in section 7.4.

7.5.2.2 Blade Pressure Loading

In this section, blade internal and external pressure distributions are discussed. These loads produce membrane and plate bending stresses that can be critical in the cross-grain direction.

The pressure loads on the blade depend upon blade venting, which influences the internal pressure. A blade sealed against the atmosphere would experience excessive pressure loads. Therefore, a vented design was adopted. Inboard and outboard vents were incorporated, because they minimize pressure loads and provide for the exit of contaminants within the blade. The trailing edge section, which extends from the blade root to the ailerons at .60R, is vented at .10R and .60R. The two forward cells of the blade cross-section are vented at .10R and the tip (1.0R).

The internal pressure in the cavities of the blade at the non-dimensional spanwise station, x , is given by:

$$p_g = p_i - p_o = q_t (x^2 - \frac{1}{2} (x_1^2 + x_2^2))$$

where,

$$q_t = \frac{1}{2} \rho V_t^2$$

ρ = air density

V_t = tip speed

x_1 and x_2 are the non-dimensional spanwise locations of the vents

p_i = absolute pressure in the cavity at station x

p_o = vent pressure (taken to be atmospheric)

p_g = gage pressure within the cavity

The external pressures on the blade surface are obtained from the airfoil pressure distribution. Figure 7-31 contains plots of airfoil pressure coefficient (C_p) vs the chordwise location for critical operating conditions. This data is furnished at three spanwise locations, $x = .25$, $.55$, and $.95$. Dimensional gage pressures on the exterior surfaces are given by

$$p_g = p_e - p_o = q_t x^2 C_p$$

The external pressures were used with the previously defined internal pressures in the blade structural analysis. The following pressures for the parked blade in hurricane conditions were also analyzed:

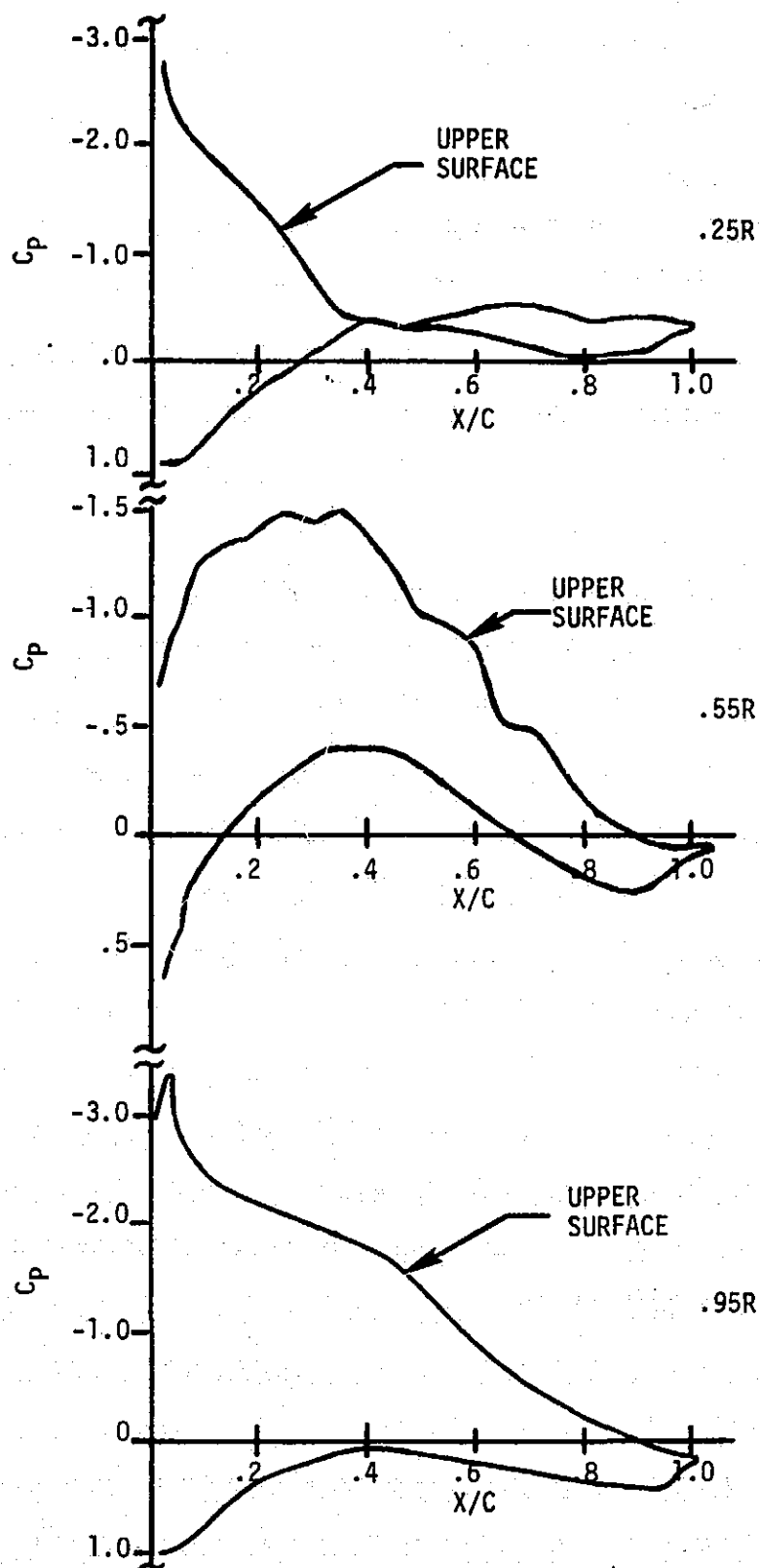


Figure 7-31 Airfoil Pressure Coefficients, Shown for Sections at $X = .25, .55$ and $.95$

internal gage pressure = 0

external gage pressure = $1/2 \rho V^2 C_{ph}$

where:

ρ = air density

V = wind speed (130 mph)

C_{ph} = 1.0 windward side (constant across surface)

= .40 leeward side (constant across surface)

These values of C_{ph} correspond to a drag coefficient of 1.4. In all the analyses, the pressures defined in this section were multiplied by a contingency factor of 1.15.

7.5.2.3 Balance Requirements

Mismatches in blade to blade mass properties cause a 1P dynamic excitation. In order to minimize this dynamic excitation, a static balance requirement of 18,000 ft.-lb. was imposed on the MOD-5A blades. That is, the manufactured blades of a rotor set will be teeter-balanced to within 18,000 ft.-lb. of one another, with respect to a fulcrum point at the blade root. The balance will be accomplished by inserting weights at 50% of the span or at the tip or in both places. While the balance can be effected with minimum weight using only the tip location, this station has the greatest influence on the natural frequency. Therefore, to minimize frequency mismatches, balance provision was made at two locations.

7.5.3 ROTOR HUB

Loads, and related dynamic requirements for the teeter brake, teeter bearings, and low speed shaft bearings are discussed in this section. The loads were either derived from the interface loads in section 7.4, or are earlier loads for the heavier partial span control. In most cases, the component specifications were not updated for the aileron configuration, recognizing that the design would be conservative using the earlier load definitions.

The structure of the yoke can be designed using the rotor center line interface loads given in section 7.4, so they will not be addressed here.

7.5.3.1 Teeter Brakes

Some form of teeter restraint is necessary to prevent impact into hard stops during abnormal operating conditions. Conditions are particularly severe during high wind shutdowns with a yaw error. Comprehensive parametric studies led to the selection of a two-stage, friction brake system as protection for the rotor, because it introduced the minimum load into the system. The brake force schedule is illustrated in Figure 7-32. During most of the operation, the teeter angle is less than 2.5° , and the brakes are totally disengaged. If for any reason the teeter angle exceeds $\pm 2.5^\circ$ the first set of brakes engages. This brake force can handle all but the most severe conditions. In the very few instances in which the teeter angle exceeds 5° , the full brake force is applied and maintained and the system will shutdown. Transient dynamic analyses have shown that this brake system will keep operational teeter angles below 6° . When parked, the brakes are set at their highest level, to protect the system from dissymmetries in the oncoming wind. During startup, the high brake force is maintained until the rotor speed exceeds 6 rpm, then the schedule illustrated in Figure 7-32 is adopted for the remaining operation.

The supporting structure for the brake system is designed to 1.15 times the maximum brake level, or 2.76×10^6 ft.-lb.

7.5.3.2 Teeter Bearings

Teeter bearing specification loads are given for both normal operating and limit conditions. These specifications were obtained from the fatigue load histograms, and the limit loads of model 304.1, with appropriate factors of safety added.

The abnormal operating loads are derived by combining the limit shears and moments. With a spacing of 17.7 ft. between bearings, the x-x load is obtained by combining half the x shear with half the z moment divided by the bearing spacing. The y-y load is equal to half the y shear. The z-z load is calculated similarly to the x-x, by combining half the z shear with half the x moment divided by the bearing spacing.

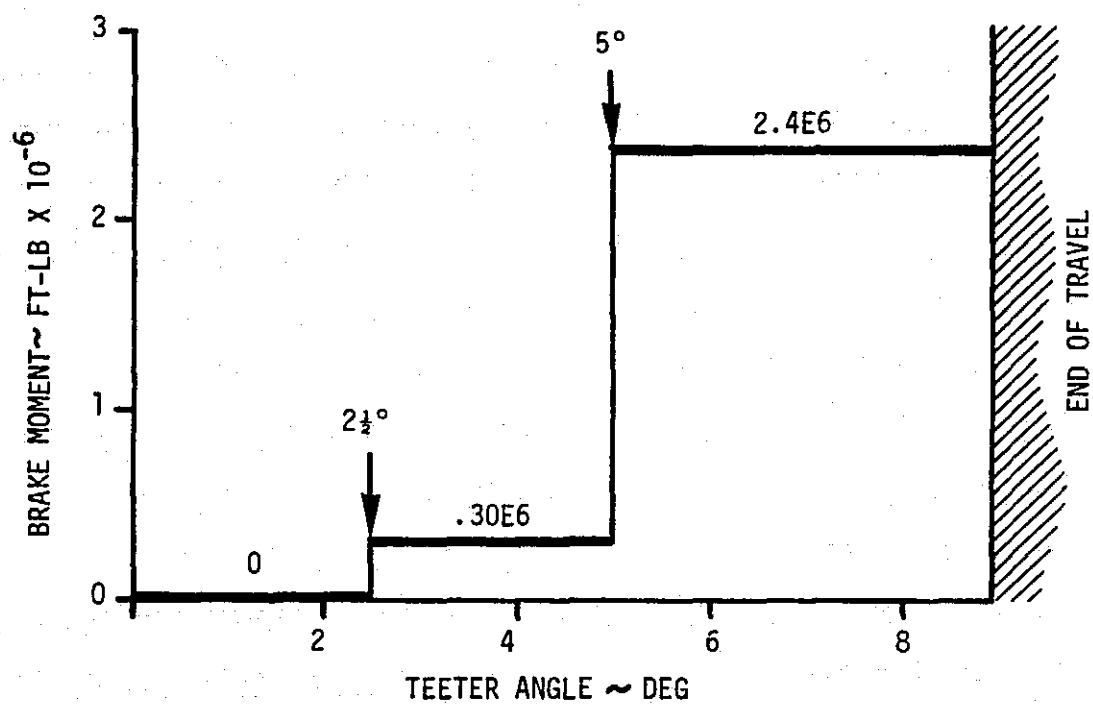


Figure 7-32 MOD-5A Teeter Brake Schedule

The normal operating loads were derived from the fatigue load histograms. The mid-range load is equal to half of the absolute value of the largest mean load from the histogram table. The alternating loads were obtained from the 99.99th percentile fatigue loads, as follows: the x-x load is equal to half of the 99.99th percentile x load, plus half of the 99.99th percentile z moment divided by the bearing spacing. The y-y load is half the y shear. The z-z load is half the z shear, plus half of the x moment divided by the bearing spacing.

The specification loads for normal operation and limit conditions are listed in Table 7-12. Table 7-13 contains ratios of these loads divided by those calculated in the more recent analysis of the final model, 304.2. The specification is conservative with respect to the model 304.2. The teeter angle probability distribution, for bearing design, is presented in Figure 7-33. Also included is Table 7-14, a reprint of the specification start-up and shut-down loads. They are divided into teeter angle bins indicating the number of load cycles encountered during 35,000 start-up to shut-down cycles.

Stiffness requirements were also defined and are presented in Table 7-15. The numerical values listed in the table as maxima or minima are those used in the frequency model for model 304.2.

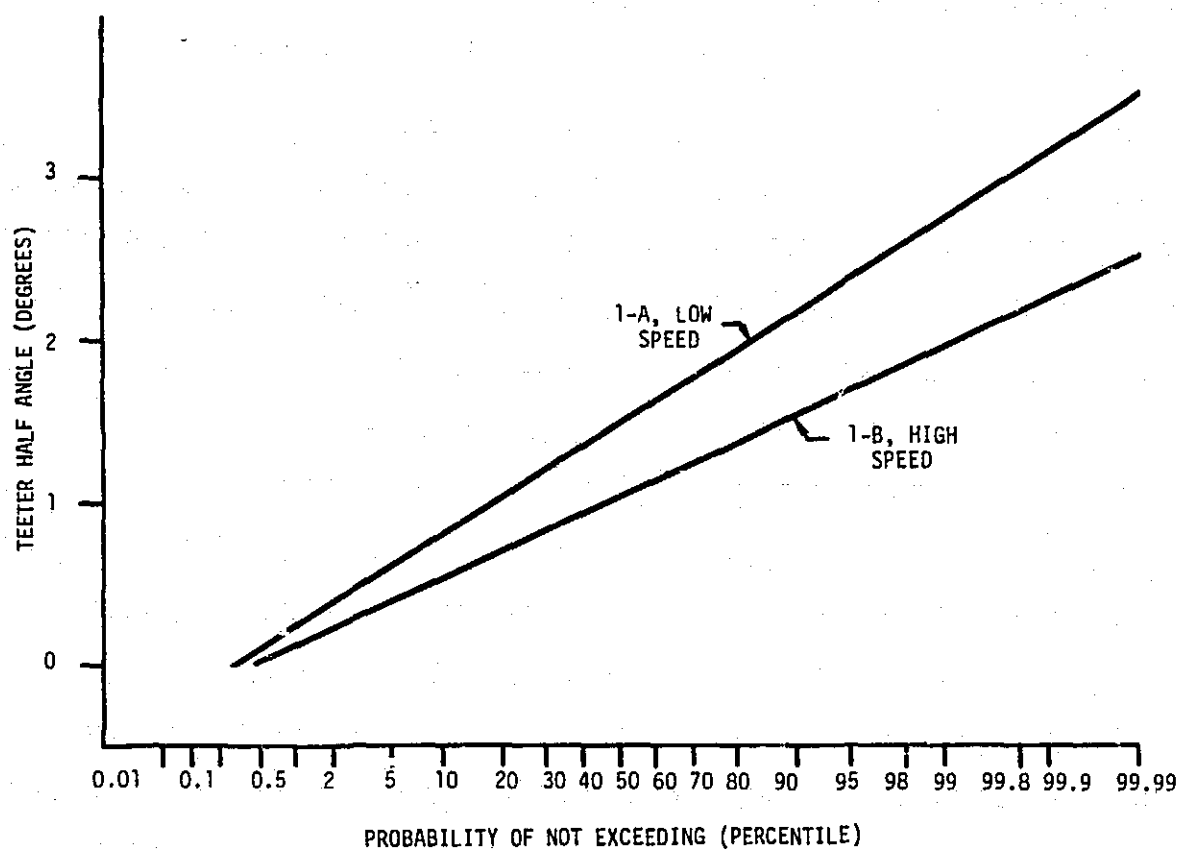


Figure 7-33 Teeter Angle Probability Distribution for Normal Operation

Table 7-12 Teeter Bearing Normal Operating and
Limit Load Specification

Normal Operating Loads (kips)

No. of Cycles	Spectrum (Degrees)	Radial Bearing		Thrust Bearing
		x-x	z-z	y-y
56 x 10 ⁶	Fig. 7-33A	140 ±336	139 ±92	225 ⁽¹⁾
135 x 10 ⁶	Fig. 7-33B	140 ±336	139 ±92	225 ⁽¹⁾
SUM 191 x 10 ⁶				

Abnormal Operating Loads (kips)

No. of Cycles	Spectrum (Degrees)	Radial Bearing		Thrust Bearing
		x-x	z-z	y-y

500	±2.0°	343 ±277	324 ± 0	225 ⁽¹⁾
-----	-------	----------	---------	--------------------

(1) 225k is the peak value - the minimum is 189k (dead weight).

Table 7-13 Ratio of Specification to Model
304.2 Loads-Teeter Bearing

Normal Operating Ratios

Radial Bearing		Thrust Bearing
x-x	z-z	y-y
1.25 ±1.34	1.01 ±1.64	1.10

Abnormal Operating Ratios

Radial Bearing		Thrust Bearing
x-x	z-z	y-y
2.30 ±1.67	1.34 ±0	1.32

Table 7-14 Normal Start-up and Shutdown Loads (kips)

	BIN	NO. OF CYCLES	SPECTRUM (degrees)	RADIAL BEARING x-x	z-z	THRUST BEARING y-y
<u>Normal</u>						
Start	E1	315,000	$< \pm 2.5^\circ$	0 ± 204	75 ⁽¹⁾	225
Up	E2	420,000	± 2.5 to 3.5°	0 ± 204	75	225
	E3	210,000	± 3.5 to 4.5°	0 ± 204	75	225
	E4	84,000	± 4.5 to 5.5°	0 ± 204	75	225
	E5	18,900	± 5.5 to 7°	0 ± 204	75	225
Shut	F1	84,000	$< \pm 2.5^\circ$	0 ± 204	160 ⁽²⁾	225
Down	F2	126,000	± 2.5 to 3.5°	0 ± 204	160	225
	F3	126,000	± 3.5 to 4.5°	0 ± 204	160	225
	F4	67,200	± 4.5 to 5.5°	0 ± 204	160	225
	F5	13,500	± 5.5 to 7°	0 ± 204	160	225
<u>Abnormal</u>						
	E6	2,100	$\pm 7^\circ$ to 9°	0 ± 204	250	225
	F6	600	$\pm 7^\circ$ to 9°	0 ± 204	330	225

(1) This value is the maximum rotor thrust expected during start-up. The load will vary from zero at 0 rpm to peak shown with an average value of 35 kips.

(2) This value is the maximum rotor thrust expected on shutdown. The load can reverse to a peak negative value, of 25k. The average shutdown value will be +40k.

Table 7-15 Teeter Bearing Stiffness Requirements

The axial and radial spring rates of the individual bearings are in the range specified below at 75°F ±15°F.

Bearing	Axial Spring Rate (lbs/in.)	Radial Spring Rate (lbs/in.)	Torsional Spring Rate (in lbs/degree)
Radial	Not applicable	$>2 \times 10^6$	$<4 \times 10^5$
Thrust	$>4 \times 10^6$	N/A	$<10^5$

7.5.3.3 Rotor Bearing

The rotor is supported by two bearings 40 in. apart, which are mounted within the yoke. The loads appearing in the bearing specification are summarized in Table 7-16. The loads were derived from the shears and moments reported at the rotor centerline and rotor and nacelle interfaces, which straddle the bearing locations. The specified loads were adjusted conservatively to accommodate possible weight increases. For example, the mean radial loads quoted are 40 to 50% higher than the 1 g loads that will be experienced during normal operations, while the alternating radial loads are 50 to 70% greater than the anticipated 99.99th percentile fatigue loads. Furthermore, the radial bearings are capable of withstanding a 100% overload, while the maximum anticipated loads, which occur when the teeter brakes are engaged, present only a 25% overload. The thrust bearing loads in Table 7-16 were also treated conservatively.

7.5.4 GEARBOX AND DRIVETRAIN

Special considerations were necessary in developing the fatigue spectrum for the gearbox design. Because the gear teeth are continually cycling between full load and no load, the absolute value of the torque governs the fatigue design. Therefore, a probability distribution of the sum of mean plus alternating rotor torques was developed. This distribution is referred to as the gearbox torque duty cycle.

The gearbox torque duty cycle is illustrated in Figure 7-34. Torque levels were normalized by the rated value. The curves depict the load level probability of a sample taken at random during the 30 years of operation. Because certain fatigue loads, such as that caused by wind shear, reach a peak magnitude at a preferred rotor azimuth, the gears that are always in contact at a given rotor position (upper curve) must be distinguished from those that are not. In the first case the design is driven by the most highly loaded tooth, while in the second case the design takes advantage of the fact that load peaks are distributed among the many teeth.

The operation of the cycloconverter limits the maximum torque during normal operation to less than 1.3 times the rated value. Hence, the probability distributions may be truncated at this level for the purposes of gearbox fatigue design. The gearbox can withstand two times the rated torque as an extreme overload. This torque is much greater than the maximum anticipated torque for the system.

Other drivetrain components, such as shafting, can use the interface torque loads that were presented in section 7.4.

7.5.5 YAW SYSTEM

The loads acting on the yaw bearing are identical to those defined at the yaw interface in section 7.4, and the actual tabulations are in Appendix B. For reference, the loads quoted in the Yaw Bearing Specification are reproduced in Table 7-17. These loads are generally greater than the interface loads for model 304.2, with the exception of V_x , which is slightly lower. The critical loads on the yaw bearing, however, are moments, not shears, so that the final design remains conservative.

The yaw drive system was designed to provide a maximum holding torque of 1.3×10^6 ft.-lb. and a maximum driving torque of 750,000 ft.-lb. The predicted maximum yaw torque, mean plus alternating, is 1.1×10^6 ft.-lb., which is below the holding torque capability. The maximum anticipated mean torque, which is what must be overcome by the yaw drive, is 5.3×10^5 ft.-lb., well below the system's capability. The yaw drive has an additional requirement: maximum yaw rate may not exceed .5°/sec. This requirement protects the rotor from excessive teeter motions.

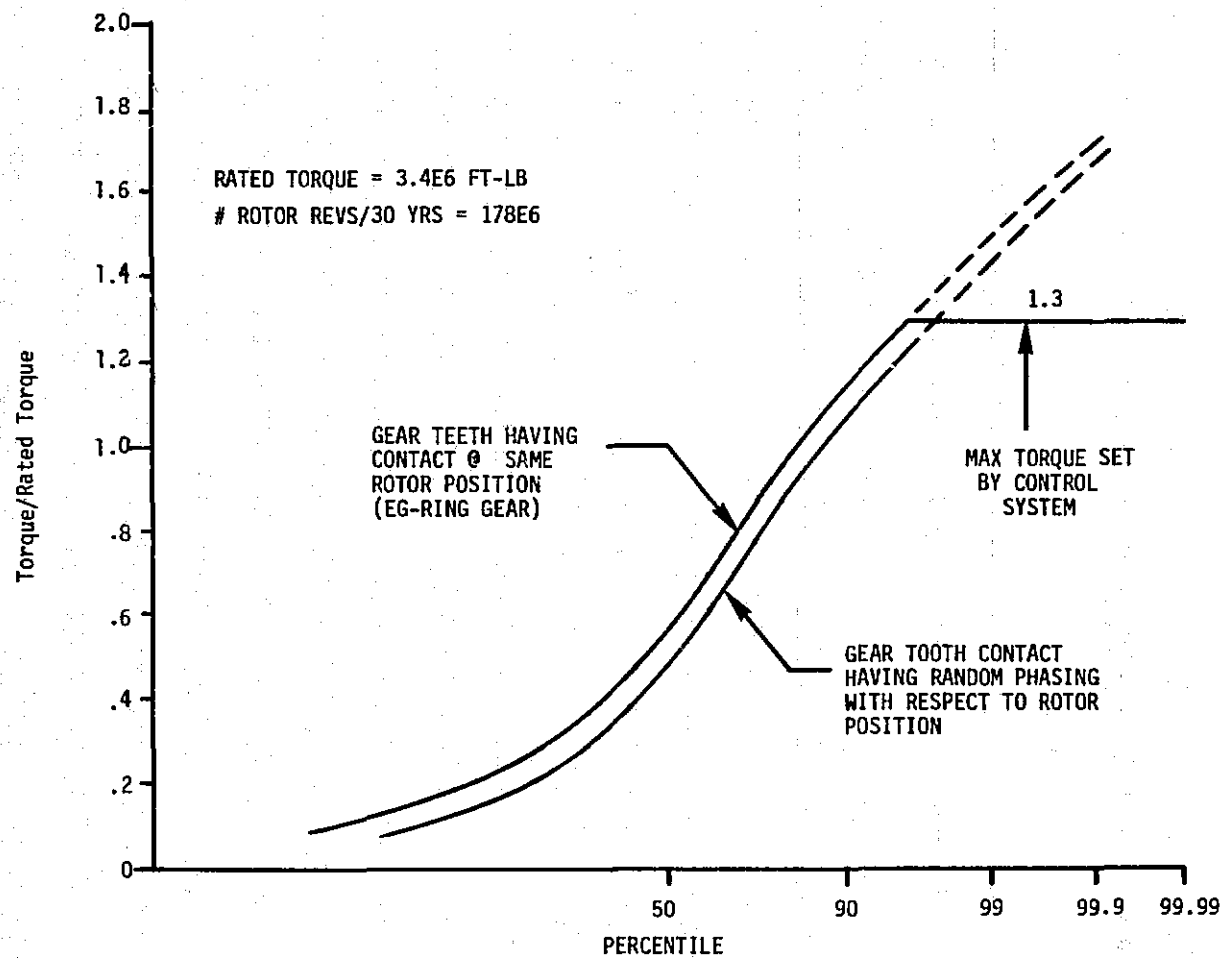


Figure 7-34 MOD-5A Gearbox Torque Duty Cycle

Table 7-16 Rotor Bearing Design Loads

Radial Bearings

	Mean	Alternating
Forward	1.5×10^6 lb.	$.15 \times 10^6$ lb.
Aft	1.0×10^6 lb.	$.10 \times 10^6$ lb.

Thrust

Peak Load = 533,000 lb.
 Rated Operating = $280,000 \pm 40,000$ lb.
 No. of Cycles = 2P for 30 years

Table 7-17 Yaw Bearing Design Loads

	V_x (kips)	V_y	V_z	M_y (ft.-lb. $\times 10^6$)	M_z
Non-Operating	-994	0	0	-11.1	0
Normal Operating					
Mean	-954	-2.5	-191	-10.1	-2.85
+99.9th percentile	26	26	59	1.0	1.79
Root Mean Cubed	18	19	18	.37	.49
Abnormal (Limit)					
Hurricane	-867	0	+455	-18.6	0
Gust	-994	60	180	-14.4	.7

References

- 7-1 1500 KW Wind Turbine Generator Program Preliminary Design Review Report, General Electric Doc. No. 77SDS4203, Jan. 1977.
- 7-2 MOD-1 WIND TURBINE GENERATOR ANALYSIS AND DESIGN REPORT, Vol. 1, DOE/NASA/0058-79/2, NASA CR-T59495, May 1979.
- 7-3 Powell, D.C., and Connell, J.R., "Definition of Gust Model Concepts and Review of Gust Models", PNL-3138, June 1980, Pacific Northwest Laboratories, Richland, Washington, 99352.

ORIGINAL PAGE IS
OF POOR QUALITY

ABBREVIATIONS

1

A	Amperes
AAO	average annual outage time
AASHTO	American Association of State Highway and Transportation Officials
ac	alternating current
ACI	American Concrete Institute
A/C	aircraft
AGMA	American Gear Manufacturers Association
AILSTAB	Aileron Stability Analysis
AISC	American Institute of Steel Construction
ASCE	American Society of Civil Engineers
ASCII	American Standard for Computer Information Interchange
ASTER	a computer program
ASTM	American Society for Testing Materials
AWG	American Wire Gauge
AWS	American Welding Society
baud	the rate of transmission of data from one part of computer to another
BESD	backup emergency shutdown
CBI	Chicago Bridge and Iron
CD	coefficient of drag
CDS	controls data system
CEC	control electronics cabinet
ccw	counterclockwise
cfm	cubic feet per minute
CGT	crack growth threshold
CI	cut-in
CIS	cycle intercept stress
CMD	command
COE	cost of energy
COV	coefficient of variation
CPU	central processing unit
CRT	cathode ray tube
CVN	Charpy V-notch test
dc	direct current
DOE	Department of Energy

ECL	Eptak control language
EHD	elastohydrodynamic
EMC	equivalent moisture content
ES	engineering instrumentation system
EPTAK	trade name for controller from Eagle Signal Division of Gulf and Western Industries
EMI	electromagnetic interference
ESD	emergency shutdown
FMEA	failure modes effects analysis
fpm	feet per minute
fpv	failures per year
FRP	glass fiber-reinforced plastic
ft.	feet
g	a unit of acceleration, equal to 32 ft/sec or 9.8 m/sec
G	giga, a prefix meaning one billion
gal.	gallons
GBI	Gougeon Brothers Incorporatedde
GETSS	GE Turbine System Analysis
GETSTAB	a computer program
gpm	gallons per minute
Hz.	Hertz
IITRI	Illinois Institute of Technology, Research Institute
I/O	input/output
in.	inch
ISM	input signal manager
k	kilo, a prefix meaning 1000
kips	a unit of force or weight, kilopounds, or 1000 pounds
ksi	a unit of stress, kips per square inch, or 1000 psi
kV	kiloVolts, or 1000 Volts
kW	kiloWatt or 1000 Watts
kWh	kiloWatt-hours, or 1000 Watt-hours
lbs.	pounds
lb/MDGL	pounds per 1000 square feet of double glue line
LEFM	linear elastic fracture mechanics
LMC	laminae moisture content
LVDT	linear variable differential transformer

m	milli, a prefix meaning .001
M	mega, a prefix meaning 1,000,000
mA	milliAmperes, or .001 of an Ampere
MC	moisture content
ml	milliliter
mph	miles per hour
mps	meters per second
MTBF	mean time between failures
MTTR	mean time to repair
MS	structural margin of safety
m/sec	meters per second
mps	meters per second
MUX	multiplexer
MW	megaWatt, or one million Watts
MWA	megaWatt-Amperes, or a million Watt-Amperes
N	Newton, the unit of force in the metric system
NASA	National Aeronautics and Space Administration
NASTRAN	a computer program
NDT	Nil-ductility transition
NEMA	National Electrical Manufacturers Association
N-m	Newton-meter, the unit of moment in the metric system
NSD	normal shutdown
O&M	operating and maintenance
OIS	operational information system
OSM	output signal manager
P	per revolution
PCS	pitch change system
PGC	Philadelphia Gear Corporation
PSC	partial span control
PIR	program information report
PLV	pitch line velocity
ppm	parts per million
PROM	programmable read only memory
psf	pounds per square feet
psi	pounds per square inch
PWHT	post-weld heat treatment
QAERO	a computer program

R	ratio of actual stress to allowable stress, or minimum fatigue stress cycle to maximum fatigue stress cycle
rad/sec	radians per second
RAM	random access memory
RAM	reliability, availability, and maintainability
RFP	request for proposal
RMC	root mean cubed
ROM	read only memory
rpm	revolutions per minute
RT	room temperature
SCAMP	Stiffness Coupling Approach Modal-Synthesis Program
SCI	Structural Composites, Incorporated
SIM-5A	a computer code for control system analysis
S_{min}	minimum stress
S_{max}	maximum stress
S-N	stress vs. number of cycles
SOW	Statement of Work
STRAP	Static Row Analysis Program
ssu	Saybolt universal seconds
TBD	to be determined
TBR	to be resolved
TFT	transverse filament tape
TRAC	Transient Rotor Analysis Code
tty	teletype
TVI	television interference
UBC	Uniform Building Code
UPS	uninterruptible power supply
UDRI	University of Dayton Research Institute
V	Volts
Vac	alternating voltage
Vdc	constant voltage
W	Watts
WEPO	Wind Energy Project Office
WTG	wind turbine generator
WT	weight
WINDLD	a computer program
WINDOPT	a computer program

1. Report No. NASA CR-174735		2. Government Accession No.		3. Recipient's Catalog No.	
4. Title and Subtitle MOD-5A Wind Turbine Generator Program Design Report Volume II - Conceptual and Preliminary Design Book 1				5. Report Date August, 1984	
				6. Performing Organization Code	
7. Author(s)				8. Performing Organization Report No.	
				10. Work Unit No.	
9. Performing Organization Name and Address General Electric Company Advanced Energy Programs Department P.O. Box 527 King of Prussia, PA 19406				11. Contract or Grant No. DEN 3-153	
				13. Type of Report and Period Covered Contractor Report	
12. Sponsoring Agency Name and Address U.S. Department of Energy Conservation and Renewable Energy Division of Wind Energy Technology Washington, D.C. 20545				14. Sponsoring Agency Code DOE/NASA/0153-2	
15. Supplementary Notes Final report. Prepared under Interagency Agreement DE-AI01-79ET20305. Project Manager, T.P. Cahill, Wind Energy Project Office, NASA Lewis Research Center, Cleveland, Ohio 44135					
16. Abstract This report documents the design, development and analysis of the 7.3MW MOD-5A wind turbine generator covering work performed between July 1980 and June 1984. The report is divided into four volumes: Volume I summarizes the entire MOD-5A program, Volume II discusses the conceptual and preliminary design phases, Volume III describes the final design of the MOD-5A, and Volume IV contains the drawings and specifications developed for the final design. In Volume II, Conceptual and Preliminary Design, the requirements and criteria for the design are presented. The conceptual design studies, which defined a baseline configuration and determined the weights, costs and sizes of each subsystem, are described. The development and optimization of the wind turbine generator are presented through the description of the ten intermediate configurations between the conceptual and final designs. The development tests, which determined or characterized many of the materials and components of the wind turbine generator, are described. Analyses of the system's loads and dynamics are presented.					
17. Key Words (Suggested by Author(s)) Renewable energy; Wind energy Wind power; Variable speed generator Wind turbine design; Wind turbine system; Wood rotor blades; Large scale wind turbine				18. Distribution Statement Unclassified - unlimited STAR Category - 44 DOE Category - UC-60	
19. Security Classif. (of this report) Unclassified		20. Security Classif. (of this page) Unclassified		21. No. of pages	
				22. Price*	